frontiers | Research Topics

Near-infrared spectroscopy technique and its application in exercise settings

Edited by
Giancarlo Condello, Salvador J. Jaime, Wei-Peng Teo and Thomas Rupp

Published in
Frontiers in Physiology
Frontiers in Sports and Active Living

ISSN 1664-8714
ISBN 978-2-83251-038-4
DOI 10.3389/978-2-83251-038-4

About Frontiers

Frontiers is more than just an open access publisher of scholarly articles: it is a pioneering approach to the world of academia, radically improving the way scholarly research is managed. The grand vision of Frontiers is a world where all people have an equal opportunity to seek, share and generate knowledge. Frontiers provides immediate and permanent online open access to all its publications, but this alone is not enough to realize our grand goals.

Frontiers journal series

The Frontiers journal series is a multi-tier and interdisciplinary set of open-access, online journals, promising a paradigm shift from the current review, selection and dissemination processes in academic publishing. All Frontiers journals are driven by researchers for researchers; therefore, they constitute a service to the scholarly community. At the same time, the *Frontiers journal series* operates on a revolutionary invention, the tiered publishing system, initially addressing specific communities of scholars, and gradually climbing up to broader public understanding, thus serving the interests of the lay society, too.

Dedication to quality

Each Frontiers article is a landmark of the highest quality, thanks to genuinely collaborative interactions between authors and review editors, who include some of the world's best academicians. Research must be certified by peers before entering a stream of knowledge that may eventually reach the public - and shape society; therefore, Frontiers only applies the most rigorous and unbiased reviews. Frontiers revolutionizes research publishing by freely delivering the most outstanding research, evaluated with no bias from both the academic and social point of view. By applying the most advanced information technologies, Frontiers is catapulting scholarly publishing into a new generation.

What are Frontiers Research Topics?

Frontiers Research Topics are very popular trademarks of the *Frontiers journals series*: they are collections of at least ten articles, all centered on a particular subject. With their unique mix of varied contributions from Original Research to Review Articles, Frontiers Research Topics unify the most influential researchers, the latest key findings and historical advances in a hot research area.

Find out more on how to host your own Frontiers Research Topic or contribute to one as an author by contacting the Frontiers editorial office: frontiersin.org/about/contact

Near-infrared spectroscopy technique and its application in exercise settings

Topic editors

Giancarlo Condello — University of Parma, Italy
Salvador J. Jaime — University of Wisconsin–La Crosse, United States
Wei-Peng Teo — Nanyang Technological University, Singapore
Thomas Rupp — Université Savoie Mont Blanc, France

Citation

Condello, G., Jaime, S. J., Teo, W.-P., Rupp, T., eds. (2022). *Near-infrared spectroscopy technique and its application in exercise settings*. Lausanne: Frontiers Media SA. doi: 10.3389/978-2-83251-038-4

Table of contents

frontiers in Physiology

SYSTEMATIC REVIEW
published: 26 October 2021
doi: 10.3389/fphys.2021.761232

Prefrontal Cortex Oxygenation During Endurance Performance: A Systematic Review of Functional Near-Infrared Spectroscopy Studies

*Jonas De Wachter[1], Matthias Proost[1], Jelle Habay[1], Matthias Verstraelen[1], Jesús Díaz-García[2], Philip Hurst[3], Romain Meeusen[1], Jeroen Van Cutsem[1,4] and Bart Roelands[1]**

[1] Human Physiology and Sports Physiotherapy Research Group, Vrije Universiteit Brussel, Brussels, Belgium, [2] Faculty of Sport Sciences, University of Extremadura, Caceres, Spain, [3] The School of Psychology & Life Sciences, Canterbury Christ Church University, Canterbury, United Kingdom, [4] VIPER Research Unit, Royal Military Academy, Brussels, Belgium

OPEN ACCESS

Edited by:
Giancarlo Condello, University of Parma, Italy

Reviewed by:
Umer Asgher, National University of Sciences and Technology, Pakistan
Atsuhiro Tsubaki, Niigata University of Health and Welfare, Japan

***Correspondence:**
Bart Roelands
Bart.Roelands@vub.be

Specialty section:
This article was submitted to Exercise Physiology, a section of the journal Frontiers in Physiology

Received: 19 August 2021
Accepted: 27 September 2021
Published: 26 October 2021

Citation:
De Wachter J, Proost M, Habay J, Verstraelen M, Díaz-García J, Hurst P, Meeusen R, Van Cutsem J and Roelands B (2021) Prefrontal Cortex Oxygenation During Endurance Performance: A Systematic Review of Functional Near-Infrared Spectroscopy Studies. Front. Physiol. 12:761232. doi: 10.3389/fphys.2021.761232

Introduction: A myriad of factors underlie pacing-/exhaustion-decisions that are made during whole-body endurance performance. The prefrontal cortex (PFC) is a brain region that is crucial for decision-making, planning, and attention. PFC oxygenation seems to be a mediating factor of performance decisions during endurance performance. Nowadays, there is no general overview summarizing the current knowledge on how PFC oxygenation evolves during whole-body endurance performance and whether this is a determining factor.

Methods: Three electronic databases were searched for studies related to the assessment of PFC oxygenation, through near-IR spectroscopy (NIRS), during endurance exercise. To express PFC oxygenation, oxygenated (HbO_2) and deoxygenated hemoglobin (HHb) concentrations were the primary outcome measures.

Results: Twenty-eight articles were included. Ten articles focused on assessing prefrontal oxygenation through a maximal incremental test (MIT) and 18 focused on using endurance tasks at workloads ranging from low intensity to supramaximal intensity. In four MIT studies measuring HbO_2, an increase of HbO_2 was noticed at the respiratory compensation point (RCP), after which it decreased. HbO_2 reached a steady state in the four studies and increased in one study until exhaustion. All studies found a decrease or steady state in HHb from the start until RCP and an increase to exhaustion. In regard to (non-incremental) endurance tasks, a general increase in PFC oxygenation was found while achieving a steady state at vigorous intensities. PCF deoxygenation was evident for near-to-maximal intensities at which an increase in oxygenation and the maintenance of a steady state could not be retained.

Discussion/Conclusion: MIT studies show the presence of a cerebral oxygenation threshold (ThCox) at RCP. PFC oxygenation increases until the RCP threshold, thereafter, a steady state is reached and HbO_2 declines. This study shows that the results obtained from MIT are transferable to non-incremental endurance exercise. HbO_2

increases during low-intensity and moderate-intensity until vigorous-intensity exercise, and it reaches a steady state in vigorous-intensity exercise. Furthermore, ThCox can be found between vigorous and near-maximal intensities. During endurance exercise at near-maximal intensities, PFC oxygenation increases until the value exceeding this threshold, resulting in a decrease in PFC oxygenation. Future research should aim at maintaining and improving PFC oxygenation to help in improving endurance performance and to examine whether PFC oxygenation has a role in other performance-limiting factors.

Keywords: near-infrared spectroscopy (NIRS), endurance exercise, prefrontal cortex, oxygenation, respiratory compensation point (RCP), systematic review

INTRODUCTION

Dynamic endurance exercise can be defined as prolonged (>75 s) exercise and can be classified into whole-body endurance and local muscle endurance (Mccormick et al., 2015). Dynamic whole-body endurance exercise involves large muscle groups (e.g., cycling, running, and rowing), whereas muscle endurance exercise involves only one muscle or muscle group (e.g., knee extension or handgrip tasks) (Kenney et al., 2012; Pageaux et al., 2013; Mccormick et al., 2015). In general, whole-body endurance tasks are most frequently measured during time-to-exhaustion (TTE), time-trials (TTs) (Amann et al., 2008), and constant intensity fixed duration (CIFD) tasks (i.e., both intensity and duration are fixed factors) (Ichinose et al., 2020). In contrast to TT and TTE performance, CIFD tasks are mainly used to assess psychological (e.g., perceived exertion rating, thermal discomfort, etc.) and physiological (e.g., heart rate (HR), blood lactate, etc.) reactions during exercise.

During both TTE and TTs, important decisions that impact performance need to be taken into consideration. In TTE, participants need to decide when to stop (e.g., "*Am I totally exhausted and have to stop this exercise?*") and in TTs, participants need to decide how much effort to give (e.g., "*When should I slow down/speed up to reach the set goal as fast/good as possible?*"). A large body of research has examined the underlying mechanisms of these decisions. Périard and Racinais (2015) suggested that decisions during TTs in hypoxic- and hot conditions are related to oxygen availability, whereas Girard and Racinais (2014) reported that decisions during TTE are related to alterations in central command. Similarly, core temperatures exceeding > 39°C and oxygen saturation dropping to less than < 70% O_2 saturation have been associated with performance-related decisions in both TT and TTE (Racinais and Girard, 2012). Psychobiological factors are also likely to play a role. Van Cutsem et al. (2019) reported an increase in subjective thermal strain resulted in a decrease in performance (i.e., an earlier exhaustion-decision). Given this evidence, it is clear that a myriad of factors plays a role in the underlying mechanisms of decisions in both TTE and TTs.

All the proposed mediating factors that play a role in decisions in TTE and TTs are likely to be located both peripherally (i.e., muscles) and centrally (i.e., the brain and central nervous system). Peripherally, for example, locomotor muscle fatigue is mediated by the accumulation of intracellular metabolites, which eventually cause failure in excitation-contraction coupling (Amann, 2011). Whereas centrally, it is theoretically hypothesized that the corollary discharge model determines the perception of effort by sending a copy of a motor command to the somatosensory areas. These corollary discharges influence performance decisions about how much effort is needed to give and highlight the brain as an important mediating factor in decision-making in both TTs and TTE.

The top-downregulation of the prefrontal cortex (PFC) during exercise tolerance and volition is also likely to play a role in performance decisions (Robertson and Marino, 2016). After applying 30-min transcranial direct current stimulation to the dorsolateral PFC, Angius et al. (2019) reported improvements in TTE, lower ratings of perceived exertion (RPE) and HR, and higher blood lactate than no-treatment controls. Angius et al. (2019) concluded that by targeting PFC using transcranial direct current stimulation, improvements in performance were the result of a change in decision-making, planning, attention, (short-term) memory, and executive function. A body of research has shown that PFC is an underlying mechanism for the termination of whole-body endurance exercise and is mediated by the oxygenation of the cerebral cortex (Ide et al., 1999; Ide and Secher, 2000; Bhambhani et al., 2007; Rupp and Perrey, 2008; Rooks et al., 2010). It is likely that PFC oxygenation during incremental exercise increases from low-to-hard intensities, and declines to preceding exhaustion (Rooks et al., 2010).

As mentioned earlier, PFC oxygenation seems to be an important and promising mediating factor of performance decisions during whole-body endurance performance. The two techniques that can be used to assess PFC oxygenation are functional MRI (fMRI) and functional near-IR spectroscopy (fNIRS). fMRI is suggested to be the gold standard for measuring changes in brain oxygenation and provides a high spatial resolution (up to 4.0 mm) that, in turn, can help to measure functional hemodynamic changes in the brain (Glover, 2011; Herold et al., 2018). On the other hand, fMRI is expensive and results in relatively low temporal resolution (≈0.5 Hz) due to its sensitivity to the movement (Ekkekakis, 2009; Herold et al., 2018). fNIRS is a non-invasive optical imaging technique that measures relative

changes in hemoglobin (Hb) concentrations. Compared to fMRI, fNIRS provides researchers with more possibilities to examine performance in ecological settings given that it is less sensitive to movement. However, the spatial resolution for fNIRS (≈10–20 mm) is inferior to that for fMRI (Glover, 2011; Scarapicchia et al., 2017). This disadvantage has, however, not held back researchers from attempting to create further insights into the role of (prefrontal) brain oxygenation in performance-related decisions during whole-body endurance performance (e.g., Rooks et al., 2010; Leff et al., 2011). Rooks et al. (2010) reported that PFC oxygenation during incremental exercise increased between moderate and hard intensities after which it drastically decreased at very hard intensities. Leff et al. (2011) replicated these results and reported that cortical oxygenation increased during the first few minutes following exercise until near-maximal exercise and a decrease in PFC oxygenation at near-maximal to intense exhaustive exercise. Herold et al. (2018) summarized the methodological knowledge of fNIRS, outlined recommendations for future research (Herold et al., 2018), and confirmed the relevance and applicability of fNIRS during exercise science. However, it has been over a decade since Rooks et al. (2010) summarized the effects of incremental exercise on cerebral oxygenation. To date, there is no general overview summarizing current knowledge on how PFC oxygenation evolves during (non-incremental) whole-body endurance exercise at different intensities and whether this influences performance. Therefore, there is a need for a state-of-the-art summary of cerebral oxygenation during whole-body endurance performance.

As mentioned earlier, it is clear that fNIRS research can help elucidate the underlying mechanisms of performance-related decisions during endurance exercise. To advance the field of whole-body endurance performance and highlight the opportunities to evaluate the impact of specific countermeasures on the performance-related changes in fNIRS variables, the aim of this systematic review is to provide an updated review of the extant research. We hypothesize that: (1) prefrontal oxygenation increases during submaximal exercise and subsequently decreases at a near-maximal intensity, (2) prefrontal oxygenation increases during prolonged submaximal exercise until a steady state is reached, and (3) at near-maximal intensities PFC oxygenation cannot be maintained, resulting in a decrease near exhaustion.

METHODS

This systematic review followed the guidelines provided by the Preferred Reporting Items for Systematic Review and Meta-Analyses statement (Page et al., 2021).

Eligibility Criteria

To determine keywords for a review, we used the participants, intervention, comparison, outcome, and study design (PICOS) search tool (see **Table 1**). Studies with a healthy human adult population, aged between 18 and 45 years old, and without gender restrictions were included. Given that an aerobic energy system predominates during maximum effort exercise after 75 s (Gastin, 2001), we included the studies using dynamic whole-body endurance performance with a duration of at least 75 s. Maximal incremental exercise tasks were also included in this review. The two main outcome parameters for inclusion were performance on the exercise task and PFC oxygenation. A baseline measure at the start of the exercise-task had to be made for cerebral oxygenation to be able to evaluate the evolution of oxygenation throughout the trials. Randomized controlled trials (RCTs), non-RCTs (nRCTs), or non-randomized non-controlled trials (nRnCTs), written in English, were considered to be eligible for inclusion. Studies were excluded when the study population was patients who were using medications. Additionally, animal studies, individual case studies, and interventions where participants performed with their eyes closed were also excluded.

TABLE 1 | "PICOS" categories (participants, interventions, comparisons, outcomes, study design) used to determine keywords.

PICOS component	Detail
Participants	Healthy humans (18–45 years)
Interventions	Whole-body endurance performance task (>75 s)
Comparisons	Baseline NIRS-measures before the start of and/or during the whole-body endurance performance task or the control condition (e.g., exercise modality)
Outcomes	Prefrontal cortex oxygenation (NIRS) during whole-body endurance task or performance
Study designs	RCTs, nRCT, nRnCTs

NIRS, Near infrared spectroscopy RCT randomized controlled trial; nRCT non-randomized controlled trials; nRnCTs non-randomized non-controlled trials.

Information Sources and Search Strategy

Three electronic databases, PubMed, Web of Science, and Cochrane Library (until August 20, 2021), were searched with no date restrictions. Medical subject heading (mesh) terms, if available in PubMed and Cochrane Library, were used for a qualitative literature search. The following keywords were applied individually or in combination: Near Infrared Spectroscopy, NIRS, Magnetic Resonance Imaging, MRI, Near Infrared Spectroscopy [MeSH], Magnetic Resonance Imaging [MeSH], Physical performance, Exercise performance, Endurance performance, Time trial, Time to exhaustion, physical endurance, Athletic performance, physical endurance [MeSH], Athletic performance [MeSH], Motor Activity [MeSH], Oxygenation, BOLD response, hemodynamic response, Cerebrovascular Circulation, Cerebrovascular Circulation [MeSH] prefrontal cortex OR frontal lobe OR frontal lobe [MeSH] (**Table 2**). The combination of keywords 1, 2, and 3 (see **Table 2**) was included in a search strategy. In addition, to ensure the literature saturation, a backward search and a forward search were performed by screening the reference lists of the included articles and by screening the citations of the included studies, respectively, to increase the likelihood of the inclusion of all relevant studies.

TABLE 2 | Search strategy: number of hits on keywords and combined keywords in PubMed, Web of Science, and Cochrane Library.

Keywords	PubMed	Web of science	Cochrane library
	No. of hits (20/08/2020)	No. of hits (20/08/2020)	No. of hits (20/08/2020)
(1) Near infrared spectroscopy OR NIRS OR magnetic resonance imaging OR MRI or near infrared spectroscopy [MeSH] OR magnetic resonance imaging [MeSH]	608,218	487,775	33,168
(2) Physical performance OR exercise performance OR endurance performance OR time trial OR time to exhaustion OR physical endurance OR athletic performance OR physical endurance [MeSH] OR athletic performance [MeSH] OR motor activity [MeSH]	336,117	137,120	31,398
(3) Oxygenation OR BOLD response OR hemodynamic response OR cerebrovascular circulation OR cerebrovascular circulation [MeSH]	124,655	77,973	51,012
(4) prefrontal cortex OR frontal lobe OR frontal lobe [MeSH]	107,239	118,480	7524
Combined key words			
(1) AND (2)	6566	549	1664
(1) AND (2) AND (3)	4650	389	352
(1) AND (2) AND (3) AND (4)*	921	202	335
(1) AND (2) AND (4)	1408	48	350

Combined keywords with a "" were included in the study.*

Study Selection and Data Collection Process

Articles from the three databases were collated in EndNote X9 where the duplicates were removed (**Table 3**). Afterward, all studies were imported into Rayyan (the web and mobile app for systematic reviewers; Ouzzani et al., 2016), where the two reviewers (JDW and JH), independently and blinded from each other, screened the title and abstracts for each study. The search resulted in 89 (7%) conflicting studies. After the conflicts were resolved, the full text of the remaining articles was screened. A general meeting with the research team was held to decide on inclusion. The full-text version of all the articles that met the inclusion criteria (**Table 3**) was retrieved for quality assessment and data extraction (see quality assessment). If, after this screening, a citation was considered potentially eligible for inclusion and relevant, the full-text article was retrieved. A flow diagram illustrating the selection of the included studies can be found in **Figure 1**.

Quality Assessment

Methodological quality was assessed using the quantitative assessment tool "QualSyst" (Kmet and Lee, 2004). The QualSyst tool is a checklist containing 14 items, which are plotted on a 3-point scale (yes = 2, partial = 1, and no = 0). Items that were not applicable to a particular study design were marked as "n/a" and were excluded from the calculation of a summary score (Kmet and Lee, 2004). A quality score was calculated for each paper by summing the total score obtained across relevant items and dividing them by the total possible score (Kmet and Lee, 2004). The two reviewers (JDW and JH) independently performed quality assessments, and disagreements were solved through a consensus. A score of $\geq$ 75%, 55–75%, and $\leq$ 55% indicated strong quality, moderate quality, and weak quality, respectively.

Classification of Intensity

Based on the ACSM position stand, the classification of exercise intensity: relative and absolute exercise intensity for cardiorespiratory endurance and resistance exercise, whole-body endurance performance tasks were classified into very light, light, moderate, vigorous, and near-maximal intensities (Garber et al., 2011). The classification, where necessary, was based on energy cost calculations using the ACSM energy equation for cycling (Swain, 2000).

TABLE 3 | Inclusion and exclusion criteria.

Inclusion	Exclusion
fNIRS	Individual case studies
Healthy participants (18–45 years)	Animal studies
Neutral ambient conditions	Eyes closed
Cycling/running/rowing	Psychiatric disorders/patients
Whole-body endurance performance task	Medication

fNIRS, functional Near-Infrared Spectroscopy.

RESULTS

Study Selection

After the removal of duplicates, the search strategy resulted in 1,260 articles. After screening the titles and abstracts of the remaining 54 (**Figure 1**), 25 met the inclusion criteria. After screening the reference lists of the full-text articles additional three articles were included, resulting in a total of 28 articles, of which 53% were scored as strong, 36% as moderate, and only 11% as weak on the quality assessment (as shown in **Table 4**).

Characteristics of Near-IR Spectroscopy

Positioning of the optodes and receivers with the associated inter-optode distances (IODs) varies and is described in **Tables 5A,B**. Nineteen studies used the international EEG 10-20 system with optode placements over the prefrontal lobe at Fp1,Fp2, Fp3, and/or Fp4 position (Rupp and Perrey, 2008; Timinkul et al., 2008; Billaut et al., 2010; Keramidas et al., 2011; Rupp et al., 2013; Giles et al., 2014; Oussaidene et al., 2015;

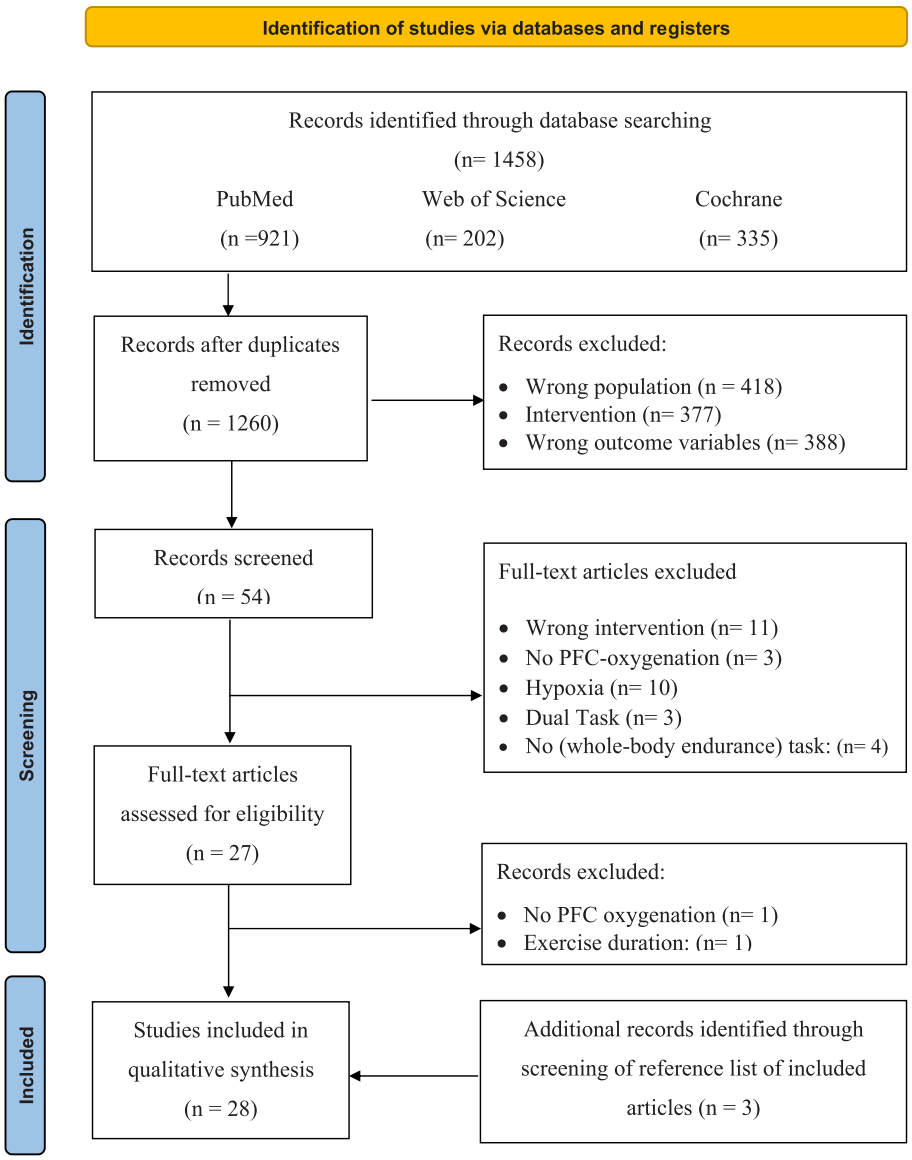

FIGURE 1 | Selection process for research articles (n = 28) included in this systematic review. Adapted version of the recommendations in the PRISMA 2020 statement (Liberati et al., 2009). *nRCT,* non-randomized controlled trial; *nRnCT,* non-randomized non-controlled trial; *RCT,* randomized controlled trial.

Santos-Concejero et al., 2015, 2017; Pires et al., 2016; Tempest and Parfitt, 2016; Tsubaki et al., 2016, 2018, 2020; Takehara et al., 2017; Tempest et al., 2017; Asahara and Matsukawa, 2018; Ohyanagi et al., 2018; Stevens et al., 2018) pecifying this location as ± 3 cm from the midline, just above the supra-orbital ridge (Bhambhani et al., 2007; Miyazawa et al., 2013). Jung et al. (2015) used Broadman area 10, Montreal Neurophysiological Institute (MNI) coordinates [(x/y/z) −40, 50, 0], two studies performed a three-dimensional T1-weighted MRI scan, marking the optode location for the left and right PFC (Suzuki et al., 2004; Fumoto et al., 2010), and finally, two studies placed the device on the participants' forehead without specifying the exact location of the optode placement (Shibuya et al., 2004; Kounalakis and Geladas, 2012). The IODs varied between 25, 30, 38, 40, 45, and 50 mm (mean ± SD: 38 ± 7 mm).

Prefrontal Cortex Oxygenation During Maximal Incremental Exercise

Eleven of the included studies evaluated the effects of exercise intensity on cerebral cortex oxygenation using an incremental cycling protocol until exhaustion (Bhambhani et al., 2007; Rupp and Perrey, 2008; Timinkul et al., 2008; Tempest et al., 2014, 2017; Jung et al., 2015; Oussaidene et al., 2015; Tempest and Parfitt, 2016; Tsubaki et al., 2016; Stevens et al., 2018; Kojima et al., 2021). Incremental exercise protocols were characterized by systematic increases in intensity over time. The protocols

TABLE 4 | Quality assessment "QualSyst" (Kmet and Lee, 2004).

Study	A	B	C	D	E	F	G	H	I	J	K	L	M	N	Rating*
Shibuya et al. (2004)	2	2	1	2	NA	NA	NA	2	1	2	2	NA	2	2	Strong: 90
Suzuki et al. (2004)	1	1	1	2	NA	NA	NA	1	1	2	1	NA	2	1	Moderate: 65
Billaut et al. (2010)	2	2	2	2	NA	NA	NA	1	1	2	2	NA	2	2	Strong: 90
Fumoto et al. (2010)	1	1	2	2	NA	NA	NA	1	1	1	2	NA	1	2	Moderate: 70
Keramidas et al. (2011)	2	1	1	2	0	0	NA	1	1	2	2	1	1	2	Moderate: 62
Miyazawa et al. (2013)	2	1	1	2	NA	NA	NA	1	1	2	2	NA	1	2	Strong: 75
Rupp et al. (2013)	2	1	1	2	NA	NA	NA	2	1	2	2	NA	1	1	Strong: 75
Giles et al. (2014)	2	1	2	2	0	0	0	2	1	1	1	1	2	2	Moderate: 61
Santos-Concejero et al. (2015)	2	2	2	2	NA	NA	NA	2	1	2	1	NA	1	2	Strong: 85
Pires et al. (2016)	2	2	2	2	NA	NA	NA	2	1	2	2	NA	2	2	Strong: 95
Santos-Concejero et al. (2017)	2	1	2	2	NA	NA	NA	2	1	2	2	NA	2	2	Strong: 90
Ohyanagi et al. (2018)	2	0	0	0	0	NA	NA	1	1	1	2	1	1	2	Weak: 46
Radel et al. (2017)	2	2	2	2	0	1	2	2	2	2	0	1	2	2	Strong: 79
Tsubaki et al. (2018)	2	2	1	1	NA	NA	NA	1	1	2	1	NA	2	1	Moderate: 70
Kounalakis and Geladas (2012)	2	2	1	2	2	0	0	2	1	1	2	2	2	2	Strong: 75
Takehara et al. (2017)	2	0	1	2	0	0	0	1	1	1	0	1	2	2	Weak: 46
Ide et al. (1999)	1	0	1	2	NA	NA	NA	2	1	1	2	NA	2	1	Moderate: 65
Bhambhani et al. (2007)	2	2	1	2	NA	NA	NA	2	1	1	2	NA	2	2	Strong: 85
Rupp and Perrey (2008)	2	2	1	2	NA	NA	NA	2	1	2	1	NA	2	2	Strong: 85
Timinkul et al. (2008)	2	2	1	2	NA	NA	NA	2	1	2	2	NA	2	2	Strong: 90
Tempest et al. (2014)	2	2	2	2	NA	NA	NA	2	2	2	2	NA	2	2	Strong: 100
Jung et al. (2015)	2	2	1	0	NA	NA	NA	2	1	1	2	NA	1	1	Moderate: 65
Oussaidene et al. (2015)	2	2	2	2	NA	NA	NA	2	1	2	2	NA	2	2	Strong: 95
Tempest and Parfitt (2016)	2	2	2	2	NA	NA	NA	2	2	1	2	NA	2	2	Strong: 95
Tempest et al. (2017)	2	2	1	1	0	0	NA	2	1	1	2	1	2	2	Moderate: 65
Stevens et al. (2018)	1	1	1	1	2	0	1	2	1	2	2	2	2	2	Moderate: 71
Hiura et al. (2018)	2	0	1	1	NA	NA	NA	2	1	1	2	NA	2	2	Moderate: 70
Kojima et al. (2020)	2	1	1	1	NA	NA	NA	1	0	1	0	NA	0	1	Weak: 40
Kojima et al. (2021)	2	1	1	1	NA	NA	NA	1	1	1	1	NA	2	1	Moderate: 60

*A, Objective sufficiently described; B, evident study design?; C, Method of subject/comparison group selection or source of information/input variables described and appropriate?; D, Subject (and comparison group, if applicable) characteristics sufficiently described?; E, If interventional and random allocation was possible, was it described?; F, If interventional and blinding of investigators was possible, was it reported?; G, If interventional and blinding of subjects was possible, was it reported?; H, Outcome and (if applicable) exposure measure(s) well de ned and robust to measurement / misclassification bias? means of assessment reported?; I, Sample size appropriate?; J, Analytic methods described/justified and appropriate?; K, Some estimate of variance is reported for the main results?; L, Controlled for confounding?; M, Results reported in sufficient detail?; N, Results support conclusion?. *Quality scores: ≥ 75% strong, 55 ≥ 75% moderate, ≤ 55% weak.*

consisted of fixed increases of 20 W (Tempest et al., 2014, 2017; Jung et al., 2015; Tempest and Parfitt, 2016; Kojima et al., 2020, 2021), 25 W (Timinkul et al., 2008), and 30 W (Rupp and Perrey, 2008) per 1 min, 30 W per 2 min (Bhambhani et al., 2007; Stevens et al., 2018), and 1 W/kg per 3 min (Oussaidene et al., 2015) until exhaustion. All protocols started from very low intensities and ranged from no resistance up to 100 W for the trained athletes. Intensities throughout all the tests were classified as low, moderate, vigorous, and near-maximal to maximal (Garber et al., 2011). From this point, oxygenated (HbO_2), deoxygenated hemoglobin (HHb), and total hemoglobin (tHb) relate to the PFC unless stated otherwise.

Ten studies reported an increase in [HbO_2] during the first part of the incremental exercise (Bhambhani et al., 2007; Rupp and Perrey, 2008; Timinkul et al., 2008; Tempest et al., 2014, 2017; Jung et al., 2015; Oussaidene et al., 2015; Stevens et al., 2018; Kojima et al., 2021). Timinkul et al. (2008) described the three distinct phases of prefrontal oxygenation during incremental exercise: (1) the linear-oxygenation phase, where HbO_2 gradually increases and HHb slightly decreases from the start until the so-called cerebral blood volume threshold (42 ± 3.9% VO_{2max}), (2) the hyper-oxygenation phase, where HbO_2 rapidly increases until the respiratory compensation point (RCP), while HHb remains stable, and (3)the desaturation phase, where HbO_2 continuously decreases and HHb increases until exhaustion. However, Timinkul et al. (2008) did not express their results as a percentage of VO_{2max}. Similarly, Rupp and Perrey (2008) described an increase in [HbO_2] from a warm-up to the second ventilatory threshold (VT2, 87.0 ± 2.0% VO_{2max}) and the cerebral oxygenation threshold (ThCox, 86.0 ± 4.0% VO_{2max} for untrained and 85.0 ± 9.0% VO_{2max} for trained). Similar results were observed for Oussaidene et al. (2015) who reported a decline in HbO_2 between VT2 or ThCox and exhaustion. These findings were replicated by Kojima et al. (2020, 2021) who reported an increase in [HbO_2] from the start of exercise until RCP and a subsequent decrease from RCP until exhaustion. Additionally,

TABLE 5A | Overview of the results within "non-incremental endurance exercise".

Study	Sample characteristics (Mean ± SD)	NIRS—devise, Inter Optode Distance (IOD), position, wave specifications	Physical task	Type of task and exercise intensity	Outcome
Shibuya et al. (2004)	5 M A: 24.6 ± 0.4 year Length: 175.3 ± 1.2 cm Mass: 62.9 ± 1.1 kg VO_{2peak}: 48.4 ± 1.3 ml/kg/min Training status: /	IOD: 50 mm Position: forehead 780, 810, and 830 nm	(Cycling) 120% VO_{2peak} exhaustive exercise test	TTE – 120% VO2peak – *Supramaximal*	• SaO_2 = throughout test • VO_2, V_E, and HR ↑ gradually over time • [HbO_2] ↑ first 30 s • [tHb] and [HbO_2] = throughout test • End of exercise: [tHb] and [HbO_2] ↓ from pre-exercise level
Suzuki et al. (2004)	7 M, 2 F A: 28.1 ± 7.4 years Training status: /	OMM-2001, Shimadzu, Kyoto, Japan IOD: / Position: anatomical 3-D T1 weighted MRI scan was performed, marking the optode location 780, 805, and 830 nm Continuous wave	(Running) 3 treadmill locomotor tasks of 90 s. each following 30 s rest: 1. Walking at 3 km/h 2. Walking at 5 km/h 3. Running at 9 km/h Randomized order	Adapting speed – 3 km/h 5 km/h 9 km/h – *Light to moderate*	• HbO_2 and tHb ↑ bilaterally before starting the locomotor tasks especially at 9 km/h and peaked before the treadmill speed got steady. • After reaching constant speed: HbO_2 and tHb ↓ and tended to return to the baseline or below baseline during performing the locomotor tasks. • After stopping locomotion: temporal drops in HbO_2 before returning to the baseline • ↑ in HbO_2 levels greatest at 9 km/h but are = between 3 and 5 km/h. • PFC-activation = greater during running at 9 km/h vs. walking at 3 and 5 km/h
Billaut et al. (2010)	11 M A: 24.8 ± 4.2 Length: 174.2 ± 5.3 cm Mass: 66.8 ± 3.1 kg Fat%: 10.3 ± 3.5% Training status: PL5	Oxymon MKIII; Artinis Medical Systems b.v., Zetten, the Netherlands IOD: 45 mm Position: Fp1 and F3, according to the modified international EEG 10–20 system 763 and 855 nm Continuous wave	(Running) T1: Familiarization trial T2: 5 km TT • 6 min self-paced warm up • 5 km TT (4°incline)	TT – Self-paced – *Near to maximal*	• HR: ↑ rapidly but remained nearly constant between 1.5 and 4 km and peaked in the last 0.5 km • SaO2: fell between 3 and 5 km • RPE ↑ throughout the trial • RBV and Cox ↑ until 2.5 km (↑△[HbO_2], ↑△[HHb], and ↑△[tHb]), o = between 2.5 and 4.5 km, f o Deoxygenation in the last 0.5 km, while RBV remained stable
Fumoto et al. (2010)	9 M, 1 F A: 32 ± 2.2 Length: 174.2 ± 5.3 cm Mass :66.8 ± 3.1 kg Fat%: 10.3 ± 3.5 Training status: PL2	OMM3000; Shimadzu Co., Kyoto, Japan IOD: 30 mm Position: anatomical 3-D T1weighted MRI scan was performed, marking the optode location 780, 805, and 830 nm	(Cycling) 15 min at 60 RPM and pre-determined intensity of 12–13 RPE	Constant load with fixed duration – 12-13 RPE – *Moderate*	• Gradual ↑ in HbO_2 and tHb, reached a steady state at the end of PE (mainly in ventral PFC regions) • Gradual ↓ in HbO_2 and tHb were observed after stopping • Small ↓ in HHb or no change in both the ventral and dorsal PFC
Miyazawa et al. (2013)	10 M A: 20.0 ± 1 year Length: 170 ± 5 cm Mass: 64 ± 9 kg Training status: /	NIRO200, Hamamatsu Photonics, Hamamatsu, Japan IOD : 40 mm Position: left forehead, ± 3 cm from midline, just above supra-orbital ridge 780 nm	(Cycling) • 4 min incremental warm-up until 60% of HR_{max} • 11-min constant load cycling o facial cooling from minute 5–8	Constant load with fixed duration – 60% HR_{max} – *Light*	• SBFhead and HbO_2 ↑ during exercise and temporally ↓ with facial cooling • HbO_2 and tHb changes correlated with the relative changes in SBFhead • HHb and TOI did not change significantly with either exercise or facial cooling • Forehead TOI was not affected by exercise or facial cooling

(Continued)

TABLE 5A | (Continued)

Study	Sample characteristics (Mean ± SD)	NIRS—devise, Inter Optode Distance (IOD), position, wave specifications	Physical task	Type of task and exercise intensity	Outcome
Rupp et al. (2013)	10 M A: 37 ± 7 year Length: 180 ± 5 cm Mass: 73 ± 7 kg Training status: PL2	Oxymon III, Artinis, the Netherlands IOD: 35 mm Position Fp1 and F3, according to the modified international EEG 10–20 system 780 and 850 nm Continuous wave	(Cycling) 4-h cycling exercise (45% max aerobic power output) 3 consecutive 80-min-bouts (B1, B2, B3), separated by 25-min of neuromuscular function testing	Constant load with fixed duration – 45% of maximal aerobic power output – *Vigorous*	• MVC ↓ after B1, B2 and B3 (-11, -19, and -25%) • RPE ↑ throughout the 3 bouts • Δ[HbO_2] and Δ[tHb] ↑ during B1 reaching a plateau after ∼40 min • [HHb] progressively ↑ during B1 from 20 to 80 min and showed a main effect of bout throughout the protocol • Δ[HHb] ↑ during B2 and B3 sign. reduced compared to B1
Giles et al. (2014)	14 M; 10 F A: 20.21 ± 2.38 year BMI: 22.51 ± 2.72 Training status: PL2	fNIR Imager 1100, fNIR Devices LLC, Potomac, Maryland, United States IOD: 25 mm Position: forehead; bottom of the probe at the Fpz, (international 10–20 system) 730 and 850 nm Continuous wave	(Cycling) 30-min recumbent cycling followed by a 5-min cool down T1: low load (52%HR_{max}) T2: moderate load (68%HR_{max}) T3: high load (84%HR_{max}) Counterbalanced	Constant load with fixed duration – 52%HR_{max} 68%HR_{max} 84%HR_{max} – *Light* *Moderate* *vigorous*	• HbO_2, HHb and tHb↑ in function of exercise load and time • No change in HbO_2 during the first minute of pedaling • HbO_2 = until minute 15, then HbO_2 ↑ (high and moderate) to low and at minute 18, HbO_2 (high) to moderate • HHb = until minute 23, then HHb ↑ (high > moderate > low) • tHb = until minute 16, then tHb ↑ (high > moderate > low)
Santos-Concejero et al. (2015)	10 M A: 23.7 ± 4.2 year Length: 170.5 ± 6.3 cm Mass: 54.8 ± 6.3 kg BMI: 18.8 ± 1.3 Fat%: 8.7 ± 0.5% Training status: PL5	NIRO-200X, Hamamatsu, Japan IOD: 30 mm Position: left prefrontal lobe between Fp1 and F3, according to the modified international EEG 10–20 system. 735, 810, and 850 nm Continuous wave	(Running) T1: 5-km time trial T2: MIT T3: constant speed running bouts (running economy determination)	TT – Self-selected speed – *Near to maximal*	5 km TT: • Cerebral oxygenation ↑ over the first half of the trial (↑ Δ[HbO_2] and Δ[HHb]) • Δ[HbO_2] = in the second half of the trial and Δ[HHb] ↑ until the end • TOI ↓ over the first 1.5 km and then remained stable until completion • tHb: stable for the first half of the test and increased progressively from 3 km until completion • SpO_2 ↓ at the beginning of the 5-km TT and then remained stable until completion
Pires et al. (2016)	10 M A: 32.9 ± 7.3 year Length: 175.7 ± 5.9 cm Mass: 75.9 ± 9.0 kg Fat%: 10.5 ± 5.2% Training status: PL3	CW6- TechEn, Milford, MA, United States IOD: 45 mm Position: prefrontal lobe at the Fp1 position (international 10–20 system) 690 and 830 nm Continuous wave	(Cycling) T1: Familiarization T2: MIT T3: Self-paced 4 km cycling TT	TT – Self-selected power – *Near to maximal*	• Δ[HbO_2], Δ[HHb], and Δ[tHb] ↑ up to ∼70% of both MIT and TT4 km, and ↓ afterward • Δ[HbO_2] was lower in TT4 km than MIT at 20, 30, 40, 50, and 60%, but higher at 100% of the exercise duration • Greater RPE slope in MIT than in TT4 km

(Continued)

TABLE 5A | (Continued)

Study	Sample characteristics (Mean ± SD)	NIRS—devise, Inter Optode Distance (IOD), position, wave specifications	Physical task	Type of task and exercise intensity	Outcome
Santos-Concejero et al. (2017)	15 M A: 23.7 ± 4.2 year Length: 170.5 ± 6.3 cm Mass: 54.8 ± 6.3 kg Training status: PL5	NIRO-200X, Hamamatsu, Japan IOD: 30 mm Position: left prefrontal lobe between Fp1 and F3, according to the modified international EEG 10–20 system. 735, 810, and 850 nm Continuous wave	(Running) T1: 5-km time trial, T2: MIT T3: Fatigue training test (FTT)	T1: TT Self-selected speed – T2: MIT – T3: FTT 5% faster than 5 km TT pace – *Near to maximal*	FTT: • SpO_2 ↓ in the first two running bouts, but ↑ in the third bout and remained stable Δ[HbO_2] • Elevated compared to baseline throughout the fatiguing session • ↑ during each bout, and ↓ during the 30 s recovery period until the end • at the end of each repetition ↓ over the course of the trial Δ[HHb] • ↓ = negatively correlated with speed at which the test was completed • < ↓ Cox between the 1st and 4th and between the 1st and last repetitions in the late fatigue group TOI • ↓ throughout the session
Ohyanagi et al. (2018)	6 M, 6 F A: 20.0 year Training status: /	OMM3000; Shimadzu Co., Kyoto, Japan IOD: 30 mm Position: Fpz position of the international 10–20 system 780, 805, and 830 nm Continuous wave	(Cycling) T1: MIT T2: Experimental trial (randomly assigned to upright or supine position): • 4-min pre exercise rest • 4-min warm-up • 20-min at 50% VO_2max • 15-min PER	Constant load with fixed duration – 50% VO_2max – *Moderate*	HbO_2: • ↑ from 3 to 6 min during the 20-min main exercise • Steady from min 6 until the end of exercise SBF: • ↑ gradually throughout the exercise • MAP ↑ during the first 3 min of exercise and then ↓ slowly throughout the exercise phase
Radel et al. (2017)	15 M, 7 F A: 21.3 ± 2.1 year Length: 174.7 ± 6.4 cm Mass: 67.0 ± 10.6 kg Peak HR: 186.5 ± 10.9 PAP: 286.1 ± 79.3 Training status: /	Oxymon Mk II, Artinis Medical Systems, Zetten, the Netherlands IOD: 40 mm Position: AF2h and F6h sites of the extended 10–5EEG system 764 and 858 nm Continuous wave	(Cycling) T1: MIT T2 and T3: 60% PAP for 10-min Participants expected one trial to last 60-min	Constant load with fixed duration – 60% PAP – *Near to maximal*	• lower general [HbO_2] in the first period vs. second- and third periods of time • rdlPFC: [HbO_2] less elevated in the 60-min than in the 10-min condition • rmPFC: [HbO_2] higher in the 60-min than in the 10-min condition • Attention was less focused on the exercise trial in the 60-min than in the 10-min condition • RPE =
Tsubaki et al. (2018)	8 M, 4 F A: 21.3 ± 0.7 year Training status: /	OMM3000; Shimadzu Co., Kyoto, Japan IOD: 30 mm Position: Cz position of the International 10–20 System 780, 805, and 830 nm Continuous wave	(Cycling) T1: MIT T2 : Experimental trial • 3-min rest • 20-min at to 50% VO_{2peak} • 15-min PER	Constant load with fixed duration – 50% VO_{2peak} – *Moderate*	• HbO_2 ↑ between start and the last 5 min of the exercise (R-PFC) • HbO_2 did not return to pre-exercise levels during the 15-min PER • HbO_2 higher during the last 5 min of PER than during the pre-exercise rest period • HbO_2 = between the last 5 min of exercise and 15-min PER. • SBF and MAP ↑ during exercise and ↓ during PER • SBF and MAP = between pre-exercise rest phase and the last 5 min of the 15-min PER.

(Continued)

TABLE 5A | (Continued)

Study	Sample characteristics (Mean ± SD)	NIRS—devise, Inter Optode Distance (IOD), position, wave specifications	Physical task	Type of task and exercise intensity	Outcome
Hiura et al. (2018)	PET-study 12 M A: 21.1 ± 2 year Training status: / NIRS-study 12 M A: 22.5 ± 2.9 year Training status: /	NIRS : Spectratech, OEG-16, Yokohama, Japan IOD:30 mm Position: Fpz position of the international 10–20 system 770 and 840 nm PET: Discovery PET/ CT 710 scanner (GE Healthcare, Milwaukee, WI	(Cycling) 15-min at 30% HR reserve	Constant load with fixed duration – 30% HR reserve – *Light*	• Δ HbO_2 ↑at Ex2 but did not change at Ex1 • ΔHHb = during exercise • rCBF ↑ at Ex1 but = at Ex2. • PET CO_2 ↑ at Ex1 and = at Ex2. • MBP ↑ during exercise but ↓ at Ex2 compared with Ex1
Kounalakis and Geladas (2012)	12 M A: 23.4 ± 3.8 year Length: 179 ± 7 cm, Mass: 78.3 ± 6.7 kg, Fat%: 10.4 ± 3.6% Training status: /	NIRS, In Spectra325, Hutchinson Technology Inc., Hutchinson, Minn IOD: / Position: middle of the forehead, just below the hairline 720 and 760 nm	(Cycling) 2 preliminary MIT at 40- and 80 RPM 2 experimental trials: T1: 40 RPM T2: 80 RPM • 8 min warm-up (50% VO_{2peak}) • Three 5 s $MVC_{isometric}$ (knee) • 25 min rest on the cycle ergometer • 90 min at 58–60% VO_{2peak}	Constant load with fixed duration – 58–60% VO_{2peak} – *Moderate*	• O_2-cost during 5 min of unloaded pedaling was significantly higher at 80- than at 40 RPM • First 8 min: VO_2 sign. ↑ (~250 ml) at 80 than at 40 RPM. • First 8 min: HR = <u>Prefrontal oxygenation:</u> • Δ[HbO_2]: ↑ from start to end of exercise • Δ[tHb] & Δ[HbO_2]: lower at 80 vs. 40 RPM at the end of exercise • Δ[HHb]: lower at the end of exercise at 80 RPM • Δ[HHb] = throughout exercise at 40 RPM • SpO_2: ↓ at 80 than at 40 RPM during exercise
Takehara et al. (2017)	5 M, 8 F A: 21.2 ± 0.6 year Length: 174.7 ± 6.4 cm Mass: 67.0 ± 10.6 kg Peak HR: 186.5 ± 10.9 PAP: 286.1 ± 79.3 Training status: /	OMM3000, Shimadzu Co., Kyoto, Japan IOD: 30 mm Position: Cz position of the International 10–20 System	2 trials: Trial 1: 30% VO_{2peak} Trial 2: 50% VO_{2peak} • 180 s rest period, 10 min continuous cycling exercise at 55 RPM	Constant load with fixed duration – 30% VO_{2peak} 50% VO_{2peak} – *Light* *Moderate*	<u>30% VO_{2peak} condition</u> • PFC [HbO_2] ↓ from 30-270s and ↑ from 300 to 600 s • SBF ↑ from 480 to 510 s <u>50% VO_{2peak} condition</u> • PFC [HbO_2] ↓ from 30 to 120 s and ↑ from 150 to 600 s • SBF ↑ from 330 to 600s MAP ↑ in both conditions from 60 to 600 s
Ide et al. (1999)	7 M, 7 F A: 20.6 ± 1.4 year Length: 171.0 ± 7.5 cm Mass: 69.3 ± 7.3 kg BMI: 23.4 ± 2.0 Training status: /	NIRO 500, Hamamatsu Photonics, Hamamatsu, Japan. IOD: 45 mm apart, Position: forehead 775, 825, and 850 nm	T1: MIT T2: experimental trial • 10 min rest • 10 min cycling at 30% VO_2max • 10 min cycling at 60% VO_2max • 10 min PER	Constant load with fixed duration – 30% VO_2max 60% VO_2max – *Light* *Moderate*	• Δ[HbO_2]: ↑ in proportion to work rate and reached a maximal level during the first few minutes of exercise • HHb and tHb: ↑ • MCA $V_{mean:}$ ↑ • MAP and HR: ↑ with exercise intensity

M, man; F, female; A, age; Y, Years; BMI, Body Mass Index; Fat%, body fat; KG, kilogram; Cm, Centimeter; mm, Millimeter; VO2peak, VO_{2max} Maximal Oxygen Uptake; PL, Performance Level; NIRS, Near Infrared Spectroscopy; IOD, Inter Optode Distance; TTE, Time To Exhaustion; SaO_2, Arterial Oxygen Saturation; VO_2, Oxygen Uptake; V_E, Ventilation; HR, Heart Rate; tHb, Total Hemoglobin; HbO_2, Oxygenated hemoglobin; HHb, Deoxygenated Hemoglobin; MRI, Magnetic Resonance Imaging; Sec, Second; Min, Minute; Km, Kilometer; H, Hour; BP, Blood Pressure; PFC, Prefrontal Cortex; PMC, Premotor Cortex; m-SMC, Medial Sensori-Motor Cortex; TT, Time-Trial; EEG, Electroencephalography; RPE, Rating of Perceived Exertion; $CPT_{(RM)}$, Constant-Power Test (Respiratory Maneuver); RPM, Rotations per Minute; SBF, Skin Blood Flow; TOI, Tissue Oxygenation Index; MVC, Maximal Voluntary Contraction; MIT, Maximal Incremental Exercise Test; Cox, Cerebral Oxygenation; FTT, Fatigue Training Test; PER, Post-Exercise Rest; MAP, Mean Arterial Pressure; PAP, Peak Aerobic Power; T, Trial.

TABLE 5B | Overview of the results within "maximal incremental exercise (MIT)".

Study	Sample characteristics (Mean ± SD)	NIRS—devise, Inter Optode Distance (IOD), position, wave specifications	Physical task	Type of task and exercise intensity	Outcome
Bhambhani et al. (2007)	7 M A: 26.7 ± 8.6 year Length: 178 ± 0.6 cm Mass :77.5 ± 9.3 kg BMI: 24.1 ± 2.5 Training status: PL1	MicroRunman, NIM Inc., Philadelphia, PA IOD: 40 mm Position: left pre-frontal lobe, ± 3 cm from midline, just above the supra-orbital ridge	(Cycling) • 2-min rest + baseline measurement • MIT: 30 W/2-min until exhaustion	MIT – ↑ 30 W/2-min	• PET_{co2} ↑ systematically until RCT-GEX • After RCT-GEX: PET_{co2} ↓ continuously until exhaustion • CBV and Cox ↑ systematically during MIT, slightly beyond the RCT-GEX-intensity, then continuous ↓until exhaustion • ↑in Cbv > ↑ in Cox • Sign. difference RCT-GEX, 76.9% and RCT-NIRS, 81.0%, as $\%VO_{2max}$
Rupp and Perrey (2008)	13 M A: 24.9 ± 1.5 year Length: 179.3 ± 1.8 cm Mass: 71.1 ± 1.2 kg Training status: PL5	NIRO-300, Hamamatsu Photonics, Japan IOD: 50 mm Position: Fp1 and F3, according to the modified international EEG 10–20 system 775, 810, 850, and 905 nm	(Cycling) • 2-min rest + baseline measurement • 3-min warm-up at 60 W MIT: 30 W/min until exhaustion Pre- and post-MIT: 2 MVICs (knee extensor)	MIT – 60 + 30 W/min	PFC-oxygenation • Δ[tHb] ↑ until VT2 and then stabilized • Δ[HHb] ↑ with the workload after warm-up until exhaustion and finally ↓ toward resting values during recovery • Δ[HbO2] ↑ from warm-up to VT2, then dropped until exhaustion and finally ↑ over resting values during recovery • Exhaustion and finally overshot the resting values during recovery
Timinkul et al. (2008)	10 M A: 21.4 ± 0.6 year Length: 175 ± 1.6 cm Mass: 68 ± 3.6 kg Training status: PL1	NIRO-300, Hamamatsu Photonics, Japan IOD: 50 mm Position: Fp1 and F3, according to the modified international EEG 10–20 system 775, 810, 850, and 905 nm Continuous wave	(Cycling) • 2-min rest + baseline measurement • MIT: 0 + 25 W/3 min until 150 W, 150 + 25 W/min until exhaustion	MIT - 150 + 25 W/min	• HR and VO2 ↑ progressively • Correlation between [Bla] and HHb and HR and HbO2 • TOI response showed a small ↑ (2–7%) or no change (one subject) with ↑ workload. However, before all-out, it began to ↓ gradually • PETCO2 ↑ gradually with ↑ workload and reached its peak, then ↓ gradually until all-out 3 distinct phases 1. Linear oxygenation phase (until blood volume threshold) • HbO_2: gradual ↑ in VO_2 from start till 15 min (100 W). • HHb: small↓ 2. Hyper-oxygenation phase: • HbO_2: rapid cerebral oxygen intake after 15-min (100 W) • HHb: ± = 3. Desaturation phase: • HbO_2: oxygenation continuously ↓from respiratory compensation threshold until exhaustion HHb: ↑
Tempest et al. (2014)	13 M, 12 F A: 25.6 ± 3.4 year Length: 174.8 ± 6.8 cm Mass: 71.8 ± 8.3 kg BMI: 23.5 ± 2.2 VO_{2peak}: 41.8 ± 5.2 $ml/kg^{-1}*min^{-1}$ Training status: PL1	Oxymon Mk II, Artinis Medical Systems, Zetten, the Netherlands IOD: 40 mm Position: AF2 h and F6 h sites of the extended 10–5EEG system Continuous wave	(Cycling) • Recumbent cycle ergometer MIT: 20 W/min until exhaustion	MIT – 20 W/min	• ΔHbO_2 ↑ from below VT to VT and VT to RCP, but remained stable from RCP to End • Δ HHb remained stable from below VT to VT, then ↑ from VT to RCP and RCP to End • Δ tHb increased from below VT, to VT, RCP, and End

(Continued)

TABLE 5B | (Continued)

Study	Sample characteristics (Mean ± SD)	NIRS—devise, Inter Optode Distance (IOD), position, wave specifications	Physical task	Type of task and exercise intensity	Outcome
Jung et al. (2015)	9 M A: 23–24 year Length: 182 ± 5 cm Mass: 77.6 ± 4.6 kg Fat%: 11.0 ± 2.8% Training status: PL3	Oxymon, Artinis, Zetten, The Netherlands IOD: 25 mm Position: left PFC (Brodmann area 10, MNI coordinates (x/y/z) -40, 50, 0) 858 and 764 nm Continuous wave	(Cycling) • MIT: 1 W/Kg + 1 W/Kg*3-min^{-1} until exhaustion 1 stage = + 1 W/Kg	MIT – 1 W/Kg + 1 W/Kg*3-min^{-1}	HbO_2 • Continuously ↑ from stage 1 to stage 2 and from stage 2 to stage 3 • Leveled between stage 3 and 4 HHb: • No changes
Oussaidene et al. (2015)	Endurance athletes (TR) 13 M A: 26 ± 5 year Length: 178.5 ± 5.8 cm Mass: 70 ± 6 kg Training status: PL3 Untrained (UNT) 11 M A: 24 ± 6 year Length: 179.7 ± 4.9 cm Mass: 77.2 ± 6.1 kg Training status: PL1	Oxymon, Artinis, Zetten, The Netherlands IOD: 50 mm Position: Fp1 and F3, according to the modified international EEG 10–20 system 780 and 857 nm Continuous wave	(Cycling) • 5 min resting period • 3-min warm-up 60 W (UNT), 100 W (TR) • MIT: warm-up workload ↑ with 1 W/3-s until exhaustion • 8-min rest (2 active, 8 passive) • TTE: o 1-min (50 W_{max}) o 105% W_{max} until exhaustion	MIT – 60 W or 100 + 1W/3-s TTE – 105%W_{max}	HbO_2: • ΔHbO2 ↑ from rest to ThCox and ↓ between ThCox and Wmax HHb: • ΔHHb ↑ between rest and Wmax in TR and UNT, but only in TR between rest and ThCox tHb: • ΔtHb ↑ from rest to W_{ThCOx} and stopped increasing between Th_{COx} and W_{max}, in the two groups Only ΔHbO_2 at Th_{Cox} was higher in TR than in UNT without a difference in W_{max} between groups
Tempest and Parfitt (2016)	High tolerance (HT) 7 M, 7 F A: 20.6 ± 1.4 year Length: 171.0 ± 7.5 cm Mass: 69.3 ± 7.3 kg BMI: 23.4 ± 2.0 Training status: PL2 Low tolerance (LT) 7 M, 7 F A: 21.5 ± 3.4 year Length: 173.2 ± 9.1 cm Mass: 68.6 ± 12.8 kg BMI: 22.4 ± 2.7 Training status: PL1	NIRO 200 Hamamatsu Photonics, Hamamatsu, Japan IOD: 40 mm Position: between Fp1 and F3 (left side) and Fp2 and F4 (right side) of the International 10–20 system	(Cycling) • MIT: 20 W/ min until exhaustion 70 RPM	MIT – ↑ 20 W/min	• Overall TTE (in seconds) = between HT- and LT-group HbO_2 • ΔHbO_2 remained stable from below VT to VT, then ↑ from VT to RCP and from RCP to end in both groups. HHb • ΔHHb remained stable from below VT to VT, that increased from VT to RCP and from RCP to end in both groups tHb • ΔtHb remained stable from below VT to VT, ↑ from VT to RCP and from RCP to end

(Continued)

TABLE 5B | (Continued)

Study	Sample characteristics (Mean ± SD)	NIRS—devise, Inter Optode Distance (IOD), position, wave specifications	Physical task	Type of task and exercise intensity	Outcome
Tempest et al. (2017)	6 M, 6 F A: 26.2 ± 3.0 year Length: 173.7 ± 7.6 cm Mass: 72.7 ± 9.1 kg Training status: PL1	Oxymon Mk II, Artinis Medical Systems, Zetten, the Netherlands IOD: 38 mm Position: 10/20 international system for electrode placement (the most inferior probes in line with Fpz)	(Cycling) • MIT: 20 W/min until exhaustion. Upright, recumbent and semi-recumbent position.	MIT – 20 W/min	HbO_2 • $\Delta HbO_2\uparrow$ from VT to RCP, but remained stable until maximal intensity, and was higher in the left than the right hemisphere. HHb • ΔHHb during upright was similar to recumbent but higher than semi-recumbent cycling • ΔHHb ↑ from VT to RCP and maximal intensities tHb • ΔtHb during upright was similar to semi-recumbent, but higher than recumbent cycling • ΔtHb ↑ from VT, to RCP and maximal intensities
Stevens et al. (2018)	15 M A: 27.8 ± 3.21 year Length: 173.7 ± 7.6 cm BMI: 24.96 ± 3.21 VO_2max: 41.80 ± 7.69 ml/kg*min^{-1} Training status: PL1	OxiplexTS, ISS, Champaign, Illinois, Unite d States IOD: 20, 25, 30, and 35 mm Position: Fp1 and F2, according to the international EEG 10–20 system 690 and 830 nm	(Cycling) • 2-min pre-exercise rest • 2-min resistance-free cycling at a self-selected cadence 30 W increments every 2 min until exhaustion	MIT – 0 + 30 W/2-min	• HbO_2 and tHb: little change up to 15% ↑VO_{2max}, quadratic increase up to 75% and a small increase above the RCT • HHb: linear trend against exercise intensity COx was unchanged with intensity
Kojima et al. (2020)	4 M, 8 F A: 21.6 ± 0.2 year Length: 162.6 ± 2 cm Mass: 57.3 ± 2.9 kg Training status: /	OMM3000, Shimadzu Co., Kyoto, Japan IOD: 30 mm Position: Cz position of the International 10–20 System	(Cycling) • 4-min pre-exercise rest • 4-min warm-up 20 W increments/min until exhaustion	MIT – 0 + 20 W/min	• HbO_2 ↑ until RCP and ↓ until exhaustion • HHb ↑ VT until exhaustion but not from rest to VT • tHb ↑ from start to RCP and further to exhaustion • SBF ↑ at VT, RCP and exhaustion compared to rest
Kojima et al. (2021)	24 M A: 20.7 ± 0 year Length: 172.6 ± 5.9 cm Mass: 64.8 ± 9.9 kg Training status: /	LABNIRS, Shimadzu Co., Kyoto, Japan IOD: 30 mm Position: Cz position of the International 10–20 System	(Cycling) • 4-min pre-exercise rest • 4-min warm-up 20 W increments/min until exhaustion	MIT – 0 + 20 W/min	• HbO_2 ↑ until RCP and ↓ until exhaustion • RCP correlated with the HbO_2 decreasing point ↑↑ΔHHb, ΔTHb, ΔCBV, and ΔSBF ↑ with load until exhaustion • $\Delta P_{ET}CO_2$ first ↑ with incremental load and then ↓ from 60 to 100% • $P_{ET}CO_2$ correlated with ΔHHb but not with HbO_2 and ΔCBV

M, man; F, female; A, age; Y, Years BMI, Body Mass Index; Fat%, body fat; KG, kilogram; Cm, Centimeter; mm, Millimeter; VO_2peak, VO_{2max} Maximal Oxygen Uptake; PL, Performance Level; NIRS, Near Infrared Spectroscopy; IOD, Inter Optode Distance; TTE, Time To Exhaustion; SaO_2, Arterial Oxygen Saturation; VO_2, Oxygen Uptake, V_E, Ventilation; HR, Heart Rate; tHb, Total Hemoglobin; HbO_2, Oxygenated hemoglobin; HHb, Deoxygenated Hemoglobin; MRI, Magnetic Resonance Imaging; Sec, Second; Min, Minute; Km, Kilometer; H, Hour; BP, Blood Pressure; PFC, Prefrontal Cortex; PMC, Premotor Cortex; m-SMC, Medial Sensori-Motor Cortex; TT, Time-Trial; EEG, Electroencephalography; RPE, Rating of Perceived Exertion; $CPT_{(RM)}$, Constant-Power Test (Respiratory Maneuver); RPM, Rotations per Minute; SBF, Skin Blood Flow; TOI, Tissue Oxygenation Index; MVC, Maximal Voluntary Contraction; MIT, Maximal Incremental Exercise Test; Cox, Cerebral Oxygenation; FTT, Fatigue Training Test; PER, Post-Exercise Rest; MAP, Mean Arterial Pressure; PAP, Peak Aerobic Power; T, Trial; $P_{ET}CO_2$, End-tidal pressure of CO_2.

Kojima et al. (2021) reported a relationship between the point of decline in [HbO_2] and RCP. Kojima et al. (2021) also reported that end-tidal CO_2 was decreased by respiratory compensation after RCP and that end-tidal CO_2 was associated with HHb.

Data in relation to HHb were inconsistent between studies. Timinkul et al. (2008) and Kojima et al. (2020) reported that HHb slightly decreased from the start of the trial until the cerebral blood volume threshold, remained stable until the RCP, and thereafter increased until exhaustion. Rupp and Perrey (2008) and Oussaidene et al. (2015), however, reported that HHb increased from a warm-up until exhaustion. Rupp and Perrey (2008) and Oussaidene et al. (2015) also reported that tHb concentrations increased between rest, VT2, and ThCox, after which it was stabilized until exhaustion. Three studies acknowledged the initial increase in [HbO_2] from the start of exercise, but instead of a subsequent decrease in [HbO_2], a steady state was reached (Tempest et al., 2014, 2017; Jung et al., 2015). Two studies reported an increase in [HbO_2] from the start of an exercise until RCP, after which [HbO_2] remained stable until exhaustion (Tempest et al., 2014, 2017; Jung et al., 2015). Tempest et al. (2014) reported that [HbO_2] increases from the value below VT (54.5 ± 4.1% VO_{2max}) until RCP (90.2 ± 4.9% VO_{2max}) and remains stable from RCP until exhaustion. The authors also showed that [HHb] remains stable between the value below VT and VT (68.2 ± 4.5% VO_{2ma}x) and increases from VT until exhaustion, whereas [tHb] continuously increases from the value below VT until exhaustion. Tempest et al. (2017) found that [HHb] increased from VT until exhaustion, whereas [HbO_2] remained stable between the start of exercise and VT (67.2 ± 2.9% VO_{2max}), increased between VT and RCP (87.9 ± 3.2% VO_{2max}), and thereafter remained stable until maximal intensity. Additionally, the results of the study by Tempest et al. (2014, 2017) were supported by Jung et al. (2015) who found a continuous increase in PFC oxygenation from stage 1 to stage 3 and stabilized HbO_2 concentrations between stages 3 and 4 during a multistage protocol that started at 1 W/kg (stage 1) and increased with 1 W/kg every stage. In contrast to Tempest et al. (2014, 2017) and Jung et al. (2015) found no significant differences in [HHb] between stages/intensities. Finally, two studies reported increases in [HbO_2] from RCP until exhaustion. Tempest and Parfitt (2016) measured prefrontal oxygenation during a maximal incremental test (MIT) between groups with high- and low-self-reported tolerance to exercise. The data indicated that [HbO_2] remains stable between the value below VT and VT (high = 49.8 ± 4.8% VO_{2max}, low = 54.6 ± 5.0% VO_{2max}) and increased between VT and RCP VT (high = 76.3 ± 5.1% VO_{2max}, low = 84.1 ± 5.9% VO_{2max}) and from RCP to exhaustion. According to Tempest et al. (2014, 2017), [HHb] and [tHb] remained stable from the value below VT to VT, increased from VT to RCP, and also increased from RCP to exhaustion in both tolerance groups. In contrast, Stevens et al. (2018) reported a small increase in [HbO_2], [HHb], and [tHb] up to 15% VO_{2max}, followed by a quadratic increase up to 75% VO_{2max} and a smaller increase above the value of RCT. Importantly, [HbO_2], [HHb], [tHb] increases were most prominent at workloads near RCP (Stevens et al., 2018). A visual representation of HbO_2 and HHb during MIT can be found in **Table 6**.

Prefrontal Cortex Oxygenation During Whole-Body Endurance Tasks

Seventeen studies measured TTE, TT, a constant load with fixed intensity- and adaptive walking/running-exercise protocols. Eleven of the included studies assessed PFC oxygenation during whole-body endurance protocols with a constant intensity and fixed duration (Ide et al., 1999; Fumoto et al., 2010; Miyazawa et al., 2013; Rupp et al., 2013; Giles et al., 2014; Tsubaki et al., 2016, 2018; Radel et al., 2017; Takehara et al., 2017; Hiura et al., 2018; Ohyanagi et al., 2018). In these studies, participants were asked to complete an endurance cycling task at a certain predetermined intensity (e.g., %HRmax and %VO_{2peak}) for a predetermined time. We classify these studies according to the following intensities: (1) light to moderate, (2) vigorous, (3) near-to-maximal, and (4) supramaximal.

Light to moderate intensity: two studies assessed PFC during 10 min of cycling at 30 and 50% VO_{2peak} (Takehara et al., 2017) and 30 and 60% VO_{2max} (Ide et al., 1999). Ide et al. (1999) found an increase in [HbO_2], [HHb], and [tHb] in proportion to work rate, at the intensities of 30 and 60% VO_{2max}. Increases were significantly higher at 60% VO_{2max}, and [HbO_2] reached a maximal level during the first few minutes of recovery. These data were replicated by Takehara et al. (2017) who reported an increase in [HbO_2] between 300 and 600 s, which was higher at 50% VO_{2peak} than 30% VO_{2peak}, but reported a decrease in [HbO_2] between 30 and 300 s. During a 4-min facial cooling intervention to reduce prefrontal skin blood flow and [HbO_2], Miyazawa et al. (2013) reported that prefrontal [HbO_2] increased during an 11-min cycling exercise at 60% HRmax (light intensity). The authors reported that neither the light-intensity cycling exercise nor the facial cooling intervention had an influence on [HHb]. The changes in [tHb] were similar to the changes in [HbO_2] and were related to prefrontal skin blood flow (Miyazawa et al., 2013). In a 15-min cycling task at 30% HR reserve (light intensity), Hiura et al. (2018) reported that [HbO_2] remained stable during the first 5 min but increased during the last 2 min of the trial and that HHb remained unchanged during the entirety. Hiura et al. (2018) also monitored the prefrontal blood flow and partial pressure of CO_2 (PCO_2) and reported that cerebral blood flow (CBF) and PCO_2 increased during the first 5 min and remained unchanged during the last 2 min. The results of the study by Ide et al. (1999) were replicated by Fumoto et al. (2010) who found a gradual increase in [HbO_2] during a 15-min cycling task at an intensity equaling 12–13 on the RPE scale (Borg, 1998) (moderate intensity), after which [HbO_2] reached a steady state until the end. Only a small decrease in [HHb] was found throughout the trial (Fumoto et al., 2010). A gradual increase in [HbO_2] during moderate-intensity exercise was supported by Tsubaki et al. (2018) who reported that [HbO_2] continually increased in right PFC during a 20-min cycling exercise trial at an intensity of 50% VO_{2peak}. Prefrontal skin blood flow also increased over the time of the trial and decreased again during the postexercise rest (Tsubaki et al., 2018). In a 20-min moderate-intensity (50%

TABLE 6 | Summary of finding on the evolution of HbO_2 and HHb during MIT.

	HbO_2			HHb		
Study	**Start—VT**	**VT—RCP**	**RCP—exhaustion**	**Start—VT**	**VT—RCP**	**RCP—exhaustion**
Bhambhani et al. (2007)	↑	↑	↓	NA	NA	NA
Timinkul et al. (2008)	↑	↑	↓	↓	=	↑
Tempest et al. (2014)	↑	↑	=	=	↑	↑
Jung et al. (2015)	↑	↑	=	=	=	=
Oussaidene et al. (2015)	↑	↑	↓	↑	↑	↑
Tempest and Parfitt (2016)	=	↑	↑	=	↑	↑
Tempest et al. (2017)	=	↑	=	=	↑	↑
Stevens et al. (2018)	↑	↑	↑	↑	↑	↑
Kojima et al. (2020)	↑	↑	↓	↓	=	↑
Kojima et al. (2021)	↑	↑	↓	↑	↑	↑

VT, Ventilatory threshold (50–70%$VO_{2max/peak}$); RCP, Respiratory compensation point (80–90% $VO_{2max/peak}$); Exhaustion (100% $VO_{2max/peak}$).

VO_{2max}) cycling trial, an increase in [HbO_2] was found between 3 and 6 min after which HbO_2 levels remained stable until the end (Ohyanagi et al., 2018). Within this research, prefrontal skin blood flow increased gradually throughout the trial, supporting the findings of Miyazawa et al. (2013) and Tsubaki et al. (2018). Finally, in two separate 90-min moderate-intensity cycling tests at 58–60% VO_{2peak}, at the cadence of 40 and 80 RPM, it was found that at the end of the exercise, [tHb] and [HbO_2] values were lower at 80 RPM than at 40 RPM, and [HHb] was lower at 80 RPM but remained unchanged at 40 RPM.

Suzuki et al. (2004) measured PFC after performing a 90-s locomotor task at three different speeds (3, 6, and 9 km/h), each with a 30-s rest. Before the start of the task, [HbO_2] and [tHb] increased, which was most prominent at 9 km/h, and peaked prior to the treadmill speed steadying. After reaching a constant speed, [HbO_2] and [tHb] decreased and returned to baseline, or lower than baseline, during the rest of the task. After stopping locomotion, temporal drops in [HbO_2] were seen before returning to baseline. PFC activation was greater, and HbO_2 was higher at 9 km/h than 3 and 6 km/h. No differences were shown between and 3 and 6 km/h (Suzuki et al., 2004).

Vigorous intensity: two studies examined the effects of vigorous cycling exercise on prefrontal oxygenation (Rupp et al., 2013; Giles et al., 2014). Rupp et al. (2013) asked participants to perform three consecutive 80-min cycling trials at 45% peak aerobic power output, each separated by 25 min of neuromuscular function testing. An increase in [HbO_2] and [tHb] was found in trial 1, reaching a plateau after approximately 40 min, whereas [HHb] progressively increased between 20 and 80 min in trials 1, 2, and 3. [HHb] was significantly lower in trials 2 and 3 than trial 1. In a sample of regular exercisers, Giles et al. (2014) found that [HbO_2], [HHb], and [tHb] increased as a result of exercise intensity. Participants completed three separate 30-min cycling trials at 52% (low intensity), 68% (moderate), and 84% (vigorous) HRmax, respectively (Giles et al., 2014). Similar HbO_2 values were found during the first 15 min among exercise intensities. After 18 min, HbO_2 was significantly higher at a moderate and high intensity than low intensity, and significantly higher at a vigorous than moderate intensity. Higher values of [HHb] were reported as a result of exercise intensity with higher values of [HHb] at a vigorous than moderate intensity, which was also higher than a low intensity (Giles et al., 2014). HHb values were steady until min 12 after which the values increased over time to min 23. From this point, HHb increased according to exercise intensity, with greater increases in [HHb] at a vigorous than moderate intensity, which in turn was higher than low intensity. [tHb] increased with each minute from the start and was similar between intensities until min 16, after which [tHb] increased between all intensities.

Near-to-maximal intensity: Two studies reported similar results in PFC during a 5-km running TT. Billaut et al. (2010) reported increased prefrontal [HbO_2], [HHb], [tHb], and CBV values from the start until a 2.5-km point, from which these values remained constant until km 4.5 and displayed evidence of deoxygenation in the last 0.5 km. Regional blood flow remained stable throughout this. Santos-Concejero et al. (2015) described increases in [HbO_2] and [HHb] over the first half of the trial, steady HbO_2 values in the second half of the trial, and further increases in [HHb] until completion. Additionally, TOI reduced over the first 1.5 km, after which it remained stable until the end. However, in contrast to Billaut et al. (2010), [tHb] remained stable for the first half of the trial and increased progressively from 3 km until completion. Pires et al. (2016), used a 4-km cycling TT and found that prefrontal [HbO_2], [HHb], and [tHb] increased until 70% of the TT and decreased upon completion. Pires et al. (2016) also assessed prefrontal oxygenation during a preliminary MIT (100 W + 25 W/min, until exhaustion), where prefrontal [HbO_2], [HHb], and [tHb] increased until 70% of the exercise, and thereafter decreased. Santos-Concejero et al. (2017) used a fatigue training test consisting of continuous 1-km repeated running trials, with 30-s recovery until exhaustion, at a pace 5% faster than their 5-km running TT (completed 2 days earlier). During the test, $\triangle$[HbO_2] was elevated compared to baseline throughout the test, decreased at the end of each repetition, and progressively decreased in the first, fifth, and final repetition. Δ[HHb] increased over the course of the test with increases during each running bout and decreases during each 30-s recovery period until completion. A decline in cerebral oxygen was negatively associated with the speed at which the test was completed. Radel et al. (2017) examined hemodynamic

changes when coping with the expectation of prolonged exercise. Participants were told that they would perform a cycling trial at an intensity equivalent to 60% peak aerobic power and that it would take 10- or 60-min according to the condition. In both experimental sessions, the trial was stopped after 10 min. A main effect of time was found, whereby [HbO_2] was lower in the first period than in the second and third. Compared to the 10-min condition, in the 60-min condition, smaller [HbO_2] elevations at the right dorsomedial PFC and higher [HbO_2] elevations at the right dorsomedial PFC were reported. No differences in RPE were found between conditions.

Supramaximal intensity: Shibuya et al. (2004) studied the effect of a supramaximal TTE performance at 120% of participants' VO_{2peak} on cerebral oxygenation. [HbO_2] increased during the first 30 s of exercise, after which [HbO_2] and [tHb] gradually decreased over time, resulting in significantly decreased values from the pre-exercise level. [HHb] remained constant throughout the test.

DISCUSSION

In this review, we outlined the current knowledge on the development of PFC oxygenation during whole-body endurance exercise through fNIRS. Research indicates that during MIT, HbO_2 increases until RCP, after which it decreases until exhaustion or remains in a steady state. Regarding submaximal exercise, prefrontal oxygenation increases during light, moderate, and vigorous intensity workloads but reaches a steady state over time. According to the findings using MIT at a near-maximal intensity, prefrontal oxygenation cannot be maintained, and deoxygenation occurs at PFC. RCP appears to act as a ThCox, with the occurrence of the deoxygenation of PFC when RCP exceeds. The findings presented in this review show no evidence for an increase in cerebral energy metabolism to be responsible for the deoxygenation of the PFC but instead indicate that an increase in respiratory ventilation in reaction exercise-induced hypocapnia results in a decrease in CBF and thus [tHb], [HbO_2], and [HHb].

Quality assessment was scored as moderate to strong in most studies, with only three studies being scored as weak (Takehara et al., 2017; Ohyanagi et al., 2018; Kojima et al., 2020). Two major limitations regarding the quality of studies were: (1) the method of participants' selection or source information variables being insufficiently described, whereby participants are often described as "healthy volunteers," and (2) insufficient data being presented to assess if the sample size was appropriate. The majority (74%) of the studies used observational study design and were therefore exempted from the subquestions E, F, G, and L of the quality assessment.

Near-IR Spectroscopy Methodology

As part of the inclusion criteria, all studies used NIRS to investigate PFC oxygenation. With this technique, near-IR light (NIR) is emitted through the scalp up to the neuronal tissue, where the light is either absorbed or scattered off. NIR with wavelengths between the optical window of 700 and 900 nm pass through most biological tissues, including bone because there is low absorption and scattering of photons (Ekkekakis, 2009). A body of research has shown that NIRS with wavelengths around 760 nm has an absorption peak within HHb, whereas in HbO_2 this is the case at 830 nm, making HHb and HbO_2 distinguishable from each other (Ekkekakis, 2009). In terms of NIRS device positioning, 23 studies used the international EEG 10–20 or 10–5 system, which is recognized to describe the placement of the scalp electrodes. This is in accordance with the methodological review of Herold et al. (2018) who stated that the international EEG 10–20/10–5 system is the most common and practical strategy for optode placement and thereby ensures that the region of interest is targeted. Next to the optode placement, the IOD is an important factor as it determines the depth of the NIRS measurement. Of the included studies, 16 applied an IOD of between 30 and 40 mm, which is appropriate for adults (Leon-Carrion and Leon-Dominguez, 2012; Herold et al., 2018). However, two studies used an IOD of 25 mm (Giles et al., 2014; Jung et al., 2015), which has been shown to include gray matter into the sample volume, and eight studies used an IOD of between 45 and 50 mm (Ide et al., 1999; Shibuya et al., 2004; Rupp and Perrey, 2008; Timinkul et al., 2008; Fumoto et al., 2010; Keramidas et al., 2011; Oussaidene et al., 2015; Pires et al., 2016), where the contribution of extracranial tissue is negligible (Leon-Carrion and Leon-Dominguez, 2012). Another effect of using a short channel (IOD $\leq$ 25 mm) is that NIRS signals are influenced by skin blood flow and CBF due to a more superficial measurement (Matsukawa et al., 2015). A consensus is needed for the studies that use NIRS devices to allow appropriate comparisons between studies. The guidelines for the usage of NIRS can be found in Herold et al. (2018).

Prefrontal Cortex Oxygenation During Incremental Exercise (Maximal Incremental Test)

It was hypothesized that prefrontal oxygenation would increase during submaximal exercise and subsequently decrease at near-maximal intensities. The results of this systematic review largely support this hypothesis but also reveal some new insights into central regulation during endurance performance. Rooks et al. (2010) concluded that cerebral oxygenation increases from low-to-vigorous intensities after which it reaches a plateau or declines toward baseline at near-to-maximal intensities. Rooks et al. (2010) focused on cerebral oxygenation in general, this review specifically focused on PFC and how oxygenation in this brain region evolves during whole-body endurance exercise. About 9 of 10 MIT studies found an increase in [HbO_2] during the first part of the incremental exercise. This initial increase can be explained by peripheral hemodynamic changes, such as increased cardiac output and metabolic demand in the function of the start of locomotion, and a gradual increase of intensity. Only in Tempest and Parfitt (2016) did [HbO_2] remain unchanged from the start until VT. All of the included studies reported an increase in [HbO_2] from VT until RCP, after which prefrontal oxygenation decreased (Bhambhani et al., 2007; Rupp and Perrey, 2008; Timinkul et al., 2008; Oussaidene et al., 2015;

Kojima et al., 2020, 2021) or reached a plateau (Tempest et al., 2014; Jung et al., 2015; Tempest and Parfitt, 2016), supporting previous research (Rooks et al., 2010). Additionally, Kojima et al. (2021) reported that the point at which [HbO_2] declined was correlated with RCP. On the other hand, two studies found a further increase in [HbO_2] (Tempest and Parfitt, 2016; Stevens et al., 2018). In comparison with a steep increase from VT until RCP, Tempest and Parfitt (2016), did not declare or provide details on the degree of the increase in [HbO_2], whereas Stevens et al. (2018) reported only a small increase in [HbO_2] from RCP until exhaustion. These results together with the other seven studies show that RCP is a crucial point for prefrontal oxygenation as after this point prefrontal oxygenation endures significant changes. RCP can be defined as the point at which arterial PCO_2 starts to decline during strenuous exercise and can be interpreted as a ventilatory response to maintain the acid-base balance by increasing ventilation (Rausch et al., 1991; van den Aardweg and de Groot, 2015).

Two studies (Timinkul et al., 2008; Kojima et al., 2021) measured end-tidal CO_2 pressure during MIT. Timinkul et al. (2008) found that end-tidal CO_2 pressure gradually increased with intensity and reached its peak at RCP, after which it gradually decreased until exhaustion. These results were supported by Kojima et al. (2021) who found an increase in end-tidal CO_2 pressure with incremental load and a subsequent decrease from 60% to 100% of the MIT. This decrease was also correlated with [HHb] and PCO_2. Research has shown that PCO_2 has a direct impact on CBF (Lassen, 1959; Poulin et al., 1996; Yoon et al., 2012). The blood-brain barrier is permeable to CO_2 but retains [H^+] and [HCO_3^-] ions, making CO_2 an important respiratory stimulant to the central chemoreceptors (Ainslie et al., 2007; Galán-Rioja et al., 2020). The brain requires a constant CBF within a narrow range of 60 and 150 mmHg despite changes in mean arterial pressure (MAP) (Ogoh and Ainslie, 2009). This regulatory mechanism is called cerebral autoregulation (Ogoh and Ainslie, 2009). Hyperventilation caused by intense exercise subsequently results in a drop in PCO_2. The state of low PCO_2 in the arterial blood, also referred to as hypocapnia, causes cerebral vasoconstriction, a cerebral autoregulatory mechanism, which results in a decrease in CBF (Ogoh and Ainslie, 2009). Nybo and Rasmussen (2007) stated that when CBF and cerebral oxygenation fall below a critical level, the motor output cannot be maintained. These results have been demonstrated in several studies that prolonged aerobic exercise was improved by increasing cerebral oxygenation through additional inspired O_2 levels (Nielsen et al., 1999; Subudhi et al., 2007). Besides the association between [HbO_2] and RCP, Kojima et al. (2021) found that end-tidal CO_2 decreases after RCP. However, no correlation between end-tidal CO_2, CBF, and cerebral O_2 exchange was reported. Kojima et al. (2021) suggests that a decrease in [HbO_2] and an increase in [HHb] before exhaustion during MIT are related to cerebral O_2 metabolism by a neural activity increase. While this is an interesting suggestion, it must be cautioned as cerebral blood volume and cerebral oxygen exchange are only the estimated values. Even though NIRS is not capable of measuring blood flow, a decrease in CBF through PCO_2 and cerebral autoregulation is a promising hypothesis to help explain changes in prefrontal oxygenation at RCP. However, there is a lack of research to objectively assess both cerebral oxygenation and CBF simultaneously. Studies combining NIRS with CBF velocity measurement techniques, such as transcranial doppler (TCD) ultrasonography and PET, could help elucidate the mediators of prefrontal oxygenation during exercise and the role of RCP as a ThCox.

Prefrontal Cortex Oxygenation During Whole-Body Endurance Tasks

This study is the first review to collect empirical evidence on PFC oxygenation during non-incremental whole-body endurance exercise. It was hypothesized that prefrontal oxygenation would increase during prolonged submaximal exercise until a steady state is reached. Additionally, we hypothesized that during near-maximal intensities PFC oxygenation cannot be maintained, resulting in a decrease near the exhaustion or end of the exercise. Maximal incremental studies have shown that PFC oxygenation is sensitive to exercise intensity. As a result, we have subdivided this section into light-to-moderate, vigorous, and near-to-maximal intensity.

Light-to-Moderate Intensity

Three low-intensity protocol studies found an increase in [HbO_2] from the start to the end of exercise (Ide et al., 1999; Miyazawa et al., 2013; Takehara et al., 2017). Although in the study of Takehara et al. (2017) an initial decrease in [HbO_2] was found between the start and 3 min into the cycling trial, this can be explained given that O_2-supply does not match the O_2-demand at the beginning of exercise (McArdle et al., 2010). Miyazawa et al. (2013) supported these findings and found a correlation between TOI, HbO_2, and tHb with prefrontal skin blood flow. This triggers the question of whether HbO_2 was measured at PFC and not superficially at the skin of the scalp, as vasoconstriction through cooling results in a decreased skin blood flow. Alternatively, HHb was not correlated with skin blood flow as HHb was not affected by the face cooling intervention, nor by an 11-min cycling task. Importantly, Miyazawa et al. (2013) implemented a 4-min incremental warm-up until reaching the intensity of 60% HRmax. This can help explain why HHb was not changed throughout the 11-min cycling exercise as several studies have pointed out that HHb is correlated with exercise intensity (Rupp and Perrey, 2008; Stevens et al., 2018; Kojima et al., 2021). Only one study objectively measured prefrontal blood flow and end-tidal CO_2 during light-intensity exercise (Hiura et al., 2018). The authors reported that the prefrontal CBF and end-tidal pressure of CO_2 initially increased but remained unchanged during the last few minutes of exercise. Similarly, the initial decrease in [HbO_2] was simultaneously associated with a steep increase in end-tidal CO_2, which can be explained though O_2 deficit at the start of the exercise. However, it is important to note that this study used both NIRS and PET to measure oxygenation and CBF, respectively, in two different samples. It is therefore unclear whether the results would be similar in the case of measurement at the same time point in the same person. Future research is

needed to examine whether these results will be the same when oxygenation and CBF are measured in the same sample.

Regarding moderate intensity endurance tasks, prefrontal oxygenation gradually increases in [HbO_2] over time until a steady state is reached. Ohyanagi et al. (2018) only found an increase in [HbO_2] between 3 and 6 min during a 20-min moderate-intensity cycling exercise, after which [HbO_2] stabilized to completion. Interestingly, Ohyanagi et al. (2018) and Tsubaki et al. (2018) both measured skin blood flow and reported that skin blood flow increased over the time of the exercise and decreased again during the postexercise rest, supporting the results of Miyazawa et al. (2013).

A gradual increase in [HbO_2] over time is present both at the light and moderate intensities and supports the results of the abovementioned incremental exercise research. In MIT, prefrontal-HbO_2 levels increase to RCP, which persist in above moderate intensities. This indicates that at light-intensity and moderate-intensity exercise, PFC oxygenation increases gradually until a steady state is reached. However, it is not clear whether the increased prefrontal oxygenation is the result of an increase in cerebral O_2 metabolism and neuronal activity. An increase in skin blood flow, through elevated MAP, seems to be correlated with increases in [HbO_2]. The changes measured by NIRS are the result of changes that occur throughout the volume of tissue traversed by the NIR light. The signal will therefore invariably contain a superficial interference from both emitter and receiver optodes. The inclusion of short-separation channels into the NIRS optode template could reduce superficial contamination through skin blood flow, which is influenceable by systemic changes (Gagnon et al., 2014). Gagnon et al. (2014) found a 33% reduction in signal noise for HbO_2 with the inclusion of one short channel and a 59% noise reduction when two short channels, one at the emitter and one at the detector, in comparison with the standard method. The role of an increased cerebral O_2 metabolism through neuronal activity can, however, not be ruled out. Suzuki et al. (2004) stated that PFC might be involved in controlling locomotion to adapt to the increasing speed in the acceleration phases during walking and running. Before the start of locomotion, an increase in [HbO_2] and [tHb] was found, especially during the 9 km/h trial, indicating a neuronal activation at PFC.

Vigorous Intensity

Two studies investigated the effects of vigorous cycling exercise on PFC oxygenation (Rupp et al., 2013; Giles et al., 2014). The results showed that prefrontal oxygenation [HbO_2] increased until reaching a steady state, which is similar during light-to-moderate intensities. Vigorous intensity ends at the verge of RCP but is still located below this threshold. In Rupp et al. (2013) and Giles et al. (2014), HHb remained unaffected during the first few minutes of exercise after which it progressively increases. Interestingly, both HbO_2 and tHb start to increase from the onset of an endurance task. However, CBF is not directly measured but can be interpreted as an estimate of tHb and HbO_2. This illustrates that there is an increase in O_2 supply to the PFC during the initiation of vigorous-intensity exercise. The continuous gradual increase of HbO_2, tHb, and, therefore, CBF, during 84% HRmax (vigorous intensity), is likely the result of RCP occurring between 85 and 91% HRmax. Given that the targeted workload of 84% HRmax is below this range, it may have resulted in being insufficient to meet RCP and thus a decrease in HbO_2 and tHb. This confirms our hypothesis that PFC increases during prolonged submaximal exercise until a steady state is reached.

Near-to-Maximal Intensity

Six studies assessed prefrontal oxygenation at near-to-maximal intensities. Incremental exercise studies have suggested that PFC oxygenation cannot be maintained and occurs in PFC. The tipping point of this deoxygenating phase is RCP. Five studies confirm this hypothesis during both running and cycling exercises. Billaut et al. (2010) and Pires et al. (2016) showed that prefrontal oxygenation could not be maintained throughout the trial, whereas in Santos-Concejero et al. (2015) HbO_2 and tHb increased from km 2.5 until the end. Despite the presence of identical TT running trials, Santos-Concejero et al. (2015) included elite Kenyan runners who underwent prenatal exposure to high altitude and high physical activity levels during childhood, which may have facilitated the maintenance of cerebral oxygenation. Prefrontal deoxygenation shown in Billaut et al. (2010) and Pires et al. (2016) did not result in a decrease in the motor output. These results may indicate that the duration of the TT task is insufficient for PFC oxygenation to influence the motor output and that deoxygenation remains within a range that does not hinder strenuous performance. However, these findings do not discount the suggestion that pacing strategies may influence the cerebral function metabolic status. Moreover, an initial increase in blood flow along with HbO_2 and HHb was thought to be the result of an increase in cardiac output. Because the near-to-maximal intensities exceed RCP, cerebral vasoconstriction could have led to prefrontal deoxygenation. This statement could, however, be questioned as to the deoxygenation in Santos-Concejero et al. (2015) was characterized by an increase in tHb through elevated HHb levels and a decrease in HbO_2. Similarly, Santos-Concejero et al. (2017) found that during a fatigue training test, $\triangle$[HbO_2] that was measured at the end of each running repetition was decreased over the course of the trial. The decrease in HbO_2 occurred simultaneously with increases in HHb over the course of the session with increases during each running bout, and a subsequent decrease during each 30-s recovery period until the end. It was stated that the speed at which participants performed was significantly faster than their expected speed at RCP, which is supported by a high lactate observation. A major limitation to this study, however, is that tHb, an indicator for CBF, is not measured in this study. Therefore, it is likely that hyperventilation-induced hypocapnia after RCP leads to deoxygenation. This study also highlights that high-intensity interval training (HIIT) results in a decrease in prefrontal oxygenation. In relation to prolonged endurance exercise, this could suggest that sequential intermediate near-to-maximal intensity efforts (e.g., repeated breakaways in cycling races) can result in a decrease in prefrontal oxygenation.

Regarding supramaximal exercise, Shibuya et al. (2004) examined TTE performance at 120% and showed that [HbO_2] increased during the first 30 s, after which [HbO_2] and [tHb]

gradually decreased and were significantly lower than pre-exercise. [HHb] remained unchanged throughout the trial. The initial increase in [HbO_2] and [tHb] is likely to be the result of a sudden increase in blood pressure through the start of locomotion against high resistance. On the other hand, the decrease in [HbO_2] and [tHb] can be linked with increasing end-tidal CO_2 concentrations, which result in cerebral vasoconstriction through hyperventilation, and in turn, lead to a decrease in CBF and thus in tHb and HbO_2. Shibuya et al. (2004) proposed a potential role for cerebral fatigue as a result of the changes in oxygenation. However, no study has provided evidence to support this hypothesis. This is the only study that has assessed PFC oxygenation during supramaximal exercise, indicating a need for further research measuring cerebral oxygenation during prolonged supramaximal exercise.

Radel et al. (2017) investigated the hemodynamic changes that arise when coping with the expectation of prolonged exercise and found that [HbO_2] increased over a 10-min cycling task, which is in accordance with the study of Rooks et al. (2010). When participants were expected to cycle for 60 min, the authors reported that [HbO_2] elevations at the right dorsolateral PFC were diminished and [HbO_2] elevations at the right dorsomedial PFC were higher. No differences in RPE between 10 and 60 min were found. The dorsolateral PFC is a representative region for the central executive network, whereas the dorsomedial PFC is a representative region for the default mode network (Fox et al., 2009). This highlights that the brain attempts to save mental resources by providing less activation of brain regions (dorsal PFC) associated with mental effort (the central executive network) and more toward those related to the resting activity (the default mode network) (Shibuya, 2011; Perrey and Besson, 2018). This study also indicates that psychological factors influence PFC oxygenation, suggesting that psychological interventions could positively influence PFC oxygenation and in turn improve endurance performance. Further, nutrition has also been shown to have a facilitating effect on PFC oxygenation. Decroix et al. (2018) reported an elevation in prefrontal oxygenation without having an impact on muscular oxygenation during a 20-min steady-state cycling exercise at 45% VO_{2max} (moderate) after the supplementation of cocoa flavanols. Given that mental fatigue negatively alters endurance performance (Marcora et al., 2009; Martin et al., 2018; Pageaux and Lepers, 2018), these findings are therefore an important factor for an examination within mental fatigue and highlight that PFC is involved in proactive behavior and goal-directed exercises (Pires et al., 2018).

Respiratory Compensation Point as a Cerebral Oxygenation Threshold

Research on PFC oxygenation within dynamic whole-body endurance performance throughout the entire spectrum of intensities (low, moderate, vigorous, near-to-maximal, and supramaximal intensities) is in accordance with research examining maximal incremental exercise. Our systematic review has found strong evidence that RCP is an important ThCox. Collectively, research indicates that PFC oxygenation increases throughout intensities below the RCP threshold and reaches a steady state during continuous sub-RCP workload tasks. However, during prolonged exercise at the intensities that exceed RCP, the increase or preservation of prefrontal HbO_2 cannot be maintained and the deoxygenation of PFC takes place. The findings presented in this review show no evidence that an increase in cerebral energy metabolism is responsible for the deoxygenation of PFC and limiting factors of endurance performance. When RCP is reached during exercise, an increase in respiratory ventilation results in hypocapnia. Cerebral autoregulation reacts to hypocapnia by causing cerebral vasoconstriction, resulting in a decrease in CBF and thus in [tHb], [HbO_2], and [HHb] (Ogoh and Ainslie, 2009).

Limitations and Future Research

Although this systematic review has provided novel insights into the influence of PFC oxygenation on whole-body endurance exercise, there are some limitations that need to be considered. Firstly, there is a need for a consensus and transparency in reporting the results within whole-body endurance exercise research. RCP acts as a tipping point/threshold for PFC oxygenation. However, this threshold was not consistently determined or referenced in every study. To ensure the adequate comparison between studies and to classify exercise intensity, we calculated VO_2 and % of VO_{2max} of the described datapoints and the metabolic equivalent of task (MET). To facilitate a comparison between studies in future research, each threshold or discussed data point should be referred to as a percentage of $VO_{2max/peak}$. Furthermore, concerning the reporting of the results, the two factors that are overlooked in most of the included studies are MAP and the training status of the subjects. MAP is closely related to oxygenation and (cerebral) blood flow and can, therefore, give interesting insights into the discussion of the results. However, recently, Castle-Kirszbaum et al. (2021) released a systematic review on a cardio-cerebral coupling and indicated that the current literature is insufficiently robust to confirm an independent relationship between the cardiac output and CBF. Regarding the training status, future research within this field should address participant characteristics related to the performance level as described by De Pauw et al. (2013) and Decroix et al. (2016) for male and female subjects, respectively. Secondly, future research should include objective measures for CBF (e.g., PET and TCD) simultaneously with NIRS to confirm the hypothesis that exceeding RCP results in cerebral vasoconstriction that in turn decreases PFC oxygenation. Moreover, a short-separation channel (8 mm) (Herold et al., 2018) needs to be included within the NIRS setup to determine whether changes in cerebral oxygenation are not the result of changes in local skin blood flow. However, there is a lack of consensus for the fNIRS application (optode placement, IOD, etc.), which complicates comparisons between studies (see Herold et al., 2018 for guidelines).

In this systematic review, only 6 of 28 studies assessed laterality. In future research, PFC laterality is an important factor given that the left and right PFC play different roles and may influence decision-making during endurance exercise. However, given a low number of studies to assess laterality, we believe

that it was inappropriate to make comparisons between all the studies. Future research should, therefore, endeavor to examine PFC laterality to provide a greater understanding of how this may influence endurance performance. Another limitation is that the environmental conditions were rarely mentioned. Given that ambient temperature and relative humidity influence endurance performance and can facilitate vasoconstriction or vasodilatation, it is likely that these could influence NIRS parameters. Further research should examine if the deoxygenation of PFC determines whether one stops or prolongs during an endurance task and if the interventions that postpone PFC deoxygenation could result in improved performances. Recently, the first study on this subject has been published (Dallaway et al., 2021). The authors reported that brain endurance training resulted in improved performance on muscular endurance handgrip tasks, which might occur with higher prefrontal oxygenation. This training-induced increase in prefrontal oxygenation was accompanied by a reduced mental effort during the physical task, making oxygenation a potential countermeasure for mental fatigue. These preliminary data are promising, and a need exists for more research to replicate this study design on whole-body endurance exercise tasks.

CONCLUSION

To conclude, this systematic review provides a detailed overview of how cerebral oxygenation at PFC reacts to various exercise intensities. As hypothesized, we found that PFC oxygenation increases at low, moderate, and vigorous intensities and decreases at near-to-maximal and supramaximal intensities. Moreover, a steady state could be reached at the intensities below RCP. RCP can also be identified as an important ThCox given that PFC oxygenation cannot be maintained and decreases until the cessation of whole-body endurance exercise at this point. The proposed mechanism behind this is that through an increase in ventilation, as a response to maintain the acid-base balance after exceeding RCP leads to cerebral vasoconstriction and therefore also in cerebral oxygenation. These findings reinforce and expand the knowledge on cerebral oxygenation during whole-body endurance exercise. Future research should examine whether maintaining/improving PFC oxygenation can improve endurance performance.

DATA AVAILABILITY STATEMENT

The original contributions presented in the study are included in the article/supplementary material, further inquiries can be directed to the corresponding author/s.

AUTHOR CONTRIBUTIONS

JDW performed the design of the search strategy. Subsequently, MP, JVC, JH, JD-G, and BR revised the design. JDW and JH did screening on title and abstract, while JDW, MP, JH, JVC, and BR conducted full text screening. JDW, MP, and JH first conducted the data analysis. JVC and BR later revised and updated the data analysis. JDW and JH performed quality assessment and also designed the quality assessment table together with MP. MV and JDW performed calculations for exercise intensity and performance level. JDW wrote the first draft of the manuscript, which was later altered by MP, JH, MV, PH, JD-G, JVC, BR, and RM. All authors read, revised, and approved the final manuscript.

ACKNOWLEDGMENTS

We would like to thank the Luxemburg Institute of Research in Orthopedics, Sport Medicine and Science (LIROMS) for their valuable contribution to this work.

REFERENCES

Ainslie, P. N., Barach, A., Murrell, C., Hamlin, M., Hellemans, J., and Ogoh, S. (2007). Alterations in cerebral autoregulation and cerebral blood flow velocity during acute hypoxia: rest and exercise. *Am. J. Physiol. Heart Circ. Physiol.* 292, H976–H983. doi: 10.1152/ajpheart.00639.2006

Amann, M. (2011). Central and peripheral fatigue: interaction during cycling exercise in humans. *Med. Sci. Sports Exerc.* 43, 2039–2045. doi: 10.1249/MSS.0b013e31821f59ab

Amann, M., Hopkins, W. G., and Marcora, S. M. (2008). Similar sensitivity of time to exhaustion and time-trial time to changes in endurance. *Med. Sci. Sports Exer.* 40, 574–578. doi: 10.1249/MSS.0b013e31815e728f

Angius, L., Santarnecchi, E., Pascual-Leone, A., and Marcora, S. M. (2019). Transcranial direct current stimulation over the left dorsolateral prefrontal cortex improves inhibitory control and endurance performance in healthy individuals. *Neuroscience* 419, 34–45. doi: 10.1016/j.neuroscience.2019.08.052

Asahara, R., and Matsukawa, K. (2018). Decreased prefrontal oxygenation elicited by stimulation of limb mechanosensitive afferents during cycling exercise. *Am. J. Physiol. Regul. Integr. Comp. Physiol.* 315, R230–R240. doi: 10.1152/ajpregu.00454.2017

Bhambhani, Y., Malik, R., and Mookerjee, S. (2007). Cerebral oxygenation declines at exercise intensities above the respiratory compensation threshold. *Respir. Physiol. Neurobiol.* 156, 196–202. doi: 10.1016/j.resp.2006.08.009

Billaut, F., Davis, J. M., Smith, K. J., Marino, F. E., and Noakes, T. D. (2010). Cerebral oxygenation decreases but does not impair performance during self-paced, strenuous exercise. *Acta Physiol.* 198, 477–486. doi: 10.1111/j.1748-1716.2009.02058.x

Borg, G. (1998). *Borg's Perceived exertion and pain scales*. Champaign, IL: Human Kinetics.

Castle-Kirszbaum, M., Parkin, W. G., Goldschlager, T., and Lewis, P. M. (2021). Cardiac output and cerebral blood flow: A systematic review of cardio-cerebral coupling. *J. Neurosurg. Anesthesiol.* 2021:768. doi: 10.1097/ANA.0000000000000768

Dallaway, N., Lucas, S. J. E., and Ring, C. (2021). Concurrent brain endurance training improves endurance exercise performance. *J. Sci. Med. Sport* 24, 405–411. doi: 10.1016/j.jsams.2020.10.008

Decroix, L., de Pauw, K., Foster, C., and Meeusen, R. (2016). Guidelines to classify female subject groups in sport-science research. *Int. J. Sports Physiol. Perform.* 11, 204–213. doi: 10.1123/ijspp.2015-0153

Decroix, L., Tonoli, C., Lespagnol, E., Balestra, C., Descat, A., Drittij-Reijnders, M. J., et al. (2018). One-week cocoa flavanol intake increases prefrontal cortex oxygenation at rest and during moderate-intensity exercise in normoxia and hypoxia. *J. Appl. Physiol.* 125, 8–18. doi: 10.1152/japplphysiol.00055.2018

De Pauw, K., Roelands, B., Cheung, S. S., de Geus, B., Rietjens, G., and Meeusen, R. (2013). Guidelines to classify subject groups in sport-science research. *Int. J. Sports Physiol. Perform.* 8, 111–122. doi: 10.1123/ijspp.8.2.111

Ekkekakis, P. (2009). Illuminating the black box: investigating prefrontal cortical hemodynamics during exercise with near-infrared spectroscopy. *J. Sport Exerc. Psychol.* 31, 505–553. doi: 10.1123/jsep.31.4.505

Fox, M. D., Zhang, D., Snyder, A. Z., and Raichle, M. E. (2009). The global signal and observed anticorrelated resting state brain networks. *J. Neurophysiol.* 101, 3270–3283. doi: 10.1152/jn.90777.2008

Fumoto, M., Oshima, T., Kamiya, K., Kikuchi, H., Seki, Y., Nakatani, Y., et al. (2010). Ventral prefrontal cortex and serotonergic system activation during pedaling exercise induces negative mood improvement and increased alpha band in EEG. *Behav. Brain Res.* 213, 1–9. doi: 10.1016/j.bbr.2010.04.017

Gagnon, L., Yücel, M. A., Boas, D. A., and Cooper, R. J. (2014). Further improvement in reducing superficial contamination in NIRS using double short separation measurements. *NeuroImage* 85, 127–135. doi: 10.1016/j.neuroimage.2013.01.073

Galán-Rioja, M., González-Mohíno, F., Poole, D. C., and González-Ravé, J. M. (2020). Relative proximity of critical power and metabolic/ventilatory thresholds: systematic review and meta-analysis. *Sports Med.* 50, 1771–1783. doi: 10.1007/s40279-020-01314-8

Garber, C. E., Blissmer, B., Deschenes, M. R., Franklin, B. A., Lamonte, M. J., Lee, I. M., et al. (2011). American college of sports medicine position stand. Quantity and quality of exercise for developing and maintaining cardiorespiratory, musculoskeletal, and neuromotor fitness in apparently healthy adults: guidance for prescribing exercise. *Med. Sci. Sports Exerc.* 43, 1334–1359. doi: 10.1249/MSS.0b013e318213fefb

Gastin, P. B. (2001). Energy system interaction and relative contribution during maximal exercise. *Sports Med.* 31, 725–741. doi: 10.2165/00007256-200131100-00003

Giles, G. E., Brunyé, T. T., Eddy, M. D., Mahoney, C. R., Gagnon, S. A., Taylor, H. A., et al. (2014). Acute exercise increases oxygenated and deoxygenated hemoglobin in the prefrontal cortex. *Neuroreport* 25, 1320–1325. doi: 10.1097/WNR.0000000000000266

Girard, O., and Racinais, S. (2014). Combining heat stress and moderate hypoxia reduces cycling time to exhaustion without modifying neuromuscular fatigue characteristics. *Eur. J. Appl. Physiol.* 114, 1521–1532. doi: 10.1007/s00421-014-2883-0

Glover, G. H. (2011). Overview of functional magnetic resonance imaging. *Neurosur. Clin. N. Am.* 22:133. doi: 10.1016/j.nec.2010.11.001

Herold, F., Wiegel, P., Scholkmann, F., and Muller, N. G. (2018). Applications of Functional Near-Infrared Spectroscopy (fNIRS) neuroimaging in exercise-cognition science: A systematic, methodology-focused review. *J. Clin. Med.* 7:466. doi: 10.3390/jcm7120466

Hiura, M., Nariai, T., Takahashi, K., Muta, A., Sakata, M., Ishibashi, K., et al. (2018). Dynamic exercise elicits dissociated changes between tissue oxygenation and cerebral blood flow in the prefrontal cortex: A study using NIRS and PET. *Adv. Exp. Med. Biol.* 1072, 269–274. doi: 10.1007/978-3-319-91287-5_43

Ichinose, Y., Morishita, S., Suzuki, R., Endo, G., and Tsubaki, A. (2020). Comparison of the effects of continuous and intermittent exercise on cerebral oxygenation and cognitive function. *Adv. Exp. Med. Biol.* 1232, 209–214. doi: 10.1007/978-3-030-34461-0_26

Ide, K., and Secher, N. H. (2000). Cerebral blood flow and metabolism during exercise. *Prog. Neurobiol.* 61, 397–414. doi: 10.1016/S0301-0082(99)00057-X

Ide, K., Horn, A., and Secher, N. H. (1999). Cerebral metabolic response to submaximal exercise. *J. Appl. Physiol.* 87, 1604–1608. doi: 10.1152/jappl.1999.87.5.1604

Jung, R., Moser, M., Baucsek, S., Dern, S., and Schneider, S. (2015). Activation patterns of different brain areas during incremental exercise measured by near-infrared spectroscopy. *Exp. Brain Res.* 233, 1175–1180. doi: 10.1007/s00221-015-4201-4

Kenney, W. L., Wilmore, J. H., and Costill, D. L. (2012). *Physiology of sport and exercise*, 5th Edn. Champaign, IL: Human Kinetics Publishers.

Keramidas, M. E., Kounalakis, S. N., Eiken, O., and Mekjavic, I. B. (2011). Muscle and cerebral oxygenation during exercise performance after short-term respiratory work. *Respir. Physiol. Neurobiol.* 175, 247–254. doi: 10.1016/j.resp.2010.11.009

Kmet, L., and Lee, R. (2004). *Standard Quality Assessment Criteria for Evaluating Primary Research Papers from a Variety of Fields AHFMRHTA Initiative20040213. HTA Initiative*, 2.

Kojima, S., Morishita, S., Hotta, K., Qin, W., Kato, T., Oyama, K., et al. (2021). Relationship between decrease of oxygenation during incremental exercise and partial pressure end-tidal carbon dioxide: near-infrared spectroscopy vector analysis. *Adv. Exp. Med. Biol.* 1269, 119–124. doi: 10.1007/978-3-030-48238-1_19

Kojima, S., Morishita, S., Qin, W., and Tsubaki, A. (2020). Cerebral oxygenation dynamics of the prefrontal cortex and motor-related area during cardiopulmonary exercise test: A near-infrared spectroscopy study. *Adv. Exp. Med. Biol.* 1232, 231–237. doi: 10.1007/978-3-030-34461-0_29

Kounalakis, S. N., and Geladas, N. D. (2012). Cardiovascular drift and cerebral and muscle tissue oxygenation during prolonged cycling at different pedalling cadences. *Appl. Physiol. Nutr. Metab.* 37, 407–417. doi: 10.1139/h2012-011

Lassen, N. A. (1959). Cerebral blood flow and oxygen consumption in man. *Physiol. Rev.* 39, 183–238. doi: 10.1152/physrev.1959.39.2.183

Leff, D. R., Orihuela-Espina, F., Elwell, C. E., Athanasiou, T., Delpy, D. T., Darzi, A. W., et al. (2011). Assessment of the cerebral cortex during motor task behaviours in adults: a systematic review of functional near infrared spectroscopy (fNIRS) studies. *Neuroimage* 54, 2922–2936. doi: 10.1016/j.neuroimage.2010.10.058

Leon-Carrion, J., and Leon-Dominguez, U. (2012). *Functional Near-Infrared Spectroscopy (fNIRS): Principles and Neuroscientific Applications*. London: IntechOpen. doi: 10.5772/23146

Liberati, A., Altman, D. G., Tetzlaff, J., Mulrow, C., Gøtzsche, P. C., Ioannidis, J. P., et al. (2009). The PRISMA statement for reporting systematic reviews and meta-analyses of studies that evaluate health care interventions: explanation and elaboration. *J. Clin. Epidemiol.* 62, e1–e34. doi: 10.1016/j.jclinepi.2009.06.006

Marcora, S. M., Staiano, W., and Manning, V. (2009). Mental fatigue impairs physical performance in humans. *J. Appl. Physiol. (1985)* 106, 857–864. doi: 10.1152/japplphysiol.91324.2008

Martin, K., Meeusen, R., Thompson, K. G., Keegan, R., and Rattray, B. (2018). Mental fatigue impairs endurance performance: A physiological explanation. *Sports Med.* 48, 2041–2051. doi: 10.1007/s40279-018-0946-9

Matsukawa, K., Ishii, K., Liang, N., Endo, K., Ohtani, R., Nakamoto, T., et al. (2015). Increased oxygenation of the cerebral prefrontal cortex prior to the onset of voluntary exercise in humans. *J. Appl. Physiol. (1985)* 119, 452–462. doi: 10.1152/japplphysiol.00406.2015

McArdle, W. D., Katch, F. I., and Katch, V. L. (2010). *Exercise physiology: nutrition, energy and human performance*. Philadelphia: Lippincott Williams & Wilkins.

Mccormick, A., Meijen, C., and Marcora, S. (2015). Psychological determinants of whole-body endurance performance. *Sports Med.* 45, 997–1015. doi: 10.1007/s40279-015-0319-6

Miyazawa, T., Horiuchi, M., Komine, H., Sugawara, J., Fadel, P. J., and Ogoh, S. (2013). Skin blood flow influences cerebral oxygenation measured by near-infrared spectroscopy during dynamic exercise. *Eur. J. Appl. Physiol.* 113, 2841–2848. doi: 10.1007/s00421-013-2723-7

Nielsen, H. B., Boushel, R., Madsen, P., and Secher, N. H. (1999). Cerebral desaturation during exercise reversed by O2 supplementation. *Am. J. Physiol.* 277, H1045–H1052. doi: 10.1152/ajpheart.1999.277.3.H1045

Nybo, L., and Rasmussen, P. (2007). Inadequate cerebral oxygen delivery and central fatigue during strenuous exercise. *Exerc. Sport Sci. Rev.* 35, 110–118. doi: 10.1097/jes.0b013e3180a031ec

Ogoh, S., and Ainslie, P. N. (2009). Cerebral blood flow during exercise: mechanisms of regulation. *J. Appl. Physiol.* 107, 1370–1380. doi: 10.1152/japplphysiol.00573.2009

Ohyanagi, H., Tsubaki, A., Morishita, S., Obata, H., Qin, W., and Onishi, H. (2018). Changes in the prefrontal cortex oxygenation levels during cycling in the supine and upright positions. *Adv. Exp. Med. Biol.* 1072, 133–137. doi: 10.1007/978-3-319-91287-5_21

Oussaidene, K., Prieur, F., Tagougui, S., Abaidia, A., Matran, R., and Mucci, P. (2015). Aerobic fitness influences cerebral oxygenation response to maximal exercise in healthy subjects. *Respir. Physiol. Neurobiol.* 205, 53–60. doi: 10.1016/j.resp.2014.10.009

Ouzzani, M., Hammady, H., Fedorowicz, Z., and Elmagarmid, A. (2016). Rayyan—a web and mobile app for systematic reviews. *Syst. Rev.* 5:210. doi: 10.1186/s13643-016-0384-4

Page, M. J., Mckenzie, J. E., Bossuyt, P. M., Boutron, I., Hoffmann, T. C., Mulrow, C. D., et al. (2021). The PRISMA 2020 statement: An updated guideline for reporting systematic reviews. *BMJ* 372:n71. doi: 10.1136/bmj.n71

Pageaux, B., and Lepers, R. (2018). The effects of mental fatigue on sport-related performance. *Prog. Brain Res.* 240, 291–315. doi: 10.1016/bs.pbr.2018.10.004

Pageaux, B., Marcora, S. M., and Lepers, R. (2013). Prolonged mental exertion does not alter neuromuscular function of the knee extensors. *Med. Sci. Sports Exerc.* 45, 2254–2264. doi: 10.1249/MSS.0b013e31829b504a

Périard, J., and Racinais, S. (2015). Performance and pacing during cycle exercise in hyperthermic and hypoxic conditions. *Med. Sci. Sports Exerc.* 48:1. doi: 10.1249/MSS.0000000000000839

Perrey, S., and Besson, P. (2018). Studying brain activity in sports performance: Contributions and issues. *Prog. Brain Res.* 240, 247–267. doi: 10.1016/bs.pbr.2018.07.004

Pires, F. O., Dos Anjos, C. A., Covolan, R. J., Pinheiro, F. A., St Clair Gibson, A., Noakes, T. D., et al. (2016). Cerebral regulation in different maximal aerobic exercise modes. *Front. Physiol.* 7:253. doi: 10.3389/fphys.2016.00253

Pires, F. O., Silva-Júnior, F. L., Brietzke, C., Franco-Alvarenga, P. E., Pinheiro, F. A., França, N. M., et al. (2018). Mental fatigue alters cortical activation and psychological responses, impairing performance in a distance-based cycling trial. *Front. Physiol.* 9:227. doi: 10.3389/fphys.2018.00227

Poulin, M. J., Liang, P. J., and Robbins, P. A. (1996). Dynamics of the cerebral blood flow response to step changes in end-tidal PCO2 and PO2 in humans. *J. Appl. Physiol.* 81, 1084–1095. doi: 10.1152/jappl.1996.81.3.1084

Racinais, S., and Girard, O. (2012). Neuromuscular failure is unlikely to explain the early exercise cessation in hot ambient conditions. *Psychophysiology* 49, 853–865. doi: 10.1111/j.1469-8986.2012.01360.x

Radel, R., Brisswalter, J., and Perrey, S. (2017). Saving mental effort to maintain physical effort: a shift of activity within the prefrontal cortex in anticipation of prolonged exercise. *Cogn. Affect. Behav. Neurosci.* 17, 305–314. doi: 10.3758/s13415-016-0480-x

Rausch, S. M., Whipp, B. J., Wasserman, K., and Huszczuk, A. (1991). Role of the carotid bodies in the respiratory compensation for the metabolic acidosis of exercise in humans. *J. Physiol.* 444, 567–578. doi: 10.1113/jphysiol.1991.sp018894

Robertson, C. V., and Marino, F. E. (2016). A role for the prefrontal cortex in exercise tolerance and termination. *J. Appl. Physiol.* 120, 464–466. doi: 10.1152/japplphysiol.00363.2015

Rooks, C., Thom, N., Mccully, K., and Dishman, R. (2010). Effects of incremental exercise on cerebral oxygenation measured by near-infrared spectroscopy: A systematic review. *Prog. Neurobiol.* 92, 134–150. doi: 10.1016/j.pneurobio.2010.06.002

Rupp, T., and Perrey, S. (2008). Prefrontal cortex oxygenation and neuromuscular responses to exhaustive exercise. *Eur. J. Appl. Physiol.* 102, 153–163. doi: 10.1007/s00421-007-0568-7

Rupp, T., Jubeau, M., Millet, G. Y., Wuyam, B., Levy, P., Verges, S., et al. (2013). Muscle, prefrontal, and motor cortex oxygenation profiles during prolonged fatiguing exercise. *Adv. Exp. Med. Biol.* 789, 149–155. doi: 10.1007/978-1-4614-7411-1_21

Santos-Concejero, J., Billaut, F., Grobler, L., Oliván, J., Noakes, T. D., and Tucker, R. (2015). Maintained cerebral oxygenation during maximal self-paced exercise in elite Kenyan runners. *J. Appl. Physiol. (1985)* 118, 156–162. doi: 10.1152/japplphysiol.00909.2014

Santos-Concejero, J., Billaut, F., Grobler, L., Oliván, J., Noakes, T. D., and Tucker, R. (2017). Brain oxygenation declines in elite Kenyan runners during a maximal interval training session. *Eur. J. Appl. Physiol.* 117, 1017–1024. doi: 10.1007/s00421-017-3590-4

Scarapicchia, V., Brown, C., Mayo, C., and Gawryluk, J. R. (2017). Functional magnetic resonance imaging and functional near-infrared spectroscopy: insights from combined recording studies. *Front. Hum. Neurosci.* 11:419. doi: 10.3389/fnhum.2017.00419

Shibuya, K. (2011). The activity of the primary motor cortex ipsilateral to the exercising hand decreases during repetitive handgrip exercise. *Physiol. Meas.* 32, 1929–1939. doi: 10.1088/0967-3334/32/12/004

Shibuya, K., Tanaka, J., Kuboyama, N., Murai, S., and Ogaki, T. (2004). Cerebral cortex activity during supramaximal exhaustive exercise. *J. Sports Med. Phys. Fitness* 44, 215–219.

Stevens, D., Halaki, M., Chow, C. M., and O'Dwyer, N. (2018). The effects of multi-stage exercise with and without concurrent cognitive performance on cardiorespiratory and cerebral haemodynamic responses. *Eur. J. Appl. Physiol.* 118, 2121–2132. doi: 10.1007/s00421-018-3942-8

Subudhi, A. W., Dimmen, A. C., and Roach, R. C. (2007). Effects of acute hypoxia on cerebral and muscle oxygenation during incremental exercise. *J. Appl. Physiol.* 103, 177–183. doi: 10.1152/japplphysiol.01460.2006

Suzuki, M., Miyai, I., Ono, T., Oda, I., Konishi, I., Kochiyama, T., et al. (2004). Prefrontal and premotor cortices are involved in adapting walking and running speed on the treadmill: an optical imaging study. *Neuroimage* 23, 1020–1026. doi: 10.1016/j.neuroimage.2004.07.002

Swain, D. P. (2000). Energy cost calculations for exercise prescription: An update. *Sports Med.* 30, 17–22. doi: 10.2165/00007256-200030010-00002

Takehara, N., Tsubaki, A., Yamazaki, Y., Kanaya, C., Sato, D., Morishita, S., et al. (2017). Changes in oxyhemoglobin concentration in the prefrontal cortex and primary motor cortex during low- and moderate-intensity exercise on a cycle ergometer. *Adv. Exp. Med. Biol.* 977, 241–247. doi: 10.1007/978-3-319-55231-6_33

Tempest, G. D., Eston, R. G., and Parfitt, G. (2014). Prefrontal cortex haemodynamics and affective responses during exercise: a multi-channel near infrared spectroscopy study. *PLoS One* 9:e95924. doi: 10.1371/journal.pone.0095924

Tempest, G. D., Eston, R. G., and Parfitt, G. (2017). A comparison of head motion and prefrontal haemodynamics during upright and recumbent cycling exercise. *Clin. Physiol. Funct. Imag.* 37, 723–729. doi: 10.1111/cpf.12365

Tempest, G., and Parfitt, G. (2016). Self-reported tolerance influences prefrontal cortex hemodynamics and affective responses. *Cogn. Affect. Behav. Neurosci.* 16, 63–71. doi: 10.3758/s13415-015-0374-3

Timinkul, A., Kato, M., Omori, T., Deocaris, C. C., Ito, A., Kizuka, T., et al. (2008). Enhancing effect of cerebral blood volume by mild exercise in healthy young men: a near-infrared spectroscopy study. *Neurosci. Res.* 61, 242–248. doi: 10.1016/j.neures.2008.03.012

Tsubaki, A., Morishita, S., Tokunaga, Y., Sato, D., Qin, W., Kojima, S., et al. (2020). Effect of exercise duration on post-exercise persistence of oxyhemoglobin changes in the premotor cortex: A near-infrared spectroscopy study in moderate-intensity cycling exercise. *Adv. Exp. Med. Biol.* 1232, 193–199. doi: 10.1007/978-3-030-34461-0_24

Tsubaki, A., Morishita, S., Tokunaga, Y., Sato, D., Tamaki, H., Yamazaki, Y., et al. (2018). Changes in cerebral oxyhaemoglobin levels during and after a single 20-minute bout of moderate-intensity cycling. *Adv. Exp. Med. Biol.* 1072, 127–131. doi: 10.1007/978-3-319-91287-5_20

Tsubaki, A., Takai, H., Kojima, S., Miyaguchi, S., Sugawara, K., Sato, D., et al. (2016). Changes in cortical oxyhaemoglobin signal during low-intensity cycle ergometer activity: a near-infrared spectroscopy study. *Oxygen transport to tissue XXXVII. Adv. Exper. Med. Biol.* 876, 79–85. doi: 10.1007/978-1-4939-3023-4_10

Van Cutsem, J., Roelands, B., de Pauw, K., Meeusen, R., and Marcora, S. (2019). Subjective thermal strain impairs endurance performance in a temperate environment. *Physiol. Behav.* 202, 36–44. doi: 10.1016/j.physbeh.2019.01.011

van den Aardweg, J. G., and de Groot, N. (2015). Tight coupling between inspiration and expiration after the respiratory compensation point. *Eur. Respir. J.* 46, A1553. doi: 10.1183/13993003.congress-2015.PA1553

Yoon, S., Zuccarello, M., and Rapoport, R. (2012). pCO2 and pH regulation of cerebral blood flow. *Front. Physiol.* 3:365. doi: 10.3389/fphys.2012.00365

Conflict of Interest: The authors declare that the research was conducted in the absence of any commercial or financial relationships that could be construed as a potential conflict of interest.

Publisher's Note: All claims expressed in this article are solely those of the authors and do not necessarily represent those of their affiliated organizations, or those of the publisher, the editors and the reviewers. Any product that may be evaluated in this article, or claim that may be made by its manufacturer, is not guaranteed or endorsed by the publisher.

frontiers in Sports and Active Living

BRIEF RESEARCH REPORT
published: 30 November 2021
doi: 10.3389/fspor.2021.725096

Brain Oxygenation in Post-concussion Combat Sport Athletes

Paolo Tiberini[1]*, *Giuseppe D'Antona*[2,3] *and Antonio Cicchella*[4]

[1] Department of Movement Sciences and Well-being, University of Naples Parthenope, Naples, Italy, [2] Criams-Sport Medicine Centre Voghera, University of Pavia, Pavia, Italy, [3] Department of Public Health, Experimental and Forensic Medicine, University of Pavia, Pavia, Italy, [4] Department for Quality of Life Studies, University of Bologna, Bologna, Italy

Purpose: Investigate the feasibility of a non-invasive method to evaluate the physical and cognitive repercussions of long-lasting post-concussion effects in professional combat sports athletes. To help athletes return to professional combat, there is a need for unbiased objective tools and techniques used as a prognostic method of recovery after Sport Related Concussion (SRC).

Methods: Six mild Traumatic Brain Injury (mTBI) athletes, age 20 ÷ 43 yr (1 female, 5 males) and 7 not concussed (NC) participants (amateur), age 24 ÷ 38 yr (3 females, 4 males), were tested Inspired/expired gas concentration, Cerebral changes in oxygenated hemoglobin ($\Delta[HbO_2]$) and deoxygenated hemoglobin ($\Delta[HHb]$) were measured using near infrared spectroscopy (NIRS) with a 3-step protocol: rest before maximal oxygen uptake (VO_2max) test, hypercapnia, and recovery after VO_2max test. The brain oxygenation and respiratory parameters of both sample sets were calculated using a non-parametric test (Mann-Whitney U test). Aerobic fitness outcome was quantified through mean average using the Bruce test. Participants performed Fitt's test using a laptop and analysis of medio-lateral and anterior-posterior range of oscillation was carried out via a force platform Romberg test.

Results: mTBI group showed statistically significant differences in saturated hemoglobin $\Delta[HbO_2]$ ($p < 0.001$) during rest and recovery phase after maximal incremental exercise, in medio-lateral sway eyes open ($p = 0.008$, NC 25.35 ± 4.11 mm and mTBI 17.65 ± 4.79 mm). VO_2max revealed no significant differences between the two groups: NC 47.47 ± 4.91 mTBI 49.58 ± 5.19 ml/kg/min^{-1}. The 2 groups didn't differ for maximum power output (NC 220 ± 34, mTBI 255 ± 50 W). End-tidal fractional concentration of O_2 ($FetO_2$ NC15.20 ± 0.41, mTBI 16.09 ± 0.68) throughout hypercapnia, saturated blood hemoglobin ($\Delta[HbO_2]$) revealed significant differences with the mTBI group. No differences emerged from Fitt's test.

Conclusions: It emerges that NIRS is able to reveal differences in long time outcomes of mTBI. The medio-lateral variations cannot be considered as a marker of long-term damage in athletes specifically trained for balance.

Keywords: brain concussion, mild traumatic brain injuries (mTBI), sway analysis, combat sport athletes, boxing athletes, brain concussion [MeSH], medio-lateral oscillation, near infrared spectroscopy (NIRS)

OPEN ACCESS

Edited by:
Wei-Peng Teo, Nanyang Technological University, Singapore

Reviewed by:
Stefano Longo, University of Milan, Italy
Aurora Daniele, University of Campania Luigi Vanvitelli, Italy

***Correspondence:**
Paolo Tiberini
paolo.tiberini001@studenti.uniparthenope.it

Specialty section:
This article was submitted to Exercise Physiology, a section of the journal Frontiers in Sports and Active Living

Received: *14 June 2021*
Accepted: *26 October 2021*
Published: *30 November 2021*

Citation:
Tiberini P, D'Antona G and Cicchella A (2021) Brain Oxygenation in Post-concussion Combat Sport Athletes. Front. Sports Act. Living 3:725096. doi: 10.3389/fspor.2021.725096

INTRODUCTION

Traumatic Brain Injuries (TBIs) can be distinguished based on the severity in: mild, moderate, and severe (Kaj, 2016). A concussion is considered as part of the mild TBI spectrum associated diseases and often the term is used as synonymous of mTBI. Generally, the term Sport-Related Concussion" (SRC) is used to represent the immediate and transient symptoms of TBI. mTBIs are the less severe brain trauma and, generally, spontaneously resolve after a short period of recovery (McCrory et al., 2017) and represent 70–90% of all treated brain injuries (Cassidy, 2004). The sequelae of chronic subclinical neurological effects of recurrent concussions are not well-understood. In the long term, it has been observed that repetitive cerebral concussions could be a possible cause of dementia-related syndromes onset (Guskiewicz Kevin, 2005) and other coexistent diseases. Concussions can also lead to psychiatric and psychological disorders (Finkbeiner et al., 2016). The effects on physical performance, on motor learning and on the coordination of movements in sub-clinical stages of post-concussion events are partly known but not yet clarified. Some studies show that there are alterations of oculomotor functions in those subjects who have suffered traumas during sports (Hecimovich et al., 2019), as a consequence of the cognitive performance decline, a slowdown in physical activity and reflexes has been observed as for example an impaired speed of movement during the walk test (Howell et al., 2019). Also, the execution of psychomotor tasks may slow in multiple-concussed athletes compared to the non-concussed. In the long run (Beaulieu et al., 2019), in addition to migraine, other concomitant conditions, such as anxiety and vestibular problems below the threshold of formal medical diagnosis-symptoms (Kontos et al., 2019), may be found. A lower incidence rate of head injuries has been also observed in more aerobically trained subjects than in less trained, even if this difference does not change the effects of neuro-cognitive decline given by a possible concussion (Kontos et al., 2006). Measurements performed with transcranial ultrasonographic doppler, showed the changes in cerebral circulation occurring in concussed subjects (Len et al., 2011). During daily life, comparable to rest, there are no persistent changes. Instead, during tests in conditions of hypo- and hypercapnia, the concussed subjects showed a fall in cerebral diffusion speed as well as an increase in recovery times compared to healthy subjects (Len et al., 2011). The limited perfusion of oxygen, determined by the autonomic nervous system, can cause limitations of brain functions or high metabolic demands to an already partially compromised brain to guarantee the required oxygen request (Jünger et al., 1997).

Post-concussive Symptoms

After a closed head injury, during which the skull and dura mater remain intact, the aforementioned symptoms may lead to post-concussion syndrome, a mild form of TBI (MeSH subject heading scope note, 2003) that could be chronic, permanent, or late-emerging. Even, some low-grade effects of concussion, such as impairments of balance, precision, attention, working memory, and oxygenation can be observed (Brush et al., 2018).

The mTBI is a complex injury that caused a large number of subjects, the development of persistent symptoms so far (Brush et al., 2018).

Persistent Post-concussive Symptoms

The "punch-drunk syndrome" also called *dementia pugilistica*, was first described in 1928 (Martland, 1928). Since then, in 2009 the VA/DoD (Veterans Administration/Department of Defense) draw up a clinical practice guideline underlining that "there is no consensus on a case definition for persistent symptoms attributed to concussion/mTBI and no consensus on the time course when acute symptoms should be considered persistent" (Cifu et al., 2009). To date, no definitive studies demonstrated the incidence of persistent symptoms after repeated concussions and no common agreement on the development of persistent symptoms.

(Guskiewicz Kevin, 2005), observed that retired professional football player that suffered three or more reported concussion had a 5-fold prevalence of problems during a questionnaire focusing on memory and issues related to Mild Cognitive Impairment (MCI) compared with retirees without a history of concussion. They also found an association between subjects who suffered a concurrent concussion during their life and an earlier onset of Alzheimer's disease. Even on the adolescent, mTBI produced cognitive function reduction, in particular verbal memory, visual memory and impulse control (Taylor et al., 2018). The cognitive functions in adolescents are compromised in performance caused by persistent effects than previously thought. Moreover, tested on a population of 5,656 adolescent aged 13–19 years, over a period of 5 years, the age at which an individual has his or her first concussion should be a related factor that influences the long-lasting effects of concussion (Taylor et al., 2018).

There is a large number of subjects such as youth and high school students or professional athletes participating in contact sports that every year are involved in repetitive brain trauma; CTE represents an important public health issue that should be considered as diseases acknowledged by the public institutions (Stern et al., 2011). A study of Neary et al. (2020) showed how NIRS (Near-Infrared Spectroscopy) can be used as a diagnostic tool in the acute assessment of concussion (1 week post-injury) but no study exists in the long term assessment of the outcomes of mTBI. The article lays the groundwork for the present research as its shows that objective measurements of cerebral hemodynamics can be performed by NIRS.

Abbreviations: TBIs, Traumatic Brain Injuries; mTBIs, Mild TBIs; SRC, Sport Related Concussion; LOC, Loss Of Consciousness; AOC, Alteration Of Consciousness; PTA, Post-traumatic amnesia; PCS, Post-Concussion Syndrome; CTE, Chronic traumatic encephalopathy; PPCS, Persistent post-concussive symptoms; MCI, Mild Cognitive Impairment; HIC, Head Injury Criteria; GSI, Gadd Severity Index; SCAT, Sport Concussion Assessment Tool; $\Delta[HbO_2]$, Oxyhaemoglobin; Δ[HHb], Deoxyhaemoglobin; tHb, Total hemoglobin; Cox, Cerebral Oxygenation; MLroo, Medio-Lateral oscillation; AProo, Anterior-Posterior range of oscillation; $FetO_2$, Fraction End Tidal O_2; OEF, Cerebral oxygen extraction fraction; MMA, Mixed Martial Arts; CBF, Cerebral Blood Flow.

TABLE 1 | Anthropometric and aerobic power data with mean values ± standard deviation values.

	Age	Body mass	Height	BMI	VO_2max/Kg	HRmax	Pmax
NC (mean ± SD)	30 ± 5	74.76 ± 12.38	173 ± 9	24.7 ± 2,4	40.1 ± 4.9	173 ± 8	220 ± 34
mTBI (mean ± SD)	29 ± 9	73.38 ± 15.62	176 ± 6	23.4 ± 4.0	45.4 ± 5.2	173 ± 17	255 ± 50

N.C, not Concussed participants; mTBI, Concussed participants; BMI, Body Mass Index; VO_2maxexpressed in (ml/min/Kg); HRmax, heart rate expressed in bpm; Pmax (W), maximum power reached during CPET test.

Aim of Research

There is a lack of studies monitoring the long-term cognitive impairment (e.g., anxiety, loss of concentration) after recurrent concussions and their neuropsychological consequences and/or behavioral impairments in several sport categories as boxing, ski, snowboarding, rugby, or American football.

The long-term neuromotor functions in concussed subjects have been poorly investigated in the literature.

The aims of the present study were to test a non-invasive method to evaluate the physical and cognitive behaviors following long-lasting concussion exposure in professional boxers and to investigate if there are differences between physiological (variation in $\Delta[HbO_2]$) and performance (VO_2max) variables and see whether differences in these variables can be highlighted between concussed (mTBI) and not concussed (NC) participants. In particular, we assessed if concussed participants showed differences between brain oxygenation, balance, maximal aerobic capacity, and power, in comparison to non-concussed healthy participants. This method was adopted in part by Len et al. (2011) but only with regard to changes in $\Delta[HbO_2]$ during rest and during hypercapnia; according to our knowledge, Δ[HHb] improvement has never been verified in the same test and never monitored during the recovery phase after maximal incremental physical exercise test in order to monitor the behavior of tissue oxygenation in mTBI participants.

Hypothesis

Our hypothesis were: significant differences exist between NC practitioners and people with mTBI in the mid-lateral oscillation, Δ[HbO2] and Δ[HHb] during the three phases of the test (Rest, Hypercapnea, Recovery).

METHODS

Thirteen participants (20–43 year old, male and female) participated in the study. Participants were recruited by public announcement addressed to gyms and specialist centers and were divided into two groups: not concussed participants (NC, $n = 7$) age 24÷38 yr (3 females, 4 males), boxers or fighters (3 boxers and 4 fighters) and repeated mTBI participants (mTBI, $n = 6$) age 20÷43 yr (1 female, 5 males) boxers and fighters (4 boxers and 2 fighters), anthropometry is reported in **Table 1**.

Inclusion criteria for the mTBI were age 20÷45 years of age, have experienced two or more mTBIs within the past 10 years but not within 6 months. Exclusion criteria for both groups included: substance abuse, major psychological disorders, the use of beta-blockers or calcium antagonists. Recruited participants were retired or professional boxers or fighters coming from martial arts like muay thai and mixed martial arts (MMA). Control participants did not experience repeated mTBIs during their entire life. Before the testing session, informed written consent was obtained by each participant. Procedures were approved by the research ethics board of the University of Bologna. Participants were asked to refrain to eat food, drink coffee ingestion, or smoke in the previous 3 h before tests or drink alcohol in the previous 12 h.

Procedure

On the day of the experiment, the participant was subjected to five subsequent tests for a total duration of ∼60 min: Romberg's test, reactivity and fine motor skills assessment, brain oxygenation measurement ($\Delta[HbO_2]$; Δ[HHb]), measurement of VO_2max, cerebral oxygenation (Cox) during recovery.

First, Romberg's test required the participants to be barefoot [30 s with eyes open (eo) and 30 s with eyes closed (EC)] on a kistler platform mod. 9286B (Kistler, Winterthur, Switzerland). For balance assessment the Sway ver. 1.4 (BTS Bioengineering, Garbagnate Milanese, Italy) software was used and the medio-lateral oscillation (MLroo) and anterior posterior range of oscillations (AProo) were calculated (Prieto et al., 1996; Mirow et al., 2016) to evaluate the origin, ocular or vestibular, of possible alterations of the balance (Błaszczyk, 2016). For an evaluation of reactivity and fine motor skills, Fitt's standardized test (Fitts, 1954) was administered on a personal computer through the use of the software PEBL (Mueller and Piper, 2014) based on Fitt's law (Fitts, 1954). This "aimed movement test" (Mueller and Piper, 2014) was performed using the computer mouse to point targets of different sizes and distances that appeared on the computer screen. For each participant, we collected 210 trials and we used the time of 100 trials for comparison. The first 50 trials were considered as training, the trials 51–150 were retained, and the last 60 trials (from 151 to 210) were not considered. Every participant was not aware of which trials were taken for the analysis. Average reaction times were compared.

Brain oxygenation measurement was performed using a standardized protocol (Len et al., 2011; Bishop and Neary, 2018). In the first phase, the participant was asked to lay supine with eyes open in resting breathing condition, in order to measure the change in concentration of oxyhaemoglobin ($\Delta[HbO_2]$)parameter used to suggest cerebral blood flow (CBF), deoxyhaemoglobin (Δ[HHb]) a reliable estimator of changes in

TABLE 2 | Sway test.

	MLroo(eo)	MLroo(ec)	AProo(eo)	AProo(ec)	TL(eo)	TL(ec)
NC	25.3 ± 4.1	29.2 ± 9.8	22.1 ± 3.1	34.2 ± 10.5	485.5 ± 161.2	808.2 ± 236.9
mTBI	17.6 ± 4.8*	29.4 ± 10.2	18.7 ± 5.7	29.6 ± 7.7	381.6 ± 116.2	601.3 ± 256.1

*MLroo, Medio-Lateral range of oscillation; AProo, Anterior-Posterior range of oscillation; TL, Trace Length, eyes open (eo) and eyes closed (ec). All the measure are expressed in millimeter (mm). *statistically significant result.*

TABLE 3 | $FetO_2$ (fractional end tidal O_2) and $FetCO_2$ (fractional end tidal CO_2) mean data during the three phases.

	Rest phase	Hyp. phase	Rec. phase
$FetO_2$ NC	13.80 ± 3.90	15.20* ± 0.41	16.37 ± 0.51
$FetO_2$ mTBI	15.45 ± 1.32	16.09* ± 0.68	16.44 ± 0.50
$FetCO_2$ NC	6.51 ± 3.82	5.04 ± 0.37	4.48 ± 0.47
$FetCO_2$ mTBI	5.14 ± 0.64	4.89 ± 0.59	4.53 ± 0.42

*$FetO_2$ NC, Fractional End Tidal O_2 Not Concussed participants; $FetO_2$ mTBI, Fractional End Tidal O_2 Concussed Subjects; $FetCO_2$ NC, Fractional End Tidal CO_2 Not Concussed participants; $FetCO_2$ mTBI, Fractional End Tidal CO_2 Concussed Subjects Rest phase (Rest Phase); Hypercapnic Phase (Hyp. phase), Recovery Phase (Rec. phase). Statistically significant between groups (p = 0.0008). *statistically significant result.*

tissue de-oxygenation status (Hoshi et al., 2001). VO_2, VCO_2, end-tidal fractional concentration of CO_2 ($FetCO_2$), end-tidal fractional concentration of O_2 ($FetO_2$) were also used.

In the second phase, a hypercapnia test was performed including 40 s of normal breathing and 20 s of breath retention for a total of 5 steps (5 min total), to allow to measure drift from the basal level (Bishop and Neary, 2018). The transition time from standing to lying between each phase has also been set to 60 s for each subject, lying on a massage table.

The measurements of oxyhaemoglobin ($\Delta[HbO_2]$) and deoxyhaemoglobin ($\Delta[HHb]$) concentrations were done using an 85 × 20 mm transcranial probe, applied 2 cm above the root of the nose and connected with a near-infrared spectroscope (NIRS, Nirox S.r.l) just above the supraorbital ridge (Kleinschmidt et al., 1996). Based on the transparency principle of human tissue to the near-infrared radiation, it uses light in the spectrum from 650 to 1,000 nm. We used a probe equipped with three low-power laser diodes (<10 mW) that emit radiation at 685, 830, and 980 nm (interoptode distance 44 mm, accuracy ± 5 μM). The 40 Hz data sampling frequency was then filtered in order to reduce the amount of data and obtain two values per second according to Wolf et al. (2007).

The breath-by-breath gases were measured using a metabolimeter Quark CPET (Cosmed S.r.l, Bologna).

The aerobic power (VO_2max) was calculated by means of a cardiopulmonary exercise Bruce ramp test (CPET) using a cycle ergometer (5 min of warming up at 80 W and then with an increase of 20 W every 2 min, until exhaustion). During CPET, the heart rate was continuously monitored with an electrocardiogram interfaced with the metabolic cart. The parameter measured were: VO_2/Kg (ml/Kg/min), hearth rate HR(bpm), maximum power P(W).

During the recovery phase following the CPET test transcranial $\Delta[HbO_2]/\Delta[HHb]$ and respiratory gases were measured in supine posture.

Statistical Analysis

The data were analyzed using the SPSS statistical software (ver. 23.0). Mean and SD values were calculated for $\Delta[HbO_2]$, $\Delta[HHb]$ and $FetO_2$, $FetCO_2$ for each participant. A Kolmogorov-Smirnov test was performed to assess the normality of data, and a Mann-Whitney U test was performed to evaluate the differences between groups (mTBI vs. NC). Significance was set at $p < 0.05$.

RESULTS

Anthropometric data and aerobic power are summarized in **Table 1**. No significant difference was found in VO_2max/kg between groups (mTBI: 45.4 ± 5.2; NC: 40.1 ± 4.9 ml/kg/min^{-1}). Sway test (**Table 2**) revealed a significant difference in medio-lateral sway at eyes open ($p = 0.008$) between mTBI (17.65 ± 4.79 mm) and NC (25.35 ± 4.11 mm). Mann-Whitney *U*-test showed a significant difference in $FetO_2$ average during the hypercapnic phase ($p = 0.008$) (**Table 3**). During rest (**Figure 1A**) and during the recovery phase (**Figure 1C**) from CPET, NIRS showed a statistically significant difference in $\Delta[HbO_2]$ ($p < 0.001$) between groups.

No statistically significant differences were observed during the hypercapnic test regarding $\Delta[HbO_2]$, $\Delta[HHb]$ (**Figure 1B**) and in reaction time that take into account total time and maximum trial duration in the Fitt's test (**Table 4**).

DISCUSSION

In post concussed athletes, compared to control participants, we found a lower mid-lateral open-eyed oscillation, significantly lower $FetO_2$ average during the hypercapnic phase and significantly lower cerebral $\Delta[HbO_2]$ during rest and recovery from a CPET test.

Posture

The change in MLroo (eyes open) was chosen for the assessment of residual postural disorders as it could be referred to an altered modulation by the autonomic nervous system (Mirow et al., 2016) and be indicative of postural abnormalities in concussed participants. Surprisingly, in mTBI a significantly lower MLroo eo(eyes open) was observed in the sway test highlighting a higher postural efficiency in the mTBI group than in the control group, expressed by a decrease in the lateral displacement

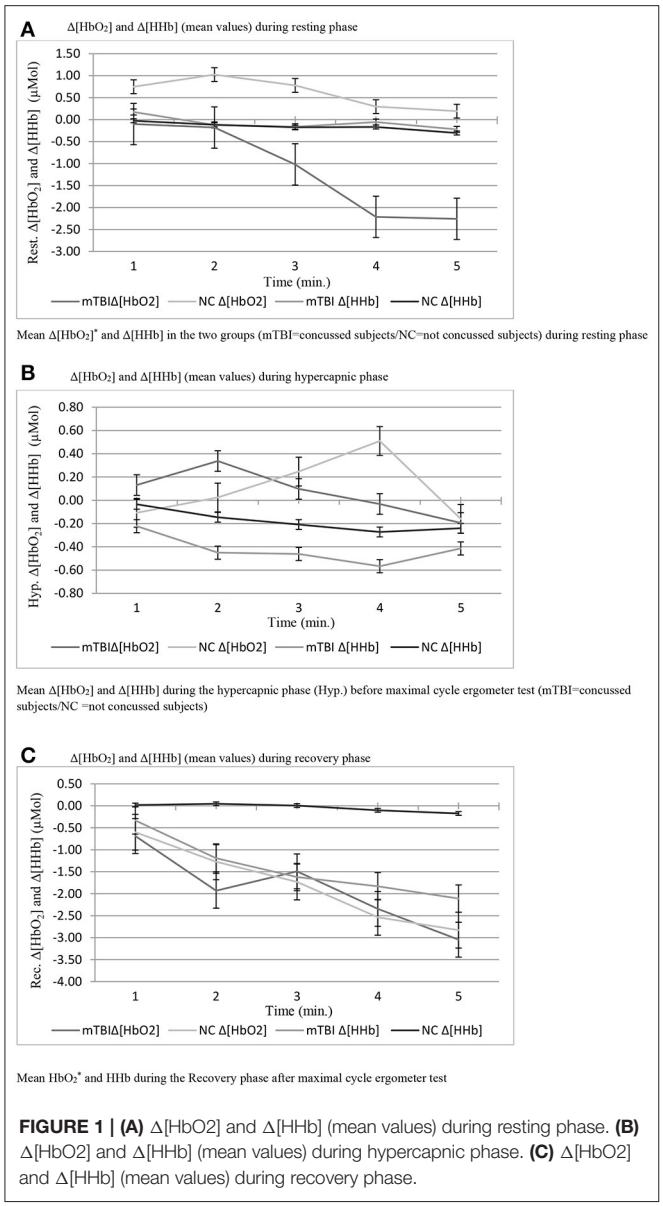

FIGURE 1 | (A) Δ[HbO2] and Δ[HHb] (mean values) during resting phase. **(B)** Δ[HbO2] and Δ[HHb] (mean values) during hypercapnic phase. **(C)** Δ[HbO2] and Δ[HHb] (mean values) during recovery phase.

valued. In agreement with previous published experimental work (Fahr et al., 2015), this result can be explained by the higher level of training of these participants. In fact, considering the MLroo at closed eyes sway values, the difference between groups disappeared. So, it is therefore possible that the observed difference may be linked to the ability of professional athletes to maintain balance and decrease the medio-lateral oscillations thanks to long-lasting training (Fahr et al., 2015). Considering these results, the values of MLroo eo may not be adequate to make assessments of the effects of medium-long-term concussions in professional mTBI when compared to non-professional athletes or sedentary controls.

Brain Oxygenation

Figure 1 reports the change of $\Delta[HbO_2]$ and $\Delta[HHb]$ during the resting phase after a maximal effort during CPET in both groups. mTBI showed a noticeable drop in $\Delta[HbO_2]$ compared to NC ($p = 0.008$) with much lower Δ hemoglobin at rest as well as reduced initial Δ oxygenation values compared to NC. Therefore, mTBI showed lower basal levels of oxygenated hemoglobin concentration, both at the beginning and at the end of the ramped test, with a constant decrease, and stabilization between the fourth and 5th min after. One of the possible causes of the physiological decline in both groups could be the redistribution of blood that takes place immediately after the change of the body posture, from supine to the sitting position leading to stabilization of the levels below the starting point when an orthostatic position is reached. However, this would not explain the lower $\Delta[HbO_2]$ values of the mTBI group compared to NC (Ivan et al., 2004). No difference in $\Delta[HbO_2]$ and $\Delta[HHb]$ between groups was observed during the hypercapnic test. Interestingly, in both groups of participants, $\Delta[HbO_2]$ reached its final value after 5 min of the test, with a similar trend in NC and mTBI. However, the initial response to the stimulus was different in the two groups: in NC, which started from higher oxygenation values, a reduced increase in oxygen demand in the transcranial zone at the initial stage was observed starting from the 2nd min. In mTBI, which started from lower oxygenation levels, the oxygenation level gradually increased. In these participants a rather fast drop-down of the oxygenation occurred from the 4th min onwards, leading to $\Delta[HbO_2]$ levels similar to those observed in NC. This is the consequences of the cerebral vasculature vasodilation (due to increased $PaCO_2$). The observed differences may also be linked to different respiratory patterns observed in well-trained mTBI as they performed deeper respiratory acts with longer inspirations compared to controls.

TABLE 4 | Fitt's test data.

	T max (ms)	Rt (ms)	Tt (s)
NC	2,313 ± 460	1,003 ± 104	100.4 ± 10.4
mTBI	2,347 ± 621	1,060 ± 75	106.0 ± 7.5

T max, Maximum Trial duration (mean of maximum ± SD); Rt, Reaction time; Tt, Total time.

As regards the changes of $\Delta[HbO_2]$ and $\Delta[HHb]$ during the recovery phase after the cycle ergometer maximal test, a higher significantly different $\Delta[HbO_2]$ decrease was observed in mTBI compared to NC. This observation could be attributed to a sub-clinical condition that leads to reduced cerebral perfusion in the time following efforts in concussed participants. These results agree with what observed by Bhambhani et al. in healthy subjects (Bhambhani et al., 2007) who experienced a collapse in cerebral oxygenation (Cox) during the final stage of maximal physical exercise to exhaustion. Another study that examines the prefrontal cortex oxygenation in healthy subjects belonging to another category of subjects is that of Rupp and Perrey (2008).

Breathing Air-Flow

Recent studies have shown that cerebral oxygen extraction fraction (OEF) is an important physiological index also defined as an "index of the homeostasis of oxygen demand and supply in the human brain." OEF has been found to be inversely related

to $FetCO_2$ (Jiang et al., 2019) in physiological conditions and is considered a potential clinical biomarker in neurodegenerative diseases such as Alzheimer's disease, multiple sclerosis and others (Jiang et al., 2019). As shown by some authors (Thomas et al., 2017), a decrease in OEF values has been reported in patients with mild cognitive impairment.

In our experimental conditions, we found a statistical difference in $FetO_2$ between groups when the participants breathed spontaneously. The values of $FetO_2$ and $FetCO_2$, change from one breath to another in relation to the natural changes of the VT (Volume Tidal). For example, increasing VT will lead to an increase in $FetO_2$ and a decrease in $FetCO_2$ (Slessarev et al., 2007). In consequence, another reason that may have been influenced the variations in $FetO_2$ is that it may have been induced by different respiratory characteristics and techniques observed in mTBI participants.

CONCLUSION

Thanks to this study we can say that the medio-lateral variations evaluated using the MLroo parameter cannot sometimes be considered as a marker for long-term changes. If, as in our case, the participants who have suffered concussion turn out to be particularly trained, their balance values and therefore MLroo will also be particularly improved compared to a non-professional participant.

Similarly, the hypercapnia phase should not be the only phase considered about brain oxygenation, but from the results obtained, we can say that the rest and recovery phases are both of particular statistical interest showing a lower level of brain oxygenation. For this reason, it would be interesting to assess if these participants, trained with a specific physical activity, can modify their brain oxygenation levels.

Finally, the values of $FetO_2$ should be considered in relation to the breathing method adopted by the participants, so it may be risky to rely only on this parameter.

Limitations

There are limitations of the present work. One of the aspects that may have negatively affected the quality of the data, is related to the great variability between the participants, in particular regarding age. To ensure the high level of performance of these participants (national, European and World champions) we neglected the uniformity of personal data, inserting participants that had $\pm$ 9 years of difference between them. In addition to this, we had to group people from very different sport categories, thus having a difference of up to $\pm$ 15.62 kg in body mass.

Another limitation regards the equipment used for measuring the amount of $\Delta[HbO_2]$ and $\Delta[HHb]$ that allowed to obtain measurements from the transcranial zone unlike the whole brain.

A limit of our study is we could not perform a confirming MRI imaging study for brain injury, because some participants refused to undergo it. This behavior was probably associated with the stigma and fear to have a brain injury and the discomfort of MRI.

Another limitation concerns the samples size that are limited because we tested available elitè athletes: the reason is that in Italy is not easy to find elitè athletes in this field of application; in addition, these athletes have to be concussed and this factor contributes to further reduce the sample.

Since we are investigating brain oxygenation, we considered male and female as comparable subjects, falling into the same group; we didn't consider sex as a discerning variable.

DATA AVAILABILITY STATEMENT

The raw data supporting the conclusions of this article will be made available by the authors, without undue reservation.

ETHICS STATEMENT

The studies involving human participants were reviewed and approved by Ethics Committee of the University of Bologna, Italy. The patients/participants provided their written informed consent to participate in this study.

AUTHOR CONTRIBUTIONS

PT and AC conceived of the presented idea, developed the theory and performed the computations, verified the analytical methods, and carried out the experiment. AC encouraged PT to investigate mTBI and NIRS exams and supervised the findings of this work. PT wrote the manuscript with support from AC and GD'A. GD'A helped supervise the final version of the manuscript. All authors discussed the results and contributed to the final manuscript.

ACKNOWLEDGMENTS

We thank all the athletes who participated in this study.

REFERENCES

Beaulieu, C., Turcotte-Giroux, A., Carrier-Toutant, F., Brisson, B., Jolicoeur, P., and De Beaumont, L. (2019). Long-term effects of concussions on psychomotor speed and cognitive control processes during motor sequence learning. *J. Psychophysiol.* 33, 96–108. doi: 10.1027/0269-8803/a000213

Bhambhani, Y., Malik, R., and Mookerjee, S. (2007). Cerebral oxygenation declines at exercise intensities above the respiratory compensation threshold. *Respir. Physiol. Neurobiol.* 156, 196–202. doi: 10.1016/j.resp.2006.08.009

Bishop, S. A., and Neary, J. P. (2018). Assessing prefrontal cortex oxygenation after sport concussion with near-infrared spectroscopy. *Clin. Physiol. Funct. Imaging* 38, 573–585. doi: 10.1111/cpf.12447

Błaszczyk, J. W. (2016). Gait & Posture The use of force-plate posturography in the assessment of postural instability. *Gait Posture* 44, 1–6. doi: 10.1016/j.gaitpost.2015.10.014

Brush, C. J., Ehmann, P. J., Olson, R. L., Bixby, W. R., and Alderman, B. L. (2018). Do sport-related concussions result in long-term cognitive impairment? A review of event-related potential research. *Int. J. Psychophysiol.* 132, 124–134. doi: 10.1016/j.ijpsycho.2017.10.006

Cassidy, J. D. (2004). Incidence, Risk factors and prevention of mild traumatic brain injury: results of the who collaborating centre task force on mild traumatic brain injury. *J. Forensic Odonto-Stomatol.* 29, 20–29. doi: 10.1080/16501960410023732

Cifu, D., Hurley, R., Peterson, M., Cornis-Pop, M., Rikli, P. A., Ruff, R. L., et al. (2009). Clinical practice guideline: Management of Concussion/Mild Traumatic Brain Injury. *J. Rehabili. Res. Dev.* 46:CP1. doi: 10.1682/JRRD.2009.06.0076

Fahr, R., Best, N., Bocker, B., Derlien, S., and Smolenski, U. C. (2015). Beeinflussung posturaler Kontrolle durch Kampfsport - eine narrative Literaturrecherche (The Effects of Martial Arts Training on Postural Control - A Narrative Review). *Physikalische Medizin Rehabilitationsmedizin Kurortmedizin* 25, 181–186. doi: 10.1055/s-0034-1398684

Finkbeiner, N. W. B., Max, J. E., Longman, S., and Debert, C. (2016). Knowing what we don't know: Long-term psychiatric outcomes following adult concussion in sports. *Canad. J. Psychiatry* 61, 270–276. doi: 10.1177/0706743716644953

Fitts, P. M. (1954). The information capacity of the human motor system in controlling the amplitude of movement. *J. Exp. Psychol.* 47, 381–391. doi: 10.1037/h0055392

Guskiewicz Kevin, M. (2005). Association between recurrent concussion and late-life cognitive impairment in retired professional football players. *Neurosurgery* 57, 719–726. doi: 10.1093/neurosurgery/57.4.719

Hecimovich, M., King, D., Dempsey, A., Gittins, M., and Murphy, M. (2019). *In situ* use of the King-Devick eye tracking test and changes seen with sport-related concussion: saccadic and blinks counts. *Phys. Sportsmed.* 47, 78–84. doi: 10.1080/00913847.2018.1525261

Hoshi, Y., Kobayashi, N., and Tamura, M. (2001). Interpretation of near-infrared spectroscopy signals: a study with a newly developed perfused rat brain model. *J. Appl. Physiol.* 90, 1657–1662. doi: 10.1152/jappl.2001.90.5.1657

Howell, D. R., Myer, G. D., Grooms, D., Diekfuss, J., Yuan, W., and Meehan, W. P. (2019). Examining motor tasks of differing complexity after concussion in adolescents. *Arch. Phys. Med. Rehabil.* 100, 613–619. doi: 10.1016/j.apmr.2018.07.441

Ivan, N., Joyce, L., and Hwee, B. W. (2004). Effect of head posture on cerebral hemodynamics. *Neurosurgery* 54, 593–597. doi: 10.1017/CBO9781107415324.004

Jiang, D., Lin, Z., Liu, P., Sur, S., Xu, C., Hazel, K., et al. (2019). Normal variations in brain oxygen extraction fraction are partly attributed to differences in end-tidal CO2. *J. Cereb. Blood Flow Metab.* 40, 1492–1500. doi: 10.1177/0271678X19867154

Jünger, E. C., Newell, D. W., Grant, G. A., Avellino, A. M., Ghatan, S., Douville, C. M., et al. (1997). Cerebral autoregulation following minor head injury. *J. Neurosurg.* 86, 425–432. doi: 10.3171/jns.1997.86.3.0425

Kaj, B., (2016). Traumatic brain injuries. *Crit. Find. Neuroradiol.* 2, 211–217. doi: 10.1007/978-3-319-27987-9_21

Kleinschmidt, A., Obrig, H., Requardt, M., Merboldt, K.-D., Dirnagl, U., Villringer, A., et al. (1996). Simultaneous recording of cerebral blood oxygenation changes during human brain activation by magnetic resonance imaging and near-infrared spectroscopy. *J. Cereb. Blood Flow Metab.* 16, 817–826. doi: 10.1097/00004647-199609000-00006

Kontos, A. P., Elbin, R. J., and Collins, M. W. (2006). "Aerobic fitness and concussion outcomes in high school football," in *Foundations of Sport-Related Brain Injuries* eds Slobounov, S., and Sebastianelli, W. (Boston, MA: Springer US). doi: 10.1007/0-387-32565-4_14

Kontos, A. P., Sufrinko, A., Sandel, N., Emami, K., and Collins, M. W. (2019). Sport-related concussion clinical profiles:clinical characteristics, targeted treatments, and preliminary evidence. *Curr. Sports Med. Rep.* 18, 82–92. doi: 10.1249/JSR.0000000000000573

Len, T. K., Neary, J. P., Asmundson, G. J. G., Goodman, D. G., Bjornson, B., and Bhambhani, Y. N. (2011). Cerebrovascular reactivity impairment after sport-induced concussion. *Med. Sci. Sports Exerc.* 43, 2241–2248. doi: 10.1249/MSS.0b013e3182249539

Martland, H. S. (1928). Punch drunk. *J. Am. Med. Assoc.* 91:1103. doi: 10.1001/jama.1928.02700150029009

McCrory, P., Meeuwisse, W., Dvorák, J., Aubry, M., Bailes, J., Broglio, S., et al. (2017). Consensus statement on concussion in sport—the 5thinternational conference on concussion in sport held in Berlin, October 2016. *Br. J. Sports Med.* 51, 838–847. doi: 10.1136/bjsports-2017-097699

MeSH subject heading scope note (2003). *Post-Concussion Syndrome*. [MeSH Subject Heading Scope Note]. Available online at: https://www.ncbi.nlm.nih.gov/mesh/?term=post$+$concussion$+$syndrome&report=Full&format=text

Mirow, S., Wilson, S., Weaver, L. K., Churchill, S., Deru, K., and Lindblad, A. S. (2016). Linear analysis of heart rate variability in post-concussive syndrome. *Undersea Hyperb Med Soc.* 43, 531–547.

Mueller, S. T., and Piper, B. J. (2014). The Psychology Experiment Building Language (PEBL) and PEBL test battery. *J. Neurosci. Methods* 184, 327–331. doi: 10.1016/j.jneumeth.2009.08.007

Neary, J. P., Dudé, C. M., Singh, J., Len, T. K., and Bhambhani, Y. N. (2020). Pre-frontal cortex oxygenation changes during aerobic exercise in elite athletes experiencing sport-related concussion. *Front. Hum. Neurosci.* 14:35. doi: 10.3389/fnhum.2020.00035

Prieto, T. E., Myklebust, J. B., Hoffmann, R. G., Lovett, E. G., and Myklebust, B. M. (1996). Measures of postural steadiness: Differences between healthy young and elderly adults. *IEEE Transact. Biomed. Eng.* 43, 956–966. doi: 10.1109/10.532130

Rupp, T., and Perrey, S. (2008). Prefrontal cortex oxygenation and neuromuscular responses to exhaustive exercise. *Eur. J. Appl. Physiol.* 102, 153–163. doi: 10.1007/s00421-007-0568-7

Slessarev, M., Han, J., Mardimae, A., Prisman, E., Preiss, D., Volgyesi, G., et al. (2007). Prospective targeting and control of end-tidal CO2 and O2 concentrations. *J. Physiol.* 581, 1207–1219. doi: 10.1113/jphysiol.2007.129395

Stern, R. A., Riley, D. O., Daneshvar, D. H., Nowinski, C. J., Cantu, R. C., and McKee, A. C. (2011). Long-term consequences of repetitive brain trauma: chronic traumatic encephalopathy. *PM and R* 3, S460–S467. doi: 10.1016/j.pmrj.2011.08.008

Taylor, K. M., Kioumourtzoglou, M.-A., Clover, J., Coull, B. A., Dennerlein, J. T., Bellinger, D. C., et al. (2018). Concussion history and cognitive function in a large cohort of adolescent athletes. *Am. J. Sports Med.* 46, 3262–3270. doi: 10.1177/0363546518798801

Thomas, B. P., Sheng, M., Tseng, B. Y., Tarumi, T., Martin-Cook, K., Womack, K. B., et al. (2017). Reduced global brain metabolism but maintained vascular function in amnestic mild cognitive impairment. *J. Cereb. Blood Flow Metabo.* 37, 1508–1516. doi: 10.1177/0271678X16658662

Wolf, M., Ferrari, M., and Quaresima, V. (2007). Progress of near-infrared spectroscopy and topography for brain and muscle clinical applications. *J. Biomed. Opt.* 12:062104. doi: 10.1117/1.2804899

Conflict of Interest: The authors declare that the research was conducted in the absence of any commercial or financial relationships that could be construed as a potential conflict of interest.

Publisher's Note: All claims expressed in this article are solely those of the authors and do not necessarily represent those of their affiliated organizations, or those of the publisher, the editors and the reviewers. Any product that may be evaluated in this article, or claim that may be made by its manufacturer, is not guaranteed or endorsed by the publisher.

frontiers in Sports and Active Living

ORIGINAL RESEARCH
published: 28 February 2022
doi: 10.3389/fspor.2022.814975

Accelerated Muscle Deoxygenation in Aerobically Fit Subjects During Exhaustive Exercise Is Associated With the *ACE* Insertion Allele

Benedikt Gasser[1], Martino V. Franchi[1†], Severin Ruoss[2], Annika Frei[1], Werner L. Popp[2], David Niederseer[3], Silvio Catuogno[4], Walter O. Frey[4†] and Martin Flück[5]**

[1] Departement für Bewegung und Sport – Universität Basel, Basel, Switzerland, [2] Spinal Cord Injury Center, Balgrist University Hospital, Zurich, Switzerland, [3] Department of Cardiology, University Hospital Zurich, University of Zurich, Zurich, Switzerland, [4] Swiss Olympic Medical Center, Balgrist University Hospital, Zurich, Switzerland, [5] Laboratory for Muscle Plasticity, University of Zurich, Balgrist Campus, Zurich, Switzerland

Introduction: The insertion/deletion (I/D) polymorphism in the gene for the major regulator of vascular tone, angiotensin-converting enzyme-insertion/deletion (ACE-I/D) affects muscle capillarization and mitochondrial biogenesis with endurance training. We tested whether changes of leg muscle oxygen saturation (SmO_2) during exhaustive exercise and recovery would depend on the aerobic fitness status and the ACE I/D polymorphism.

Methods: In total, 34 healthy subjects (age: 31.8 ± 10.2 years, 17 male, 17 female) performed an incremental exercise test to exhaustion. SmO_2 in *musculus vastus lateralis* (VAS) and musculus gastrocnemius (GAS) was recorded with near-IR spectroscopy. Effects of the aerobic fitness status (based on a VO_{2peak} cutoff value of 50 ml O_2 min^{-1} kg^{-1}) and the ACE-I/D genotype (detected by PCR) on kinetic parameters of muscle deoxygenation and reoxygenation were assessed with univariate ANOVA.

Results: Deoxygenation with exercise was comparable in VAS and GAS ($p = 0.321$). In both leg muscles, deoxygenation and reoxygenation were 1.5-fold higher in the fit than the unfit volunteers. Differences in muscle deoxygenation, but not VO_2peak, were associated with gender-independent ($p > 0.58$) interaction effects between aerobic fitness × ACE-I/D genotype; being reflected in a 2-fold accelerated deoxygenation of VAS for aerobically fit than unfit ACE-II genotypes and a 2-fold higher deoxygenation of GAS for fit ACE-II genotypes than fit D-allele carriers.

Discussion: Aerobically fit subjects demonstrated increased rates of leg muscle deoxygenation and reoxygenation. Together with the higher muscle deoxygenation in aerobically fit ACE-II genotypes, this suggests that an ACE-I/D genotype-based personalization of training protocols might serve to best improve aerobic performance.

Keywords: cycling, aerobic metabolism, oxygen saturation, gene, exhaustive pedaling

OPEN ACCESS

Edited by:
Giancarlo Condello, University of Parma, Italy

Reviewed by:
Christos Yapijakis, National and Kapodistrian University of Athens, Greece
Hemant Kumar Mishra, University of Minnesota Twin Cities, United States

****Correspondence:***
Benedikt Gasser
benediktandreas.gasser@unibas.ch
Martin Flück
martin.flueck@tutanota.com

†Present addresses:
Martino V. Franchi, Department of Biomedical Sciences, Institute of Physiology, University of Padova, Padova, Italy
Walter O. Frey, Klinik Hirslanden, Zürich, Switzerland

Specialty section:
This article was submitted to Exercise Physiology, a section of the journal Frontiers in Sports and Active Living

Received: *14 November 2021*
Accepted: *24 January 2022*
Published: *28 February 2022*

Citation:
Gasser B, Franchi MV, Ruoss S, Frei A, Popp WL, Niederseer D, Catuogno S, Frey WO and Flück M (2022) Accelerated Muscle Deoxygenation in Aerobically Fit Subjects During Exhaustive Exercise Is Associated With the ACE Insertion Allele. Front. Sports Act. Living 4:814975. doi: 10.3389/fspor.2022.814975

INTRODUCTION

Exercise pronouncedly elevates the energy expenditure of working skeletal muscle due to increased ATPase activity of the actin-myosin filaments and ion pumps (Rolfe and Brown, 1997). The resultant energy demand is met by enhanced aerobic combustion of organic substrates in mitochondria (Tonkonogi and Sahlin, 2002; Ryan et al., 2014); giving rise to the commonly observed oxygen deficit with exercise (Lukin and Ralston, 1962; Nioka et al., 1998). The implicated enhancement of mitochondrial respiration in contracting skeletal muscle can be readily, and indirectly, detected based on an increased signal for deoxygenated myoglobin/hemoglobin as measurable with near-IR spectroscopy (NIRS) (Nioka et al., 1998; Richardson et al., 2001; Perrey and Ferrari, 2018). The thereby observable decreases in muscle oxygen saturation (SmO_2) are graded to the duration and intensity of exercise (Nioka et al., 1998; Chuang et al., 2002) and seem to be faster at the local, compared to the systemic (i.e., cardiopulmonary) level (Nioka et al., 1998; Grassi and Quaresima, 2016).

The changes in muscle oxygen saturation during intense prolonged exercise are dependent on the endurance capacity, respectively, aerobic fitness (Hoppeler et al., 1985). Thereby the general consensus is that endurance-trained individuals demonstrate elevated rates of oxygen desaturation with the onset of exercise (deoxygenation), compared to unfit subjects. Accordingly, an improved regain of oxygen saturation (reoxygenation) with the offset of exercise (Jones et al., 2017; Perrey and Ferrari, 2018).

Plausibly the alterations changes in oxygen saturation with on and offset of exercise are in a linear relationship to the aerobic capacity of skeletal muscle (Hoppeler et al., 1985; Jones et al., 2002; Tonkonogi and Sahlin, 2002; di Prampero, 2003; Fluck and Hoppeler, 2003; Flueck et al., 2010; Grassi and Quaresima, 2016). The capacity is set by the volume content of mitochondria which demonstrates itself considerable variability in relation to the maximal or peak oxygen uptake ($peakVO_2$) (Hoppeler et al., 1985; Jones et al., 2002; Tonkonogi and Sahlin, 2002; di Prampero, 2003; Fluck and Hoppeler, 2003; Flueck et al., 2010; Grassi and Quaresima, 2016). Aside, vaso-regulatory factors modulate mitochondria-dependent muscle respiration by modulating the perfusion and consequently oxygen supply of recruited muscle fibers with the onset of contraction (Hoppeler et al., 1985; Zoll et al., 2002; Clifford and Hellsten, 2004; Roseguini et al., 2010; Korthuis, 2011; Hellsten and Nyberg, 2015).

Genetic influences on the regulation of blood flow with exercise are known to contribute to muscle energy metabolism (van Ginkel et al., 2015). Particularly, we have identified that a frequent insertion/deletion polymorphism in the gene that codes for angiotensin-converting enzyme (*ACE*) is associated with differences in blood flow with the onset of intense cyclic exercise, and oxygen-dependent mitochondria metabolism as well as with fluctuations in gene expression (Jackman et al., 2008; Dimitriou et al., 2010; Williams et al., 2017; Fluck et al., 2019). The implicated genetic mechanism is mediated by differences in the expression of the encoded ACE protease, which processes the main vasoconstrictor peptide, angiotensin 2, and the degradation of the vasodilatative kinin peptides (Jones et al., 2002). The presence of a 287-basepair insertion (the I-allele) in intron 16 of the *ACE* gene silences tissue expression of *ACE* transcripts, reducing ACE activity and angiotensin 2 levels in the blood; whereas its absence (i.e., deletion, D-allele) is associated with the inverse effects (Jackman et al., 2008; Vaughan et al., 2013; Mathes et al., 2015; van Ginkel et al., 2016; Fluck et al., 2019). *ACE* I-allele carriers demonstrate exaggerated gains in the volume density of mitochondria in knee extensor muscle with repeated endurance training (Vaughan et al., 2013; Fluck et al., 2019); indicating that ACE-insertion/deletion (I/D) genotype-associated differences in aerobic metabolism develop with repeated sessions of endurance exercise.

Importantly, healthy ACE-DD genotypes demonstrate a lower muscle capillarization and a reduced capillary perfusion with endurance exercise than *ACE* I-allele carriers (van Ginkel et al., 2015; Valdivieso et al., 2017). Collectively, the observed ACE-I/D-related response to acute and repeated endurance exercise indicated either an elevated vasoconstriction or a lower potential for vasodilatation, in *ACE* D-allele carriers; giving rise to a lowered capacity for oxygen delivery to recruited skeletal muscles during and after exercise (Buikema et al., 1996; O'Donnell et al., 1998; van Dijk et al., 2000; Williams et al., 2000; Woods et al., 2002; Fluck and Hoppeler, 2003; Flueck et al., 2010).

Whether the reported influence of the ACE-I/D gene polymorphism on mitochondria and capillary processes and connected metabolic processes of skeletal muscle results in differences in muscle oxygen saturation during intense exercise is not known. Toward this end we tested the hypotheses, the ACE-I/D polymorphism is associated with (i) an accelerated and more extensive deoxygenation in aerobically fit subjects I-allele carriers compared to non-I-allele carriers, and whether (ii) the reoxygenation is accelerated in *ACE* I-allele carriers and may be further accelerated by a good fitness state.

METHODS

Study Design

This study had a cross-sectional design in which the subjects performed a ramp test to determine VO_{2peak}, Peak Power Output (PPO) and SmO_2 in a knee extensor muscle (VAS) and an ankle extensor muscle (GAS). Prospective power analysis on the association of the ACE-I/D genotype with aerobic processes in skeletal muscle indicated that a total number of 24 replicas (distributing equally according to each of the four combinations of genotype and fitness type) is sufficient enough to reveal statistically significant associations between the ACE-I/D genotype × fitness state and differences in muscle deoxygenation (**Supplementary Table 1**). As the average age of participants was 31.81 ± 10.18 years in line with standard guidelines subjects were assigned as being aerobically fit or unfit based on whether their respective VO_{2peak} met the criteria of being above or below 50 $mL \cdot min^{-1} \cdot kg^{-1}$ (Valdivieso et al., 2017; ACSM, 2021). ACE I/D gene polymorphism genotyping was performed retrospectively.

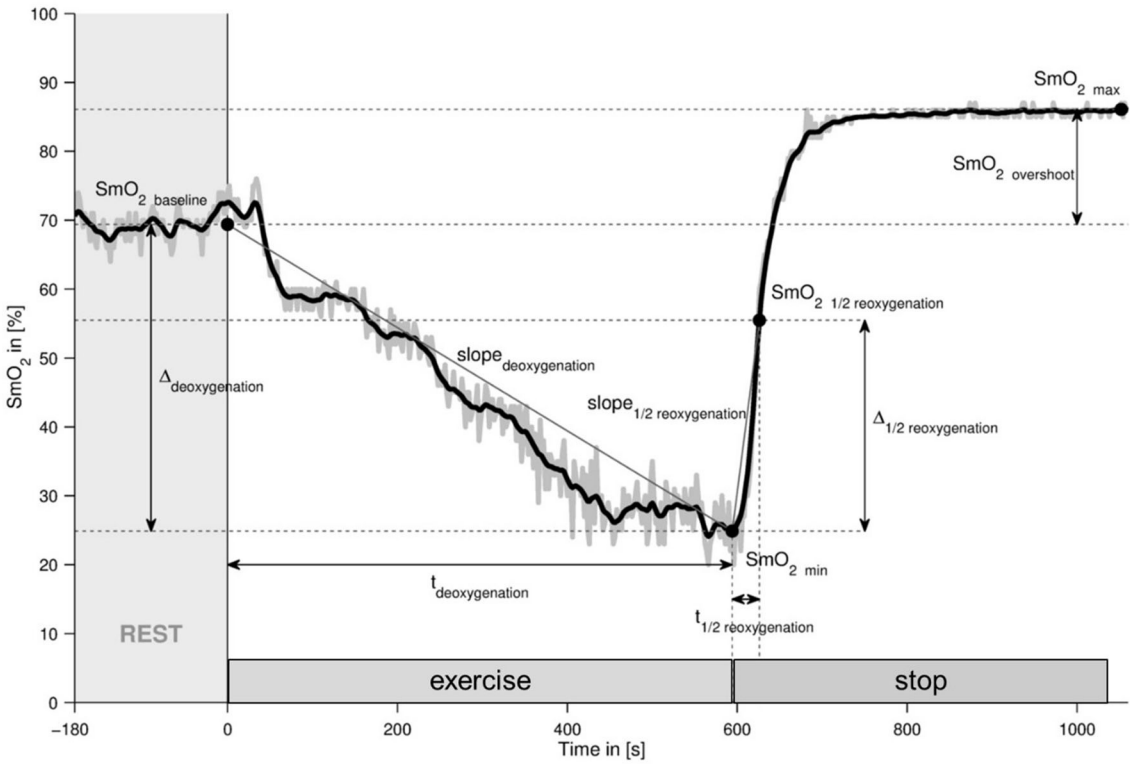

FIGURE 1 | Representative example of the recorded SmO_2 course during the ramp test. Line graph visualizing the raw (gray) and processed data (black) and the derived parameters. SmO_2, muscle oxygen saturation; t, time; min, minimum; max, maximum. The extracted parameters are declared.

Subjects/Ethics

A total of 34 recreational active healthy subjects, i.e., 17 women and 17 men, participated in this study. Subject recruitment was by word-of-mouth and a public announcement with flyers in the professional or private environment of the research group. All subjects volunteered after their self-assessment that they met the requirements of presenting a good health and an age between 20 and 70 years. Upon the provision of an informed consent, the further specific inclusion criterium of an unobtrusive cardiovascular system was verified based on an inconspicuous ECG during exercise in a ramp test on a cycle ergometer. The exclusion criteria comprised evidence for a relevant valvular heart disease, arterial hypertension (blood pressure at rest > 140/90 mm Hg), arrhythmogenic cardiomyopathy, smoker, drug, or alcohol disease, known or suspected non-compliance with the protocol, or a contraindication for ethical reasons. All the 34 participating volunteers qualified for the inclusion in this study. The study has been approved by the Ethics Committee of the Canton of Zurich. All the investigations were conducted in accordance with the ethical standards of the Declaration of Helsinki of 1964.

Ramp Test

Subjects performed a test of incremental exercise on an electrically braked cycle ergometer (Ergoselect 200, Ergoline, Bitz, Germany, UK) being accompanied with spiroergometric and NIRS measurements. Prior to the test, anthropometric data (height and body mass) were collected, and the body mass index (BMI) was calculated. A resting ECG was recorded and verified by a physician to ensure that the subjects did not demonstrate a counter-indication to conduct the ramp test.

The test protocol was conducted in an air-conditioned laboratory at a standardized temperature of 20°C according to a modified version of a published protocol (Whipp et al., 1981). In brief, the test started with a 3 min period of rest, when subjects sat still on the cycle ergometer while maintaining a normal breathing pattern. Subsequently, subjects started pedaling at an initial power (75 W for women and 100 W for men). Target power was increased every 20 s (18 $W \cdot min^{-1}$ for women and 30 $W \cdot min^{-1}$ for men). The subjects were asked to keep a constant self-chosen pedal cadence throughout the test (optimally between 70 and 100 rpm). The test was stopped when the subjects experienced volitional exhaustion and/or were not able to maintain the target pedal cadence. Subsequently, recordings continued during a period of 8 min, when subjects rested in a seated position on the cycle ergometer.

Pulmonary gas exchange (oxygen uptake) was measured after proper calibration through a breath-by-breath spiroergometry system (MetaLyzer® 3B-R2, CORTEX Biophysics, Leibzig, Germany). VO_{2peak} and PPO were defined as the last achieved, and peak, values before exhaustion manifested. To non-invasively measure SmO_2 during the ramp test, a muscle NIRS

TABLE 1 | Physiological characteristics.

Group	*n*	Age	Body mass	Height	BMI	VO2peak	PPO
		[years]	[kg]	[m]	[kg m^{-2}]	[mL·min-1·kg^{-1}]	[W]
All	34	31.81 ± 10.18	69.34 ± 10.43	173.00 ± 8.40	23.08 ± 2.39	46.03 ± 9.61	298.26 ± 79.29
Aerobically unfit	20	32.07 ± 12.09	69.00 ± 10.80	170.60 ± 7.63	23.61 ± 2.55	39.89 ± 7.32	251.90 ± 61.09
Aerobically fit	14	31.43 ± 7.00	69.83 ± 10.26	176.43 ± 8.53	22.31 ± 1.98	54.79 ± 3.94	364.50 ± 49.75
D-allele carriers	25	32.17 ± 10.71	67.67 ± 10.46	172.92 ± 9.33	22.51 ± 1.96	46.42 ± 9.60	295.76 ± 80.51
D-allele non-carriers	9	30.81 ± 9.02	73.99 ± 9.35	173.22 ± 5.49	24.66 ± 2.87	44.94 ± 10.14	305.22 ± 80.09
Unfit D-allele carriers	14	31.97 ± 12.91	67.43 ± 10.51	170.36 ± 8.60	23.11 ± 1.91	39.75 ± 6.88	249.36 ± 68.56
Unfit D-allele non-carriers	6	32.30 ± 11.04	72.67 ± 11.55	171.17 ± 5.31	24.78 ± 3.58	40.22 ± 8.97	257.83 ± 43.57
Aerobically fit D-allele carriers	11	32.41 ± 7.65	67.97 ± 10.91	176.18 ± 9.58	21.74 ± 1.81	54.90 ± 4.28	354.82 ± 50.95
Aerobically fit D-allele non-carriers	3	27.84 ± 1.03	76.63 ± 0.55	177.33 ± 3.51	24.40 ± 0.82	54.40 ± 3.02	400.00 ± 26.46
Aerobic fitness	*p*	0.644	0.601	0.084	0.339	<0.001	<0.001
	η2	0.007	0.009	0.096	0.031	0.516	0.486
Genotype	*p*	0.626	0.114	0.772	0.022	0.995	0.258
	η2	0.008	0.081	0.003	0.163	0.000	0.042
Aerobic fitness	*p*	0.574	0.691	0.960	0.590	0.853	0.436
× genotype	η2	0.011	0.005	0.000	0.010	0.001	0.020

Values represent mean ± SD of the measurements for the studied 34 subjects, as well as the p-values and effect sizes (η2) and observed power, for the effect of ACE-I/D genotype and aerobic fitness status, and their respective interaction. ANOVA with post-hoc test of Fisher. Underlined p-values were deemed to reflect significant effects.

monitor (Moxy, Fortiori Design LLC, Minnesota, USA) was used as established (Fitze et al., 2019). The device uses four different light sources covering wavelengths in the range of 630 to 850 nm and a modified Beer–Lambert law to perform measurements of SmO_2. For measurements, two NIRS monitors were positioned on specific sites of the skin that were shaved using a disposable razor (Gallant, Dynarex, Orangeburg, USA) and cleaned with an alcohol swab (Webcol™, Covidien™, Dublin, Ireland). One monitor was placed on the lower third of the VAS in the middle of the muscle belly on the left leg of the subjects. The other monitor was placed on the GAS, onto a fictive line between the Malleolus medialis and medial plateau of the tibia. Sensors were attached using the recommended tape (Moxy Adhesive Attachments, Fortiori Design LLC, Minnesota, USA). In order to protect the NIRS device from ambient light, it was covered with an adhesive non-woven fabric (Hypafix®, BSN medical, Hamburg, Germany). Recording started synchronized with the start of the ramp test (with 3 min of rest).

Genotyping

Buccal swabs were collected with an ear-bud, air-dried in a laboratory fume cupboard (Secuflow 1500, Waldner, Wangen, Germany, UK) for 2 h and then stored at +4°C. Subjects were told not to consume any food or to drink in the 30 min prior to sample collection.

Deoxyribonucleic acid extraction was performed according to a commercially available protocol (QIAamp® DNA Mini Kit, Qiagen, Hilden, Germany, UK). In brief, the cotton swab was separated from the stick with scissors, followed by incubation steps in a 2 ml microcentrifuge tube to degrade contaminating ribonucleic acids, lyse the cells with QIAGEN® proteinase K, and enrich the contained genomic DNA with QIAamp Mini spin columns with the help of an air-cooled microcentrifuge (Prism™, Labnet International, Edison, USA). The resulting sample (150 µl) elute was stored at +4°C until genotyping was performed.

Genotyping was carried out by polymerase chain reactions in 48 well-plates followed by high-resolution melt analysis using a real-time PCR system (Eco™, illumina®, San Diego, USA) according to the instructions. The reaction mix per well-included for each sample 2 µl of the DNA solution, 1 µl distilled H_2O, 1 µl of $MgCl_2$ (25 mmol), 5 µl of KAPA HRM FAST Master Mix (2×) and 1 µl of the I- or D-allele-specific primer mix (2 µmol). The primer mix for the detection of the 66 bp amplicon, which is specific for the I-allele, contained the primer ACE2 (5′-TGGGATTACAGGCGTGATACAG-3′) and the primer ACE3 (5′-ATTTCAGAGCTGGAATAAAATT-3′). The primer mix for the detection of the 83 bp amplicon, which is specific to the D allele, contained primers ACE1 (5′-CATCCTTTCTCCCATTTCTC-3′) and ACE3 (5′-ATTTCAGAGCTGGAATAAAATT-3′). The sealed plate was centrifuged to remove any bubbles and was submitted to a standardized thermal protocol as published (Valdivieso et al., 2017). Genotype analysis was carried out using a genetic variation analysis software (EcoStudy Version 5.0, Illumina®, San Diego, California, USA). The respective genotype was verified based on the presence of an allele-specific melting curve for the amplified products in the respective PCR reactions, as established by microsequencing of PCR reactions from reference samples at a commercial provider (Microsynth, Balgach, Switzerland, UK) (Valdivieso et al., 2017).

Data Processing

A representative example of the recorded and processed timeline of SmO_2 during the ramp test, as well as the extracted parameters,

TABLE 2 | Association between fitness status and angiotensin-converting enzyme-insertion/deletion (ACE-I/D) genotype on parameters of muscle oxygen kinetics during the ramp test of cycling exercise.

Phase	Parameter	Statistical size	Fitness	Genotype	Fitness × genotype	Muscle	Muscle × fitness	Muscle × genotype	Fitness × genotype
Rest	$SmO_{2baseline}$	*p*-value	0.018	0.027	0.151	0.004	0.355	0.812	0.305
		η^2	0.090	0.079	0.034	0.123	0.014	0.001	0.018
Exercise	SmO_{2min}	*p*-value	≤0.001	0.597	0.098	0.052	0.208	0.031	0.296
		η^2	0.240	0.005	0.045	0.058	0.026	0.075	0.018
Exercise	$\Delta_{deoxygenation}$	*p*-value	≤0.001	0.141	0.020	0.321	0.891	0.174	0.920
		η^2	0.302	0.036	0.087	0.015	0.000	0.031	0.000
Exercise	$t_{deoxygenation}$	*p*-value	0.011	0.174	0.151	0.586	0.834	0.519	0.472
		η^2	0.104	0.031	0.034	0.005	0.001	0.007	0.009
Exercise	$Slope_{deoxygenation}$	*p*-value	0.005	0.598	0.006	0.175	0.902	0.306	0.575
		η^2	0.125	0.005	0.118	0.029	0.000	0.017	0.005
Stop	SmO_{2max}	*p*-value	0.013	0.364	0.357	≤0.001	0.526	0.945	0.451
		η^2	0.098	0.014	0.014	0.674	0.007	0.000	0.009
Stop	$\Delta 1/2_{reoxygenation}$	*p*-value	≤0.001	0.705	0.101	≤0.001	0.105	0.131	0.765
		η^2	0.270	0.002	0.044	0.392	0.043	0.038	0.001
Stop	$t1/2_{reoxygenation}$	*p*-value	0.262	0.818	0.571	0.123	0.822	0.639	0.828
		η^2	0.021	0.001	0.005	0.037	0.001	0.004	0.001
Stop	$Slope_{1/2reoxygenation}$	*p*-value	0.031	0.598	0.365	0.823	0.682	0.607	0.592
		η^2	0.076	0.005	0.014	0.001	0.003	0.004	0.005
Stop	$SmO_{2overshoot}$	*p*-value	0.838	0.273	0.687	≤0.001	0.182	0.793	0.842
		η^2	0.001	0.020	0.003	0.473	0.030	0.001	0.001

Values refer to the calculated level of statistical significance (p) and effect size (η^2) for the effect of the aerobic fitness state, ACE-I/D genotype (ACE-II vs. ACE-ID/ACE-DD), and muscle type on assessed parameters of deoxygenation and reoxygenation in the leg muscles of the studied 34 subjects. P-values that were deemed statistically significant (i.e., $p < 0.05$) are underlined. ANOVA with post-hoc test of least significant difference.

is shown in **Figure 1**. Data pre-processing and analysis were performed as previously described using a data processing program (MATLAB 2015a, The Mathworks, Natick, USA) (Fitze et al., 2019). In short, SmO_2 data were filtered using a 2nd order zero-phase shift Butterworth low-pass filter with a cutoff frequency of 0.03 Hz. Extraction of the values for relevant parameters was performed as previously described: $SmO_{2baseline}$ was declared as the mean value of the t3-min prerest period. The minimum SmO_2 value during the ramp test (SmO_{2min}) was determined based on the last local minimum of the filtered SmO_2 prior to reoxygenation. $\Delta_{deoxygenation}$ was set as the difference between $SmO_{2baseline}$ and SmO_2 min. $t_{deoxygenation}$ was the time from the beginning of the ramp test until SmO_{2min} was reached. $slope_{deoxygenation}$ was calculated of the values of $\Delta_{deoxygenation}$ over $t_{deoxygenation}$. SmO_{2max} was defined as the highest value achieved within the period between the start of reoxygenation and test termination. $SmO_{21/2reoxygenation}$ was defined as 50% of the difference between SmO_{2max} and SmO_{2min}. $\Delta_{1/2reoxygenation}$ was the difference between $SmO_{21/2reoxygenation}$ and SmO_{2min}. $t_{1/2reoxygenation}$ was defined as the time between SmO_{2min} and $SmO_{21/2reoxygenation}$. Slope $_{1/2reoxygenation}$ was calculated using $\Delta_{1/2reoxygenation}$ over $t_{1/2reoxygenation}$. $SmO_{2overshoot}$ represented the difference between SmO_{2max} and $SmO_{2baseline}$. Concerning the assumption of a linear process over the ramp protocol before exhaustion of SmO_2 and Power a high correlation was detected ($R = -0.981 \pm 0.214$). For the display of the average course of SmO_2 in VAS and GAS during the ramp test, the recorded raw values were averaged over 9 s intervals, and the mean and SE over all 34 samples calculated for each time point/9 s interval. For the values from the exercise phases, the "time coordinates" were scaled to the duration of a reference data set for a study participant which ceased pedaling nearest to the duration of the lower 25% quartile of $t_{deoxygenation}$, i.e., 358 s.

Statistical Analysis

An online calculator was used to determine whether the observed genotype frequency is consistent with the Hardy–Weinberg equilibrium (Rodriguez et al., 2009). Prospective and retrospective power analyses were conducted with G-Power (version 3.1.9.6, http://www.gpower.hhu.de/) and the Statistical Package for the Social Sciences (SPSS version 23, IBM, Armonk, USA), respectively. Variance homogeneity for sub-samples was analyzed with Levene Test, whereby only for $t_{1/2reoxygenation}$ ($p = 0.027$) variance inhomogeneity was deduced. Therefore, a multivariate ANOVA was used to assess the effects of the ACE I/D genotype and aerobic fitness status, and their interaction, and the influence of the muscle type and gender, on parameters of muscle oxygenation (SmO_2) during the ramp test. A co-dominant genetic model was applied to calculate the effects of the ACE I/D genotype, i.e., carriers vs. non-carriers of the D-allele. A *post-hoc* test of the least significant difference was applied to localize effects. Statistical analyses and graphical presentations were calculated with SPSS (SPSS version 23, IBM, Armonk,

USA) and assembled for presentation using MS-Office Excel and Powerpoint (Microsoft Office Professional Plus 10, Kildare, Ireland, UK). Significance was declared depending on whether a p-value below 0.05 was met.

RESULTS

Subjects Characteristics

Table 1 summarizes selected physiological and characteristics of the 34 volunteers per genotype and fitness status. Aerobically fit subjects demonstrated on average a 14.9 ml O_2 min^{-1} kg^{-1} higher specific VO_2 peak and a 112.6 W higher PPO than the unfit subjects. Body mass, BMI, height, and weight did not differ between the aerobically fit and unfit subjects.

The studied population was found to stand in Hardy-Weinberg equilibrium ($p = 0.261$). The ACE-I/D genotype was not associated with differences in VO_2peak or PPO independent of whether assessed as single effect ($p = 1.00$, $p = 0.26$) or interaction effect with the aerobic fitness state ($p = 0.85$, $p = 0.44$; **Table 1**). BMI was 2.2 kg/m^2 higher in non-carriers than carriers of the *ACE* D-allele.

Muscle Oxygen Saturation During the Ramp-Incremental Pedaling Exercise

Figure 1 visualizes an example of the alterations in SmO_2 in *musculus vastus lateralis* during the ramp-incremental pedaling exercise. SmO_2 was fairly stable during the first phase of rest (SmO_2 baseline) and then fell with the onset of contraction (deoxygenation) at an average rate of $-0.060 \pm 0.028\%$ SmO_2 s^{-1} to a minimal value (SmO_2 min) until voluntary exhaustion manifested. SmO_2 rapidly recovered with a rate of $0.736 \pm 0.459\%$ SmO_2 s^{-1}, to, or above, baseline values with the cessation of exercise (reoxygenation).

Muscle deoxygenation was similar between VAS and GAS muscle ($p = 0.321$, **Table 2**; **Figure 2**). Muscle type differences resolved for parameters of reoxygenation (Δ1/2 reoxygenation, SmO_2 max, SmO2 overshoot; **Supplementary Figure 1**), and SmO_2 at baseline (59.9 vs. 52.9%; $p = 0.004$), all being higher in VAS than GAS.

Aerobic Fitness Affects Muscle Deoxygenation and Reoxygenation During Ramp-Incremental Exercise

Parameters that characterized the deoxygenation and reoxygenation kinetics in the two-leg muscles with ramp-incremental pedaling exercise demonstrated associations with aerobic fitness (**Table 2**). **Figure 3** depicts the differences for the corresponding effect of the aerobic fitness status for the combined values for both the leg muscles.

The values for SmO_2 min (25.6%), $\Delta_{deoxygenation}$ (59.1%) and the $slope_{deoxygenation}$ (22.1%), were lower in aerobically fit compared to unfit subjects, when the $t_{deoxygenation}$ was higher in fit than unfit subjects (+24.2%). Conversely, the values for $\Delta_{1/2reoxygenation}$ (44.2%), slope $_{1/2reoxygenation}$ (+39.0%) and SmO_2 max (+9.4%) were higher in aerobically fit than unfit subjects.

When assesses separately for VAS and GAS, the values for SmO_2 min (24.8 vs. 35.1%, 22.8 vs. 28.9%), $\Delta_{deoxygenation}$ (−34.9 vs. −21.7%, −31.1 vs. −19.8%) and the $slope_{deoxygenation}$ (i.e., −0.065 vs. −0.054% SmO_2 s^{-1}, −0.056 vs. −0.045% SmO_2 s^{-1}) were all lower in aerobically fit compared to unfit subjects. Conversely, the values for $\Delta_{1/2reoxygenation}$ (27.8 vs. 18.4%, 15.5 vs. 11.6%) were higher in aerobically fit than unfit subjects. Additionally, the values for baseline SmO_2 min in GAS (53.9 vs. 48.7%), SmO_2 max in VAS (80.2 vs. 71.8%) and $t_{deoxygenation}$ in VAS (543.7 s vs. 430.3 s) were higher in fit than unfit subjects.

Differences in Muscle Deoxygenation During Ramp-Incremental Exercise Are Associated With the Interaction Between Aerobic Fitness × ACE-I/D Genotype

Baseline values for SmO2, alone, were associated with the ACE-I/D genotype ($p = 0.027$, **Table 2**). The values of two kinetic parameters resuming muscle deoxygenation, i.e., Δdeoxygenation and slope deoxygenation, demonstrated interactions between the aerobic fitness status and the ACE-I/D genotype (**Table 2**).

For both parameters, the interaction was localized to the lowest values in fit non-carriers of the *ACE* D-allele (**Figure 4**). For Δdeoxygenation, the values in the fit ACE-II genotypes were 29.4% lower than in fit non-carriers of the D-allele and 56.4% lower than in unfit ACE-II genotypes. Alike for the slope deoxygenation, the values in fit ACE-II genotypes were 52.5% lower than in unfit ACE-II genotypes and 31.3% lower than in fit carriers of the D-allele.

The interaction effect of aerobic fitness status and the ACE-I/D genotype for Δdeoxygenation and $slope_{deoxygenation}$ was not affected by the muscle type ($p = 0.920$, $p = 0.575$), and sex (**Supplementary Table 2**), where Δdeoxygenation and $slope_{deoxygenation}$ in VAS and GAS were the lowest in the fit ACE-II genotypes (**Supplementary Figure 2**).

Supplementary Table 3 depicts the average values for the observed parameters of deoxygenation and reoxygenation in both studied leg muscles for each genotype and fitness status.

DISCUSSION

The aim of this study was to investigate whether a NIRS-based measure of the balance between supply and use of oxygen during exhaustive pedaling exercise is associated with the ACE-I/D genotype and stands in dependence of the fitness state (Casey and Joyner, 2015; Ross et al., 2019). The mechanism underpinning muscle deoxygenation involves local reactions in skeletal muscle, such as contraction-induced elevations in capillary perfusion and an increased mitochondrial respiration (Badtke, 1987; Zoll et al., 2002; Clifford and Hellsten, 2004; Korthuis, 2011; Grassi and Quaresima, 2016).

The observed higher slopes and minima/maxima of muscle oxygen saturation during and after exhaustive ramp exercise are in line with previous observations on the enhanced and accelerated capacity for muscle deoxygenation of aerobically fit individuals during exhaustive pedaling exercise and subsequent

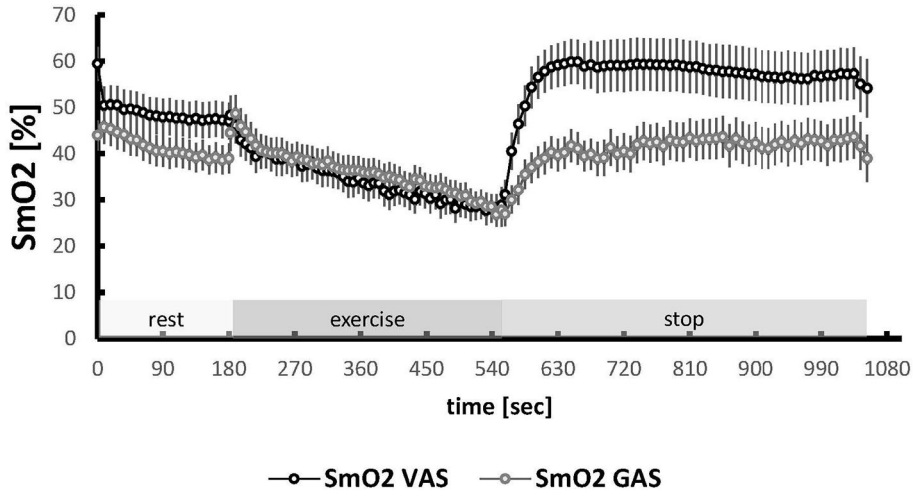

FIGURE 2 | Oxygen saturation in VAS and GAS during the ramp test. Line graph visualizing the mean + SE (circle and vertical bars) of values for SmO_2 in VAS and GAS during the course of the ramp test. The three phases of the test are indicated. Values were averaged to each 9 s interval for the measures from the 34 subjects. The time coordinates for the values during the exercise phase were scaled for each subject to the duration of a reference data set.

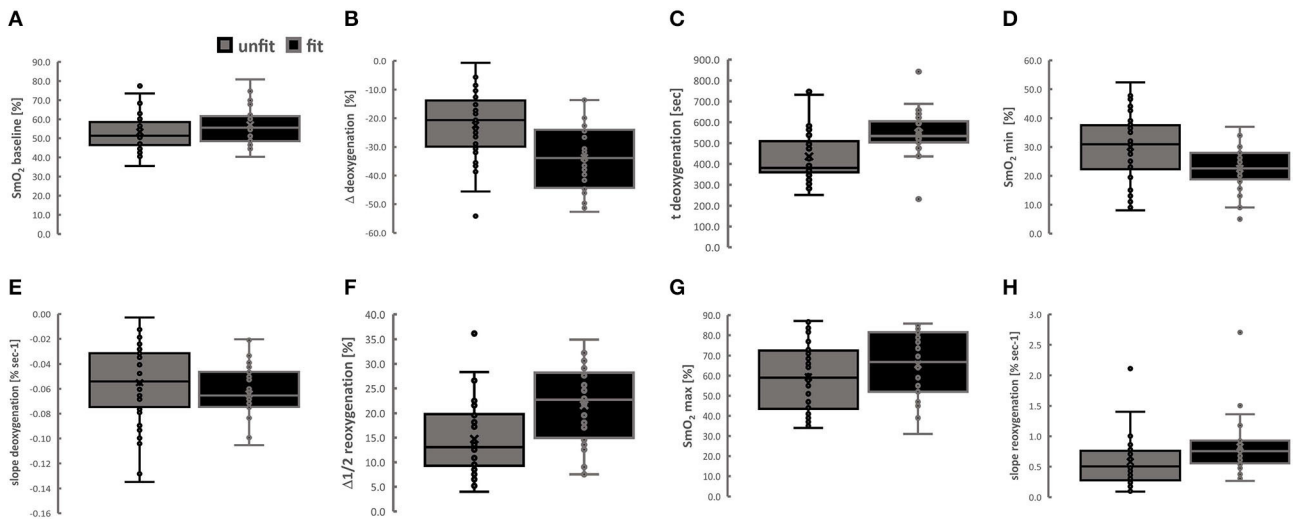

FIGURE 3 | Aerobic fitness state affects the kinetics of muscle oxygenation during exercise. Box Whisker plots (Box, 5 and 95% confidence intervals; Whisker, minima-maxima; central line, median; circle, individual values) for kinetic parameters of muscle deoxygenation **(A–E)** and reoxygenation **(F–H)** in VAS and GAS combined. Lines connect conditions demonstrating significant differences at $p < 0.05$. ANOVA for the factor "aerobic fitness" with *post-hoc* test of Fisher for the least significant difference.

reoxygenation with the offset of pedaling (**Figure 2**) (Ding et al., 2001; Brizendine et al., 2013; Casey and Joyner, 2015; Perrey and Ferrari, 2018; Ross et al., 2019). These observations support the view that NIRS-based measures of oxygen saturation are a proxy of mitochondrial activity (Pilegaard et al., 2002; Ryan et al., 2014). The resulting difference in the proxy for the local respiratory capacity between fit and unfit subjects indicated that this study would allow to identify whether the hypothesized association between the ACE-I/D genotype and kinetic aspects of oxygen saturation with exhaustive muscle work would depend on the aerobic fitness state.

Based on previous observations on ACE-I/D associated differences on angiotensin-modulated vasoconstriction (Korthuis, 2011; van Ginkel et al., 2015, 2016; Valdivieso et al., 2017), variability in exercise-induced changes in muscle oxygen saturation during the exhaustive type of pedaling exercise were expected to be associated, with the ACE-I/D genotype and the aerobic fitness status. We observed a 1.5-fold increased

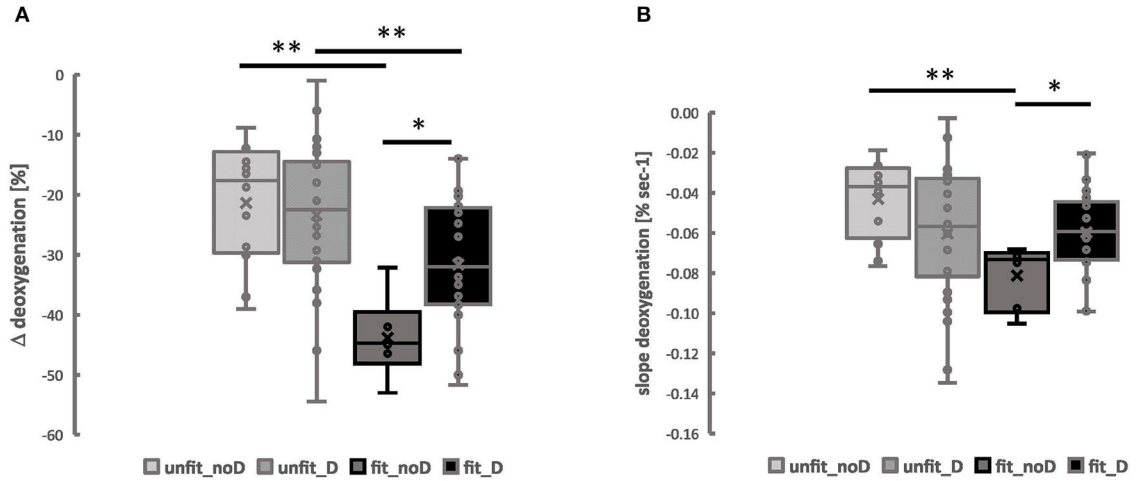

FIGURE 4 | Muscle deoxygenation during exercise is associated with the interaction between the aerobic fitness state and the angiotensin-converting enzyme-insertion/deletion (ACE-I/D) genotype. Box Whisker plots for the Δ_deoxgenation **(A)** and the slope of deoxygenation **(B)** in VAS and GAS combined in the function of the aerobic fitness status and the ACE-I/D genotype. Lines connect conditions demonstrating significant differences at $^{*}p < 0.05$ and $^{**}p < 0.01$. ANOVA for the factor "aerobic fitness" with *post-hoc* test of least significant difference.

muscle deoxygenation in the aerobically fit than unfit subjects (**Figure 3**). Accordingly, the identified slopes of deoxygenation during exhaustive ramp exercise emphasized that this difference was due to an accelerated rate of deoxygenation for both investigated leg muscles in the aerobically fit compared to the unfit subjects, i.e., VAS: −3.5 vs. 2.9% per minute; GAS: −4.1 vs. −3.3% per minute). The slope 1/2 reoxygenation was overall 1.5-fold enhanced in aerobically fit compared to unfit subjects relating to the reportedly 2-fold faster recovery rates of oxygen consumption in *musculus vastus lateralis* of endurance athletes than inactive controls (Brizendine et al., 2013).

We explain the former observations in terms of the model that the precipitous drop of muscle oxygen saturation with contraction is due to enhanced oxygen consumption in mitochondria, which is not matched by the increase in muscle perfusion (Baker et al., 2010; Jones et al., 2017). Conversely, muscle reoxygenation postexercise arises because the respiratory activity of mitochondria levels off, while muscle perfusion continues to be elevated due to the fact that muscle capillaries remain maximally perfused for a longer time (Egginton and Hudlicka, 1999; Korzeniewski, 2003; Clifford and Hellsten, 2004). Anatomical factors that modify quantitative aspects of muscle oxygen saturation, such as the content of mitochondria and the capillarization, are an integral part of the underpinning processes. Accordingly, as muscle oxygen saturation is related to mitochondrial respiratory capacity (Ryan et al., 2014), the increased muscle deoxygenation and steeper negative slope of deoxygenation with pedaling exercise in the aerobically fit subjects would be explained by the functionally more developed capacity for mitochondrial respiration due to typical increases in mitochondrial volume density in trained skeletal muscles (Hoppeler et al., 1985). By contrast, the increased slope of reoxygenation for *Musculus vastus lateralis* during recovery from exhaustive exercise in the aerobically fit compared to the unfit individuals would be driven by the total capacity for capillary perfusion because the arterioles are in a fully dilated state in the recruited knee extensor muscles (Egginton and Hudlicka, 1999; Clifford and Hellsten, 2004). This suggestion would be supported by the observation that the estimated rate of reoxygenation was 9–15-fold accelerated in the studied leg muscles for both the fit and unfit subjects, compared to the corresponding rate of deoxygenation. Consequently, our results imply that capacitive differences in capillary perfusion exist between the aerobically fit and unfit participants of our investigation. Interestingly, the slope $_{1/2reoxygenation}$ was 3-fold higher in VAS than GAS muscle (i.e., 69 vs. 21%), indicting higher capacities for reperfusion in the knee extensor than ankle extensor muscle.

The observed interaction effect between the aerobic fitness status × ACE-I/D genotype for the slope of deoxygenation and trend for such an effect on SmO_2 min in the leg muscles during ramp-incremental exercise (**Table 2**, **Figure 3**) meets the expectation emanating from the aerobic fitness-associated influence of the ACE-I/D gene polymorphism on mitochondrial volume density (van Ginkel et al., 2015). In this article, we had reported that the volume density of mitochondria in *musculus vastus lateralis* is elevated in aerobically fit non-carriers compared to carriers of the *ACE* D-allele (i.e., endurance athletes) (van Ginkel et al., 2015). As well we had identified that the increase in the volume density of subsarcolemmal mitochondria in *musculus vastus lateralis* with cycling endurance training is amplified in non-carriers compared to carriers of the D-allele (Vaughan et al., 2013). As the content of mitochondria sets the capacity for muscle oxygen consumption, it appears reasonable to expect that the capacity for oxygen consumption, and, conversely, the

reduction in muscle oxygen saturation during exercise (Ryan et al., 2014), was largest in the knee extensor muscles of the aerobically fit subjects that did not carry the *ACE* D-allele.

By contrast, we did not find an aerobic fitness-associated interaction effect of the ACE-I/D-genotype on parameters of muscle reoxygenation in *musculus vastus lateralis* during ramp-incremental exercise (**Table 2**). The ACE-I/D genotype has been found to be associated with altered capillary perfusion of distal limbs (i.e., the fingers) during exhaustive pedaling leg exercise and the capillarization of *Musculus vastus lateralis* (Valdivieso et al., 2017; Fluck et al., 2019) in not-specifically endurance-trained subjects. We observed however a trend ($p = 0.10$) for an interaction between ACE-I/D genotype and fitness state for $\Delta 1/2$ reoxygenation, which resolved for VAS in unfit subjects to a trend ($p = 0.07$) for a 10.7% higher $\Delta_{1/2reoxygenation}$ in carriers compared to non-carriers of the D-allele (**Supplementary Table 3**). As well we observed a shallower slope of muscle deoxygenation during ramp-incremental exercise in unfit non-carriers compared to unfit D-allele carriers. This observation may in addition to differences in mitochondria respiration be reflective of the before mentioned better capillary perfusion of D-allele non-carriers during strenuous exercise, overriding of angiotensin 2-mediated vasoconstriction (van Ginkel et al., 2015). Concomitantly, our data relate to findings in ACE-DD genotypes on an altered balance between biochemical reactions that replenish and deplete intermediates of the TCA cycle, which releases energy through the oxidation of acetyl-CoA (Mathes et al., 2015). Nevertheless, an increased respiratory capacity of skeletal muscle is understood to contribute in an over-proportional manner to gains in maximal oxygen uptake with endurance training (Hoppeler et al., 1985) and add together with cardiovascular and pulmonary factors to the systemically measurable maximal oxygen uptake (di Prampero, 2003). Intriguingly, although the slope of muscle deoxygenation during exhaustive ramp exercise (i.e., −0.081 vs. −0.034% SmO_2 s^{-1}) and VO_2 peak (i.e., 54.4 vs. 40.2 mlO_2 min^{-1} kg^{-1}) differed substantially between the aerobically fit and unfit ACE-II genotypes, the slope of muscle deoxygenation did not differ between the aerobically fit and unfit carriers of the *ACE* D-allele, despite a different VO_2 peak (i.e., 54.9 vs. 39.8 ml O_2 min^{-1} kg^{-1}). Thus, the fitness × genotype-related effects on muscle deoxygenation were not reflected at the level of statistical significance for VO_2 peak. ACE-I/D genotypes have been found to demonstrate different hemodynamic responses during maximal exercise (Hellsten and Nyberg, 2015). Collectively our results, therefore, support the view that the association between ACE-I/D × fitness state for oxygen saturation in working skeletal muscle may not always manifest in statistically different maximal oxygen uptake due to a lower effect size at the system level and a possibly different contribution of knee extensor muscle between ACE-I/D genotypes to systemic oxygen uptake (Hoppeler et al., 1985; Jones et al., 2002; Flueck et al., 2010; Valdivieso et al., 2017; Williams et al., 2017).

The identified effects should be viewed in terms of the limitations of this study. First, NIRS-based measures only allow to compute values of oxygen concentration from a rather small volume of tissue which may bear the risk of being confounded by subcutaneous tissue material (Richardson et al., 2001; Grassi and Quaresima, 2016; Jones et al., 2017; Perrey and Ferrari, 2018). The recorded values, however, have been reported to be reliable, especially at the moderate exercise intensities used in this investigation, thus allowing to conduct real-time measurements in a non-invasive manner (Grassi and Quaresima, 2016; Crum et al., 2017; Jones et al., 2017; Perrey and Ferrari, 2018). Furthermore, within our investigation, we also identify considerable reductions for the computed levels of oxygen saturation that are in line with the reported larger degrees for muscle deoxygenation and reoxygenation between the aerobically fit and unfit subjects (Brizendine et al., 2013; Perrey and Ferrari, 2018). As well, for the purpose of data interpretation, it needs to be considered that oxygen saturation reflects the difference between oxygen supply and demand, thus providing only an indirect estimate of the possibly larger changes in the flux of oxygen with exercise (Collins et al., 2011; Rosenberry et al., 2019). This may especially come into account with the onset, and offset, of exercise when metabolic processes are not in a steady-state. Also, we note that in order to avoid other vasodilatation-related influences that may camouflage fitness state and genotype effects, we carried out the ramp-incremental exercise in the mere absence of a warm-up or muscle work to avoid the activation of mitochondrial respiration by unloaded contractions (Nioka et al., 1998; Boone et al., 2012; Perrey and Ferrari, 2018). Finally, we note that our observations are based on a rather heterogeneous population of volunteers, which were not matched for physical fitness between the ACE-I/D genotypes. Both the men and women were recruited to achieve the prospectively determined number of observations to reach the statistical significance of effects, although it had been shown that gender affects muscle deoxygenation during incremental ramp exercise (Murias et al., 2013).

CONCLUSION

Our measurements resolve that the ACE-I/D genotype affects aerobic fitness state-related differences in muscle oxygen saturation in recruited skeletal muscle during exhaustive pedaling exercise. Our findings corroborate the view that aerobic metabolism in exercised muscle importantly contributes to the variability of the systemically assessed values for aerobic capacity.

DATA AVAILABILITY STATEMENT

The datasets presented in this study can be found in online repositories. The names of the repository/repositories and accession number(s) can be found in the article/**Supplementary Materials**.

ETHICS STATEMENT

The studies involving human participants were reviewed and approved by Ethics Committee of

University of Zürich. The patients/participants provided their written informed consent to participate in this study.

AUTHOR CONTRIBUTIONS

DN, WF, and MF: study design. MF: funding. MVF, SR, AF, SC, and WF performed experiments. MVF, AF, WP, SC, and MF analyzed experiments. AF, WP, and MF analyzed the data. BG, DN, and MF interpreted the results. BG, MVF, and MF drafted the manuscript. BG, SR, MVF, DN, and MF revised the manuscript. All authors contributed to the article and approved the submitted version.

FUNDING

This study was supported by the Swiss Heart Foundation and the RESORTHO Foundation.

ACKNOWLEDGMENTS

We thank Daniel Fitze, Karin Camenisch, Deborah Lehmann, and Milena Gemperle for their excellent technical assistance during the ramp-incremental exercise test and Dr. Paola Valdivieso for dedicated technical training for the genotyping.

SUPPLEMENTARY MATERIAL

The Supplementary Material for this article can be found online at: https://www.frontiersin.org/articles/10.3389/fspor.2022.814975/full#supplementary-material

Supplementary Figure 1 | Muscle-type dependent differences in reoxygenation after exercise. Box Whisker plots showing the $\Delta 1/2$ reoxygenation **(A)**, SmO_2 max **(B)** and SmO_2 overshoot **(C)** in VAS and GAS. Lines connect conditions demonstrating significant differences at $^{***}p < 0.001$. ANOVA for the factor "aerobic fitness" with *post-hoc* test of least significant difference.

Supplementary Figure 2 | Aerobic fitness × angiotensin-converting enzyme-insertion/deletion (ACE-I/D) genotype associated differences in deoxygenation in leg muscles. Box Whisker plots for the Δ_deoxgenation **(A)** and the slope of deoxygenation **(B)** in VAS and GAS in the function of the aerobic fitness status and the ACE-I/D genotype. Lines connect conditions demonstrating significant differences at $^{*}p < 0.05$ and $^{**}p < 0.01$. ANOVA for the factor "aerobic fitness" with *post-hoc* test of least significant difference.

Supplementary Table 1 | Prospective power analysis. Calculation of the prospectively required number of biological replica to reveal statistically significant associations.

Supplementary Table 2 | Association of variability is assessed parameters with sex. List of the p-values and effect sizes of the MANOVA for fitness state × genotype × sex. nc, not computable.

Supplementary Table 3 | Muscle deoxygenation and re-oxygenation in both studied leg muscles for each genotype and fitness status. List of the average/median (+ SE) values of the MANOVA for fitness state × genotype × muscle type.

Supplementary Table 4 | Retrospective power analysis of the observed effects.

REFERENCES

ACSM (2021). *Guidelines for Exercise Testing and Prescription, 11th Edn*. Philadelphia, PA: Wolters Kluwer Health.

Badtke, G. (1987). *Sportmedizinsche Grundlagen der Körpererziehung und des sportlichen Trainings*. Leipzig.

Baker, J. S., McCormick, M. C., and Robergs, R. A. (2010). Interaction among skeletal muscle metabolic energy systems during intense exercise. *J. Nutr. Metab.* 2010, 905612. doi: 10.1155/2010/905612

Boone, J., Bouckaert, J., Barstow, T. J., and Bourgois, J. (2012). Influence of priming exercise on muscle deoxy[Hb + Mb] during ramp cycle exercise. *Eur. J. Appl. Physiol.* 112, 1143–1152. doi: 10.1007/s00421-011-2068-z

Brizendine, J. T., Ryan, T. E., Larson, R. D., and McCully, K. K. (2013). Skeletal muscle metabolism in endurance athletes with near-infrared spectroscopy. *Med. Sci. Sports Exerc.* 45, 869–875. doi: 10.1249/MSS.0b013e31827e0eb6

Buikema, H., Pinto, Y. M., Rooks, G., Grandjean, J. G., Schunkert, H., and van Gilst, W. H. (1996). The deletion polymorphism of the angiotensin-converting enzyme gene is related to phenotypic differences in human arteries. *Eur. Heart J.* 17, 787–794. doi: 10.1093/oxfordjournals.eurheartj.a014947

Casey, D. P., and Joyner, M. J. (2015). Regulation of increased blood flow (hyperemia) to muscles during exercise: a hierarchy of competing physiological needs. *Physiol. Rev.* 95, 549–601. doi: 10.1152/physrev.00035.2013

Chuang, M. L., Ting, H., Otsuka, T., Sun, X. G., Chiu, F. Y., Hansen, J. E., et al. (2002). Muscle deoxygenation as related to work rate. *Med. Sci. Sports Exerc.* 34, 1614–1623. doi: 10.1097/00005768-200210000-00013

Clifford, P. S., and Hellsten, Y. (2004). Vasodilatory mechanisms in contracting skeletal muscle. *J. Appl. Physiol.* 97, 393–403. doi: 10.1152/japplphysiol.00179.2004

Collins, J. A., Rudenski, A., Gibson, J., Howard, L., and O'Driscoll, R. (2011). Relating oxygen partial pressure, saturation and content: the haemoglobin–oxygen dissociation curve. *Breathe* 11, 194–201. doi: 10.1183/20734735.001415

Crum, E. M., O'Connor, W. J., Van Loo, L., Valckx, M., and Stannard, S. R. (2017). Validity and reliability of the Moxy oxygen monitor during incremental cycling exercise. *Eur. J. Sport Sci.* 17, 1037–1043. doi: 10.1080/17461391.2017.1330899

di Prampero, P. E. (2003). Factors limiting maximal performance in humans. *Eur. J. Appl. Physiol.* 90, 420–429. doi: 10.1007/s00421-003-0926-z

Dimitriou, G., Papakonstantinou, D., Stavrou, E. F., Tzifas, S., Vervenioti, A., Athanassiadou, A., et al. (2010). Angiotensin-converting enzyme gene polymorphism and respiratory muscle function in infants. *Pediatr. Pulmonol.* 45, 1233–1239. doi: 10.1002/ppul.21316

Ding, H., Wang, G., Lei, W., Wang, R., Huang, L., Xia, Q., et al. (2001). Non-invasive quantitative assessment of oxidative metabolism in quadriceps muscles by near infrared spectroscopy. *Br. J. Sports Med.* 35, 441–444. doi: 10.1136/bjsm.35.6.441

Egginton, S., and Hudlicka, O. (1999). Early changes in performance, blood flow and capillary fine structure in rat fast muscles induced by electrical stimulation. *J. Physiol.* 515(Pt 1), 265–275. doi: 10.1111/j.1469-7793.1999.265ad.x

Fitze, D. P., Franchi, M., Popp, W. L., Ruoss, S., Catuogno, S., Camenisch, K., et al. (2019). Concentric and eccentric pedaling-type interval exercise on a soft robot for stable coronary artery disease patients: toward a personalized protocol. *JMIR Res. Protoc.* 8, e10970. doi: 10.2196/10970

Fluck, M., and Hoppeler, H. (2003). Molecular basis of skeletal muscle plasticity–from gene to form and function. *Rev. Physiol. Biochem. Pharmacol.* 146, 159–216. doi: 10.1007/s10254-002-0004-7

Fluck, M., Kramer, M., Fitze, D. P., Kasper, S., Franchi, M. V., and Valdivieso, P. (2019). Cellular aspects of muscle specialization demonstrate genotype - phenotype interaction effects in athletes. *Front. Physiol.* 10, 526. doi: 10.3389/fphys.2019.00526

Flueck, M., Vaughan, D., and Westerblad, H. (2010). Linking genes with exercise: where is the cut-off?. *Eur. J. Appl. Physiol.* 110, 1095–1098. doi: 10.1007/s00421-010-1662-9

Grassi, B., and Quaresima, V. (2016). Near-infrared spectroscopy and skeletal muscle oxidative function in vivo in health and disease: a review

from an exercise physiology perspective. *J. Biomed. Opt.* 21, 091313. doi: 10.1117/1.JBO.21.9.091313

Hellsten, Y., and Nyberg, M. (2015). Cardiovascular adaptations to exercise training. *Compr. Physiol.* 6, 1–32. doi: 10.1002/cphy.c140080

Hoppeler, H., Howald, H., Conley, K., Lindstedt, S. L., Claassen, H., Vock, P., et al. (1985). Endurance training in humans: aerobic capacity and structure of skeletal muscle. *J. Appl. Physiol.* 59, 320–327. doi: 10.1152/jappl.1985.59.2.320

Jackman, M. R., Ravussin, E., Rowe, M. J., Pratley, R., Milner, M. R., and Willis, W. T. (2008). Effect of a polymorphism in the ND1 mitochondrial gene on human skeletal muscle mitochondrial function. *Obesity* 16, 363–368. doi: 10.1038/oby.2007.40

Jones, A., Montgomery, H. E., and Woods, D. R. (2002). Human performance: a role for the ACE genotype?. *Exerc. Sport Sci. Rev.* 30, 184–190. doi: 10.1097/00003677-200210000-00008

Jones, S., D'Silva, A., Bhuva, A., Lloyd, G., Manisty, C., Moon, J. C., et al. (2017). Improved exercise-related skeletal muscle oxygen consumption following uptake of endurance training measured using near-infrared spectroscopy. *Front. Physiol.* 8, 1018. doi: 10.3389/fphys.2017.01018

Korthuis, R. (2011). *Skeletal Muscle Circulation*. San Rafael, CA: Morgan & Claypool Life Sciences.

Korzeniewski, B. (2003). Regulation of oxidative phosphorylation in different muscles and various experimental conditions. *Biochem. J.* 375, 799–804. doi: 10.1042/bj20030882

Lukin, L., and Ralston, H. J. (1962). Oxygen deficit and repayment in exercise. *Int. Z. Angew. Physiol.* 19, 183–193. doi: 10.1007/BF00693749

Mathes, S., van Ginkel, S., Vaughan, D., Valdivieso, D., and Flück, M. (2015). Gene-pharmacologial effects on exercise-induced muscle gene expression in healthy men. *Anatomy Physiol. Curr. Res.* S5, 2161–0940. doi: 10.4172/2161-0940.S5-005

Murias, J. M., Keir, D. A., Spencer, M. D., and Paterson, D. H. (2013). Sex-related differences in muscle deoxygenation during ramp incremental exercise. *Respir. Physiol. Neurobiol.* 189, 530–536 doi: 10.1016/j.resp.2013.08.011

Nioka, S., Moser, D., Lech, G., Evengelisti, M., Verde, T., Chance, B., et al. (1998). Muscle deoxygenation in aerobic and anaerobic exercise. *Adv. Exp. Med. Biol.* 454, 63–70. doi: 10.1007/978-1-4615-4863-8_8

O'Donnell, C. J., Lindpaintner, K., Larson, M. G., Rao, V. S., Ordovas, J. M., Schaefer, E. J., et al. (1998). Evidence for association and genetic linkage of the angiotensin-converting enzyme locus with hypertension and blood pressure in men but not women in the Framingham Heart Study. *Circulation* 97, 1766–1772. doi: 10.1161/01.CIR.97.18.1766

Perrey, S., and Ferrari, M. (2018). Muscle oximetry in sports science: a systematic review. *Sports Med.* 48, 597–616. doi: 10.1007/s40279-017-0820-1

Pilegaard, H., Keller, C., Steensberg, A., Wulff Helge, J., Klarlund Pedersen, B., Saltin, B., et al. (2002). Influence of pre-exercise muscle glycogen content on exercise-induced transcriptional regulation of metabolic genes. *J Physiol.* 541(Pt 1), 261–271. doi: 10.1113/jphysiol.2002.016832

Richardson, R. S., Newcomer, S. C., and Noyszewski, E. A. (2001). Skeletal muscle intracellular PO(2) assessed by myoglobin desaturation: response to graded exercise. *J. Appl. Physiol.* 91, 2679–2685. doi: 10.1152/jappl.2001.91.6.2679

Rodriguez, S., Gaunt, T. R., and Day, I. N. (2009). Hardy-Weinberg equilibrium testing of biological ascertainment for Mendelian randomization studies. *Am. J. Epidemiol.* 169, 505–514. doi: 10.1093/aje/kwn359

Rolfe, D. F., and Brown, G. C. (1997). Cellular energy utilization and molecular origin of standard metabolic rate in mammals. *Physiol. Rev.* 77, 731–758. doi: 10.1152/physrev.1997.77.3.731

Roseguini, B. T., Davis, M. J., and Harold Laughlin, M. (2010). Rapid vasodilation in isolated skeletal muscle arterioles: impact of branch order. *Microcirculation* 17, 83–93. doi: 10.1111/j.1549-8719.2009.00005.x

Rosenberry, R., Tucker, W. J., Haykowsky, M. J., Trojacek, D., Chamseddine, H. H., Arena-Marshall, C. A., et al. (2019). Determinants of skeletal muscle oxygen consumption assessed by near-infrared diffuse correlation spectroscopy during incremental handgrip exercise. *J. Appl. Physiol.* 127, 698–706. doi: 10.1152/japplphysiol.00273.2019

Ross, R., Goodpaster, B. H., Koch, L. G., Sarzynski, M. A., Kohrt, W. M., Johannsen, N. M., et al. (2019). Precision exercise medicine: understanding exercise response variability. *Br. J. Sports Med.* 53, 1141–153. doi: 10.1136/bjsports-2018-100328

Ryan, T. E., Brophy, P., Lin, C. T., Hickner, R. C., and Neufer, P. D. (2014). Assessment of in vivo skeletal muscle mitowchondrial respiratory capacity in humans by near-infrared spectroscopy: a comparison with in situ measurements. *J. Physiol.* 592, 3231–3241. doi: 10.1113/jphysiol.2014.274456

Tonkonogi, M., and Sahlin, K. (2002). Physical exercise and mitochondrial function in human skeletal muscle. *Exerc. Sport Sci. Rev.* 30, 129–137. doi: 10.1097/00003677-200207000-00007

Valdivieso, P., Vaughan, D., Laczko, E., Brogioli, M., Waldron, S., Rittweger, J., et al. (2017). The metabolic response of skeletal muscle to endurance exercise is modified by the ACE-I/D gene polymorphism and training state. *Front. Physiol.* 8, 993. doi: 10.3389/fphys.2017.00993

van Dijk, M. A., Kroon, I., Kamper, A. M., Boomsma, F., Danser, A. H., and Chang, P. C. (2000). The angiotensin-converting enzyme gene polymorphism and responses to angiotensins and bradykinin in the human forearm. *J. Cardiovasc. Pharmacol.* 35, 484–490. doi: 10.1097/00005344-200003000-00020

van Ginkel, S., de Haan, A., Woerdeman, J., Vanhees, L., Serne, E., de Koning, J., et al. (2015). Exercise intensity modulates capillary perfusion in correspondence with ACE I/D modulated serum angiotensin II levels. *Appl. Transl. Genom.* 4, 33–37. doi: 10.1016/j.atg.2015.03.002

van Ginkel, S., Ruoss, S., Valdivieso, P., Degens, H., Waldron, S., de Haan, A., et al. (2016). ACE inhibition modifies exercise-induced pro-angiogenic and mitochondrial gene transcript expression. *Scand. J. Med. Sci. Sports* 26, 1180–1187. doi: 10.1111/sms.12572

Vaughan, D., Huber-Abel, F. A., Graber, F., Hoppeler, H., and Fluck, M. (2013). The angiotensin converting enzyme insertion/deletion polymorphism alters the response of muscle energy supply lines to exercise. *Eur. J. Appl. Physiol.* 113, 1719–1729. doi: 10.1007/s00421-012-2583-6

Whipp, B. J., Davis, J. A., Torres, F., and Wasserman, K. (1981). A test to determine parameters of aerobic function during exercise. *J. Appl. Physiol. Respir. Environ. Exerc. Physiol.* 50, 217–221. doi: 10.1152/jappl.1981.50.1.217

Williams, A. G., Rayson, M. P., Jubb, M., World, M., Woods, D. R., Hayward, M., et al. (2000). The ACE gene and muscle performance. *Nature*. 403, 614. doi: 10.1038/35001141

Williams, C. J., Williams, M. G., Eynon, N., Ashton, K. J., Little, J. P., Wisloff, U., et al. (2017). Genes to predict VO2max trainability: a systematic review. *BMC Genomics* 18, 831. doi: 10.1186/s12864-017-4192-6

Woods, D. R., Pollard, A. J., Collier, D. J., Jamshidi, Y., Vassiliou, V., Hawe, E., et al. (2002). Insertion/deletion polymorphism of the angiotensin I-converting enzyme gene and arterial oxygen saturation at high altitude. *Am. J. Respir. Crit. Care Med.* 166, 362–366. doi: 10.1164/rccm.2103060

Zoll, J., Sanchez, H., N'Guessan, B., Ribera, F., Lampert, E., Bigard, X., et al. (2002). Physical activity changes the regulation of mitochondrial respiration in human skeletal muscle. *J. Physiol.* 543, 191–200. doi: 10.1113/jphysiol.2002.019661

Conflict of Interest: The authors declare that the research was conducted in the absence of any commercial or financial relationships that could be construed as a potential conflict of interest.

Publisher's Note: All claims expressed in this article are solely those of the authors and do not necessarily represent those of their affiliated organizations, or those of the publisher, the editors and the reviewers. Any product that may be evaluated in this article, or claim that may be made by its manufacturer, is not guaranteed or endorsed by the publisher.

frontiers in Physiology

REVIEW
published: 04 March 2022
doi: 10.3389/fphys.2022.838450

Effects of Cardiorespiratory Fitness on Cerebral Oxygenation in Healthy Adults: A Systematic Review

*Talia Salzman[1], Olivier Dupuy[2,3] and Sarah Anne Fraser[4]**

[1] Faculty of Health Sciences, School of Human Kinetics, University of Ottawa, Ottawa, ON, Canada, [2] Laboratory MOVE, University of Poitiers, Poitiers, France, [3] Faculty of Medicine, School of Kinesiology and Physical Activity Sciences (EKSAP), University of Montreal, Montreal, QC, Canada, [4] Faculty of Health Sciences, Interdisciplinary School of Health Sciences, University of Ottawa, Ottawa, ON, Canada

Introduction: Exercise is known to improve cognitive functioning and the cardiorespiratory hypothesis suggests that this is due to the relationship between cardiorespiratory fitness (CRF) level and cerebral oxygenation. The purpose of this systematic review is to consolidate findings from functional near-infrared spectroscopy (fNIRS) studies that examined the effect of CRF level on cerebral oxygenation during exercise and cognitive tasks.

Methods: Medline, Embase, SPORTDiscus, and Web of Science were systematically searched. Studies categorizing CRF level using direct or estimated measures of $\dot{V}O_{2max}$ and studies measuring cerebral oxygenation using oxyhemoglobin ([HbO_2]) and deoxyhemoglobin ([HHb]) were included. Healthy young, middle-aged, and older adults were included whereas patient populations and people with neurological disorders were excluded.

Results: Following PRISMA guidelines, 14 studies were retained following abstract and full-text screening. Cycle ergometer or treadmill tests were used as direct measures of CRF, and one study provided an estimated value using a questionnaire. Seven studies examined the effects of CRF on cerebral oxygenation during exercise and the remaining seven evaluated it during cognitive tasks. Increased [HbO_2] in the prefrontal cortex (PFC) was observed during cognitive tasks in higher compared to lower fit individuals. Only one study demonstrated increased [HHb] in the higher fit group. Exercise at submaximal intensities revealed increased [HbO_2] in the PFC in higher compared to lower fit groups. Greater PFC [HHb] was also observed in long- vs. short-term trained males but not in females. Primary motor cortex (M1) activation did not differ between groups during a static handgrip test but [HHb] increased beyond maximal intensity in a lower compared to higher fit group.

Conclusion: Consistent with the cardiorespiratory hypothesis, higher fit young, middle-aged, and older adults demonstrated increased cerebral oxygenation compared to lower fit groups. Future research should implement randomized controlled trials to evaluate the effectiveness of interventions that improve CRF and cerebral oxygenation longitudinally.

Keywords: cardiorespiratory fitness, functional near-infrared spectroscopy, cerebral oxygenation, younger adults, older adults, exercise, cognition

Edited by:
Giancarlo Condello, University of Parma, Italy

Reviewed by:
Hamoon Zohdi, University of Bern, Switzerland
Atsuhiro Tsubaki, Niigata University of Health and Welfare, Japan

***Correspondence:**
Sarah Anne Fraser
sarah.fraser@uottawa.ca

Specialty section:
This article was submitted to Exercise Physiology, a section of the journal Frontiers in Physiology

Received: *17 December 2021*
Accepted: *28 January 2022*
Published: *04 March 2022*

Citation:
Salzman T, Dupuy O and Fraser SA (2022) Effects of Cardiorespiratory Fitness on Cerebral Oxygenation in Healthy Adults: A Systematic Review. Front. Physiol. 13:838450. doi: 10.3389/fphys.2022.838450

INTRODUCTION

Considerable evidence has supported that maintaining a good level of physical activity is associated with better cognitive performances across the lifespan (Colcombe and Kramer, 2003; Hillman et al., 2008; Stillman et al., 2020). Themanson et al. (2006) suggest that such effects may be driven by exercise-related improvements in cardiorespiratory fitness (CRF). From childhood to adulthood, a greater CRF will have a positive impact on cognitive performance. More specifically, executive performance seems to be preferentially favored. Indeed, there is considerable evidence from cross-sectional studies and meta-analyses that CRF has beneficial effects on multiple cognitive domains, particularly executive functions (Colcombe and Kramer, 2003; Predovan et al., 2012; Dupuy et al., 2015; Chaparro et al., 2019; Goenarjo et al., 2020a). This is partly because the prefrontal cortex, which governs these functions, seems to be very sensitive to physical activity-related changes (Yuki et al., 2012). Therefore, the interactions between exercise and cognition are multifaceted and examining them requires a deeper understanding of cognitive and physiological concepts.

The clinical benefits of CRF on cognitive function appear in the form of enhanced brain functioning, as suggested by neuroimaging studies that report increased brain activity in physically active older adults when compared to less active ones (Voelcker-Rehage and Niemann, 2013). Evidence from functional magnetic resonance imaging (fMRI) studies also supports the effects of CRF on brain activation during cognitive tasks. For instance, active older adults exhibited increased brain activity in the prefrontal cortex (PFC) and decreased activity in the anterior cingulate cortex compared to less active older adults during Flanker and Stroop tasks (Colcombe et al., 2004). This is consistent with the cardiorespiratory hypothesis which suggests that higher levels of fitness are related to increased cerebral blood flow (Agbangla et al., 2019b).

Many underlying neurophysiologic and structural changes may be used to explain this improvement in brain functioning (Hillman et al., 2008; Ploughman, 2008). For example, structural brain changes after physical training including both the improvement of the density and integrity of gray and white matter has been observed (Weinstein et al., 2012; Voelcker-Rehage and Niemann, 2013; Erickson et al., 2014; Sexton et al., 2016; d'Arbeloff, 2020; Kundu et al., 2021). However, it should be noted that the functional activity of the brain is related to blood supply and that neuronal activation requires an increase in cerebral blood flow and metabolism. This mechanism has been illustrated by Mehagnoul-Schipper et al. (2002) who reported simultaneous increases in cerebral blood volume and cerebral oxygenation during motor tasks in younger and older adults using functional near-infrared spectroscopy (fNIRS) and fMRI. It also appears that the magnitude of this adaptation is proportional to the complexity of the task. Several studies have reported that during exercise (Mekari et al., 2015) or by using hypoxic paradigms (Ando et al., 2013; Williams et al., 2019), cerebral oxygen availability affects cognitive performance and shows that cerebral oxygenation plays a key role in brain functioning.

Among neuroimaging techniques, however, fMRI has limited applications during exercise tasks that involve a full range of motion. FNIRS can overcome these challenges since it is portable, non-invasive, and robust to motion artifacts, which is also convenient for examining participants of all ages (Quaresima and Ferrari, 2016). Both fMRI and fNIRS function based on the principles of neurovascular coupling but fNIRS dissociates oxyhemoglobin ($[HbO_2]$) and deoxyhemoglobin ([HHb]) unlike the blood oxygen level dependent (BOLD) response measure used in fMRI (Villringer, 1997). This is because fNIRS devices emit near-infrared light into the scalp at specific wavelengths (i.e., 650–950 nm) that coincide with the absorption properties of $[HbO_2]$ and [HHb] (Scholkmann et al., 2014). The reflected light is then measured by continuous wave, frequency domain, or time domain techniques, which differ based on how the incident light is emitted and reflection is detected. Continuous wave devices, which are the most commercially available, rely on a constant intensity of light and quantify the relative changes in reflected light (Scholkmann et al., 2014). In contrast, frequency and time domain devices are more complex but capture absolute measures of cerebral oxygenation. Frequency domain devices modulate the incident light and measure the phase shift of the reflected light compared to time domain devices that emit short pulses of light and measure the dispersion of reflected light (Scholkmann et al., 2014). Lastly, fNIRS also has the advantage of better temporal and spatial resolution than fMRI and electroencephalography (EEG), respectively, and at relatively a low cost (Pinti et al., 2018). For these reasons, fNIRS publications have grown exponentially with many studies focusing on exercise and cognition (Yan et al., 2020). However, few reviews focus on the role of CRF on cerebral oxygenation during cognitive or physical activity and to our knowledge none have examined this systematically (Agbangla et al., 2021).

One factor that increases heterogeneity amongst reviewed studies is the assessment of CRF. The gold standard index of CRF, $\dot{V}O_{2max}$, reflects a point where an individual's maximum oxygen uptake remains constant despite an increase in workload (Buttar et al., 2019). It also provides the most accurate assessment of CRF and can be evaluated using direct or estimated measures (Vanhees et al., 2005; Aadahl et al., 2007). Direct measures typically involve running or cycling tests with incremental loads (Vanhees et al., 2005). Therefore, direct measures are generally assessed in a laboratory setting using cardiopulmonary exercise systems and gas analyzers that are worn during the test and capture ventilatory measurements, oxygen consumption, and expired carbon monoxide. Since direct measures require specialized equipment and settings, a valid alternative is to use maximal or submaximal tests that require minimal equipment or self-report questionnaires that estimate CRF (i.e., $\dot{V}O_{2max}$) using an equation. For example, indirect tests include the Rockport test (Jurca et al., 2005; Dupuy et al., 2018), Balke test (Balke and Ware, 1959; Goenarjo et al., 2020b, 2021), or 1.5 mile (George et al., 1993) run where participants may or may not be equipped with heart rate monitors. Accordingly, aerobic capacity may be estimated based on heart rate, distance covered, or trial time using the validated protocols for each type of test (George et al., 1993; Buttar et al., 2019). Lastly, self-report cardiorespiratory

measures have been shown to correlate with $\dot{V}O_{2max}$ but risk leading to overestimations of fitness levels in sedentary people (Aadahl et al., 2007).

The present review aims to consolidate findings from previous reports that demonstrated an interaction between CRF level and cerebral oxygenation. More specifically, this systematic review will summarize evidence from cross-sectional and interventional fNIRS studies that used direct or estimated measures of CRF and examined changes in cerebral oxygenation in healthy younger, middle-aged, and older adult groups during cognitive and exercise tasks. Findings will provide insights into the physiological mechanisms underlying changes in brain activation that are associated with CRF.

METHODS

This systematic review followed the Preferred Reporting Items for Systematic Reviews and Meta-Analyses (PRISMA) guidelines (Liberati et al., 2009).

Eligibility Criteria

The PICO (population, intervention, comparison, and outcome) model was used to outline the inclusion and exclusion criteria for this systematic review (Eriksen and Frandsen, 2018). The population being studied included healthy younger, middle-aged, and older adults (i.e., participants aged 18 years and older). As this review focuses on healthy adults, studies that examined participants who are obese or patient populations including those with chronic neurological disorders were excluded. Intervention type included cognitive, physical, or a combination of both while fNIRS was used to assess changes in cerebral oxygenation during task performance. The studies must have also compared a high- and low-fit group or an active and control group that were created based on direct or estimated measures of CRF. Cross-sectional and longitudinal studies were included whereas those without full-texts, systematic reviews, and animal studies were excluded.

Search Strategy

Following PRISMA guidelines, the systematic literature search was conducted in July 2021 using four online databases: Medline, Embase, SPORTDiscus, and Web of Science. There were no restrictions set for language or publication year. The search terms encompassed Medical Subject Headings (MeSH) and keywords that described fNIRS, the hemodynamic response as well as CRF levels (**Supplementary Table 1**). For example, the following keywords and MeSH terms were used: "Spectroscopy, Near-Infrared" AND "Cardiorespiratory fitness" OR "$\dot{V}O_{2max}$" AND "[HbO_2]" OR "[HHb]."

The resulting studies were imported and managed in Covidence (Melbourne, Australia) where duplicates were automatically removed and visually inspected by TS. Titles and abstracts were then independently screened by OD and TS. SF resolved all conflicts and relevant studies were retained for the full-text review. SF, TS, and OD reviewed the full-texts and disagreements were resolved by a consensus between authors. The reference lists of the included full-texts were hand-searched as well as recent publications since the initial search for additional studies meeting the inclusion and exclusion criteria.

Quality Assessment

The Joanna Briggs Institute (JBI) checklist for analytical cross-sectional studies was used to assess the methodological quality of the included studies (Ma et al., 2020). It is suitable for non-randomized experimental studies because it evaluates eight criteria: (1) Inclusion criteria in the sample were clearly defined; (2) The study subjects and the setting were described in detail; (3) The exposure was measured in a valid and reliable way; (4) Objective, standard criteria were used for measurement of the condition; (5) Confounding factors were identified; (6) Strategies to deal with confounding factors were stated; (7) The outcomes were measured in a valid and reliable way; and (8) An appropriate statistical analysis was used. The overall appraisal to determine whether a study is of sufficient quality to include, exclude, or seek further information, was decided based on a consensus between TS and SF.

Synthesis of Results

Data extraction was conducted by TS and SF. The form included information on study and participant characteristics, study design, CRF measures, and fNIRS measures. Significant differences between CRF scores were identified across both direct and estimated measures. The hemodynamic response was extracted based on the study's primary outcome measure. In addition, the type of task during which the hemodynamic response was measured (e.g., cycling, Stroop task) was analyzed while accounting for variables such as age, sex, and exercise intensity.

RESULTS

Study Selection and Characteristics

The initial database search resulted in 2,592 studies and 1,495 after duplicates were removed. After screening the titles and abstracts, 1,450 records were excluded. The full-texts of 45 studies were then reviewed and 31 studies were excluded due to the wrong study design (n = 18), wrong comparator (n = 5), wrong outcomes (n = 4), abstract only (n = 2), wrong population (n = 1), and no full-text available (n = 1) (**Figure 1**). No additional papers were included following a hand-search. Fourteen studies were retained for analysis. The publication period ranged from 2010 to 2020 and all the studies were cross-sectional except for one which was a pre-/post-intervention design. Four studies took place in France, followed by three in Japan, two in Australia and Canada, and one in Belgium, Germany, and the United States, respectively. Study characteristics for all 14 included studies are shown in **Table 1**.

Seven studies examined the effects of CRF during an exercise task, five studies evaluated the effects during a cognitive task, one study examined a cognitive-motor dual-task, and one study examined a visual task. CRF was assessed using direct and estimated measures. Ten studies used a cycle ergometer test, two studies used a treadmill test, one study used self-report

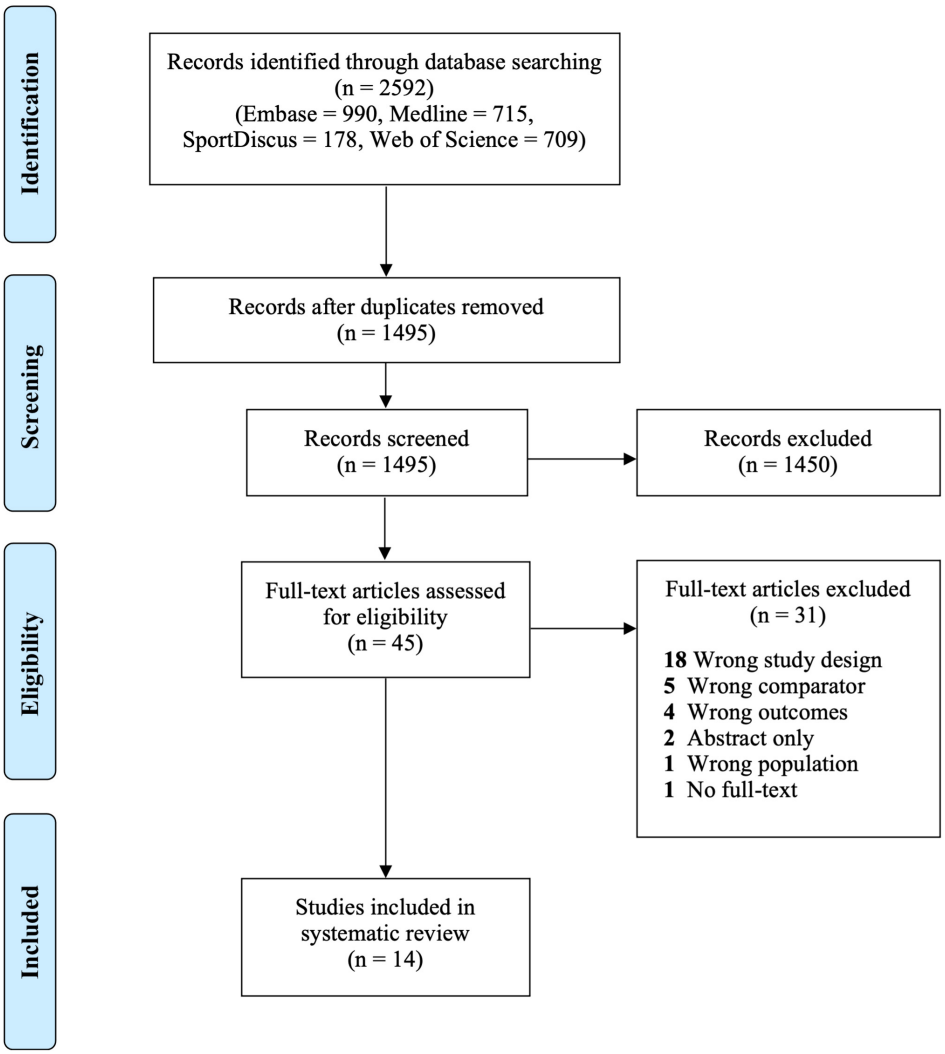

FIGURE 1 | PRISMA flow diagram.

questionnaires, and one study did not specify which test was used but provided a $\dot{V}O_{2max}$ cut-off score for each group (Shibuya and Kuboyama, 2010). In addition, the hemodynamic response was measured using both [HbO_2] and [HHb] in 10 studies whereas two studies exclusively examined [HbO_2], and two studies only examined [HHb]. These measurements were taken in the PFC across 11 studies, motor cortices in two studies, and visual cortex in one study.

Participant Characteristics

A total of 530 participants were examined and sample sizes ranged from 11 to 66. Seven studies consisted exclusively of male participants whereas three studies only enrolled females, and four studies evaluated both males and females. The age groups being examined varied across studies including five that evaluated younger adults (18–26 years old), four examined older adults (≥60 years old), three studies compared older and younger adults, and two studies evaluated middle-aged adults (40–60 years old). Amongst the studies that compared older and younger adults, high and low levels of CRF were only established in the older adult group in two studies (Fabiani et al., 2014; Agbangla et al., 2019a). Participant characteristics for included studies are indicated in **Table 2**.

Cardiorespiratory Fitness Terminology

In the included studies, various terms were used to describe CRF levels. More specifically, the studies evaluating CRF during exercise tasks used terms such as moderately active and sedentary (Brugniaux et al., 2014; Caen et al., 2019), short-term and long-term training (Buzza et al., 2016, 2020), trained and untrained (Oussaidene et al., 2015), endurance athlete and control (Seidel et al., 2019), and athlete and non-athlete (Shibuya and Kuboyama, 2010). In studies measuring cerebral oxygenation during cognitive tasks, the terms higher and lower fit were used to characterize CRF level.

TABLE 1 | Study characteristics of included studies.

Author (Year)	Study design	Brain region	Task	Cerebral oxygenation outcomes
Cognitive				
Agbangla et al. (2019a)	Cross-sectional	PFC	N-back (0–3 back)	Bilateral increase [HbO_2] in PFC during 2-back ($p < 0.05$) and 3-back ($p < 0.05$) compared to 1-back condition in high fit group. Decreased [HbO_2] overall in low compared to high fit group ($ps < 0.05$). Greater decrease in [HHb] in the left hemisphere in high compared to low fit group ($p = 0.003$).
Albinet et al. (2014)	Cross-sectional	DLPFC	Control counting task and Random Number Generation at a fast (one tone every 1 s) or slow pace (one tone every 1.5 s)	Increased [HbO_2] in left and right DLPFC during the Random Number Generation task in high fit group ($p < 0.05$). Decreased [HbO_2] in right DLPFC in low compared to high fit group ($p < 0.05$). Decreased [HbO_2] in left compared to right DLPFC in low fit group ($p < 0.05$). No change in [HbO_2] or [HHb] between groups during the counting number task ($ps > 0.3$).
Dupuy et al. (2015)	Cross-sectional	DLPFC, VLPFC,	Computerized Stroop task	Greater increase in [HbO_2] right inferior frontal gyrus of the VLPFC in high fit group compared to low fit ($p < 0.01$).
Hyodo et al. (2016)	Cross-sectional	DLPFC	Color-word Stroop task	Left lateralized DLPFC activation in high compared to low fit group. No differences in [HHb] ($p > 0.05$).
Mekari et al. (2019)	Cross-sectional	Left PFC	Trail making test A and B	Cerebral oxygenation mediated the relationship between cardiorespiratory fitness and Trail Making Test part B performance in the higher fit group ($p = 0.004$).
Dual-task				
Goenarjo et al. (2020a)	Cross-sectional	PFC	Auditory n-back (2-back) and walking	Greater decrease in [HHb] in the right and left PFC in high compared to low fit group ($p = 0.01$). Negative correlation between [HHb] and $\dot{V}O_{2peak}$ ($r = -0.36$, $p = 0.04$). No differences in [HbO_2].
Exercise				
Brugniaux et al. (2014)	Cross-sectional	Left PFC	Incremental cycling test	Increased [HbO_2] from low to moderate intensity exercise in the active group compared to sedentary group ($p < 0.05$).
Buzza et al. (2016)	Cross-sectional	Left PFC	Ramp incremental peak and submaximal square wave cycling	No differences during ramp incremental task ($p = 0.773$) or submaximal square wave cycling ($p = 0.788$) in [HHb] between long and short term trained individuals.
Buzza et al. (2020)	Cross-sectional	Left PFC	Ramp incremental peak and submaximal square wave cycling	Increased [HHb] in PFC at 90% GET during submaximal square wave cycling ($p = 0.011$) in long compared to short term trained individuals.
Caen et al. (2019)	Pre-/post-intervention	Right PFC	6-week incremental ramp exercise	Steeper [HbO_2] ($p = 0.034$) and [HHb] ($p < 0.001$) and increased [HbO_2] amplitude ($p < 0.001$) at moderate intensities post-intervention compared to pre-intervention.
Oussaidene et al. (2015)	Cross-sectional	Left PFC	Maximal ramp cycle exercise test and supramaximal test	Increased [HbO_2] ($p < 0.05$) at submaximal intensity in endurance trained compared to untrained group. No differences in [HHb] between groups.
Seidel et al. (2019)	Cross-sectional	M1, PMC, SMA, SPL, IPL	Incremental cycling test and multi-intensity cycling test	No differences in [HbO_2] ($0.444 \leq p$ adjusted ≤ 0.980) or [HHb] between groups during multi-intensity cycling test ($0.462 \leq p\ adjusted \leq 0.993$) between endurance athletes and active controls. Across exercise intensities, decreased [HbO_2] in PMC, SMA, and left IPL in endurance group and right PMC at 20% for active control. Bilateral decrease in [HHb] in motor cortices in both groups except at 20% in active control.
Shibuya and Kuboyama (2010)	Cross-sectional	M1	Maximal voluntary static handgrip test	No differences in [HbO_2] between groups. Increased [HbO_2] in M1 at voluntary exhaustion compared to baseline in non-athlete group and decrease in [HHb] below baseline ($p < 0.05$). Decreased [HbO_2] ($p < 0.05$) in M1 at voluntary exhaustion and decrease in [HHb] below baseline ($p < 0.05$) in the athlete group.
Visual				
Fabiani et al. (2014)	Cross-sectional	Primary visual cortex	Visual stimulation (Checkerboard reversals at different frequencies)	Positive correlation between [HbO_2] and $\dot{V}O_{2max}$ ($p < 0.05$) in older adults. Correlation between age and [HHb] was significant ($p < 0.05$) whereas [HHb] and $\dot{V}O_{2max}$ was not.

DLPFC, Dorsolateral prefrontal cortex; GET, Gas exchange threshold; IPL, Inferior parietal lobe; M1, Primary motor cortex; PFC, Prefrontal cortex; PMC, Premotor cortex; SMA, Supplementary motor area; SPL, Superior parietal lobe; VLPFC, Ventrolateral prefrontal cortex; VTP, Ventilatory turn point.

Effects of Cardiorespiratory Fitness During Cognitive Tasks

Two studies examined the effects of CRF level on [HbO_2] activation during the Stroop task (Dupuy et al., 2015; Hyodo et al., 2016), one study used the n-back task (Agbangla et al., 2019a), control counting and random number generation (Albinet et al., 2014), and trail making tests part A and B (Mekari et al., 2019). Four studies measured [HbO_2] and [HHb] (Albinet et al., 2014; Dupuy et al., 2015; Hyodo et al., 2016; Agbangla et al., 2019a) whereas one study only measured [HbO_2] (Mekari et al., 2019). All studies measured PFC activation in older adults and divided the participants into high and low fit groups based on

TABLE 2 | Participant characteristics for included studies.

Author (Year)	Sample size (Females)	Age ± SD	Cardiorespiratory fitness test	Cardiorespiratory fitness level (mL/kg/min)
Cognitive				
Agbangla et al. (2019a)	Males and females YA: *n* = 19 (2F) OA LF: *n* = 16 (9F) OA HF: *n* = 21(13F)	YA: 19.1 ± 1 OA LF: 70.31 ± 4.33 OA HF: 67.90 ± 4.86	YA: Maximal fitness test (20 m shuttle run) OA: NASA/JSC physical activity scale	$\dot{V}O_{2max}$ in OA ($p = 0.0004$) YA: 54.83 ± 7.21 OA LF: 17.4 ± 6.6 OA HF: 26.1 ± 6.7
Albinet et al. (2014)	Females OA LF: *n* = 17 OA HF: *n* = 17	LF: 68.88 ± 3.87 HF: 67.32 ± 4.48	Maximal continuous graded exercise test, cycle ergometer	$\dot{V}O_{2max}$ (*p*-value not specified) LF: 20 ± 2.7 HF: 29.8 ± 6.5
Dupuy et al. (2015)	Females YA: *n* = 22 OA: *n* = 36	YA LF: 23.5 ± 5.3 YA HF: 24.5 ± 3.1 OA LF: 60.8 ± 5.6 OA HF: 63.0 ± 3.1	Maximal continuous graded exercise test, cycle ergometer	$\dot{V}O_{2max}$ ($p < 0.05$) in YA and OA groups YA LF: 36.4 ± 5.3 YA HF: 46.6 ± 7.0 OA LF: 21.4 ± 7.1 OA HF: 30.1 ± 1.5
Hyodo et al. (2016)	Males OA: *n* = 60	OA: 70.3 ± 3.2	Graded exercise test, cycle ergometer	Ventilatory threshold OA: 14.9 ± 3.8
Mekari et al. (2019)	Males and females OA: *n* = 66 (44F)	LF: 69.6 ± 4.68 HF: 66.5 ± 7.41	Maximal continuous graded exercise test, cycle ergometer	$\dot{V}O_{2peak}$ ($p > 0.05$) LF: 18.4 ± 4.77 HF: 27.5 ± 5.92
Dual-task				
Goenarjo et al. (2020a)	Males YA LF: *n* = 12 YA HF: *n* = 12	HF: 22.8 ± 4.2 LF: 24.8 ± 5.1	Maximal continuous graded exercise test, treadmill	$\dot{V}O_{2peak}$ ($p < 0.05$) LF: 36.7 ± 4.1 HF: 56.0 ± 6.7
Exercise				
Brugniaux et al. (2014)	Males YA sedentary: *n* = 12 YA active: *n* = 12	Sedentary: 24 ± 5 Active: 26 ± 7	Incremental exercise, cycle ergometer	$\dot{V}O_{2max}$ ($p < 0.05$) Sedentary: 33 ± 5 Active: 52 ± 9
Buzza et al. (2016)	Females Middle age STT: *n* = 13 Middle age LTT: *n* = 13	STT: 51.5 ± 5.0 LTT: 47.5 ± 5.0	Ramp incremental exercise, cycle ergometer	VTP ($p < 0.05$) STT: 20.2 ± 5.1 LTT: 29.0 ± 6.4
Buzza et al. (2020)	Males Middle age STT: *n* = 14 Middle age LTT: *n* = 14	STT: 48.6 ± 5.5 LTT: 46.1 ± 4.6	Ramp incremental exercise, cycle ergometer	GET $\dot{V}O_2$ ($p < 0.05$) STT: 26.6 ± 5.5 LTT: 37.7 ± 5.4
Caen et al. (2019)	Males YA: *n* = 11	YA: 21.8 ± 1.2	Maximal ramp incremental exercise, cycle ergometer	$\dot{V}O_{2peak}$ ($p < 0.05$) Pre: 52.4 ± 3.5 Post: 56.4 ± 3.8
Oussaidene et al. (2015)	Males Untrained: *n* = 11 Endurance trained: *n* = 13	Endurance trained: 24 ± 6 Untrained: 26 ± 5	Ramp cycle exercise test, cycle ergometer	$\dot{V}O_{2max}$ ($p < 0.05$) Endurance trained: 61.2 ± 8.0 Untrained: 47.3 ± 4.0
Seidel et al. (2019)	Males and females Endurance trained: *n* = 22 (8F) Active control: *n* = 20 (8F)	Endurance trained: 28.82 ± 3.92 Control: 24.80 ± 3.14	Incremental cycling test, cycle ergometer	$\dot{V}O_{2max}$ ($p < 0.001$) Endurance trained: 64.59 ± 10.07 Active control: 52.20 ± 7.21
Shibuya and Kuboyama (2010)	Males Athletes: *n* = 7 Non-athletes: *n* = 7	Males Whole sample: 25.2 ± 1.4	Not specified	$\dot{V}O_{2max}$ (*p*-value not specified) Highly trained athletes: 60 Non-athletes: < 45
Visual				
Fabiani et al. (2014)	Males and females YA: *n* = 19 (9F) OA HF: *n* = 20 (11F) OA LF: *n* = 24 (13F)	YA: 22.3 ± 2.0 OA HF: 70.3 ± 4.2 OA LF: 72.2 ± 5.2	YA: Self-reported physical activity OA: Modified Balke protocol	$\dot{V}O_{2max}$ ($p < 0.0001$) YA: Not measured OA HF: 30.7 ± 6.7 OA LF: 18.9 ± 3.8

GET, Gas exchange threshold; HF, High fit; LF, Low fit; LTT, Long term trained; NASA/JSC, NASA/Johnson Space Center; OA, Older adults; STT, Short term trained; VTP, Ventilatory turn point; YA, Younger adults.

$\dot{V}O_{2max}$ measured by cycle ergometer tests except for one study that used a self-report questionnaire in older adults (Agbangla et al., 2019a).

Oxyhemoglobin During Executive Function Tasks

High fit groups demonstrated greater activation in the frontal lobe than low fit groups. More specifically, increased [HbO_2]

change was observed in the right inferior frontal gyrus and bilaterally in the dorsolateral PFC in high compared to low fit women during a Stroop task, regardless of age (Dupuy et al., 2015), and random number generation task (Albinet et al., 2014), respectively. This between groups effect was not observed during a control counting task, which was considered to be less demanding (Albinet et al., 2014). Within the high fit group, similar activation was observed in the right and left PFC whereas significantly lower [HbO_2] was observed in the right dorsolateral PFC compared to left in the low fit group. Right dorsolateral PFC activation was also greater overall in the high fit group compared to low fit group (Albinet et al., 2014). A second study examining the effects of CRF in males during the Stroop task revealed that the higher fit group was associated with more left-lateralized dorsolateral PFC activation compared to the lower fit group (Hyodo et al., 2016).

The final two studies measured cerebral oxygenation during an n-back task (Agbangla et al., 2019a) and a trail making task (Mekari et al., 2019) in a mixed sample of older males and females. Cerebral oxygenation mediated the relationship between CRF and executive function performance on the trail making test part B (Mekari et al., 2019). In other words, increased PFC [HbO_2] in high fit older adults resulted in better performance on part B of the trail making test than the low fit group. A similar interaction was observed during the n-back task in which PFC [HbO_2] increased in the high compared to low fit group on the 2- and 3-back tasks resulting in better accuracy performance (Agbangla et al., 2019a). In addition, the lower fit group exhibited less [HbO_2] activation overall compared to the high fit group.

Deoxyhemoglobin During Executive Function Tasks

Four studies measured the effects of CRF on [HHb] during executive functions tasks. Each study measured PFC activation but only one found a greater [HHb] decrease in high compared to low fit groups (Agbangla et al., 2019a). More specifically, this study used an n-back task in a mixed sample of female and male older adults whose CRF was assessed using a self-report questionnaire (Agbangla et al., 2019a). There were no significant differences in the other three studies that evaluated CRF using a cycle ergometer test and changes in cerebral oxygenation in the PFC (Albinet et al., 2014; Dupuy et al., 2015; Hyodo et al., 2016). In addition, these studies only examined female (Albinet et al., 2014; Dupuy et al., 2015) or male (Hyodo et al., 2016) participants during a controlled counting or random number generation task (Albinet et al., 2014) or Stroop task (Dupuy et al., 2015; Hyodo et al., 2016).

Oxyhemoglobin and Deoxyhemoglobin During Visual Tasks

One study measured the effects of CRF level on [HbO_2] and [HHb] in older adults (Fabiani et al., 2014). By measuring cerebral oxygenation changes in the visual cortex, findings revealed a significant positive correlation between [HbO_2] and $\dot{V}O_{2max}$ whereby low fit older adults demonstrated reduced [HbO2] activation compared to the high fit group. There was no correlation, however, between [HHb] and $\dot{V}O_{2max}$.

Oxyhemoglobin and Deoxyhemoglobin During Cognitive-Motor Dual-Tasks

One study measured the effects of CRF level on [HbO_2] and [HHb] during a dual-task (Goenarjo et al., 2020b). The dual-task was composed of an auditory n-back task and walking and there were no significant differences in [HbO_2] in either PFC hemisphere and between high and low fit younger adults. However, there was a significantly greater decrease in [HHb] in the high compared to low fit group in the right and left PFC during dual-tasks and a negative correlation between $\dot{V}O_{2peak}$ and [HHb].

Effects of Cardiorespiratory Fitness During Exercise Tasks

Oxyhemoglobin During Acute Exercise Tasks

Oxyhemoglobin was measured across acute bouts of exercise that included cycle ergometer tests and incremental cycling (Brugniaux et al., 2014), maximal and submaximal ramp exercises (Oussaidene et al., 2015), cycling with a constant load (Seidel et al., 2019), and a maximal voluntary static handgrip task (Shibuya and Kuboyama, 2010). During acute exercise, PFC activation differed between high and low fit groups (Brugniaux et al., 2014; Oussaidene et al., 2015). There were progressive [HbO2] increases during incremental cycling in the moderately active group until 80% of $\dot{V}O_{2max}$ after which [HbO2] leveled off and declined (Brugniaux et al., 2014). [HbO_2] remained constant despite increased exercise intensity in the low fit group. At submaximal exercise intensity, [HbO_2] was higher in an endurance trained compared to untrained younger adults (Oussaidene et al., 2015). The maximum cerebral oxygenation threshold was also higher in the trained group, but the threshold occurred at a similar $\dot{V}O_{2max}$ in both groups.

Cerebral oxygenation of the parietal lobe and motor cortices including the primary motor cortex (M1), supplementary motor area (SMA), and premotor cortex (PMC) were measured during a maximal voluntary static handgrip test (Shibuya and Kuboyama, 2010), and a cycle ergometer test (Seidel et al., 2019). There were no [HbO_2] and CRF level interactions during the cycling test but within the endurance trained group, there was a decrease in [HbO_2] in the PMC, SMA, and left inferior parietal lobe (Seidel et al., 2019). In the active control group, this effect was only observed in the right-hemispheric PMC at 20% intensity (Seidel et al., 2019). During the handgrip exercise test, there was continued activation in the contralateral M1 in the non-athlete group at voluntary exhaustion compared to M1 activation that dropped below baseline values in the athlete group (Shibuya and Kuboyama, 2010).

Deoxyhemoglobin During Acute Exercise Tasks

Two studies, one examining male and the other examining female older adults, measured deoxyhemoglobin during a ramp incremental test at 25, 80, or 90% intensity or square wave constant load test at 90% or peak intensity (Buzza et al., 2016, 2020). In the study examining females, there were no significant interactions between CRF level and PFC activation at 25, 80,

and 90% or peak intensity in short-term (6–24 months) or long-term (>5 years) groups (Buzza et al., 2016). However, the study examining males revealed greater [HHb] changes in the PFC during the square wave constant load test in the long compared to short-term trained group at 90% intensity (Buzza et al., 2020). In a study measuring left PFC activation, there were no differences in [HHb] between endurance-trained and untrained young males (Oussaidene et al., 2015).

Two studies measured changes in [HHb] in the motor cortex. The first study did not find significant interactions between endurance-trained athletes and active controls during a cycling test (Seidel et al., 2019). There was, however, a larger [HHb] decrease at 60% compared to 20% intensity across all participants in the left PMC. A second study evaluated the effect of a static handgrip exercise test on contralateral M1 activation in athlete and non-athlete younger adults (Shibuya and Kuboyama, 2010). Findings revealed that [HHb] activation decreased after 20 s of exercise and continued below baseline values from 30 s to exhaustion in the non-athlete group. The athlete group demonstrated lower [HHb] levels than baseline values at 30 s to exhaustion.

Oxyhemoglobin and Deoxyhemoglobin Following a Training Intervention

Cerebral oxygenation was measured during a maximal incremental test before and after a 6-week cycling training intervention (Caen et al., 2019). Findings revealed that after an aerobic training intervention, participants who displayed greater $\dot{V}O_{2max}$ had a higher total [HbO_2] and total hemoglobin amplitude during maximal exercise compared to pre-training (Caen et al., 2019).

Functional Near-Infrared Spectroscopy Processing and Analysis Methods

FNIRS recordings during exercise tasks lasted between 2 and 32 min, which was substantially longer than studies using cognitive tasks where brain activity was recorded for 30–150 s. Physiological and/or motion filters were used to remove artifacts from noisy data in all studies evaluating cerebral oxygenation during cognitive and visual tasks. In contrast, the study evaluating dual-tasks stated that they did not use any filters but artifacts were identified through visual inspection and replaced by interpolation of adjacent data (Goenarjo et al., 2020a). Of the studies examining exercise tasks, filtering methods were not specified except for one study that used short-distance channels to eliminate physiological artifacts (Seidel et al., 2019).

All but one study used continuous wave fNIRS, which are the most commercially available devices (Scholkmann et al., 2014). Fabiani et al. (2014) used a frequency domain device. Accordingly, thirteen studies measured relative changes in cerebral oxygenation by subtracting baseline values from task-evoked changes. A linear regression approach was used by one study to assign a slope coefficient to [HbO_2] and [HHb] for the entire response signal (Albinet et al., 2014). Channel configuration varied between studies with four using three channels (Buzza et al., 2016, 2020; Mekari et al., 2019; Goenarjo et al., 2020b), three studies using two (Shibuya and Kuboyama, 2010; Albinet et al., 2014; Caen et al., 2019) or eight channels (Brugniaux et al., 2014; Oussaidene et al., 2015; Agbangla et al., 2019a), and one study using 16 (Dupuy et al., 2015), 22 (Seidel et al., 2019), 32 (Fabiani et al., 2014), or 48 (Hyodo et al., 2016) channels, respectively. Across all studies, the lower wavelength ranged from 690 to 794 nm and the upper wavelength ranged from 830 to 905 nm, which was largely dependent on the fNIRS device.

Differences Between Cardiorespiratory Fitness Measures

CRF was measured using direct measures of $\dot{V}O_{2max}$, $\dot{V}O_{2peak}$, ventilatory threshold, or peak power output in 11 studies and self-report questionnaires in three studies. The study using a ventilatory threshold justified using this measure because it was more convenient for older adults (Hyodo et al., 2016). Amongst the studies using direct measures, four studies divided the participants into high and low fit groups based on a median split or by excluding the middle group of CRF scores and analyzing the upper and lower thirds (Albinet et al., 2014; Fabiani et al., 2014; Mekari et al., 2019; Goenarjo et al., 2020a). The remaining studies divided groups based on published age and gender norms of CRF. In addition to direct measures of CRF, five studies assessed whether participants had a background in different types of physical activity or training during the recruitment stage (Albinet et al., 2014; Brugniaux et al., 2014; Oussaidene et al., 2015; Caen et al., 2019; Seidel et al., 2019). This included a 7-point physical activity rating used to estimate $\dot{V}O_{2max}$ (Albinet et al., 2014), a self-report physical activity questionnaire (Brugniaux et al., 2014), a simple question about past involvement in recreational sports (Caen et al., 2019), or questions that determined the number of hours per week of physical activity (Oussaidene et al., 2015; Seidel et al., 2019).

The three studies using self-report questionnaires to determine CRF consisted of the NASA/Johnson Space Center physical activity questionnaire, which required older adults to rate their physical activity on a scale from 0 to 7 and was adjusted for their age, body mass index (BMI), and sex (Agbangla et al., 2019a). In comparison, two studies used self-reported physical activity logs to track training minutes of moderate to vigorous exercise per week (Buzza et al., 2016, 2020).

Assessment of Risk of Bias

Based on the JBI quality assessment checklist, each of the 14 studies was of sufficient quality to be included in this review (**Table 3**). In all studies, the exposure was clearly described, the outcomes were clearly defined, and statistical analyses were appropriately chosen. All studies described the participant characteristics in sufficient detail, but two studies did not clearly describe the setting. Despite this, it can be assumed that these studies were conducted in a university lab setting due to the specialized equipment involved in CRF testing. Objective criteria were used to measure CRF in 13 studies whereas one study indicated the cut-offs between high and low groups but did not indicate what test was used to measure $\dot{V}O_{2max}$ in each group (Shibuya and Kuboyama, 2010). Lastly, seven studies identified

and controlled for confounding variables such as education level. Five studies did not control for confounding variables, and two studies were unclear. These studies were not excluded because they reported confounding characteristics in a table format, which were not significantly different between groups. Therefore, it is unlikely that they contributed to sources of bias between studies.

DISCUSSION

Effects of Cardiorespiratory Fitness on Cerebral Oxygenation During Cognitive Tasks

Previous reviews have outlined the effects of chronic exercise on cognitive performance (Li et al., 2017; Rathore and Lom, 2017), but few have assessed the impact of CRF on cerebral oxygenation. In a meta-analysis, Rooks et al. (2010) examined the impact of training status on cerebral oxygenation during incremental tests without considering how CRF and training status were measured (i.e., $\dot{V}O_{2max}$ or physical activity level). More recently, Agbangla et al. (2021) reviewed the impact of CRF on cerebral oxygenation during cognitive tasks. This review examined the effects of CRF level, as determined by direct or estimated measures, on cerebral oxygenation during exercise and cognitive task performance. Exercise-related effects on cognition have been explored using the cardiorespiratory hypothesis, which maintains that improvements in cognitive performance are moderated by factors such as increased cerebral perfusion in individuals with greater CRF (Agbangla et al., 2019b).

Studies examining the PFC revealed increased [HbO_2] in higher compared to lower fit groups during cognitive tasks. In fact, most studies in this review used tasks that draw on executive functions since they are susceptible to age-related declines and can be improved with exercise interventions (Colcombe and Kramer, 2003). There is evidence that the frontal lobe is disproportionately affected by aging but is activated during executive function tasks (West, 1996). In older adults, this results in bilateral PFC activation compared to younger adults who demonstrate unilateral activation to support task performance (Reuter-Lorenz and Cappell, 2008). This is outlined in the Compensation-Related Utilization of Neural Circuits Hypothesis (CRUNCH) which accounts for the effect of task demands and processing capacity that when exceeded, results in performance declines (Reuter-Lorenz and Cappell, 2008). Therefore, PFC activation is more pronounced with increasing executive function demands and greater CRF can facilitate these processes (Albinet et al., 2014; Agbangla et al., 2019a; Goenarjo et al., 2020a). In the case of M1, activation is observed in the contralateral hemisphere to the movement being performed (Shibuya and Kuboyama, 2010). Previous studies have reported that right-handed individuals activate the left M1 but recruit M1 bilaterally during exhaustive exercise to compensate for decreased muscle force (Shibuya et al., 2008). Therefore, both the PFC and M1 can demonstrate bilateral activation as a mechanism of compensation.

In studies comparing younger and older adults, higher $\dot{V}O_{2max}$ only contributed to increased cerebral oxygenation in

TABLE 3 | JBI quality assessment.

	Criteria							
Author (Year)	**1**	**2**	**3**	**4**	**5**	**6**	**7**	**8**
Agbangla et al. (2019a)	Yes	Yes	Yes	Yes	Yes	Yes	Yes	Yes
Albinet et al. (2014)	Yes	Yes	Yes	Yes	Yes	Yes	Yes	Yes
Brugniaux et al. (2014)	Yes	Unclear	Yes	Yes	No	No	Yes	Yes
Buzza et al. (2016)	Yes	Yes	Yes	Yes	Yes	Yes	Yes	Yes
Buzza et al. (2020)	Yes	Unclear	Yes	Yes	Yes	Yes	Yes	Yes
Caen et al. (2019)	Unclear	Yes	Yes	Yes	No	No	Yes	Yes
Dupuy et al. (2015)	Yes	Yes	Yes	Yes	No	No	Yes	Yes
Fabiani et al. (2014)	Yes	Yes	Yes	Yes	Unclear	Unclear	Yes	Yes
Goenarjo et al. (2020a)	Yes	Yes	Yes	Yes	Yes	Yes	Yes	Yes
Hyodo et al. (2016)	Yes	Yes	Yes	Yes	Yes	Yes	Yes	Yes
Mekari et al. (2019)	Yes	Yes	Yes	Yes	Yes	Yes	Yes	Yes
Oussaidene et al. (2015)	Yes	Yes	Yes	Yes	No	No	Yes	Yes
Seidel et al. (2019)	Yes	Yes	Yes	No	Unclear	Unclear	Yes	Yes
Shibuya and Kuboyama (2010)	Yes	Yes	Yes	Unclear	No	No	Yes	Yes

1. Were the criteria for inclusion in the sample clearly defined?
2. Were the study subjects and the setting described in detail?
3. Was the exposure measured in a valid and reliable way?
4. Were objective, standard criteria used for measurement of the condition?
5. Were confounding factors identified?
6. Were strategies to deal with confounding factors stated?
7. Were the outcomes measured in a valid and reliable way?
8. Was appropriate statistical analysis used?

older adults (Dupuy et al., 2015; Agbangla et al., 2019a). In other words, high and low fit younger adults (Dupuy et al., 2015) as well as a pooled group (Agbangla et al., 2019a) did not exhibit increased cerebral oxygenation or differences in performance. These findings have been attributed to the high functioning status of young adults and intact brain structures that help maintain cognitive performance regardless of CRF level. In addition, older adults aged 65 and over have shown the greatest capacity to demonstrate improvements in executive function compared to younger adults (Colcombe and Kramer, 2003). Therefore, differences in CRF may only lead to small improvements in cerebral oxygenation, which may be less evident in younger compared to older adults.

[HHb] findings prove to be more variable with studies reporting both decreased and insignificant changes based on CRF. Two studies found decreased [HHb] during executive function and dual-tasks in high compared to low fit younger and older adults (Agbangla et al., 2019a; Goenarjo et al., 2020b). In contrast, one study indicated that the lack of significant findings was due to their fNIRS device, which was not configured to measure [HHb] (Hyodo et al., 2016). Insignificant differences in [HHb] can also be attributed to its low signal to noise ratio making it hard to identify the hemodynamic component of the signal. Nonetheless, [HHb] is less likely to be influenced by systemic and motion artifacts making it a reliable measure during tasks that require unrestricted movements (Menant et al., 2020). To better interpret these results, it is important to remember that during cognitive stimulation, the fNIRS responses are manifested by an increase in [HbO_2] and a decrease in [HHb] (Villringer, 1997). [HHb] is also strongly correlated with brain activity and inversely correlated with the BOLD signal (Villringer, 1997). The greater the decrease in [HHb], the more the BOLD signal increases. Based on this information, a greater decrease in [HHb] during a cognitive task in high fit subjects could represent greater brain activity as shown by Colcombe et al. (2004).

Studies examining mixed samples of male and female participants demonstrated that increased CRF was associated with increased cerebral oxygenation and better performance (Agbangla et al., 2019a; Mekari et al., 2019). There are, however, known differences in CRF between males and females that contribute to changes in cerebral oxygenation (Colcombe and Kramer, 2003; Erickson et al., 2007; Dimech et al., 2019). For example, findings differed across male and female groups in the present review such that high fit females demonstrated increased bilateral activation in the PFC (Albinet et al., 2014) and increased right activation as task demands increased (Dupuy et al., 2015). Older males, however, only demonstrated left lateralized PFC activation in the higher fit group, which is a pattern typically observed in younger adults (Hyodo et al., 2016). This is outlined in the hemispheric asymmetry reduction in older adults (HAROLD) model whereby bilateral activation is expected due to decreased white matter integrity, vascularization, and less efficient adaptations to task-related metabolic demands (Cabeza, 2002; Hyodo et al., 2016; Agbangla et al., 2019b). Upon re-examining the studies investigating mixed samples, participants were predominantly female. Therefore, data from female participants may be contributing to bilateral activation in mixed samples more so than males. More evidence is needed that directly compares activation in males and females across different CRF levels.

Effect of Cardiorespiratory Fitness on Cerebral Oxygenation During Exercise

Incremental and maximal exercise elicit an increased metabolic demand for oxygen. In the present review, cerebral oxygenation was measured during acute cycling exercise and in one case during a static handgrip task (Shibuya and Kuboyama, 2010). During submaximal exercise, [HbO_2] was greater in the PFC of trained compared to untrained young males (Oussaidene et al., 2015). In addition, moderately active young males demonstrated increased PFC oxygenation until 80% $\dot{V}O_{2max}$ compared to the sedentary group, which displayed constant but lower cerebral oxygenation (Brugniaux et al., 2014). These findings build on a previous meta-analysis where healthy participants demonstrated steady increases in cerebral oxygenation during incremental exercise compared to their baseline resting levels (Rooks et al., 2010).

In terms of [HHb], two studies measured middle-aged females and males, respectively (Buzza et al., 2016, 2020). Only the male long-term training group (higher fit) demonstrated greater PFC [HHb] compared to the short-term training group (lower fit) at 90% intensity on a cycle ergometer (Buzza et al., 2020). A similar interaction was observed in younger adults whereby left PFC [HHb] increased in a trained vs. untrained group (Oussaidene et al., 2015). From low to submaximal intensities, PFC [HbO_2] is expected to increase until it reaches a plateau near maximum intensity (Jung et al., 2015). During the handgrip exercise test, however, activation in M1, which is responsible for sending efferent information to the contracting hand muscles, continued to rise in the non-athlete group at voluntary exhaustion whereas it dropped below baseline values in the athlete group (Shibuya and Kuboyama, 2010). More specifically, participants were right-handed and cerebral oxygenation was measured in the contralateral M1. Continued activation may be a mechanism used to compensate for decreased muscle force when exhausted (Shibuya et al., 2008). A second mechanism is the bilateral activation of M1, which has been observed during low intensity static handgrip tasks (Shibuya et al., 2008). For the same task, compensation and greater oxygenation in the lower compared to higher fit group reflects how [HbO_2] and [HHb] are regulated in M1 during exhaustive motor tasks (Shibuya and Kuboyama, 2010).

Effects of Exercise Training on Cerebral Oxygenation

Numerous studies have demonstrated that aerobic training is beneficial for cognitive performance, but few interventional studies have evaluated the effect of aerobic training on brain oxygenation during physical exercise or cognitive tasks. Only one study in this review measured a 6-week aerobic exercise training intervention and demonstrated that [HbO_2] and [HHb] amplitude and slope increased post-intervention in younger adults during maximal incremental exercise test

(Caen et al., 2019). It is unclear if this is the case for older adults, but previous reports have demonstrated improvements in executive functions following exercise interventions (Voss et al., 2012; Northey et al., 2018; Domingos et al., 2021). In addition, fitness training selectively improved executive control processes compared to speed, controlled, and spatial ability in older adults (Colcombe and Kramer, 2003). Fewer studies have examined cerebral oxygenation following exercise interventions but changes in cerebral blood flow have been observed in cortical and subcortical regions (Brown et al., 2010; Chapman, 2013). To the best of our knowledge, only Coetsee and Terblanche (2017) reported lower cerebral oxygenation in older adults after aerobic training, but the measure of $\dot{V}O_{2max}$ was not explicitly stated. In addition, the meta-analysis by Rooks et al. (2010) reported greater cerebral oxygenation during incremental exercise tests between trained and untrained participants but lacked defined criteria for training status making the results difficult to compare. Previous reports have used direct measures of CRF in older adults (Dupuy et al., 2015) while others suggest that estimated measures are more feasible to obtain in older adults (Agbangla et al., 2019a). Nonetheless, more training interventions are needed to assess the effects of CRF on cerebral oxygenation.

Possible Mechanisms Underlying Improved Cerebral Oxygenation With Higher Cardiorespiratory Fitness

Exercise has known benefits on cerebrovascular health such that the cardiovascular system is involved in delivering oxygen and regulating cerebral metabolism to sustain cognitive processing. From a cognitive perspective, exercise may increase angiogenesis, neurovascular plasticity, and oxygen saturation in brain regions related to cognitive performance including prefrontal and motor cortices and the hippocampus (Stimpson et al., 2018). Exercise also upregulates growth factors like brain-derived neurotrophic factor (BDNF), insulin-like growth factor (IGF), and vascular endothelial growth factor (VEGF), which are involved in synaptic plasticity, neurogenesis, promote angiogenesis, and support memory (Cotman and Berchtold, 2002; Ploughman, 2008; Davenport et al., 2012; Hayes et al., 2013). These neurotrophins can also offset the effects of age-related cerebral atrophy that interfere with adequate oxygen delivery to the brain (Ainslie et al., 2008; Erickson et al., 2014). For example, 3 months of aerobic exercise have been reported to increase neurotrophins and cerebral blood volume (Pereira et al., 2007). Therefore, higher fit individuals demonstrate increased BDNF compared to lower fit individuals because of improved cerebral blood flow and better vascularization, which foster neurotrophic and growth factors in the brain (Brown et al., 2010; Stimpson et al., 2018). In addition, older adults who are more physically active have been found to display a higher number of small cerebral vessels than less physically active older adults (Bullitt et al., 2009). Angiogenesis is upregulated by VEGF which also promotes endothelial cell proliferation (Cotman and Berchtold, 2002). Similarly, exercise increases the production of plasmatic VEGF which is the main growth factor associated with capillary formation in the brain (Cotman and Berchtold, 2002; Duman, 2005). Stimpson et al. (2018) and Dupuy et al. (2019) summarized these factors in a simplified model that describes the relationship between physical activity and cognition. In combination with these molecular mechanisms, it has also been observed that higher fit individuals have higher cerebral blood flow at rest, and during the tilt test and exercise than lower fit people (Murrell et al., 2011a,b). This explains the reports of greater cerebral oxygenation in higher fit individuals. Given that higher CRF is associated with increased cerebral oxygenation, fNIRS measures can complement the existing literature on the mechanisms involved in exercise and improved cognition.

Functional Near-Infrared Spectroscopy Devices and Processing Variability

Given the growing popularity of fNIRS in cognitive and exercise physiology research, guidelines have been established to increase reporting transparency and the reproducibility of different study designs (Menant et al., 2020; Yücel et al., 2021). In terms of fNIRS devices, most commercially available continuous wave fNIRS systems have the capability of measuring [HbO_2] and [HHb], which is an advantage over fMRI. Therefore, studies should report on both measures to broaden our understanding of potential shifts between increases and decreases in these measures related to CRF. Amongst the studies in this review, the most common justification for only reporting [HbO_2] is that it better reflects cortical activation, but it should be noted that it contains a larger signal-to-noise ratio (Strangman et al., 2002). In terms of [HHb], it is less contaminated by systemic artifacts, but the signal is attenuated compared to [HbO_2], and certain devices are not configured to assess both measures (Kirilina et al., 2012; Hyodo et al., 2016).

As stated in the guidelines and consensus measures by Menant et al. (2020) and Yücel et al. (2021), signal processing methods should be clearly described. Many studies in this review were unclear or did not specify the methods used to process motion artifacts. For example, cycling tasks are expected to produce greater motion artifacts than seated cognitive tasks due to increased movement (Yücel et al., 2021). Removing irrelevant artifacts from the signal can be achieved through filtering, visual inspection, and is sometimes overcome with specific instructions for participants to minimize sudden head movements (Menant et al., 2020). In order to adequately compare and contrast different research studies and to fully understand cerebral oxygenation changes associated with CRF level, detailed reporting is imperative.

The duration of fNIRS measurements also differed between cognitive and exercise tasks. Exercise measures were significantly longer than cognitive tasks given the nature of incremental cycling. In both cases, the segment analyzed was of sufficient duration to capture the hemodynamic response. Longer measures, however, could increase participant discomfort and affect brain activation due to drifts in the signal (Menant et al., 2020).

Limitations

This systematic review included cross-sectional studies with relatively small sample sizes. In addition, only one study examined the effects of exercise training on cerebral oxygenation. Future studies should consider implementing randomized controlled trials to ensure a comprehensive examination and minimal bias is introduced when examining the effects of CRF on cerebral oxygenation. The self-reported questionnaires to estimate $\dot{V}O_{2max}$ may have introduced biased responses if participants overestimated their physical activity levels. However, the questionnaires were reliable and a more feasible method to measure CRF in older adults. $\dot{V}O_{2max}$ also significantly differed between high and low fit groups in these studies.

Continuous wave fNIRS devices are most frequently reported in the literature, but only provide relative changes in cerebral oxygenation rather than absolute values. This limitation can be overcome by frequency and time domain fNIRS devices, which come at a greater cost, but allow for more in-depth measures. Although it is also limited to surface cortex measurements, changes in PFC and motor cortex activation were identified between studies. The interaction between these two regions should be further examined as connectivity between the PFC and motor regions is important for exercise load management, coordination, and preparation of motor movements, which may differ between high and low fit groups (Voss et al., 2016). In addition, similar deoxygenation between PFC and motor cortices has been reported during maximum intensity exercise (Subudhi et al., 2009). Lastly, preprocessing is essential for removing physiological (e.g., systemic) and motion artifacts (e.g., head movements) in the fNIRS signal. Due to the nature of physical exercise, these variables may be especially prominent. Future studies should report all preprocessing steps to increase signal quality and methodological reproducibility.

CONCLUSION

CRF can affect cerebral oxygenation in young, middle-aged, and older adults. Due to the widespread applications of fNIRS in both aerobic exercise and cognitive tasks, careful attention should be placed on reporting detailed processing methods to increase study reproducibility. Nonetheless, increased CRF was generally associated with increased cerebral oxygenation in the prefrontal and motor cortices. Lastly, this review predominantly featured cross-sectional studies. Future research should attempt to reproduce these effects using fNIRS in a randomized controlled trial to identify whether these findings hold true across larger samples, populations, and training interventions.

AUTHOR CONTRIBUTIONS

TS developed the search with a Health Sciences librarian, translated the search for the different databases, conducted the search, screened and extracted the articles, wrote up the findings, and drafted the manuscript. OD assisted with the screening of the articles, reviewed the findings, and participated in the write-up of the manuscript. SF assisted with the screening and extraction of the articles, reviewed the findings, and participated in the write-up of the manuscript. All authors contributed to the article and approved the submitted version.

FUNDING

This publication received scholarly communication support from the University of Ottawa for online publication fees.

ACKNOWLEDGMENTS

We would like to acknowledge the scholarly communications open access publishing support from the library at the University of Ottawa, as well as the support of the librarian.

SUPPLEMENTARY MATERIAL

The Supplementary Material for this article can be found online at: https://www.frontiersin.org/articles/10.3389/fphys.2022.838450/full#supplementary-material

REFERENCES

Aadahl, M., Kjaer, M., Kristensen, J. H., Mollerup, B., and Jørgensen, T. (2007). Self-reported physical activity compared with maximal oxygen uptake in adults. *Eur. J. Cardiovasc. Prev. Rehabilit.* 14, 422–428. doi: 10.1097/HJR.0b013e3280128d00

Agbangla, N. F., Fraser, S. A., and Albinet, C. T. (2019b). An Overview of the Cardiorespiratory Hypothesis and Its Potential Contribution to the Care of Neurodegenerative Disease in Africa. *Medicina* 55:601. doi: 10.3390/medicina55090601

Agbangla, N. F., Maillot, P., and Vitiello, D. (2021). Mini-Review of Studies Testing the Cardiorespiratory Hypothesis With Near-Infrared Spectroscopy (NIRS): overview and Perspectives. *Front. Neurosci.* 15:699948. doi: 10.3389/fnins.2021.699948

Agbangla, N. F, Audiffren, M., Pylouster, J., and Albinet, C. (2019a). Working Memory, Cognitive Load and Cardiorespiratory Fitness: Testing the CRUNCH Model with Near-Infrared Spectroscopy. *Brain Sci.* 9:38. doi: 10.3390/brainsci9020038

Ainslie, P. N., Cotter, J. D., George, K. P., Lucas, S., Murrell, C., Shave, R., et al. (2008). Elevation in cerebral blood flow velocity with aerobic fitness throughout healthy human ageing: Cerebral blood flow and aerobic fitness. *J. Physiol.* 586, 4005–4010. doi: 10.1113/jphysiol.2008.158279

Albinet, C. T., Mandrick, K., Bernard, P. L., Perrey, S., and Blain, H. (2014). Improved cerebral oxygenation response and executive performance as a function of cardiorespiratory fitness in older women: a fNIRS study. *Front. Aging Neurosci.* 6:272. doi: 10.3389/fnagi.2014.00272

Ando, S., Hatamoto, Y., Sudo, M., Kiyonaga, A., Tanaka, H., and Higaki, Y. (2013). The Effects of Exercise Under Hypoxia on Cognitive Function. *PLoS One* 8:e63630. doi: 10.1371/journal.pone.0063630

Balke, B., and Ware, R. W. (1959). An experimental study of physical fitness of Air Force personnel. *U S Arm. For. Med. J.* 10, 675–688.

Brown, A. D., McMorris, C. A., Longman, R. S., Leigh, R., Hill, M. D., Friedenreich, C. M., et al. (2010). Effects of cardiorespiratory fitness and cerebral blood

flow on cognitive outcomes in older women. *Neurobiol. Aging* 31, 2047–2057. doi: 10.1016/j.neurobiolaging.2008.11.002

Brugniaux, J. V., Marley, C. J., Hodson, D. A., New, K. J., and Bailey, D. M. (2014). Acute exercise stress reveals cerebrovascular benefits associated with moderate gains in cardiorespiratory fitness. *J. Cereb. Blood Flow Metab.* 34, 1873–1876. doi: 10.1038/jcbfm.2014.142

Bullitt, E., Rahman, F. N., Smith, J. K., Kim, E., Zeng, D., Katz, L. M., et al. (2009). The effect of exercise on the cerebral vasculature of healthy aged subjects as visualized by MR angiography. *AJNR* 30, 1857–1863. doi: 10.3174/ajnr.A1695

Buttar, K., Saboo, N., and Kacker, S. (2019). A review: Maximal oxygen uptake (VO2 max) and its estimation methods. *Internat. J. Phys. Educ. Sport Health* 6, 24–32.

Buzza, G., Lovell, G. P., Askew, C. D., Kerherve, H., and Solomon, C. (2016). The Effect of Short and Long Term Endurance Training on Systemic, and Muscle and Prefrontal Cortex Tissue Oxygen Utilisation in 40—60 Year Old Women. *PLoS One* 11:e0165433. doi: 10.1371/journal.pone.0165433

Buzza, G., Lovell, G. P., Askew, C. D., and Solomon, C. (2020). A Comparison of VO 2, and Muscle and Prefrontal Cortex Tissue Oxygen Extraction between Short and Long-term Aerobically Trained Men Aged 40—60 Years. *Internat. J. Exerc. Sci.* 13, 964–978.

Cabeza, R. (2002). Hemispheric asymmetry reduction in older adults: the HAROLD model. *Psychol. Aging* 17, 85–100. doi: 10.1037/0882-7974.17.1.85

Caen, K., Vermeire, K., Pogliaghi, S., Moerman, A., Niemeijer, V., Bourgois, J. G., et al. (2019). Aerobic Interval Training Impacts Muscle and Brain Oxygenation Responses to Incremental Exercise. *Front. Physiol.* 10:1195. doi: 10.3389/fphys.2019.01195

Chaparro, G. N., Stine-Morrow, E. A. L., and Hernandez, M. E. (2019). Effects of aerobic fitness on cognitive performance as a function of dual-task demands in older adults. *Exp. Gerontol.* 118, 99–105. doi: 10.1016/j.exger.2019.01.013

Chapman, R. F. (2013). The individual response to training and competition at altitude. *Br. J. Sports Med.* 47, i40–i44. doi: 10.1136/bjsports-2013-092837

Coetsee, C., and Terblanche, E. (2017). Cerebral oxygenation during cortical activation: The differential influence of three exercise training modalities. a randomized controlled trial. *Eur. J. Appl. Physiol.* 117, 1617–1627. doi: 10.1007/s00421-017-3651-8

Colcombe, S., and Kramer, A. F. (2003). Fitness effects on the cognitive function of older adults: a meta-analytic study. *Psychol. Sci.* 14, 125–130. doi: 10.1111/1467-9280.t01-1-01430

Colcombe, S. J., Kramer, A. F., Erickson, K. I., Scalf, P., McAuley, E., Cohen, N. J., et al. (2004). Cardiovascular fitness, cortical plasticity, and aging. *Proc. Natl. Acad. Sci.U S A* 101, 3316–3321. doi: 10.1073/pnas.0400266101

Cotman, C. W., and Berchtold, N. C. (2002). Exercise: a behavioral intervention to enhance brain health and plasticity. *Trends Neurosci.* 25, 295–301. doi: 10.1016/s0166-2236(02)02143-4

d'Arbeloff, T. (2020). Cardiovascular fitness and structural brain integrity: an update on current evidence. *GeroScience* 42, 1285–1306. doi: 10.1007/s11357-020-00244-7

Davenport, M. H., Hogan, D. B., Eskes, G. A., Longman, R. S., and Poulin, M. J. (2012). Cerebrovascular Reserve: the Link Between Fitness and Cognitive Function? *Exerc. Sport Sci. Rev.* 40, 153–158. doi: 10.1097/JES.0b013e3182553430

Dimech, C. J., Anderson, J. A. E., Lockrow, A. W., Spreng, R. N., and Turner, G. R. (2019). Sex differences in the relationship between cardiorespiratory fitness and brain function in older adulthood. *J. Appl. Physiol.* 126, 1032–1041. doi: 10.1152/japplphysiol.01046.2018

Domingos, C., Pêgo, J. M., and Santos, N. C. (2021). Effects of physical activity on brain function and structure in older adults: a systematic review. *Behav. Brain Res.* 402:113061. doi: 10.1016/j.bbr.2020.113061

Duman, R. S. (2005). Neurotrophic factors and regulation of mood: Role of exercise, diet and metabolism. *Neurobiol. Aging* 26(Suppl. 1), 88–93. doi: 10.1016/j.neurobiolaging.2005.08.018

Dupuy, O., Bosquet, L., Fraser, S. A., Labelle, V., and Bherer, L. (2018). Higher cardiovascular fitness level is associated to better cognitive dual-task performance in Master Athletes: Mediation by cardiac autonomic control. *Brain Cogn.* 125, 127–134. doi: 10.1016/j.bandc.2018.06.003

Dupuy, O., Gauthier, C. J., Fraser, S. A., Desjardins-Crèpeau, L., Desjardins, M., Mekary, S., et al. (2015). Higher levels of cardiovascular fitness are associated with better executive function and prefrontal oxygenation in younger and older women. *Front. Hum. Neurosci.* 9:66. doi: 10.3389/fnhum.2015.00066

Dupuy, O., Goenarjo, R., Fraser, S. A., Bherer, L., and Bosquet, L. (2019). Master Athletes and cognitive performance: what are the potential explanatory neurophysiological mechanisms? *Mov. Sport Sci.* 104, 55–67. doi: 10.1051/sm/2019023

Erickson, K. I., Colcombe, S. J., Elavsky, S., McAuley, E., Korol, D. L., Scalf, P. E., et al. (2007). Interactive effects of fitness and hormone treatment on brain health in postmenopausal women. *Neurobiol. Aging* 28, 179–185. doi: 10.1016/j.neurobiolaging.2005.11.016

Erickson, K. I., Leckie, R. L., and Weinstein, A. M. (2014). Physical activity, fitness, and gray matter volume. *Neurobiol. Aging* 35, S20–S28. doi: 10.1016/j.neurobiolaging.2014.03.034

Eriksen, M. B., and Frandsen, T. F. (2018). The impact of patient, intervention, comparison, outcome (PICO) as a search strategy tool on literature search quality: a systematic review. *J. Med. Lib. Assoc.* 106, 420–431. doi: 10.5195/jmla.2018.345

Fabiani, M., Gordon, B., Maclin, E., Pearson, M., Brumback-Peltz, C., Low, K., et al. (2014). Neurovascular coupling in normal aging: A combined optical, ERP and fMRI study. *Neuroimage* 85, 592–607. doi: 10.1016/j.neuroimage.2013.04.113

George, J. D., Vehrs, P. R., Allsen, P. E., Fellingham, G. W., and Fisher, A. G. (1993). VO2max estimation from a submaximal 1-mile track jog for fit college-age individuals. *Med. Sci. Sports Exerc.* 25, 401–406.

Goenarjo, R., Bosquet, L., Berryman, N., Metier, V., Perrochon, A., Fraser, S. A., et al. (2020a). Cerebral Oxygenation Reserve: the Relationship Between Physical Activity Level and the Cognitive Load During a Stroop Task in Healthy Young Males. *Internat. J. Env. Res. Public Health* 17:4. doi: 10.3390/ijerph17041406

Goenarjo, R., Dupuy, O., Fraser, S., Perrochon, A., Berryman, N., and Bosquet, L. (2020b). Cardiorespiratory fitness, blood pressure, and cerebral oxygenation during a dual-task in healthy young males. *Behav. Brain Res.* 380:112422. doi: 10.1016/j.bbr.2019.112422

Goenarjo, R., Dupuy, O., Fraser, S., Berryman, N., Perrochon, A., and Bosquet, L. (2021). Cardiorespiratory fitness and prefrontal cortex oxygenation during Stroop task in older males. *Physiol. Behav.* 242:113621. doi: 10.1016/j.physbeh.2021.113621

Hayes, S. M., Hayes, J. P., Cadden, M., and Verfaellie, M. (2013). A review of cardiorespiratory fitness-related neuroplasticity in the aging brain. *Front. Aging Neurosci.* 5:31. doi: 10.3389/fnagi.2013.00031

Hillman, C. H., Erickson, K. I., and Kramer, A. F. (2008). Be smart, exercise your heart: Exercise effects on brain and cognition. *Nat. Rev. Neurosci.* 9, 58–65. doi: 10.1038/nrn2298

Hyodo, K., Dan, I., Kyutoku, Y., Suwabe, K., Byun, K., Ochi, G., et al. (2016). The association between aerobic fitness and cognitive function in older men mediated by frontal lateralization. *NeuroImage* 125, 291–300. doi: 10.1016/j.neuroimage.2015.09.062

Jung, R., Moser, M., Baucsek, S., Dern, S., and Schneider, S. (2015). Activation patterns of different brain areas during incremental exercise measured by near-infrared spectroscopy. *Exp. Brain Res.* 233, 1175–1180. doi: 10.1007/s00221-015-4201-4

Jurca, R., Jackson, A. S., LaMonte, M. J., Morrow, J. R., Blair, S. N., Wareham, N. J., et al. (2005). Assessing cardiorespiratory fitness without performing exercise testing. *Am. J. Prev. Med.* 29, 185–193. doi: 10.1016/j.amepre.2005.06.004

Kirilina, E., Jelzow, A., Heine, A., Niessing, M., Wabnitz, H., Brühl, R., et al. (2012). The physiological origin of task-evoked systemic artefacts in functional near infrared spectroscopy. *NeuroImage* 61, 70–81. doi: 10.1016/j.neuroimage.2012.02.074

Kundu, S., Huang, H., Erickson, K. I., McAuley, E., Kramer, A. F., and Rohde, G. K. (2021). Investigating impact of cardiorespiratory fitness in reducing brain tissue loss caused by ageing. *Brain Commun.* 3:fcab228. doi: 10.1093/braincomms/fcab228

Li, J. W., O'Connor, H., O'Dwyer, N., and Orr, R. (2017). The effect of acute and chronic exercise on cognitive function and academic performance in adolescents: A systematic review. *J. Sci. Med. Sport* 20, 841–848. doi: 10.1016/j.jsams.2016.11.025

Liberati, A., Altman, D. G., Tetzlaff, J., Mulrow, C., Gotzsche, P. C., Ioannidis, J. P. A., et al. (2009). The PRISMA statement for reporting systematic reviews and meta-analyses of studies that evaluate healthcare interventions: explanation and elaboration. *BMJ* 339, b2700–b2700. doi: 10.1136/bmj.b2700

Ma, L.-L., Wang, Y.-Y., Yang, Z.-H., Huang, D., Weng, H., and Zeng, X.-T. (2020). Methodological quality (risk of bias) assessment tools for primary and secondary medical studies: What are they and which is better? *Milit. Med. Res.* 7:7. doi: 10.1186/s40779-020-00238-8

Mehagnoul-Schipper, D. J., van der Kallen, B. F. W., Colier, W. N. J. M., van der Sluijs, M. C., van Erning, L. J. T. O., Thijssen, H. O. M., et al. (2002). Simultaneous measurements of cerebral oxygenation changes during brain activation by near-infrared spectroscopy and functional magnetic resonance imaging in healthy young and elderly subjects. *Hum. Brain Map.* 16, 14–23. doi: 10.1002/hbm.10026

Mekari, S., Dupuy, O., Martins, R., Evans, K., Kimmerly, D. S., Fraser, S., et al. (2019). The effects of cardiorespiratory fitness on executive function and prefrontal oxygenation in older adults. *GeroScience* 41, 681–690. doi: 10.1007/s11357-019-00128-5

Mekari, S., Fraser, S., Bosquet, L., Bonnéry, C., Labelle, V., Pouliot, P., et al. (2015). The relationship between exercise intensity, cerebral oxygenation and cognitive performance in young adults. *Eur. J. Appl. Physiol.* 115, 2189–2197. doi: 10.1007/s00421-015-3199-4

Menant, J. C., Maidan, I., Alcock, L., Al-Yahya, E., Cerasa, A., Clark, D. J., et al. (2020). A consensus guide to using functional near-infrared spectroscopy in posture and gait research. *Gait Post.* 82, 254–265. doi: 10.1016/j.gaitpost.2020.09.012

Murrell, C. J., Cotter, J. D., George, K., Shave, R., Wilson, L., Thomas, K., et al. (2011a). Cardiorespiratory and cerebrovascular responses to head-up tilt II: influence of age, training status and acute exercise. *Exp. Gerontol.* 46, 1–8. doi: 10.1016/j.exger.2010.06.004

Murrell, C. J., Cotter, J. D., George, K., Shave, R., Wilson, L., Thomas, K., et al. (2011b). Cardiorespiratory and cerebrovascular responses to head-up tilt I: Influence of age and training status. *Exp. Gerontol.* 46, 9–17. doi: 10.1016/j.exger.2010.06.005

Northey, J. M., Cherbuin, N., Pumpa, K. L., Smee, D. J., and Rattray, B. (2018). Exercise interventions for cognitive function in adults older than 50: a systematic review with meta-analysis. [Review]. *J. Sports Med.* 52, 154–160. doi: 10.1136/bjsports-2016-096587

Oussaidene, K., Prieur, F., Tagougui, S., Abaidia, A., Matran, R., and Mucci, P. (2015). Aerobic fitness influences cerebral oxygenation response to maximal exercise in healthy subjects. *Respirat. Physiol. Neurobiol.* 205, 53–60. doi: 10.1016/j.resp.2014.10.009

Pereira, A. C., Huddleston, D. E., Brickman, A. M., Sosunov, A. A., Hen, R., McKhann, G. M., et al. (2007). An in vivo correlate of exercise-induced neurogenesis in the adult dentate gyrus. *Proc. Natl. Acad. Sci.* 104, 5638–5643. doi: 10.1073/pnas.0611721104

Pinti, P., Tachtsidis, I., Hamilton, A., Hirsch, J., Aichelburg, C., Gilbert, S., et al. (2018). The present and future use of functional near-infrared spectroscopy (fNIRS) for cognitive neuroscience: Advances in using fNIRS in cognitive neuroscience. *Ann. N Y Acad. Sci.* 2018:13948. doi: 10.1111/nyas.13948

Ploughman, M. (2008). Exercise is brain food: The effects of physical activity on cognitive function. *Dev. Neurorehabil.* 11, 236–240. doi: 10.1080/17518420801997007

Predovan, D., Fraser, S. A., Renaud, M., and Bherer, L. (2012). The Effect of Three Months of Aerobic Training on Stroop Performance in Older Adults. *J. Aging Res.* 2012:e269815. doi: 10.1155/2012/269815

Quaresima, V., and Ferrari, M. (2016). Functional Near-Infrared Spectroscopy (fNIRS) for Assessing Cerebral Cortex Function During Human Behavior in Natural/Social Situations: a Concise Review. *Org. Res. Methods* 2016:109442811665895. doi: 10.1177/1094428116658959

Rathore, A., and Lom, B. (2017). The effects of chronic and acute physical activity on working memory performance in healthy participants: a systematic review with meta-analysis of randomized controlled trials. *Syst. Rev.* 6:124. doi: 10.1186/s13643-017-0514-7

Reuter-Lorenz, P. A., and Cappell, K. A. (2008). Neurocognitive Aging and the Compensation Hypothesis. *Curr. Direct. Psychol. Sci.* 17, 177–182. doi: 10.1111/j.1467-8721.2008.00570.x

Rooks, C. R., Thom, N. J., McCully, K. K., and Dishman, R. K. (2010). Effects of incremental exercise on cerebral oxygenation measured by near-infrared spectroscopy: a systematic review. *Prog. Neurob.* 92, 134–150. doi: 10.1016/j.pneurobio.2010.06.002

Scholkmann, F., Kleiser, S., Metz, A. J., Zimmermann, R., Mata Pavia, J., Wolf, U., et al. (2014). A review on continuous wave functional near-infrared spectroscopy and imaging instrumentation and methodology. *NeuroImage* 85, 6–27. doi: 10.1016/j.neuroimage.2013.05.004

Seidel, O., Carius, D., Roediger, J., Rumpf, S., and Ragert, P. (2019). Changes in neurovascular coupling during cycling exercise measured by multi-distance fNIRS: A comparison between endurance athletes and physically active controls. *Exp. Brain Res.* 237, 2957–2972. doi: 10.1007/s00221-019-05646-4

Sexton, C. E., Betts, J. F., Demnitz, N., Dawes, H., Ebmeier, K. P., and Johansen-Berg, H. (2016). A systematic review of MRI studies examining the relationship between physical fitness and activity and the white matter of the ageing brain. *NeuroImage* 131, 81–90. doi: 10.1016/j.neuroimage.2015.09.071

Shibuya, K., and Kuboyama, N. (2010). Decreased activation in the primary motor cortex area during middle-intensity hand grip exercise to exhaustion in athlete and nonathlete participants. *Percept. Motor Skills* 111, 19–30. doi: 10.2466/15.25.26.PMS.111.4.19-30

Shibuya, K., Sadamoto, T., Sato, K., Moriyama, M., and Iwadate, M. (2008). Quantification of delayed oxygenation in ipsilateral primary motor cortex compared with contralateral side during a unimanual dominant-hand motor task using near-infrared spectroscopy. *Brain Res.* 1210, 142–147. doi: 10.1016/j.brainres.2008.03.009

Stillman, C. M., Esteban-Cornejo, I., Brown, B., Bender, C. M., and Erickson, K. I. (2020). Effects of exercise on brain and cognition across age groups and health states. *Trends Neurosci.* 43, 533–543. doi: 10.1016/j.tins.2020.04.010

Stimpson, N. J., Davison, G., and Javadi, A.-H. (2018). Joggin' the Noggin: Towards a Physiological Understanding of Exercise-Induced Cognitive Benefits. *Neurosci. Biobehav. Rev.* 88, 177–186. doi: 10.1016/j.neubiorev.2018.03.018

Strangman, G., Culver, J. P., Thompson, J. H., and Boas, D. A. (2002). A quantitative comparison of simultaneous BOLD fMRI and NIRS recordings during functional brain activation. *NeuroImage* 17, 719–731. doi: 10.1006/nimg.2002.1227

Subudhi, A. W., Miramon, B. R., Granger, M. E., and Roach, R. C. (2009). Frontal and motor cortex oxygenation during maximal exercise in normoxia and hypoxia. *J. Appl. Physiol.* 106, 1153–1158. doi: 10.1152/japplphysiol.91475.2008

Themanson, J. R., Hillman, C. H., and Curtin, J. J. (2006). Age and physical activity influences on action monitoring during task switching. *Neurobiol. Aging* 27, 1335–1345. doi: 10.1016/j.neurobiolaging.2005.07.002

Vanhees, L., Lefevre, J., Philippaerts, R., Martens, M., Huygens, W., Troosters, T., et al. (2005). How to assess physical activity? How to assess physical fitness? *Eur. J. Cardiovasc. Prevent. Rehabil.* 12, 102–114. doi: 10.1097/01.hjr.0000161551.73095.9c

Villringer, A. (1997). Non-invasive optical spectroscopy and imaging of human brain function. *Trends Neurosci.* 20, 435–442. doi: 10.1016/S0166-2236(97)01132-6

Voelcker-Rehage, C., and Niemann, C. (2013). Structural and functional brain changes related to different types of physical activity across the life span. *Neurosci. Biobehav. Rev.* 37, 2268–2295. doi: 10.1016/j.neubiorev.2013.01.028

Voss, M. W., Heo, S., Prakash, R. S., Erickson, K. I., Alves, H., Chaddock, L., et al. (2012). The influence of aerobic fitness on cerebral white matter integrity and cognitive function in older adults: results of a one-year exercise intervention. *Hum. Brain Map.* 34, 2972–2985. doi: 10.1002/hbm.22119

Voss, M. W., Weng, T. B., Burzynska, A. Z., Wong, C. N., Cooke, G. E., Clark, R., et al. (2016). Fitness, but not physical activity, is related to functional integrity of brain networks associated with aging. *NeuroImage* 131, 113–125. doi: 10.1016/j.neuroimage.2015.10.044

Weinstein, A. M., Voss, M. W., Prakash, R. S., Chaddock, L., Szabo, A., White, S. M., et al. (2012). The association between aerobic fitness and executive function is mediated by prefrontal cortex volume. *Brain Behav. Immun.* 26, 811–819. doi: 10.1016/j.bbi.2011.11.008

West, R. L. (1996). An application of prefrontal cortex function theory to cognitive aging. *Psycholog. Bull.* 120, 272–292. doi: 10.1037//0033-2909.120.2.272

Williams, T. B., Corbett, J., McMorris, T., Young, J. S., Dicks, M., Ando, S., et al. (2019). Cognitive performance is associated with cerebral oxygenation and peripheral oxygen saturation, but not plasma catecholamines, during graded normobaric hypoxia. *Exp. Physiol.* 104, 1384–1397. doi: 10.1113/EP087647

Yan, W., Zheng, K., Weng, L., Chen, C., Kiartivich, S., Jiang, X., et al. (2020). Bibliometric evaluation of 2000–2019 publications on functional near-infrared spectroscopy. *NeuroImage* 220:117121. doi: 10.1016/j.neuroimage.2020.117121

Yücel, M. A., Lühmann, A. V., Scholkmann, F., Gervain, J., Dan, I., Ayaz, H., et al. (2021). Best practices for fNIRS publications. *Neurophotonics* 8:012101. doi: 10.1117/1.NPh.8.1.012101

Yuki, A., Lee, S., Kim, H., Kozakai, R., Ando, F., and Shimokata, H. (2012). Relationship between Physical Activity and Brain Atrophy Progression. *Med. Sci. Sports Exerc*. 44, 2362–2368. doi: 10.1249/MSS.0b013e3182667d1d

Conflict of Interest: The authors declare that the research was conducted in the absence of any commercial or financial relationships that could be construed as a potential conflict of interest.

Publisher's Note: All claims expressed in this article are solely those of the authors and do not necessarily represent those of their affiliated organizations, or those of the publisher, the editors and the reviewers. Any product that may be evaluated in this article, or claim that may be made by its manufacturer, is not guaranteed or endorsed by the publisher.

frontiers in Sports and Active Living

OPINION
published: 07 March 2022
doi: 10.3389/fspor.2022.864825

Muscle Oxygenation Unlocks the Secrets of Physiological Responses to Exercise: Time to Exploit it in the Training Monitoring

*Stephane Perrey**

EuroMov Digital Health in Motion, Univ Montpellier, IMT Mines Ales, Montpellier, France

Keywords: training, NIRS, muscle, monitoring, internal load

INTRODUCTION

Our understanding of the human physiology during exercise lags behind our understanding of human behavior for decades. However, the number of available technologies for monitoring physiological functions "in the wild" and for assessing various training related-parameters has increased dramatically in recent years. In order to maximize exercise performance, mitigate fatigability as well as minimize the risk of injury, coaches and practitioners need a tough understanding of the relationship(s) between the external work outputs and its physiological impacts among other performance determinants (Vallance et al., 2020). Quantifying of how muscles respond to physical exercise conditions with sufficient accuracy and response time is important in athletes to unveil in dynamic fashion the adaptations to the training bouts and potential limiting factors of exercise performance. In exercise physiology, measurements of systemic changes (i.e., heart rate, HR; oxygen consumption, VO2; blood lactate) in the body are widely used in the prescription of exercise intensity and monitoring of physical conditioning. Besides, monitoring of the working muscles was proposed for tracking the muscle physiology adaptability during exercise, but it still remains nascent and not so used in the athletic field (Perrey and Ferrari, 2018). However, there is a strong demand in the monitoring of athlete training to use alternative indicators or metrics, to allow drawing of an accurate and reliable reflection of muscle status over time. Muscular activation (recorded by surface electromyography) and muscle oxygenation (assessed by near infrared spectroscopy, NIRS) are considered as the main approaches in the monitoring of working muscle (Ferrari et al., 2011). While electromyographic technique represents the electrical activity generated in muscle fibers, NIRS aims to assess the local oxygenation responses reflecting the balance between oxygen (O_2) delivery and utilization at the level of the microvasculature within skeletal muscle. In 2019, Barstow proposed a deep physiological explanation of the NIRS technique, and described its strengths, limitations and a few applications to skeletal muscle research during common exercise modalities (i.e., incremental exercise, square wave transitions). The NIRS technique is based on the light absorption of oxygenated and deoxygenated hemoglobin (Hb) and myoglobin (Mb) in the near infrared tissue, using the interaction of light at different wavelengths. It allows to measure the changes in oxyhemoglobin (O2Hb), deoxyhemoglobin (HHb), total hemoglobin, and tissue saturation index (StO2) in skeletal muscle during exercise. These last years, small wireless and portable NIRS devices have been built for sports applications.

Thus, NIRS technique presents an exciting opportunity to measure human physiological indicators in a continuous, real-time, and non-intrusive manner. Current wearable NIRS monitors (e.g., Moxy, BSI Insight, and Portamon devices) growing in availability, offer promising approaches but formal longitudinal and cohort studies are still needed to assess their use-case for sports (Perrey and Ferrari, 2018). In this context, allowing continuous and sensitive

OPEN ACCESS

Edited by:
Salvador J. Jaime, University of Wisconsin–La Crosse, United States

Reviewed by:
Mathieu Gruet, Université de Toulon, France

***Correspondence:**
Stephane Perrey
stephane.perrey@umontpellier.fr

Specialty section:
This article was submitted to Exercise Physiology, a section of the journal Frontiers in Sports and Active Living

Received: *28 January 2022*
Accepted: *09 February 2022*
Published: *07 March 2022*

Citation:
Perrey S (2022) Muscle Oxygenation Unlocks the Secrets of Physiological Responses to Exercise: Time to Exploit it in the Training Monitoring. Front. Sports Act. Living 4:864825. doi: 10.3389/fspor.2022.864825

monitoring with high frequency of NIRS signal capture may contribute to the improvement of the organization of exercise and training load monitoring aimed at improving performance.

This opinion article concentrates on the benefits of utilizing NIRS technique in measuring the muscle physiological status and determining how the working muscles are being exerted. Some questions are addressed: are NIRS-derived hemodynamic variables able in delineating different levels of physical workload? Are these measures sufficiently sensitive to varying changes in exercise conditions (e.g., intensity, terrain)? What are the current challenges?

A PLETHORA OF POSSIBILITIES FOR PRESCRIBING AND CONTROLLING EXERCISE INTENSITY

Systemic responses, such as VO2 and blood lactate, which are associated with intramuscular changes, are typically used as indicators of homeostatic perturbations in response to different exercise intensities. An alternative approach for prescribing exercise intensity could be based on a local indicator providing specific information about the working muscle(s) status. These last two decades, much attention has been devoted primarily to muscle oxygenation time course analysis during incremental exercise tests (Bhambhani et al., 1997). It has been emphasized that NIRS measurements may represent a simple, safe, reliable, and fast way to determine training intensity zones based on the determination of several thresholds representing shifts in the metabolic status of the working muscle (Grassi et al., 1999; Racinais et al., 2014; Borges and Driller, 2016; Crum et al., 2017; Rodrigo-Carranza et al., 2021). Those studies observed moderate to high correlations between NIRS breakpoints and traditional thresholds detection methods (i.e., the gas exchange, the first and second lactate or ventilatory thresholds). Reproducibility for NIRS derived breakpoints is however still limited to laboratory setup (see Barstow, 2019). In the field, on the one hand, these breakpoints might be used as a valid surrogate of ventilatory and/or lactate thresholds while being assessed on a regularly basis according to the training phases. Accordingly, based on a systemic physiological approach, muscle oxygenation recording should be implemented further by coaches and practitioners as portable devices for monitoring changes in the workload at various threshold levels in endurance training (Driller et al., 2016). Data collection with gas exchange measurement requires tedious and unique laboratory equipment while multiple blood sample withdrawal for lactate threshold is rather inconvenient for the athletes and the staff, especially if larger numbers of athletes are tested. In the daily training environment, reducing the number of devices, and reducing installation time before every test is important. It means that with NIRS the use of only one muscle (primary locomotor muscle) should be target according to the specificity of the task. Obviously, it might be an oversimplification of the underpinning and complex whole-body physiology to exercise. On the other hand, based on a more local physiological approach (e.g., fiber type distribution), expected heterogeneity of response profiles across different muscle sites (upper vs. lower body, locomotor vs. non locomotor, and among locomotor muscles) should be considered according to the physical task demands. Such multiple NIRS breakpoints metrics may allow for a better categorization of training stimulus into zones of exercise intensity for specific muscle groups (resistance/strength training), and in turn will favor the expected local muscle adaptations. In short-endurance event, oxygenation in *biceps brachii*, *latissimus dorsi* and *vastus lateralis* muscles was shown to be more relevant than VO2max in predicting canoe-kayak performance (Paquette et al., 2018).

Demarcating exercise intensity zones can be assessed with other metrics, such as the critical power/speed derived from the power-duration relationship. For constant-load heavy exercise, the maximal lactate steady state and critical power/speed were determined accurately by measuring the level of deoxygenated hemoglobin or StO2 (Snyder and Parmenter, 2009; Bellotti et al., 2013; Feldmann and Erlacher, 2021). Since critical power, the greatest metabolic rate achieved through the oxidative pathways, is influenced by the balance of oxygen delivery and utilization in working muscles, muscle oxygenation may be used to approximate the power-duration relationship in real-time. Based on a physiological framework, critical oxygenation as a counterpart of critical power method calculated at various workloads and over various durations was proposed by Feldmann and Erlacher (2021). This new individual metric can be useful in the understanding of the origin of muscle performance and fatigue for various sporting disciplines. Interestingly, the balance between muscle O_2 supply and metabolic demand as a critical metabolic rate in two sites (quadriceps and forearm), allows for predicting time to exhaustion during continuous and intermittent exercise (Kirby et al., 2021).

A BETTER INSIGHT OF THE INTERNAL TRAINING LOAD

The goal of physical training is to deliver the appropriate physiological stimuli (volume*intensity*frequency) to achieve adaptations. As a consequence, accurate assessment and monitoring of training load is of paramount importance. To quantify the training load, both external (amount and quality of workload performed) and internal (the individual psycho-physiological responses to the external workload imposed) indicators can be used (Vallance et al., 2020). To date, there is a need for future advancements toward precision training monitoring for dynamic adjustment based on the individual response to physical workouts. However, while perceptual (rating of perceived exertion, RPE) and physiological (systemic variables) metrics are often proposed for evaluating athlete's response to exercise, it is currently not clear which physiological indicator(s) with sufficient sensitivity to exercise loading is/are the most suitable to target. Traditional physiological indicators used are blood lactate and HR measurements. Regarding lactate, its measure requiring capillary blood to be collected at limited epochs is a reliable metabolite occurring during steady-state exercise conditions. Although HR measure has been commonly used, some limitations do exist. Literature has shown relatively

low usefulness of HR measurements in strength training, interval endurance training, and when training in naturally hilly terrain (uphill and downhill sections). Furthermore, HR depends on many factors related to emotional state, degree of rest and hydration, and environmental conditions (temperature, humidity, time of day, caffeine, altitude, etc.). One of the main limitations of HR monitoring in athletes appears to be the low sensitivity of HR response to some exercise features. Indeed, while systemic physiological (HR and VO2) responses are characterized by a certain lag (Perrey et al., 2001), the local deoxygenation is responding faster to changing exercise intensity in control lab setup (Bringard and Perrey, 2014). Recent field studies showed that muscle NIRS measurement can give a better indication of exercise intensity than HR across varied terrain (trail running in Born et al., 2017; long-distance cross-country skiing race in Stöggl and Born, 2021). Altogether, these findings suggest that NIRS may provide a robust method to track rapid changes of muscle activation and its metabolic status in exercise conditions (e.g., changes in altitude and locomotion speed), as well as a more detailed information of training potential by discerning upper and lower body muscles participation. Using multiple NIRS sensors to different muscle groups, comparing local metabolic responses among each muscle toward the energy demand of the exercise is possible, and may help to diagnose weakness and strengths within a tailored training approach. Additionally, NIRS devices allow for the measurements in the applied settings as evidenced for a while in various challenging and even extreme sports such as speed skating (Hesford et al., 2013), swimming (Jones et al., 2018), and kayaking (Paquette et al., 2018–2020). In aquatic environments with a specially waterproofed NIRS device, Jones et al. (2018) observed that improved oxidative metabolism of the muscle following 8-weeks endurance training in adolescents was strongly associated (not for HR and RPE) with the improved swim exercise performance. Due to rapid time resolution with NIRS, practical insights of changes in oxygenation and blood volume were observed also during typical swim movements (sprints, turns). In junior kayakers, peripheral adaptations, as assessed *via* NIRS-derived changes in muscle oxygenation (for upper- and lower-body muscles), appear stronger predictors of kayak performance compared to VO2max in both short and long events (Paquette et al., 2018). Noteworthy, benefit of using portable NIRS as a monitoring tool to track 3-weeks training effects on muscle oxygen extraction was even highlighted in male elite senior kayakers (Paquette et al., 2020) although important variability in muscle oxygenation response to training occurs. In summary, it means that the easy implementation of such technology purporting to the specificity of the sports in the field, should be driven by a rethinking of internal load characteristics according to the context. Due to its better sensitivity, a prescription of exercise intensity using NIRS-derived muscle parameters should be implemented in a manner comparable to routinely used conventional internal parameters (e.g., HR, lactate, VO2, RPE). As reported previously, the practicability and effectiveness of this approach has been tested successfully in various acute exercise setting, but is currently underutilized over a competitive season.

CURRENT CHALLENGES AND PERSPECTIVES

To date, there are still obstacles plaguing the widespread use of portable NIRS sensors in sports settings. The development of NIRS applications during exercise faces some challenges including methodological considerations and the knowledge of the collected metrics on what constitute a good interpretation. The first main limitation to all NIRS devices is the reduced sensitivity (due to scattering attenuation) to muscles in the presence of subcutaneous adipose tissue where thin adipose layers provide larger changes in StO2 values (Ferrari et al., 2011). Personalized correcting for this attenuation has been suggested based on the strength of the relationship between NIRS-derived measurements and the adipose tissue thickness using muscle site-specific factors (Craig et al., 2017). Second, the hemoglobin concentration spatial distribution throughout the muscle needs to be considered with NIRS (Hamaoka et al., 2011); muscle oxygenation of the most relevant muscle groups for the physical activity can be tracked. Third, it is important to consider the potential increase in skin blood flow associated with prolonged exercise (Ferrari et al., 2011), inducing increased muscle oxygenation values (Davis et al., 2006). All these limitations can be tackled through current and next developments, which will increase the NIRS practical usefulness. Finally, the assessment of muscle status based on NIRS data requires computational tools explaining the observed intra- and inter-individual variability responses to exercise and training programs. With NIRS monitoring, the continuous traces collected could be analyzed *via* time-series segmentation to detect how the working muscle status is evolving as a function of time. Implementation of evidence-based training framework should lead to the development of basic analysis for NIRS indicators (StO2, reoxygenation rate, blood flow) and methods for diagnosing muscle oxygenation in a personalized manner and identifying responders/non-responders to exercise bouts. Modeling the inter-individual differences of muscle oxygenation and the intra-individual responses according to the muscle groups in responses to exercise would lead to propose more accurate exercise prescription. Machine learning and data-driven artificial intelligence approaches can help to achieve this goal. Last potential limitation to consider may be for most practitioners and club the relatively substantial cost of current NIRS devices although their costs have dramatically decreased during recent years, as compared to HR monitors.

CONCLUSION

To continuously monitor muscle oxygenation during exercise in the field, small portable NIRS devices have been built. Despite important advances in athlete monitoring technologies, few muscle NIRS devices are currently used in sports settings. But NIRS is able for assessing two of the major determinants of exercise capacity: oxygen delivery and oxygen utilization. The reliability of the microvascular oxygenation measurements observed in the literature, along with the portability of the

wireless NIRS device, not too cumbersome (small size and lightweight) for the athlete suggest that it may be very useful for measuring changes in local microvascular oxygenation in diverse sports settings. Portable NIRS devices provide vital insights into how muscles are exerting during training that are not provided by other systemic metrics. In addition, it can be used to compliment other external load metrics (e.g., distance, power, speed, force) to give a clearer picture during training. NIRS devices could provide a collection of athlete internal load data, whereby coaches and practitioners can use various derived oxygenation metrics to monitor, evaluate, and prescribe training (and competition) characteristics. It is now time to integrate muscle oxygenation metrics beside the most common methods (i.e., HR and RPE) for quantifying internal training loads.

AUTHOR CONTRIBUTIONS

The author confirms being the sole contributor of this work and has approved it for publication.

REFERENCES

Barstow, T. J. (2019). Understanding near infrared spectroscopy and its application to skeletal muscle research. *J. Appl. Physiol.* 126,1360–1376. doi: 10.1152/japplphysiol.00166.2018

Bellotti, C., Calabria, E., Capelli, C., and Pogliaghi, S. (2013). Determination of maximal lactate steady state in healthy adults: can NIRS help? *Med. Sci. Sports Exerc*. 45,1208–1216. doi: 10.1249/MSS.0b013e3182828ab2

Bhambhani, Y. N., Buckley, S. M., and Susaki, T. (1997). Detection of ventilatory threshold using near infrared spectroscopy in men and women. *Med. Sci. Sports Exerc*. 29, 402–409. doi: 10.1097/00005768-199703000-00017

Borges, N. R., and Driller, M. W. (2016). wearable lactate threshold predicting device is valid and reliable in runners. *J. Strength Cond. Res*. 30, 2212–2218. doi: 10.1519/JSC.0000000000001307

Born, D. P., Stöggl, T., Swarén, M., and Björklund, G. (2017). Near-Infrared spectroscopy: more accurate than heart rate for monitoring intensity in running in hilly terrain. *Int. J. Sports Physiol. Perform.* 12, 440–447. doi: 10.1123/ijspp.2016-0101

Bringard, A., and Perrey, S. (2014). Influence of repeated isometric contractions on muscle deoxygenation and pulmonary oxygen uptake kinetics in humans. *Clin. Physiol. Funct. Imaging*. 24, 229–236. doi: 10.1111/j.1475-097X.2004.00554.x

Craig, J. C., Broxterman, R. M., Wilcox, S. L., Chen, C., and Barstow, T. J. (2017). Effect of adipose tissue thickness, muscle site, and sex on near-infrared spectroscopy derived total-[hemoglobin + myoglobin]. *J. Appl. Physiol.* 123, 1571–1578. doi: 10.1152/japplphysiol.00207.2017

Crum, E. M., O'Connor, W. J., Van Loo, L., Valckx, M., and Stannard, S. R. (2017). Validity and reliability of the moxy oxygen monitor during incremental cycling exercise. *Eur. J. Sport Sci.* 17, 1037–1043. doi: 10.1080/17461391.2017.1330899

Davis, S. L., Fadel, P. J., Cui, J., Thomas, G. D., and Crandall, C. G. (2006). Skin blood flow influences near-infrared spectroscopy-derived measurements of tissue oxygenation during heat stress. *J. Appl. Physiol.* 100, 221–224. doi: 10.1152/japplphysiol.00867.2005

Driller, M. W., Borges, N. R., and Plews, D. (2016). Evaluating a new wearable lactate threshold sensor in recreational to highly trained cyclists. *Sports Eng.* 19, 229–235. doi: 10.1007/s12283-016-0198-6

Feldmann, A., and Erlacher, D. (2021). Critical oxygenation: can muscle oxygenation inform us about critical power? *Med. Hypotheses*. 150, 110575. doi: 10.1016/j.mehy.2021.110575

Ferrari, M., Muthalib, M., and Quaresima, V. (2011). The use of near-infrared spectroscopy in understanding skeletal muscle physiology: recent developments. *Philos. Trans. A Math. Phys. Eng. Sci*. 369, 4577–4590. doi: 10.1098/rsta.2011.0230

Grassi, B., Quaresima, V., Marconi, C., Ferrari, M., and Cerretelli, P. (1999). Blood lactate accumulation and muscle deoxygenation during incremental exercise. *J. Appl. Physiol.* 87, 348–355. doi: 10.1152/jappl.1999.87.1.348

Hamaoka, T., McCully, K. K., Niwayama, M., and Chance, B. (2011). The use of muscle near-infrared spectroscopy in sport, health and medical sciences: recent developments. *Philos. Trans. A Math. Phys. Eng. Sci.* 369, 4591–4604. doi: 10.1098/rsta.2011.0298

Hesford, C. M., Laing, S., Cardinale, M., and Cooper, C. E. (2013). Effect of race distance on muscle oxygenation in short-track speed skating. *Med. Sci. Sports Exerc.* 45, 83–92. doi: 10.1249/MSS.0b013e31826c58dd

Jones, B., Parry, D., and Cooper, C. E. (2018). Underwater near-infrared spectroscopy can measure training adaptations in adolescent swimmers. *Peer J.* 6, e4393. doi: 10.7717/peerj.4393

Kirby, B. S., Clark, D. A., Bradley, E. M., and Wilkins, B. W. (2021). The balance of muscle oxygen supply and demand reveals critical metabolic rate and predicts time to exhaustion. *J. Appl. Physiol.* 130, 1915–1927. doi: 10.1152/japplphysiol.00058.2021

Paquette, M., Bieuzen, F., and Billaut, F. (2018). Muscle oxygenation rather than VO2max as a strong predictor of performance in sprint Canoe-Kayak. *Int. J. Sports Physiol. Perform*. 19, 1–9. doi: 10.1123/ijspp.2018-0077

Paquette, M., Bieuzen, F., and Billaut, F. (2020). Effect of a 3-weeks training camp on muscle oxygenation, VO_2 and performance in Elite Sprint Kayakers. *Front. Sports Act Liv*. 2, 47. doi: 10.3389/fspor.2020.00047

Perrey, S., Betik, A., Candau, R., Rouillon, J. D., and Hughson, R. L. (2001). Comparison of oxygen uptake kinetics during concentric and eccentric cycle exercise. *J. Appl. Physiol.* 91, 2135–2142. doi: 10.1152/jappl.2001.91.5.2135

Perrey, S., and Ferrari, M. (2018). Muscle oximetry in sports science: a systematic review. *Sports Med.* 48, 597–616. doi: 10.1007/s40279-017-0820-1

Racinais, S., Buchheit, M., and Girard, O. (2014). Breakpoints in ventilation, cerebral and muscle oxygenation, and muscle activity during an incremental cycling exercise. *Front. Physiol.* 5, 142. doi: 10.3389/fphys.2014.00142

Rodrigo-Carranza, V., González-Mohíno, F., Turner, A. P., Rodriguez-Barbero, S., and González-Ravé, J. M. (2021). Using a portable near-infrared spectroscopy device to estimate the second ventilatory threshold. *Int. J. Sports Med.* 42, 905–910. doi: 10.1055/a-1343-2127

Snyder, A. C., and Parmenter, M. A. (2009). Using near-infrared spectroscopy to determine maximal steady state exercise intensity. *J. Strength Cond. Res*. 23, 1833–1840. doi: 10.1519/JSC.0b013e3181ad3362

Stöggl, T., and Born, D. P. (2021). Near infrared spectroscopy for muscle specific analysis of intensity and fatigue during cross-country skiing competition-a case report. *Sensors* 21, 2535. doi: 10.3390/s21072535

Vallance, E., Sutton-Charani, N., Imoussaten, A., Montmain, J., and Perrey, S. (2020). Combining internal- and external-training-loads to predict non-contact injuries in soccer. *Appl. Sci.* 10:5261. doi: 10.3390/app10155261

Conflict of Interest: The author declares that the research was conducted in the absence of any commercial or financial relationships that could be construed as a potential conflict of interest.

Publisher's Note: All claims expressed in this article are solely those of the authors and do not necessarily represent those of their affiliated organizations, or those of the publisher, the editors and the reviewers. Any product that may be evaluated in this article, or claim that may be made by its manufacturer, is not guaranteed or endorsed by the publisher.

frontiers in Physiology

BRIEF RESEARCH REPORT
published: 24 March 2022
doi: 10.3389/fphys.2022.843574

Comparisons Between Normobaric Normoxic and Hypoxic Recovery on Post-exercise Hemodynamics After Sprint Interval Cycling in Hypoxia

Masahiro Horiuchi[1]*, *Ayano Nishida*[2], *Shohei Dobashi*[2,3] and *Katsuhiro Koyama*[4,5]

[1]Division of Human Environmental Science, Mount Fuji Research Institute, Fuji-yoshida, Japan, [2]Graduate School of Education, University of Yamanashi, Kofu, Japan, [3]Graduate School of Health and Sports Science, Juntendo University, Inzai, Japan, [4]Gradulate School Department of Interdisciplinary Research, University of Yamanashi, Kofu, Japan, [5]Faculty of Sport Science, Yamanashi Gakuin University, Kofu, Japan

The aim of this study was to investigate the effects of either normoxic or hypoxic recovery condition on post-exercise hemodynamics after sprint interval leg cycling exercise rather than hemodynamics during exercise. The participants performed five sets of leg cycling with a maximal effort (30 s exercise for each set) with a 4-min recovery of unloaded cycling between the sets in hypoxia [fraction of inspired oxygen (FiO_2) = 0.145]. The load during pedaling corresponded to 7.5% of the individual's body weight at the first set, and it gradually reduced from 6.5 to 5.5%, 4.5, and 3.5% for the second to fifth sets. After exercise, the participants rested in a sitting position for 30 min under normoxia (room-air) or hypoxia. Mean arterial pressure decreased over time during recovery ($p < 0.001$) with no condition and interaction effects ($p > 0.05$). Compared to pre-exercise values, at 30 min after exercise, mean arterial pressure decreased by 5.6 ± 4.8 mmHg (mean ± standard deviation) during hypoxic recovery, and by 5.3 ± 4.6 mmHg during normoxic recovery. Peripheral arterial oxygen saturation (SpO_2) at all time points (5, 10, 20, and 30 min) during hypoxic recovery was lower than during normoxic recovery (all $p < 0.05$). The area under the hyperemic curve of tissue oxygen saturation (StO_2) at vastus lateralis defined as reperfusion curve above the baseline values during hypoxic recovery was lower than during normoxic recovery ($p < 0.05$). Collectively, post-exercise hypotension after sprint interval leg cycling exercise was not affected by either normoxic or hypoxic recovery despite marked differences in SpO_2 and StO_2 during recovery between the two conditions.

Keywords: blood lactate concentration, hypotension, hypoxic vasodilation, mean arterial pressure, near infrared spectroscopy, tissue oxygen saturation

OPEN ACCESS

Edited by:
Thomas RUPP,
Université Savoie Mont Blanc, France

Reviewed by:
Tadej Debevec,
University of Ljubljana, Slovenia
Samuel Verges,
Université Grenoble Alpes, France

***Correspondence:**
Masahiro Horiuchi
mhoriuchi@mfri.pref.yamanashi.jp

Specialty section:
This article was submitted to Exercise Physiology, a section of the journal Frontiers in Physiology

Received: *26 December 2021*
Accepted: *09 March 2022*
Published: *24 March 2022*

Citation:
Horiuchi M, Nishida A, Dobashi S and Koyama K (2022) Comparisons Between Normobaric Normoxic and Hypoxic Recovery on Post-exercise Hemodynamics After Sprint Interval Cycling in Hypoxia. Front. Physiol. 13:843574. doi: 10.3389/fphys.2022.843574

INTRODUCTION

After an acute single bout of physical exercise irrespective of exercise mode, intensity, and duration, arterial blood pressure decreases for approximately up to 2 h compared to the baseline (pre-exercise) levels; this phenomenon is called "Post Exercise Hypotension (PEH)" (Halliwill et al., 2014). While previous studies about PEH have primarily used moderate-intensity prolonged exercise (about 60% of peak aerobic capacity for up to 60 min) (McCord et al., 2006; Francisco et al., 2021), few existing studies have investigated PEH and related phenomena using short-duration high-intensity exercise

(Lacewell et al., 2014). However, after such high-intensity exercise (e.g., Wingate test, or sprint interval exercise), the incidence rate of presyncope symptoms was more than 50% among the individuals (Halliwill et al., 2014). Additionally, as orthostatic tolerance is reduced at high altitude (Rowell and Seals, 1990; Nicholas et al., 1992; Westendorp et al., 1997), it can be expected that the risk of presyncope or syncope might increase when exercise and/or recovery is performed at a high altitude.

However, only a few studies have assessed the impact of hypoxic exercise on PEH. PEH was more significant in 2-h aerobic exercise (Horiuchi et al., 2016) or high-intensity resistance exercise under hypoxia versus normoxia (Horiuchi et al., 2018) possibly due to hypoxic-induced vasodilation (Joyner and Casey, 2014). Another study found that there were no significant differences in the occurrence of PEH between hypoxic or normoxic 45-min aerobic exercises (Kleinnibbelink et al., 2020). The different exercise modes and recovery conditions (normoxia or hypoxia) make it difficult to obtain consensus (Horiuchi et al., 2016; Horiuchi et al., 2018; Kleinnibbelink et al., 2020). To the best of our knowledge, there have been no studies on PEH after a sprint interval leg cycling exercise performed in hypoxia.

Exercise-induced arterial hypoxemia has been observed both at higher altitude and sea level, but the magnitude of exercise-induced arterial hypoxemia was greater at high altitude than sea level (Chapman et al., 1999). Recovery from arterial hypoxemia in the hours after exercise may be important in some cases since arterial hypoxemia is associated with the occurrence or the severity of acute mountain sickness, which is mainly characterized by headache (Erba et al., 2004; Nespoulet et al., 2012). In contrast, when considering practical implications of exercise at high-altitude, continuous hypoxic stress (both during exercise and recovery) may be more effective for athletes to generate specific training adaptations (Puype et al., 2013; Gibala and Hawley, 2017). However, no studies have examined the effect of different recovery conditions (e.g., normoxia vs. hypoxia) on post-exercise hemodynamics after a sprint interval leg cycling exercise in hypoxia. A previous study reported that elevated post-exercise oxygen consumption was not associated with PEH, although their study was conducted under normoxia with a moderate exercise intensity (Williams et al., 2005); therefore, it is still uncertain about a relationship between PEH and post-exercise oxygen consumption (e.g., systemic and muscle oxygenation).

Accordingly, the aim of this study was to investigate the effects of either normobaric normoxic or hypoxic recovery condition on post-exercise hemodynamics, systemic and muscle oxygenation after sprint interval leg cycling exercise in hypoxia. We hypothesized that PEH would occur in both recovery conditions, but that the magnitude of PEH would be greater during hypoxic recovery.

MATERIALS AND METHODS

Sample Size and Participants

Based on a previous study that observed decreases in mean arterial pressure (MAP) after hypoxic exercise (Horiuchi et al., 2016), a sample size estimation for the primary analysis (MAP) indicated that 10 participants were needed to produce an 80% chance of obtaining statistical significance at the level of 0.05 (G Power 3.1) (Faul et al., 2007).

Ten healthy young men with a mean age of 21 ± 1 years, a height of 174 ± 5 cm, and a body mass of 66.8 ± 8.7 kg [mean ± standard deviation (SD)] were enrolled. The participants engaged in regular physical activity (1–2 h per day, 3–5 days per week). None of the participants were exposed to an altitude higher than 1,500 m within 6 months prior to the study, and had a history of cardiovascular or orthopedic disease. They were non-smokers. After detailed explanations regarding the study, including the procedures, possible risks, and benefits of participation, a written informed consent was obtained from each participant. This study was approved by the Ethical Committee of the University of Yamanashi, in Japan, and was performed in accordance with the guidelines of the Declaration of Helsinki (No. 201509).

Experimental Procedures

The participants were asked to abstain from caffeinated beverages for 12 h, strenuous exercise and alcohol consumption for 24 h before each session. The room temperature was set at 24 ± 1°C, and external stimuli were minimized. All experiments were performed using a cycle ergometer (Powermax V, Combi Co. Ltd., Tokyo, Japan). On the first visit, they familiarized themselves with 1) leg cycling with maximal pedaling revolutions while wearing all the devices as well as 2) the BP measurement and blood sampling. On the second and third visits, participants performed main experiment. The experiment consisted of three consecutive protocols; 1) a 10-min sitting/resting period, 2) warm-up cycling (5-min at the pedaling load corresponded to a 2.0% of body weight at 80 revolutions per minute of pedaling frequency, including maximal pedaling for 3 s at 2 and 4 min), followed by 3) the five sets of the sprint interval leg cycling exercise in hypoxia. In the normobaric hypoxic recovery condition, participants inspired hypoxic gas vias tube attached on a face mask, from a tent, while in the normobaric normoxic recovery condition, after the five sets of the sprint interval leg cycling exercise in hypoxia, the tube was taken out from the tent immediately, then, participants could inspire normobaric normoxic gas (room air). The load during pedaling corresponded to 7.5% of the individual's body weight at the first set, and it gradually reduced from 6.5 to 5.5%, 4.5, and 3.5% of body weight in the second to third, fourth, and fifth sets, respectively. During each five set, participants performed leg cycling for 30 s. The applied load was set according to a previous study (Kasai et al., 2015). In the preliminary test at our laboratory, we decided that decremental settings of the load was an optimal protocol to allow the participants to produce the maximal mean power despite fatigue. A 4-min recovery at 0 W (unloaded cycling at 60 revolutions per minute) was inserted between the sets. After the five sets of leg cycling exercise, they rested for 30-min sitting recovery period: in 1) normobaric normoxia (room air; equivalent to 400 m), and 2) normobaric hypoxia [fraction of inspired oxygen (FiO_2) = 0.145; equivalent to 3,000 m]. These two tests were performed in a random order with a 1-week wash out period as shown in **Figure 1**.

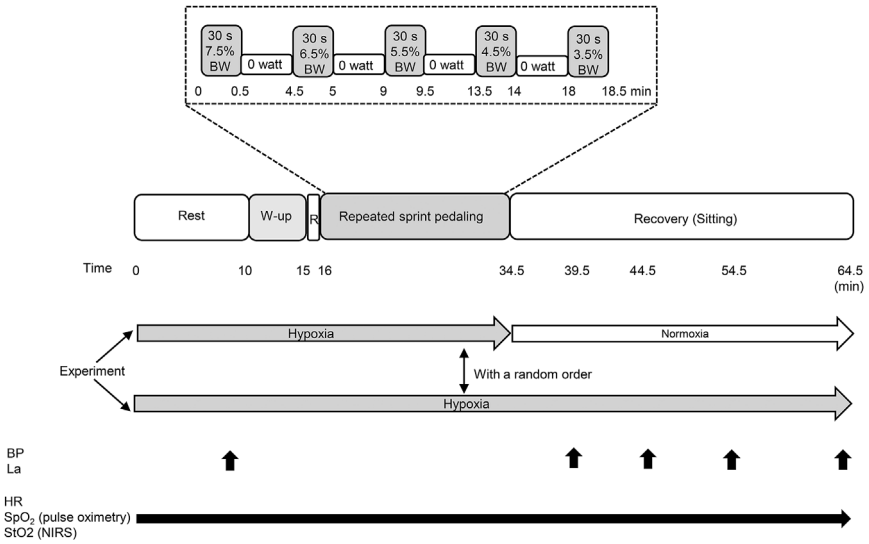

FIGURE 1 | Experimental protocol of the present study. BW, body weight; W-up, warm up; R, rest; BP, blood pressure; La, blood lactate concentration; HR, heart rate; SpO_2, arterial oxygen saturation; StO_2, tissue oxygen saturation. Black arrows indicate the measuring points and periods.

A commercial hypoxic generator (Hypoxico Everest Summit II: Will Co., Ltd., Tokyo, Japan) supplied hypoxic gas based on a previous study (Horiuchi et al., 2017). Briefly, hypoxic gas was supplied into a custom-made tent (approximately 4,000 L) *via* one tube connected to the gas generator, and hypoxic gas was mixed in the tent. Participants inspired the hypoxic gas *via* another tube from the tent. They wore a two-way, non-rebreathing valve (for inspired and expired gas, respectively) and face mask (Horiuchi et al., 2017). Participants were blinded to inspire normoxic or hypoxic gas during recovery. The inspired oxygen concentration was verified before and after each experiment (AE-310; Minato Medical Science, Osaka, Japan).

Measurements

The last 2 min of a 10-min resting hypoxic exposure was used to measure hypoxic baseline values before exercise. Blood pressure (BP) and blood lactate concentration (La) were measured at baseline, and at 5, 10, 20, and 30 min during recovery. BP was measured using the oscillometric method (HEM-907, OMRON, Tokyo, Japan). Resting BP was measured twice, and the average of the two measurements was considered as the participant's BP value. We also confirmed the difference in the systolic BP or diastolic BP was <5 mmHg compared to the values of one before measurement at rest (Horiuchi et al., 2018). During the recovery period, BP was measured at 5, 10, 20, and 30 min of the period. Fingertip blood samples (0.3 μL) were taken to measure La (Lactate Pro 2LT-1730; Arkray, Tokyo, Japan). Heart rate (HR) and peripheral arterial oxygen saturation (SpO_2) were continuously monitored throughout the experiment using a wireless HR monitor (RS 800CX, Polar Electro, Japan) and pulse oximeter (TM-256, A&D, Tokyo, Japan), respectively. The probe of pulse oximeter was attached on the left middle finger. Local tissue oxygenation profiles of the vastus lateralis muscle were also continuously measured at 1-s intervals throughout the experiment using NIRS device (BOML1TRW, Omegawave, Tokyo, Japan) (Horiuchi et al., 2017). This instrument uses three laser diodes (780, 810, and 830 nm) and calculates the relative levels of oxygenated and deoxygenated hemoglobin (Hb) in the tissue according to the modified Beer–Lambert law. The oxygen saturation of the skeletal muscle (StO_2) was calculated by dividing oxygenated Hb by the total Hb, and was expressed as percentage (Horiuchi et al., 2017). NIRS optodes were placed on the lower third of the vastus lateralis muscle. The probe holder contained one light source probe, and two detectors were placed 2.0 cm (detector 1) and 4 cm (detector 2) away from the source at the vastus lateralis. Hb concentrations received by detector 1 were subtracted from those received by detector 2. This procedure minimized the influence of skin blood flow. Since NIRS signals can reach half the depth of the distance between the probe and detector, it can traverse at a depth of 10–20 mm at the target muscle.

Data Analysis

The mean arterial pressure (MAP) was calculated using the following equation (Horiuchi et al., 2018):

$$\boldsymbol{MAP} = \frac{(\boldsymbol{systoloc\ BP}\ [\boldsymbol{SBP}] - \boldsymbol{distolic\ BP}\ [\boldsymbol{DBP}])}{3} + \boldsymbol{DBP}$$

The values of HR and SpO_2 were adopted at baseline, and at 5, 10, 20, and 30 min of recovery for further analysis. These values were averaged during the last 1 min at the sitting baseline and during the 10 s immediately after each recovery period.

Baseline values of StO_2 were determined by the average value during the last 5 min prior to the warm-up exercise. The minimum StO_2 values were defined as the lowest StO_2 values during the five sets of the sprint interval leg cycling exercise. The

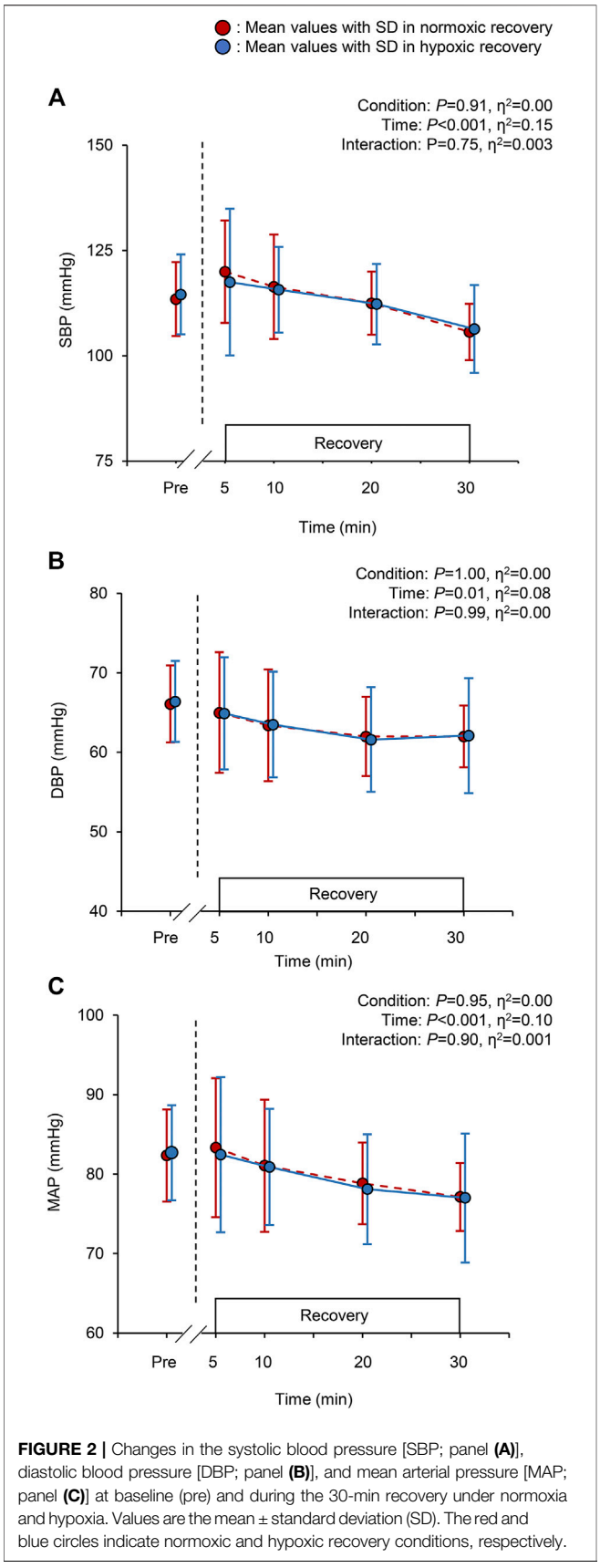

FIGURE 2 | Changes in the systolic blood pressure [SBP; panel **(A)**], diastolic blood pressure [DBP; panel **(B)**], and mean arterial pressure [MAP; panel **(C)**] at baseline (pre) and during the 30-min recovery under normoxia and hypoxia. Values are the mean ± standard deviation (SD). The red and blue circles indicate normoxic and hypoxic recovery conditions, respectively.

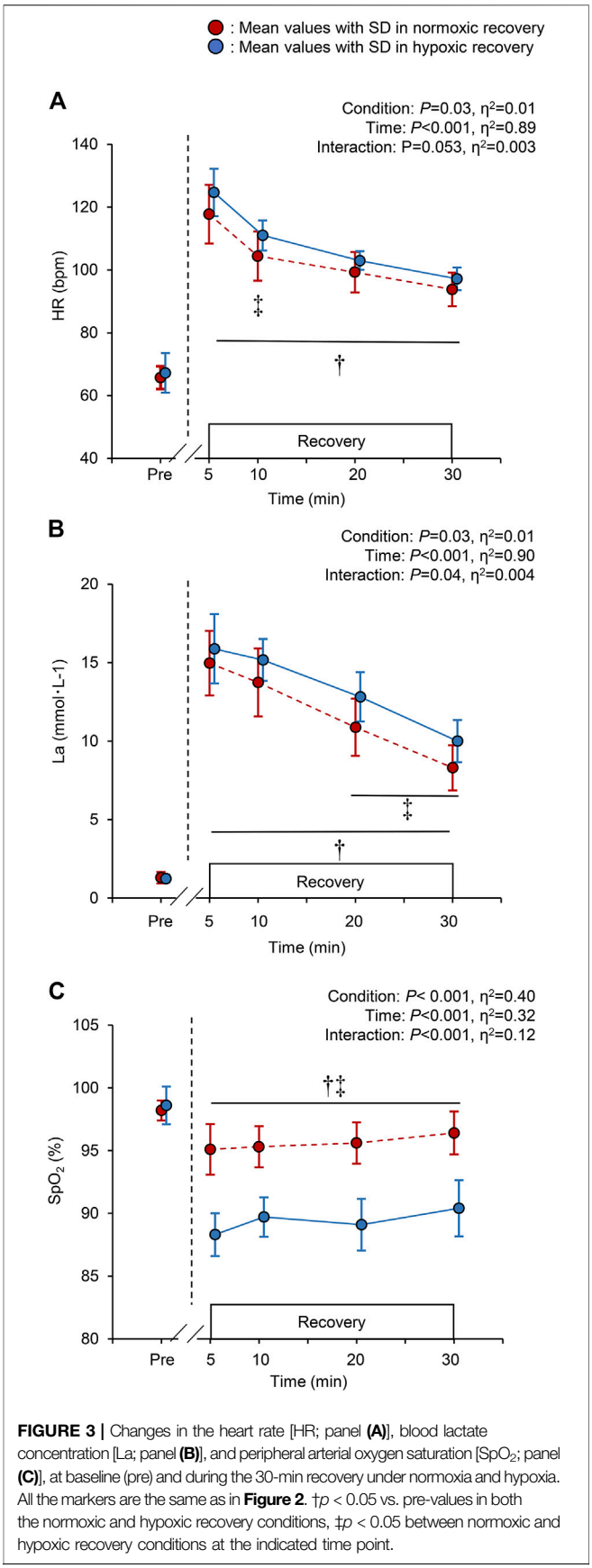

FIGURE 3 | Changes in the heart rate [HR; panel **(A)**], blood lactate concentration [La; panel **(B)**], and peripheral arterial oxygen saturation [SpO_2; panel **(C)**], at baseline (pre) and during the 30-min recovery under normoxia and hypoxia. All the markers are the same as in **Figure 2**. †$p < 0.05$ vs. pre-values in both the normoxic and hypoxic recovery conditions, ‡$p < 0.05$ between normoxic and hypoxic recovery conditions at the indicated time point.

hyperemic phase (i.e., the time from baseline values to the end of 30 min of recovery) was analyzed for the peak StO_2 (%) and the area under the hyperemic curve (AUC; % s). The peak StO_2 value was defined as the highest StO_2 value achieved during the hyperemic phase. The AUC was calculated as the total area under the reperfusion curve above the baseline values (Soares et al., 2018; Horiuchi and Okita, 2020). The mean power was calculated for each set of sprint cycling, and the mean values of five sets was identified as exercise performance.

Statistics

Data are presented mean ± standard deviation. Statistical analyses were performed using the R programming language (RKWard, Version 0.7.2). A paired *t*-test was performed to compare the sprint interval leg cycling exercise performance and NIRS indices between the two conditions. A two-way (time × recovery condition) repeated measures analysis of variance (ANOVA) was used to compare time course changes in other physiological variables (SBP, DBP, MAP, HR, La, and SpO_2). Effect size was calculated as Cohen's d and η^2, defined as a trivial (<0.2), small (0.2), moderate (0.5), or large (0.8) for paired *t*-test "Cohen's d" (Hopkins et al., 2009) and as small (η^2 = 0.01), medium (η^2 = 0.06), and large (η^2 = 0.14) for ANOVA "η^2" effects (Lakens, 2013). Statistical significance was set at $p < 0.05$.

RESULTS

There were no significant differences in the averaged values of mean power output between the two conditions (488 ± 38 W vs. 486 ± 33 W for normoxic vs. hypoxic recovery, p = 0.62).

The changes in SBP, DBP, and MAP are shown in **Figure 2**. A significant main effect of time was observed in SBP, DBP, and MAP (all $p < 0.001$, **Figures 2A–C**), whereas there were no significant condition effects and interactions for these BP variables (all $p > 0.05$, **Figures 2A–C**). The mean PEH response (differences between values pre-exercise and at 30 min) for SBP, DBP, and MAP in normoxic recovery were −7.8 ± 8.5, −4.1 ± 3.1, and −5.3 ± 4.6 mmHg respectively, and in hypoxic recovery −8.2 ± 6.8, −4.3 ± 4.6, and −5.6 ± 4.8 mmHg, respectively.

There were significant main effects of time and recovery condition on HR, La, and SpO_2 (all $p < 0.05$. **Figures 3A–C**). During hypoxic recovery, HR at 10 min was significantly higher than that in normoxic recovery (p = 0.03), and showed marginal higher values at 5, 20, and 30 min (all $p < 0.1$ **Figure 3A**). La at 20 and 30 min during hypoxic recovery was significantly higher than those in normoxic recovery (p = 0.02, respectively; **Figure 3B**). SpO_2 during hypoxic recovery was significantly lower than normoxic recovery throughout the recovery period (all $p <$ 0.05, **Figure 3C**). Specifically, the mean values of SpO_2 during recovery were 95.6 ± 1.8% in normoxia and 88.7 ± 1.9% in hypoxia.

Time course changes in StO_2 for a typical single subject and mean values of StO_2 and total Hb during the recovery period are shown in **Figure 4**. At rest, during warm-up, and sprint interval leg cycling exercise, the StO_2 showed similar values between the two conditions. Conversely, the StO_2 during hypoxic recovery appeared to be markedly lower than that during normoxic recovery. Between the two recovery conditions, baseline (54.9 ± 2.9% vs. 54.7 ± 2.7% for normoxic vs. hypoxic recovery, p = 0.74, Cohen's d = 0.11) and nadir values (20.2 ± 6.2% vs. 21.2 ± 6.9%, p = 0.40, Cohen's d = −0.28) at the five sets of

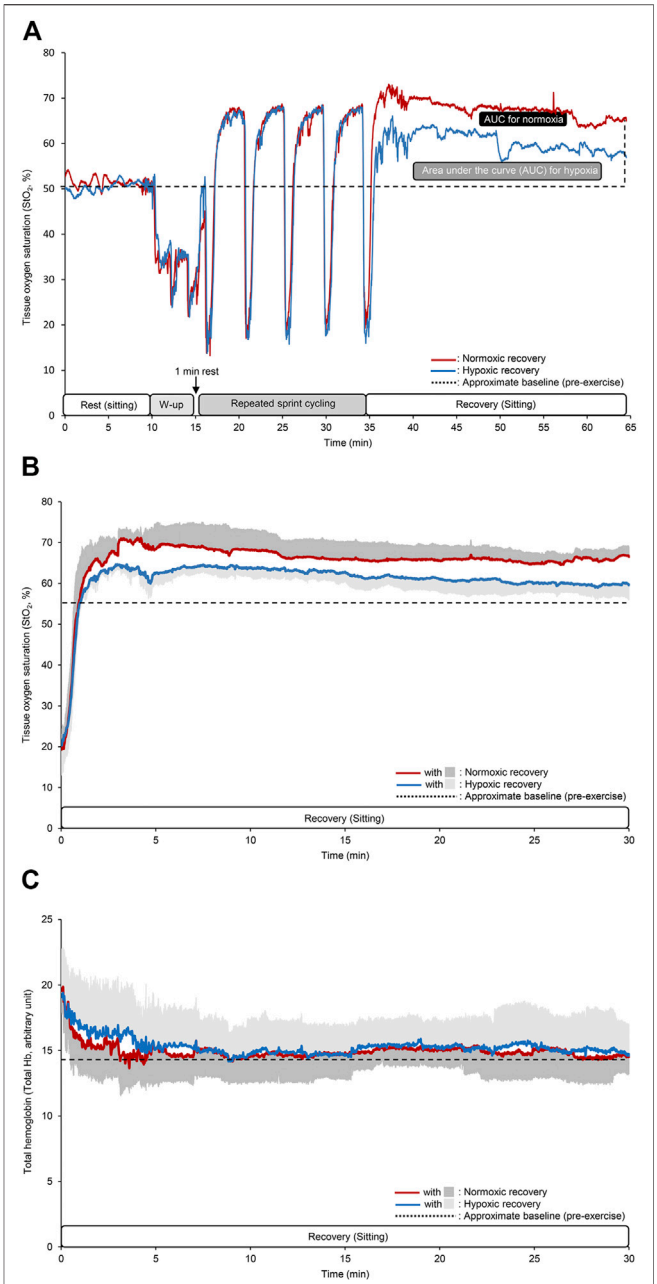

FIGURE 4 | Time course changes in the tissue oxygen saturation (StO_2) at the vastus lateralis muscle for a typical single subject **(A)**, mean values of StO_2 and total hemoglobin (Hb) during the recovery period **(B,C)**. The different colored lines indicate the same as that in **Figure 2**. In the panels **(B,C)**, dark and light gray areas indicate SD for normoxic and hypoxic recovery, respectively, and black dotted lines indicate approximate baseline (pre-exercise) values. Note that SD area are given only upper or lower side.

the sprint interval leg cycling exercise were not statistically different. By contrast, peak values (70.8 ± 2.8% vs. 66.8 ± 2.3% for normoxic vs. hypoxic recovery, p = 0.02, Cohen's d = 0.90) and StO_2 AUC in normoxic recovery (14,500 ± 6,794%·s) were significantly greater than hypoxic recovery (9,535 ± 2,206%·s, p = 0.04, Cohen's d = 0.75) (**Figures 4A,B**). After exercise, total Hb decreased exponentially within 10 min, and showed similar values as the baseline (pre-exercise) values, irrespective of recovery conditions. There were no significant differences in the mean values of total Hb during the recovery (14.7 ± 1.9 arbitrary unit in normoxia and 15.3 ± 2.3 arbitrary unit in hypoxia, p = 0.62, Cohen's d = 0.16) (**Figure 4C**).

DISCUSSION

The present study demonstrated the three findings as follows: 1) MAP significantly decreased over time during the 30-min recovery period after a sprinting exercise in hypoxia, with no difference depending on this recovery is performed in normoxia or hypoxia, 2) HR and La in hypoxic recovery were significantly higher than those in normoxic recovery, and 3) SpO_2 and StO_2 AUC during hypoxic recovery were significantly lower than those during normoxic recovery. These results suggest that post-exercise hypotension was not affected by either nomoxic or hypoxic recovery condition despite marked differences in arterial and muscle tissue oxygen saturation, during recovery between the two conditions.

Results showed that compared to pre-exercise (baseline) values, MAP at 30 min during hypoxic recovery decreased by approximately ~6 mmHg, and by approximately ~5 mmHg during normoxic recovery, supporting the occurrence of PEH, independently of the conditions. The results coincide with previous studies that found the presence of PEH after hypoxic exercise (Horiuchi et al., 2016; Horiuchi et al., 2018; Kleinnibbelink et al., 2020). Theoretically, a reduction in MAP can be caused by a decrease in HR, stroke volume, or total vascular resistance (TVR). It has been suggested that PEH may be explained by a decrease in TVR, likely due to a combination of central and locally mediated vasodilation, which is not compensated to maintain cardiac output (Halliwill et al., 2014). Since stroke volume has been reported to be unchanged (Talbot et al., 2005) or reduced (Stembridge et al., 2015) in hypoxia, higher HR during hypoxic recovery in the present study may suggest the possibility of maintaining cardiac output. The elevated HR in hypoxic recovery may be explained by hypoxia-induced chemoreceptor stimulation promoting greater sympathetic activation (Bärtsch and Gibbs, 2007; Fisher, 2015) and more commonly, is thought to preserve oxygen delivery. Changes in the TVR is another consideration as it is proven that hypoxia is a powerful vasodilator for peripheral arteries (Dinenno et al., 2003), subsequently leading to a decrease in TVR. Additionally, hypoxic condition has been linked to vasodilation of the splanchnic (Rowell and Blackmon, 1989; Westendorp et al., 1997) and of cutaneous circulation (Simmons et al., 2010; Simmons et al., 2011). As we did not evaluate TVR, we must acknowledge that effects of TVR on PEH is highly speculative; however, the results of the present study might indicate that changes in TVR did not affect PEH in hypoxic recovery condition. Further studies measuring stroke volume, cardiac output, and vascular conductance are required.

Blood lactate concentration as another candidate promoting PEH was higher in hypoxic recovery than in normoxic recovery. An animal experiment found dose-dependent vasodilation by administration of lactate in isolated small arteries (Chen et al., 1996). However, significant differences in the La at 20 and 30 min of normoxic and hypoxic recovery (**Figure 3B**) in our study did not support the aforementioned hypothesis that vasodilation occurs due to elevated blood lactate concentration.

The StO_2 AUC during recovery (reactive hyperemia) was markedly greater in normoxic recovery than in hypoxic recovery. In both conditions, the participants performed maximal cycling which resulted in successive intense ischemic episodes in the exercising muscle (i.e., StO_2 < 20%, **Figure 4A**). Previous studies have evaluated muscle reoxygenation responses (oxygen delivery to tissues) after exercise (Kemps et al., 2009; Mankowski et al., 2017; Zebrowska et al., 2021), and confirmed the validity and utility of NIRS device when assessing individuals' recovery kinetics between different oxygen levels (Mankowski et al., 2017). Arterial inflow to thigh muscles may have increased during recovery irrespective of different oxygen recovery conditions, and that normoxic recovery further enhanced these responses compared to hypoxic recovery, probably due to greater arterial O_2 supply (higher arterial O_2 content). We found no differences in total Hb responses during recovery between the two conditions. It has been reported that changes in total Hb are associated with changes in blood flow (Alvares et al., 2020) and in vascular conductance (Watanabe et al., 2005). Thus, our results suggest that leg vascular conductance may not vary between normoxic and hypoxic recovery, causing no differences in PEH between the two conditions. Although we can only speculate, regional differential vascular conductance might be associated with the similar PEH finding. It is known that hypoxic conditions promote vasodilation in skeletal muscles during exercise (Dinenno et al., 2003), and we can expect hyperventilation-induced hypocapnia during hypoxic recovery. A previous study demonstrated hypocapnia-induced reductions in cerebral oxygenation and total hemoglobin, suggesting cerebral vasoconstriction (Rupp et al., 2014). Similarly, acute exposure to hypoxia increases pulmonary vasoconstriction (Bärtsch and Gibbs, 2007). In contrast, hypoxia causes cutaneous vasodilation (Simmons et al., 2007) and vasodilation of the splanchnic circulation (Rowell and Blackmon, 1989; Westendorp et al., 1997). Given these possibilities, the mechanisms linking hypoxic conditions and BP regulation are likely complex and multi-factorial, and thus, future studies with measurements of regional vascular conductance may be required.

Methodological Considerations

First, only young men were enrolled in this study, which makes the results inapplicable to other populations, such as women and elite sport athletes. Second, the present study did not conduct normoxic exercise, followed by normoxic recovery as a control condition. However, our main aim was to compare between

normoxic and hypoxic recovery after sprint interval leg cycling exercise in hypoxia. Although future studies are needed, our results may have following future outlooks. Finally, we evaluated only StO_2 among the indicators of NIRS technique. Venous occlusion technique has been suggested to estimate O_2 supply and consumption in working muscles during exercise (Homma et al., 1996). Similarly, a recent study demonstrated that combination of arterial and venous occlusion provides valid estimates of blood flow and oxygen consumption at rest and during exercise (Dennis et al., 2021). Although we must acknowledge that these techniques are useful and that we should have performed this technique to obtain more insight interpretations, we considered that further arterial occlusion may not be required after exhaustion. This is because, in the preliminary test, most of the participants complained of intolerable pain and nausea during arterial occlusion after exercise. Thus, we considered a safety for participants preferentially in the present study.

Perspectives

Sprint interval training in hypoxia has been considered to be a useful strategy to improve exercise both at sea level and high-altitude (Kon et al., 2015). Similarly, it was reported that repeated-sprint training, defined to consist of the repetition of short (<30 s) "all-out" sprints with incomplete recoveries (<60 s) (Girard et al., 2020), in hypoxia significantly improved cardiorespiratory fitness level (Camacho-Cardenosa et al., 2020). Additionally, even though under normoxic environments, a recent review summarized that sprint interval training improves glucose metabolism (Jiménez-Maldonado et al., 2020). Although these previous findings are beyond of the present study, studies including various combination of hypoxic (normoxic) exercise and recovery conditions may be required. As the present study is the first study to compare the effects of a normoxic versus hypoxic recovery on post-exercise hemodynamics, the present results may be informative for populations who perform an exercise at high-altitude, particularly from the viewpoint of safe implementation for conducting sprint interval training in hypoxia. For example, while the average magnitude of PEH in the present study was approximately 6 mmHg, regardless of different recovery conditions, previous studies reported PEH magnitudes of approximately 3 mmHg after 45 min of a high-intensity running exercise (85% of maximal HR) (Kleinnibbelink et al., 2020), approximately 6 mmHg after a 2-h leg cycling exercise (50% of peak oxygen uptake) (Horiuchi et al., 2016), and more than 10 mmHg after a resistance exercise (bilateral leg squat) (Horiuchi et al., 2018). These different magnitudes of PEH may be influenced by different study settings. Since these previous studies (Horiuchi et al., 2016; Horiuchi et al., 2018; Kleinnibbelink et al., 2020) and our study did not evaluate symptoms leading to presyncope, it is still uncertain whether sprint interval exercise in hypoxia increases the risk of presyncope. Nevertheless, the current findings suggest that the risks of presyncope may be similar with either normoxic or hypoxic recovery. Moreover, a recent study demonstrated that an acute exercise-induced reduction in BP was related to a greater chronic reduction in the BP-lowering effect of exercise training (Kleinnibbelink et al., 2020). Therefore, the greater magnitude of PEH in the present study, compared with the previous study (Kleinnibbelink et al., 2020), might indicate that regular sprint interval training in hypoxia could be a future strategy for antihypertensive therapy.

CONCLUSION

Sprint interval leg cycling exercise in hypoxia caused significant reductions in BP variables, regardless of hypoxic and normoxic recovery. SpO_2 and StO_2 AUC were also lower than that with normoxic recovery. These results suggest that PEH after sprint interval leg cycling exercise in hypoxia was not affected by either normoxic or hypoxic recovery despite marked differences in SpO_2 and StO_2 between the two recovery conditions.

DATA AVAILABILITY STATEMENT

The original contributions presented in the study are included in the article/Supplementary Materials, further inquiries can be directed to the corresponding author.

ETHICS STATEMENT

The studies involving human participants were reviewed and approved by the University of Yamanashi. The patients/participants provided their written informed consent to participate in this study.

AUTHOR CONTRIBUTIONS

MH, AN, SD, and KK conceived and designed the study. MH, AN and SD performed the experiments. MH, AN and SD analyzed data. MH, AN, SD, and KK interpreted results. MH prepared tables and figures. MH drafted the first manuscript. MH, SD and KK critically revised the manuscript, and all authors approved the final version of the manuscript.

FUNDING

This work was supported in part by Japan Society for the Promotion of Science (JSPS, KAKENHI, Numbers; 26440268 to MH, and 17K01757 to KK).

ACKNOWLEDGMENTS

We appreciate the time and effort spent by our volunteer participants. We would like to thank Miss. Misato Watanabe for her technical assistant. The authors would like to thank Editage (https://www.editage.jp) for the English language service.

REFERENCES

Alvares, T. S., Oliveira, G. V. d., Soares, R., and Murias, J. M. (2020). Near-infrared Spectroscopy-Derived Total Haemoglobin as an Indicator of Changes in Muscle Blood Flow during Exercise-Induced Hyperaemia. *J. Sports Sci.* 38, 751–758. doi:10.1080/02640414.2020.1733774

Bärtsch, P., and Gibbs, J. S. (2007). Effect of Altitude on the Heart and the Lungs. *Circulation* 116, 2191–2202. doi:10.1161/CIRCULATIONAHA.106.650796

Camacho-Cardenosa, A., Camacho-Cardenosa, M., Brazo-Sayavera, J., Timón, R., González-Custodio, A., and Olcina, G. (2020). Repeated Sprint in Hypoxia as a Time-Metabolic Efficient Strategy to Improve Physical Fitness of Obese Women. *Eur. J. Appl. Physiol.* 120, 1051–1061. doi:10.1007/s00421-020-04344-2

Chapman, R. F., Emery, M., and Stager, J. M. (1999). Degree of Arterial Desaturation in Normoxia Influences &OV0312;O2max Decline in Mild Hypoxia. *Med. Sci. Sports Exerc.* 31, 658–663. doi:10.1097/00005768-199905000-00006

Chen, Y. L., Wolin, M. S., and Messina, E. J. (1996). Evidence for cGMP Mediation of Skeletal Muscle Arteriolar Dilation to Lactate. *J. Appl. Physiol.* 81, 349–354. doi:10.1152/jappl.1996.81.1.349

Dennis, J. J., Wiggins, C. C., Smith, J. R., Isautier, J. M. J., Johnson, B. D., Joyner, M. J., et al. (2021). Measurement of Muscle Blood Flow and O2 Uptake via Near-Infrared Spectroscopy Using a Novel Occlusion Protocol. *Sci. Rep.* 11, 918. doi:10.1038/s41598-020-79741-w

Dinenno, F. A., Joyner, M. J., and Halliwill, J. R. (2003). Failure of Systemic Hypoxia to Blunt α-Adrenergic Vasoconstriction in the Human Forearm. *J. Physiol.* 549, 985–994. doi:10.1113/jphysiol.2003.042507

Erba, P., Anastasi, S., Senn, O., Maggiorini, M., and Bloch, K. E. (2004). Acute Mountain Sickness Is Related to Nocturnal Hypoxemia but Not to Hypoventilation. *Eur. Respir. J.* 24, 303–308. doi:10.1183/09031936.04.00006504

Faul, F., Erdfelder, E., Lang, A.-G., and Buchner, A. (2007). G*Power 3: a Flexible Statistical Power Analysis Program for the Social, Behavioral, and Biomedical Sciences. *Behav. Res. Methods* 39, 175–191. doi:10.3758/bf03193146

Fisher, J. P. (2015). Cardiac Autonomic Regulation During Hypoxic Exercise. *Am J Physiol Heart Circ Physiol.* 308, H1474–H1475. doi:10.1152/ajpheart.00311.2015

Francisco, M. A., Colbert, C., Larson, E. A., Sieck, D. C., Halliwill, J. R., and Minson, C. T. (2021). Hemodynamics of post-exercise vs. post Hot Water Immersion Recovery. *J. Appl. Physiol. (1985)* 130, 1362. doi:10.1152/japplphysiol.00260.2020

Gibala, M. J., and Hawley, J. A. (2017). Sprinting toward Fitness. *Cel Metab.* 25, 988–990. doi:10.1016/j.cmet.2017.04.030

Girard, O., Brocherie, F., Goods, P. S. R., and Millet, G. P. (2020). An Updated Panorama of "Living Low-Training High" Altitude/Hypoxic Methods. *Front. Sports Act. Living* 2, 26. doi:10.3389/fspor.2020.00026

Halliwill, J. R., Sieck, D. C., Romero, S. A., Buck, T. M., and Ely, M. R. (2014). Blood Pressure Regulation X: what Happens when the Muscle Pump Is Lost? Post-exercise Hypotension and Syncope. *Eur. J. Appl. Physiol.* 114, 561–578. doi:10.1007/s00421-013-2761-1

Homma, S., Eda, H., Ogasawara, S., and Kagaya, A. (1996). Near-infrared Estimation of O2 Supply and Consumption in Forearm Muscles Working at Varying Intensity. *J. Appl. Physiol. (1985)* 80, 1279–1284. doi:10.1152/jappl.1996.80.4.1279

Hopkins, W. G., Marshall, S. W., Batterham, A. M., and Hanin, J. (2009). Progressive Statistics for Studies in Sports Medicine and Exercise Science. *Med. Sci. Sports Exerc.* 41, 3–12. doi:10.1249/mss.0b013e31818cb278

Horiuchi, M., and Okita, K. (2020). Microvascular Responses during Reactive Hyperemia Assessed by Near-Infrared Spectroscopy and Arterial Stiffness in Young, Middle-Aged, and Older Women. *Microvasc. Res.* 129, 103972. doi:10.1016/j.mvr.2019.103972

Horiuchi, M., Dobashi, S., Kiuchi, M., Endo, J., Koyama, K., and Subudhi, A. W. (2016). Reduction in Cerebral Oxygenation after Prolonged Exercise in Hypoxia Is Related to Changes in Blood Pressure. *Adv. Exp. Med. Biol.* 876, 95–100. doi:10.1007/978-1-4939-3023-4_12

Horiuchi, M., Oda, S., Uno, T., Endo, J., Handa, Y., and Fukuoka, Y. (2017). Effects of Short-Term Acclimatization at the Summit of Mt. Fuji (3776 M) on Sleep Efficacy, Cardiovascular Responses, and Ventilatory Responses. *High Alt. Med. Biol.* 18, 171–178. doi:10.1089/ham.2016.0162

Horiuchi, M., Ni-I-Nou, A., Miyazaki, M., Ando, D., and Koyama, K. (2018). Impact of Resistance Exercise under Hypoxia on Postexercise Hemodynamics in Healthy Young Males. *Int. J. Hypertens.* 2018, 1456972. doi:10.1155/2018/1456972

Jiménez-Maldonado, A., García-Suárez, P. C., Rentería, I., Moncada-Jiménez, J., and Plaisance, E. P. (2020). Impact of High-Intensity Interval Training and Sprint Interval Training on Peripheral Markers of Glycemic Control in Metabolic Syndrome and Type 2 Diabetes. *Biochim. Biophys. Acta Mol. Basis Dis.* 1866, 165820. doi:10.1016/j.bbadis.2020.165820

Joyner, M. J., and Casey, D. P. (2014). Muscle Blood Flow, Hypoxia, and Hypoperfusion. *J. Appl. Physiol. (1985)* 116, 852–857. doi:10.1152/japplphysiol.00620.2013

Kasai, N., Mizuno, S., Ishimoto, S., Sakamoto, E., Maruta, M., and Goto, K. (2015). Effect of Training in Hypoxia on Repeated Sprint Performance in Female Athletes. *Springerplus* 4, 310. doi:10.1186/s40064-015-1041-4

Kemps, H. M., Prompers, J. J., Wessels, B., De Vries, W. R., Zonderland, M. L., Thijssen, E. J., et al. (2009). Skeletal Muscle Metabolic Recovery Following Submaximal Exercise in Chronic Heart Failure Is Limited More by O(2) Delivery Than O(2) Utilization. *Clin. Sci. (Lond)* 118, 203–210. doi:10.1042/cs20090220

Kleinnibbelink, G., Stens, N. A., Fornasiero, A., Speretta, G. F., Van Dijk, A. P. J., Low, D. A., et al. (2020). The Acute and Chronic Effects of High-Intensity Exercise in Hypoxia on Blood Pressure and post-exercise Hypotension. *Medicine (Baltimore)* 99, e22411. doi:10.1097/md.0000000000022411

Kon, M., Nakagaki, K., Ebi, Y., Nishiyama, T., and Russell, A. P. (2015). Hormonal and Metabolic Responses to Repeated Cycling Sprints under Different Hypoxic Conditions. *Growth Horm. IGF Res.* 25, 121–126. doi:10.1016/j.ghir.2015.03.002

Lacewell, A. N., Buck, T. M., Romero, S. A., and Halliwill, J. R. (2014). Postexercise Syncope: Wingate Syncope Test and Effective Countermeasure. *Exp. Physiol.* 99, 172–186. doi:10.1113/expphysiol.2013.075333

Lakens, D. (2013). Calculating and Reporting Effect Sizes to Facilitate Cumulative Science: a Practical Primer for T-Tests and ANOVAs. *Front. Psychol.* 4, 863. doi:10.3389/fpsyg.2013.00863

Mankowski, R. T., Niemeijer, V. M., Jansen, J. P., Spraakman, L., Stam, H. J., and Praet, S. F. E. (2017). Oxygen Delivery Is Not a Limiting Factor during post-exercise Recovery in Healthy Young Adults. *J. Exerc. Sci. Fitness* 15, 43–47. doi:10.1016/j.jesf.2017.07.001

McCord, J. L., Beasley, J. M., and Halliwill, J. R. (2006). H2-receptor-mediated Vasodilation Contributes to Postexercise Hypotension. *J. Appl. Physiol. (1985)* 100, 67–75. doi:10.1152/japplphysiol.00959.2005

Nespoulet, H., Wuyam, B., Tamisier, R., Saunier, C., Monneret, D., Remy, J., et al. (2012). Altitude Illness Is Related to Low Hypoxic Chemoresponse and Low Oxygenation during Sleep. *Eur. Respir. J.* 40, 673–680. doi:10.1183/09031936.00073111

Nicholas, R., O'meara, P. D., and Calonge, N. (1992). Is Syncope Related to Moderate Altitude Exposure? *JAMA* 268, 904–906. doi:10.1001/jama.268.7.904

Puype, J., Van Proeyen, K., Raymackers, J.-M., Deldicque, L., and Hespel, P. (2013). Sprint Interval Training in Hypoxia Stimulates Glycolytic Enzyme Activity. *Med. Sci. Sports Exerc.* 45, 2166–2174. doi:10.1249/mss.0b013e31829734ae

Rowell, L. B., and Blackmon, J. R. (1989). Hypotension Induced by central Hypovolaemia and Hypoxaemia. *Clin. Physiol.* 9, 269–277. doi:10.1111/j.1475-097x.1989.tb00979.x

Rowell, L. B., and Seals, D. R. (1990). Sympathetic Activity during Graded central Hypovolemia in Hypoxemic Humans. *Am. J. Physiol. Heart Circulatory Physiol.* 259, H1197–H1206. doi:10.1152/ajpheart.1990.259.4.h1197

Rupp, T., Esteve, F., Bouzat, P., Lundby, C., Perrey, S., Levy, P., et al. (2014). Cerebral Hemodynamic and Ventilatory Responses to Hypoxia, Hypercapnia, and Hypocapnia during 5 Days at 4,350 M. *J. Cereb. Blood Flow Metab.* 34, 52–60. doi:10.1038/jcbfm.2013.167

Simmons, G. H., Minson, C. T., Cracowski, J.-L., and Halliwill, J. R. (2007). Systemic Hypoxia Causes Cutaneous Vasodilation in Healthy Humans. *J. Appl. Physiol. (1985)* 103, 608–615. doi:10.1152/japplphysiol.01443.2006

Simmons, G. H., Fieger, S. M., Minson, C. T., and Halliwill, J. R. (2010). Hypoxic Cutaneous Vasodilation Is Sustained during Brief Cold Stress and Is Not

Affected by Changes in CO2. *J. Appl. Physiol. (1985)* 108, 788–792. doi:10.1152/japplphysiol.01221.2009

Simmons, G. H., Barrett-O'Keefe, Z., Minson, C. T., and Halliwill, J. R. (2011). Cutaneous Vascular and Core Temperature Responses to Sustained Cold Exposure in Hypoxia. *Exp. Physiol.* 96, 1062–1071. doi:10.1113/expphysiol.2011.059147

Soares, R. N., George, M. A., Proctor, D. N., and Murias, J. M. (2018). Differences in Vascular Function between Trained and Untrained Limbs Assessed by Near-Infrared Spectroscopy. *Eur. J. Appl. Physiol.* 118, 2241–2248. doi:10.1007/s00421-018-3955-3

Stembridge, M., Ainslie, P. N., and Shave, R. (2015). Short-term Adaptation and Chronic Cardiac Remodelling to High Altitude in Lowlander Natives and Himalayan Sherpa. *Exp. Physiol.* 100, 1242–1246. doi:10.1113/expphysiol.2014.082503

Talbot, N. P., Balanos, G. M., Dorrington, K. L., and Robbins, P. A. (2005). Two Temporal Components within the Human Pulmonary Vascular Response to ~2 H of Isocapnic Hypoxia. *J. Appl. Physiol. (1985)* 98, 1125–1139. doi:10.1152/japplphysiol.00903.2004

Watanabe, S., Ishii, C., Takeyasu, N., Ajisaka, R., Nishina, H., Morimoto, T., et al. (2005). Assessing Muscle Vasodilation Using Near-Infrared Spectroscopy in Cardiac Patients. *Circ. J.* 69, 802–814. doi:10.1253/circj.69.802

Westendorp, R. G., Blauw, G. J., Frölich, M., and Simons, R. (1997). Hypoxic Syncope. *Aviat Space Environ. Med.* 68, 410–414.

Williams, J. T., Pricher, M. P., and Halliwill, J. R. (2005). Is Postexercise Hypotension Related to Excess Postexercise Oxygen Consumption through Changes in Leg Blood Flow? *J. Appl. Physiol. (1985)* 98, 1463–1468. doi:10.1152/japplphysiol.01211.2004

Zebrowska, M., Weippert, M., and Petelczyc, M. (2021). Oxyhemoglobin Concentration and Oxygen Uptake Signal during Recovery from Exhaustive Exercise in Healthy Subjects-Relationship with Aerobic Capacity. *Front. Physiol.* 12, 695569. doi:10.3389/fphys.2021.695569

Conflict of Interest: The authors declare that the research was conducted in the absence of any commercial or financial relationships that could be construed as a potential conflict of interest.

Publisher's Note: All claims expressed in this article are solely those of the authors and do not necessarily represent those of their affiliated organizations, or those of the publisher, the editors and the reviewers. Any product that may be evaluated in this article, or claim that may be made by its manufacturer, is not guaranteed or endorsed by the publisher.

frontiers in Physiology

ORIGINAL RESEARCH
published: 24 March 2022
doi: 10.3389/fphys.2022.818733

Comparing the Respiratory Compensation Point With Muscle Oxygen Saturation in Locomotor and Non-locomotor Muscles Using Wearable NIRS Spectroscopy During Whole-Body Exercise

Assaf Yogev[1], Jem Arnold[1], Dave Clarke[2], Jordan A. Guenette[3,4], Ben C. Sporer[5,6] and Michael S. Koehle[1,6]*

[1]Environmental Physiology Laboratory, School of Kinesiology, University of British Columbia, Vancouver, BC, Canada, [2]Department of Biomedical Physiology and Kinesiology and Centre for Cell Biology, Development and Disease, Simon Fraser University, Burnaby, BC, Canada, [3]Department of Physical Therapy, University of British Columbia, Vancouver, BC, Canada, [4]Providence Health Care Research Institute, Centre for Heart Lung Innovation, University of British Columbia, Vancouver, BC, Canada, [5]Vancouver Whitecaps FC, Vancouver, BC, Canada, [6]Division of Sport Medicine, University of British Columbia, Vancouver, BC, Canada

OPEN ACCESS

Edited by:
Thomas Rupp,
Université Savoie Mont Blanc, France

Reviewed by:
Danilo Iannetta,
University of Calgary, Canada
Susanna Rampichini,
University of Milan, Italy

***Correspondence:**
Assaf Yogev
yogevass@student.ubc.ca

Specialty section:
This article was submitted to Exercise Physiology, a section of the journal Frontiers in Physiology

Received: 19 November 2021
Accepted: 25 February 2022
Published: 24 March 2022

Citation:
Yogev A, Arnold J, Clarke D, Guenette JA, Sporer BC and Koehle MS (2022) Comparing the Respiratory Compensation Point With Muscle Oxygen Saturation in Locomotor and Non-locomotor Muscles Using Wearable NIRS Spectroscopy During Whole-Body Exercise.
Front. Physiol. 13:818733.
doi: 10.3389/fphys.2022.818733

The relationship between the muscle deoxygenation breakpoint (Deoxy-BP) measured with near-infrared spectroscopy (NIRS), and the respiratory compensation point (RCP) has been well established. This relationship has also been reported using wearable NIRS, however not in locomotor and non-locomotor muscles simultaneously during whole-body cycling exercise. Our aim was to measure muscle oxygen saturation (SmO_2) using wearable NIRS sensors, and to compare the Deoxy-BPs at each muscle with RCP during a ramp cycling exercise test. Twenty-two trained female and male cyclists completed a ramp exercise test to task intolerance on a cycling ergometer, at a ramp rate of 1 W every 2 s (30 W/min). SmO_2 was recorded at the subjects' right vastus lateralis (VL) and right lateral deltoid. SmO_2 and the Deoxy-BPs were assessed using a piecewise double-linear regression model. Ventilation ($\dot{V}_E$) and gas exchange were recorded, and RCP was determined from $\dot{V}_E$ and gas exchange using a V-slope method and confirmed by two physiologists. The SmO_2 profiles of both muscles and gas exchange responses are reported as $\dot{V}O_2$, power output (W), and time of occurrence (TO). SmO_2 profiles at both muscles displayed a near-plateau or breakpoint response near the RCP. No differences were detected between the mean RCP and mean Deoxy-BP from either the locomotor or non-locomotor muscles; however, a high degree of individual variability was observed in the timing and order of occurrence of the specific breakpoints. These findings add insight into the relationships between ventilatory, locomotor, and non-locomotor muscle physiological breakpoints. While identifying a similar relationship between these breakpoints, individual variability was high; hence, caution is advised when using wearable NIRS to estimate RCP in an incremental ramp test.

Keywords: muscle oxygenation, near-infrared spectroscopy, respiratory compensation point, breakpoint, wearable, exercise, exercise testing, cardiorespiratory fitness

INTRODUCTION

The close relationship between the respiratory compensation point (RCP) and the muscle deoxygenation breakpoint (Deoxy-BP) measured by near-infrared spectroscopy (NIRS) during incremental ramp cycling test has been well documented in recent years (Murias et al., 2013; Racinais et al., 2014; Fontana et al., 2015; Keir et al., 2015; Iannetta et al., 2017a; Caen et al., 2018). The ability to use changes in muscle oxygenation signals [deoxy(heme), oxy(heme), saturation, etc.] as a proxy for systemic pulmonary response yields far reaching possibilities for improving athletic performance, such as improving pacing strategies, simplifying performance assessment with non-invasive measures, and the potential for better understanding of central and peripheral limitations during exercise. The wider availability of affordable, portable NIRS devices that can be recorded to commercially available sport watches and cycling computers has made it more feasible for athletes, coaches, and teams to use muscle oxygenation as part of their regular training data collection (McManus et al., 2018; Perrey and Ferrari, 2018; Kirby et al., 2021; Rodrigo-Carranza et al., 2021). Wearable NIRS devices are typically based on continuous wave (CW) NIR light technology, which despite having some technical limitations compared to more robust, non-portable NIRS equipment, introduces the significant advantages of cost reduction and portability for field applications (Perrey and Ferrari, 2018).

In 2013, Murias et al. (2013) compared the recently described breakpoint (BP) in the NIRS-derived deoxygenated hemoglobin (Δ[HHb]) measurement at the VL with both the gas exchange threshold (GET) and the RCP, in 10 young males and 10 young females during a continuous ramp exercise test on a bicycle ergometer (Murias et al., 2013). They showed strong correlation in VO_2 obtained at the RCP and Δ[HHb]-BP. Other studies demonstrated a strong agreement between RCP and Δ[HHb]-BP both cross-sectionally (Racinais et al., 2014; Fontana et al., 2015; Keir et al., 2015; Inglis et al., 2017; Caen et al., 2018), in a heterogeneous fitness group (Boone et al., 2015), as well as longitudinally (Inglis et al., 2019). Contradicting evidence demonstrated that RCP and Δ[HHb]-BP occur at slightly different %VO_2max (Boone et al., 2015) and to be somewhat dissociated based on power output (PO), when evaluated across time following an exercise training intervention (Caen et al., 2018). This evidence comes mostly from two laboratories. Therefore, more studies are needed to corroborate the presence, or lack thereof, of this correspondence. Several studies observed the relationship between different muscles' Deoxy-BP during incremental exercise, and short, maximal intensity exercise, and the RCP during cycling and running. Iannetta et al. (2017a) assessed muscle oxygenation heterogeneity across quadricep muscles during a ramp exercise test on a cycling ergometer and compared the oxygenation response of the vastus lateralis (VL), vastus medialis, and rectus femoris muscles with the RCP (Iannetta et al., 2017b). Their findings showed a strong correlation between the pulmonary gas exchange (VO_2) corresponding to the NIRS-derived Δ[HHb]-BP measured across the different muscle sites and the VO_2 at RCP. Similar relationships have been observed between the VO_2 detected at the RCP, and the VO_2 observed at both the VL and respiratory muscle oxygenation breakpoints (Legrand et al., 2007; Contreras-Briceño et al., 2019), during similar cycling ergometer exercise protocols.

Several studies measured inactive forearm muscle oxygenation response to lower limb cycling exercise using ramp exercise tests (Ogata et al., 2004; Tanaka et al., 2006; Shiroishi et al., 2010). Their findings showed accelerated deoxygenation response past the RCP at the inactive forearm. Conversely, muscle oxygenation response in the biceps brachii (BB) and VL were compared during a 30 s maximal running on a treadmill (Manchado-Gobatto et al., 2020). This study found significant differences between these muscle groups during the final 15 s of the effort, with the BB reporting greater dynamic range in percent muscle deoxygenation (76 ± 2 to 31 ± 3) compared with the VL (79 ± 2 to 50 ± 4). These findings lead to further questions about the relationship between the systemic VO_2 response and the non-locomotor muscle deoxygenation response, and whether the latter can be used to accurately estimate the heavy - severe intensity threshold. If it is possible to detect a heavy - severe threshold using either locomotor or non-locomotor muscles, both endurance athletes and their coaches would be able to use it to optimize pacing strategy for specific competitions and environments, without the need to rely on expensive, invasive gas exchange or blood lactate measurements. The use of both lactate and gas exchange for these applications has been well documented, and thresholds such as the RCP, critical power, and maximal lactate steady state have shown strong agreements in the intensity at which they occur (Keir et al., 2015; Iannetta et al., 2018; Inglis et al., 2019). The primary limitations of both methods are a need for controlled environments for both operation and safety, trained personnel to conduct them due to their invasiveness, and expensive running cost. These limitations can be resolved using wearable NIRS, which requires very little experience to operate as data can be recorded using existing sport computers and applications, and can be done both indoors and in real-world training environments and competition at a relatively affordable cost. Therefore, should a muscle deoxygenation breakpoint be detectable with a wearable unit as described previously with other NIRS devices, at an intensity associated with RCP, it may provide a more accessible physiological measure of intensity dependent effects on muscle metabolism, without the need to rely on laboratory equipment or expert interpretation.

It is important to note that differences do exist between wearable CW-NIRS sensors and more technologically advanced, laboratory-based NIRS devices used in previous reports. Meaning results may not be directly transferable between different NIRS devices. These more advanced NIRS equipment may have multiple emitter-receptor optodes, more precise signal resolution, and higher sampling frequency. This improved measurement sensitivity may provide greater accuracy and reliability with absolute measurements, especially when evaluating subjects of heterogeneous tissue composition and fitness characteristics (McManus et al., 2018; Perrey and Ferrari, 2018; Barstow, 2019).

To translate findings from stationary NIRS in the lab to portable NIRS in the field, it is important to replicate findings obtained using advanced NIRS technology with those from commercially available portable devices. A recent study compared muscle oxygenation profiles using a wearable NIRS sensor (Humon Hex, Cambridge, MA, United States) with the RCP in elite runners. They reported no differences in $\dot{V}O_2$ or PO between the Deoxy-BP measured at the VL muscle and RCP, during an incremental ramp test on a treadmill (Rodrigo-Carranza et al., 2021). However, it is unknown whether this relationship holds in trained cyclists.

The RCP represents a systemic metabolic threshold. If Deoxy-BP is associated with the RCP, then it may not be limited to a local locomotor phenomenon. As such, a breakpoint may be detectable in non-locomotor muscle sites that reflect this systemic shift in metabolic homeostasis. The purpose of this study was 2-fold (1) to compare muscle Deoxy-BP as detected using a commercially available wearable NIRS with the RCP during a ramp exercise test performed on the subjects' own bicycles, as they would be performing in everyday training. (2) To measure this response at both locomotor and non-locomotor muscle sites. We hypothesized that wearable NIRS sensors would show a breakpoint or plateau-like response near the RCP, both at the locomotor and non-locomotor muscles, and that an association exists between the PO at RCP and muscle deoxygenation during a ramp exercise test on a bicycle ergometer.

MATERIALS AND METHODS

Subjects

Twenty-two trained cyclists (17 males and 5 females, 31 ± 8 yr.; 75 ± 12 kg; and 179 ± 10 cm) volunteered and provided written informed consent to participate in the study. To obtain sufficient power of $\beta = 0.8$ with $\alpha = 0.05$, an *a priori* sample size calculation was made in G*Power software (version 3.1.9.7, Kiel, Germany), using previously reported data from other groups that compared performance parameters for either gas exchange or PO between RCP and muscle oxygenation response (Murias et al., 2013; Boone et al., 2014; Racinais et al., 2014; Keir et al., 2015; Zwaard et al., 2016; Iannetta et al., 2017a, 2018; Caen et al., 2018; Rodrigo-Carranza et al., 2021). This study was approved by the research ethics committee of University of British Columbia and was conducted in accordance with principles established in the Declaration of Helsinki.

Experimental Design

The study required a single visit that included an incremental ramp cycling test from rest to task intolerance completed on an electronically controlled, stationary bicycle trainer (KICKR, Wahoo Fitness Inc., Atlanta, GA, United States) using each participant's bicycle and riding gear to simulate their regular indoor training environment. The ramp rate increased by 1 W every 2 s (30 W/min; **Figure 1**), with task intolerance determined as the point at which the participant cadence went down by more than 10 revolutions per minute from their self-selected cadence. Resistance was controlled in ergometer mode using PerfPRO Studio Software© (Hartware Technologies, Rockford, MI, United States) installed on a personal laptop.

Pulmonary oxygen uptake ($\dot{V}O_2$) was measured with an open-circuit expired-gas analysis system (TrueOne 2,400; ParvoMedics, Inc., Sandy, UT). $\dot{V}O_2$ data were averaged to 15 s and interpolated to 1 Hz for analysis. $\dot{V}O_2$peak was considered the highest average 30-s measurement. The RCP was determined at the point of deflection of $\dot{V}_E$ relative to $\dot{V}CO_2$ and the second deflection of $\dot{V}_E$ relative to $\dot{V}O_2$ (Davis, 1985; Beaver et al., 1986).

An individual mean response time (MRT) representing the delay between muscular metabolic activity and pulmonary response was determined using a recently described protocol (Murias et al., 2013; Iannetta et al., 2019). Briefly, the subjects performed a baseline warm-up for 6 min at a moderate PO of either 110 W (females) or 140 W (males). Average baseline $\dot{V}O_2$ was determined from the final 2 min of the baseline step. The ramp exercise test began with 4 min at 70 W (females) or 100 W (males), before the continuous ramp commenced at 1 W per 2 s. The subject's $\dot{V}O_2$ response during the ramp test was compared to their average baseline $\dot{V}O_2$. The difference in the instantaneous PO that elicited the same $\dot{V}O_2$ response was used to determine the MRT in watts and in seconds. The MRT was then used to shift PO relative to $\dot{V}O_2$ for estimation of the PO that elicited RCP and the $\dot{V}O_2$ response at the Deoxy-BP (further described below).

Near-Infrared Spectroscopy

Three wearable NIRS sensors (Moxy Monitor, Fortiori Design LLC., Hutchinson, United States) were used during the test. The Moxy monitor employs four wavelengths of NIR light (680, 720, 760, and 800 nm), with source detector separation of 12.5 and 25 mm (McManus et al., 2018). The sensors were placed on the following locations: on the vastus lateralis (VL) of the right and left leg, and right lateral deltoid. The right VL (RVL) was used for analysis unless signal quality was poor ($n = 1$), in which case the left side was used. The anatomical location on the VL was 1/3 the distance from the proximal pole of the patella to the greater trochanter. Left and right VL sensors were held in place by the participants' elastic cycling shorts. The deltoid sensor was positioned on the midline of the lateral deltoid muscle belly inferior to the acromion and maintained in place with a fiber-elastic band. All sensors were covered using a light shield supplied by the manufacturer to minimize interference.

According to the manufacturer, the Moxy sensor does not require calibration. A skinfold measurement with a Harpenden skinfold caliper (Slim Guide Skinfold Caliper) was made on the RVL to ensure all subjects were below 15 mm skinfold thickness, during the initial visit (Perrey and Ferrari, 2018).

Power Output

Power output was recorded using each participant's individual onboard power meter. Power meters were zero-offset following

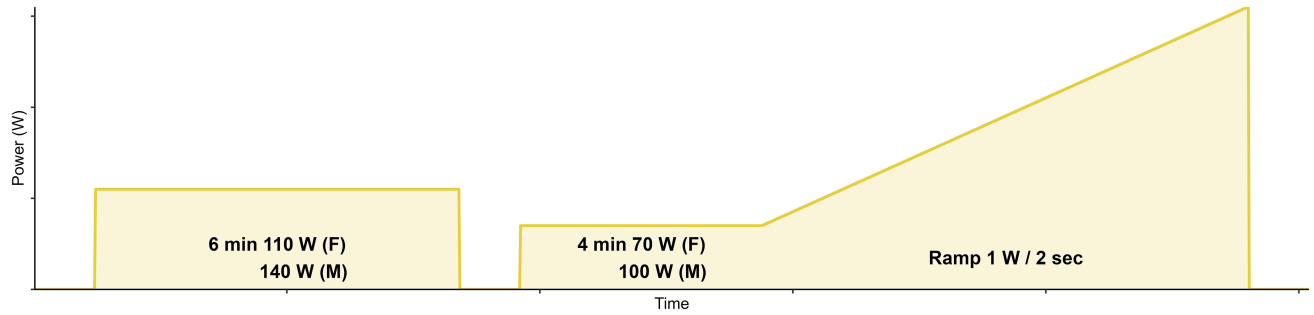

FIGURE 1 | Ramp exercise protocol. An initial baseline warm-up of 6 min at a moderate PO of either 110 W (females) or 140 W (males) was performed. It was then followed by 4 min at 70 W (females) or 100 W (males), before the continuous ramp commenced at 1 W per 2 s. Cessation of exercise was determined by the point at which the participant cadence went down by more than 10 revolutions per minute from their self-selected cadence.

manufacturer specifications before each test. The electronic trainer was calibrated immediately after the warm-up of each test to ensure accurate resistance was provided. Peak PO (W_{peak}) was defined as the highest 30-s PO recorded during the ramp test.

Data Collection

All three NIRS sensors and power data were collected using a Garmin Edge 520 cycling computer (Garmin Ltd., Lenexa, United States). Gas exchange and V_E were collected using Parvo Medics software.

Data Analysis

Methods used for measuring VO_{2peak} and detecting RCP are described above. The Moxy sensor provided measures of estimated total heme concentration ([tHb + Mb] in arbitrary units) and muscle O_2 saturation (SmO_2 as a percent). Computation of oxygenated hemoglobin [O_2Hb + Mb] and deoxygenated hemoglobin [HHb + Mb] can be derived from [tHb + Mb] and SmO_2 (McManus et al., 2018; Feldmann et al., 2019).

The SmO_2 signal was used as the primary output variable in this study (Crum et al., 2017; McManus et al., 2018; Feldmann et al., 2019). SmO_2 was measured every 2 s (0.5 Hz) and raw data were smoothed to 5-s moving averages as per manufacturer default settings. The Deoxy-BP was operationally defined as an inflection point in the SmO_2 profile plotted against time, analogous to the approach using the [HHb + Mb] plateau described by. This gives a time of occurrence (TO) from which the corresponding PO and VO_2 can be determined using the MRT correction detailed above. The breakpoint was located using a piecewise "double-linear" regression model implemented in the training analysis software WKO5 (TrainingPeaks, LLC, Boulder, CO, United States). This method is similar to the V-slope method for detecting RCP from the inflection of V_E vs. VCO_2 (Davis, 1985; Beaver et al., 1986). Following estimation of both the RCP and Deoxy-BP, each data set was reviewed by two physiologists for confirmation of the RCP and Deoxy-BP detection. Power output, VO_2, and time of occurrence (TO) at the RCP and Deoxy-BP were estimated, accounting for the muscle-pulmonary delay (MRT) as outlined above (**Figure 2**).

Statistical Analysis

GraphPad statistical software (GraphPad Software Inc., CA, United States) was used for statistical analysis. To test the hypothesis of non-differences between RCP and the two Deoxy-BP, as well as between the two Deoxy-BP (deltoid and VL), we performed one-way ANOVAs for the three outcome variables (VO_2, PO, and TO) and factors (RCP, Deoxy-BP deltoid, and Deoxy-BP VL). Regression analyses were used to calculate an association between RCP and the two Deoxy-BP, as well as between the two Deoxy-BP (deltoid and VL). Correlation was classified as followed: negligible (0.00–0.30), weak (0.30–0.50), moderate (0.50–0.70), strong (0.70–0.90), or very strong (0.90–1.00; Mukaka, 2012). A post-hoc Tukey Test was employed when significant differences were detected, and a Bland Altman test was used for agreement in the VO_2 between the breakpoints ($p < 0.05$).

RESULTS

Means for participant characteristics are presented in **Table 1**. Means for VO_2, PO, and TO at RCP, and both VL and deltoid Deoxy-BP are presented in **Table 2**. Mean comparison of RCP with both Deoxy-BP showed no difference in VO_2, PO, or TO ($p > 0.05$). **Figures 3A–C** presents individual data comparison between the three measurements as a function of VO_2, PO, and TO.

Figures 4A–C presents Pearson correlations between the VO_2 at RCP and the two Deoxy-BP, as well as between the two Deoxy-BP (VL and deltoid). The relationships across all variables showed positive, moderate relationships ($r = 0.58–0.69$). All correlations were statistically significant ($p < 0.01$).

Figures 5A–C presents Bland–Altman plots depicting the agreement between the VO_2 at RCP and both Deoxy-BP. Relative VO_2 ($ml \cdot kg^{-1} \cdot min^{-1}$) detected for each of the measurements was used to assess their agreement. The mean average error for RCP and VL Deoxy-BP was

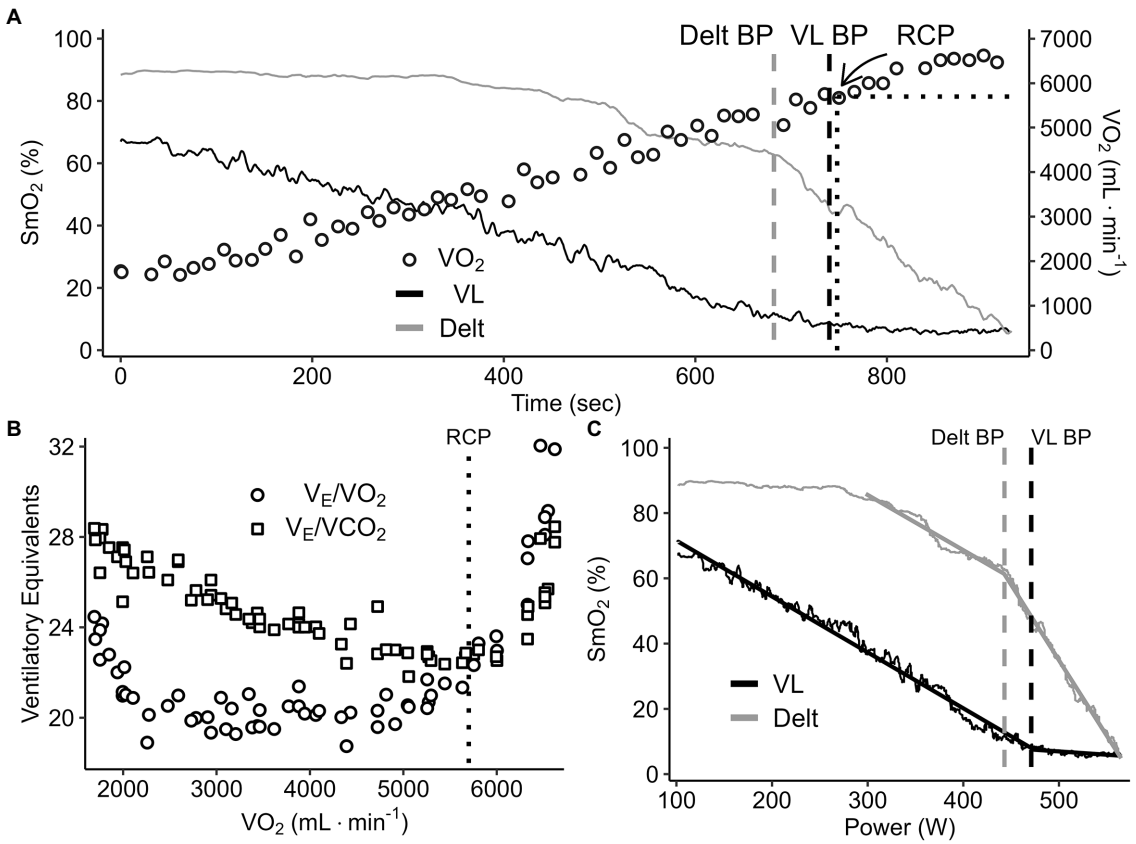

FIGURE 2 | A representative data set of breakpoint detection and comparison between the change in $\%SmO_2$ (VL and deltoid) and $\dot{V}O_2$ (panel **A**), ventilatory equivalents of O_2 and CO_2 (panel **B**), and $\%SmO_2$ VL and deltoid profiles (panel **C**) during a continuous graded exercise test from rest to task intolerance.

TABLE 1 | Characteristics of study participants.

Age (y)	Weight (kg)	Height (cm)	$\dot{V}O_2$peak ($ml \cdot kg^{-1} \cdot min^{-1}$)	MRT (sec)	W_{peak} (W)	SF (mm)	HR_{max} (bpm)
30.9 ± 8.3	75.0 ± 12.3	178.9 ± 10.1	61.4 ± 11.4	31.1 ± 10.8	406.4 ± 66.1	9.8 ± 4.9	188.9 ± 10.0

Mean data displayed as mean ± standard deviation, for the following variables: age, weigh, height, peak VO_2 (VO_{2peak}), mean response time (MRT), peak power output (W_{peak}), skinfold tissue thickness (SF), and maximum heart rate (HR_{max}).

$-2.1\ ml \cdot kg^{-1} \cdot min^{-1}$ ($p > 0.05$; limits of agreement: lower = $-14.6\ ml \cdot kg^{-1} \cdot min^{-1}$; upper = $10.5\ ml \cdot kg^{-1} \cdot min^{-1}$). The mean average error for RCP and deltoid Deoxy-BP was $-1.2\ ml \cdot kg^{-1} \cdot min^{-1}$ ($p > 0.05$; limits of agreement: lower = $-12.6\ ml \cdot kg^{-1} \cdot min^{-1}$; upper = $10.1\ ml \cdot kg^{-1} \cdot min^{-1}$). Lastly, the mean average error for VL and deltoid Deoxy-BP was $0.8\ ml \cdot kg^{-1} \cdot min^{-1}$ ($p > 0.05$; limits of agreement: lower = $-11.1\ ml \cdot kg^{-1} \cdot min^{-1}$; upper = $12.7\ ml \cdot kg^{-1} \cdot min^{-1}$).

DISCUSSION

The aim of this study was to compare VO_2, PO, and TO corresponding to the RCP, and the breakpoint of muscle oxygenation in the vastus lateralis and deltoid muscles (VL and deltoid Deoxy-BP respectively) measured using wearable NIRS sensors, during a ramp exercise protocol on a bicycle ergometer. From our results, we were unable to detect significant differences across our mean variables which were in support of our main hypothesis. It is important, however, to point out that despite our Bland Altman plots presenting a bias that was not different from zero, they depicted large limits of agreement of $> 10\ ml \cdot kg^{-1} \cdot min^{-1}$ between the variables. Our findings were in agreement with previous studies that compared the VO_2 and PO at the RCP and at the NIRS-derived Deoxy-BP (Iannetta et al., 2017a,b). Additionally, our results presented that the Deoxy-BP derived from a wearable sensor was not different from the RCP in a group of trained male and female cyclists with heterogeneous fitness. That said, the limits of agreement were poor; hence, caution is advised when using wearable NIRS devices to estimate RCP in an incremental ramp test. This may suggest that the protocol used should

TABLE 2 | Mean comparison between respiratory compensation point (RCP), vastus lateralis (VL), and deltoid Deoxy-BP as a function of VO2, power output (PO), and time of occurrence (TO).

	RCP	VL	deltoid
VO_2 (ml·kg^{-1}·min^{-1})	51.2 ± 7.5	53.3 ± 6.3	52.5 ± 7.3
PO (W)	304 ± 63	321 ± 65	317 ± 60
TO (s)	448 ± 116	451 ± 115	442 ± 106

Mean data displayed as mean ± standard deviation. No significant difference was observed between RCP, VL, and deltoid Deoxy-BP for those variables.

be considered when evaluating metabolic thresholds and intensity domains with either gas exchange, blood lactate, or muscle oxygenation. The demarcation of metabolic breakpoints is specific to the assessment protocol and measurement device used.

When all three breakpoints were compared in terms of corresponding VO_2 and PO, no mean differences were observed, and significant moderate to strong correlations between the measures were detected. Previous studies showing no differences used similar analysis; however, a majority of these studies used healthy participants with a lower mean VO_{2peak} of approximately 50 ml·kg^{-1}·min^{-1} (Iannetta et al., 2017a,b). A study by Boone et al. (2015) had 64 participants with a similar range of heterogeneous fitness as seen in our group, who underwent a similar exercise protocol. Our results showed a similar range at Deoxy-BP at the VL and deltoid when presented in relative VO_2 (ml·kg^{-1}·min^{-1}). Despite these similarities, our results show large individual variation, which raises concerns about using these indices interchangeably. It is possible that the difference between the findings of Boone, et al., compared with our results is related to the different sensors used for the detection of the Deoxy-BP (laser-based, frequency domain versus CW-NIRS, respectively). Therefore, caution is warranted for practitioners using wearable NIRS sensors when attempting to interpret similar thresholds, using similar exercise protocols.

Although there were no significant differences between the mean VO_2 and PO corresponding to the Deoxy-BP and the RCP, individual data showed that the VL Deoxy-BP and RCP did not occur in a consistent sequence. The difference between the TO for VL Deoxy-BP and RCP ranged from −210 to 180 s, and for deltoid Deoxy-BP and RCP was −155 to 145 (where negative indicates the RCP occurred before the Deoxy-BP, and positive indicates that the Deoxy-BP occurred before the RCP). The TO of the VL Deoxy-BP preceded the RCP TO in 11 of the 22 subjects, and the deltoid Deoxy-BP TO occurred before the RCP TO in 12 subjects, although not necessarily in the same individuals. The inclusion of TO in the analysis was to account for methodological limitations in accounting for MRT (discussed further below) and the differences that might have resulted when shifting either VO_2 or PO to compare the different breakpoints (Murias et al., 2013; Iannetta et al., 2019). In terms of corresponding VO_2, nine subjects had lower VO_2 at their VL Deoxy-BP than at their RCP, and nine subjects

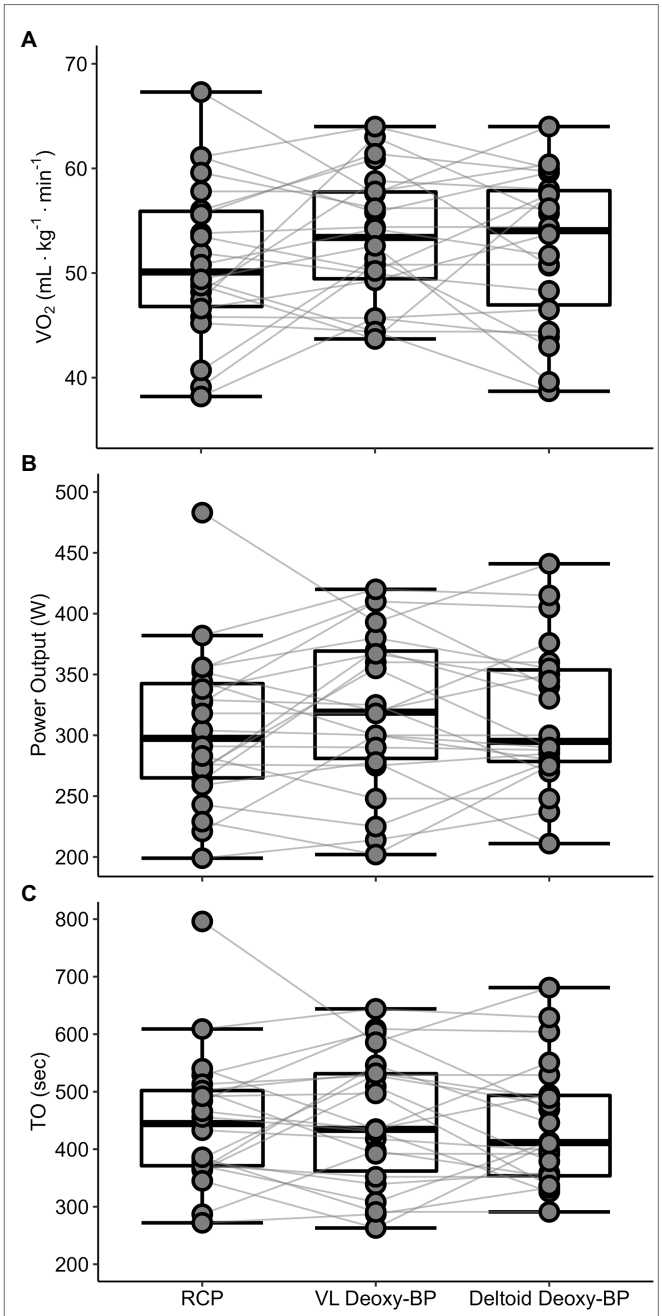

FIGURE 3 | Individual data comparison between RCP, VL, and deltoid Deoxy-BP for VO_2 (ml·kg^{-1}·min^{-1}; panel **A**), power output (PO in W; panel **B**), and time of occurrence (TO in s; panel **C**).

(not necessarily the same individuals) had lower VO_2 at their deltoid Deoxy-BP. Such differences have also been shown by Boone et al. between the VO_2 at the RCP and the deoxygenated hemoglobin breakpoint BP deoxy[Hb+Mb] similar to Deoxy-BP used in our study), with the RCP preceding the breakpoint in deoxy[Hb+Mb] during an incremental ramp cycle test (Boone et al., 2015). They suggested two hypotheses for the potential mechanism responsible for this sequence. These hypotheses are focused

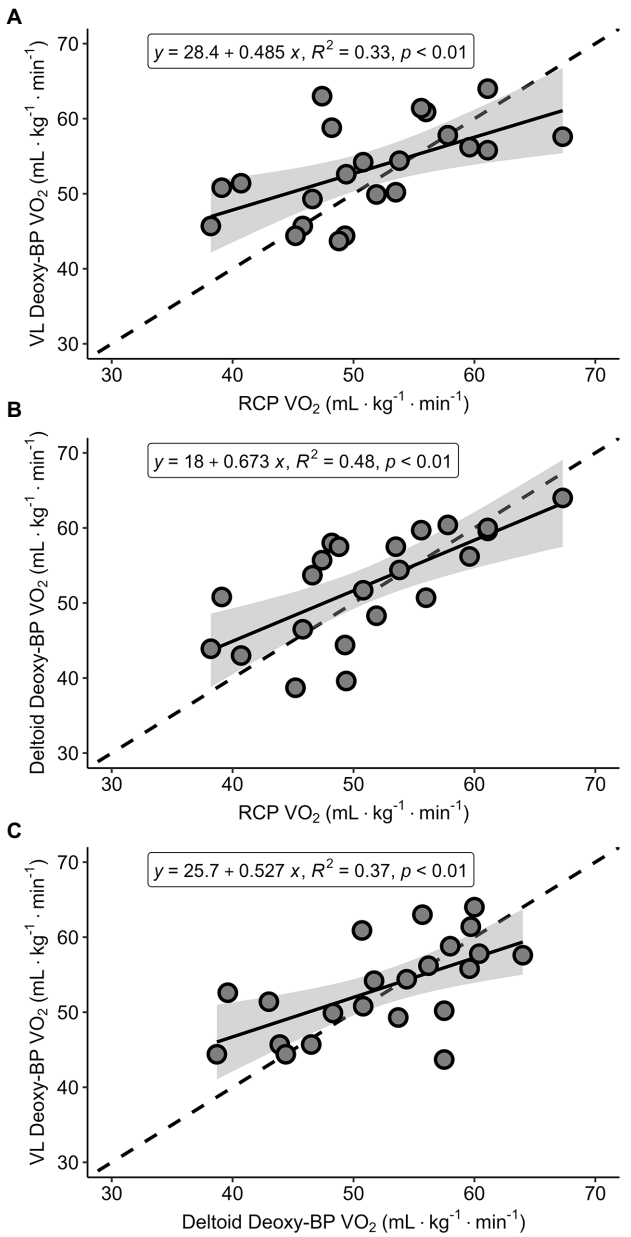

FIGURE 4 | Regression analyses for VO_2 (ml·kg^{-1}·min^{-1}) between RCP and VL Deoxy-BP (panel **A**), RCP and deltoid Deoxy-BP (panel **B**), and VL Deoxy-BP and deltoid Deoxy-BP (panel **C**).

on (1) muscle metabolism changes during a ramp exercise test stimulating both V_E and respiratory alkalosis and vasodilation, resulting in increased blood delivery to the working muscles. (2) An increase in less oxidatively efficient type IIa and type IIx muscle fiber recruitment above the RCP to maintain power production in response to the increased resistance (Boone et al., 2015). These hypotheses are likely not mutually exclusive and potentially responsible for the variability observed in this study. Conversely, other reports have described a close agreement, with no significant differences between the RCP and NIRS breakpoints (Murias et al., 2013; Fontana et al., 2015; Keir et al., 2015; Iannetta et al., 2017a), suggesting further investigation is warranted.

Our results, however, do not rule out the concept of disparate tissues reaching a local breakpoint at different times, which cumulatively produce the systemic response. It is possible that the breakpoint at the VL is led by elevated whole-body oxygen during cycling (Boone et al., 2015). As for the deltoid, recruitment during cycling may vary between different riding techniques and riding positions. As such, the presence of a Deoxy-BP at the deltoid may result from (1) an increase in O_2 extraction to produce work of upper body stabilization with increasing locomotor PO and (2) systemic redistribution of blood flow primarily toward working skeletal muscle, respiratory muscles, the heart, and the brain *via* vasoconstriction of non-priorities tissues (Özyener et al., 2012). Our results highlight the importance of including multiple muscle sites during whole-body exercise testing to investigate the sequential and mechanistic relationships between peripheral and systemic expression of metabolic breakpoints. This relationship is important as it may contribute to field application of wearable NIRS for intensity monitoring for the following reasons: (1) it may not be limited only to primary locomotor muscle measurements and (2) other anatomical locations may be less affected by movement artifacts, providing better signal quality during real-world training and competition. Further investigations should be made to address these points.

For practitioners and athletes, the ability to describe local oxygenation responses at multiple muscle sites may help understand the distribution of muscle recruitment, metabolic supply and demand, and cumulative local fatigue in the context of whole-body exercise. However, from our results, we conclude that using wearable NIRS to determine metabolic breakpoints remains premature, insofar as a high degree of individual variability exist even in well-controlled laboratory conditions. Contextual observations of muscle oxygenation responses and their reliability, apart from the determination of metabolic breakpoints, may still provide relevant information for practitioners to understand an individual athlete's response to exercise. Such observations could focus on stochastic exercise, recovery and repeated efforts, warm-up, and simulation of sport-specific activities to better understand metabolic demand and individual responses.

STUDY LIMITATIONS

As mentioned previously, VO_2 was measured with an open-circuit respiratory gas analysis system, with mixed expired gases averaged every 15 s and interpolated to 1 Hz for analysis. Unlike a breath-by-breath system, this could have potentially introduced timing errors into the calculation of MRT that may have contributed to the individual variability observed in this parameter. This in turn could have affected the adjustment of VO_2 and PO at Deoxy-BP and RCP, respectively. For this reason, we chose to report the original time of occurrence for all breakpoints as they were measured during exercise, in

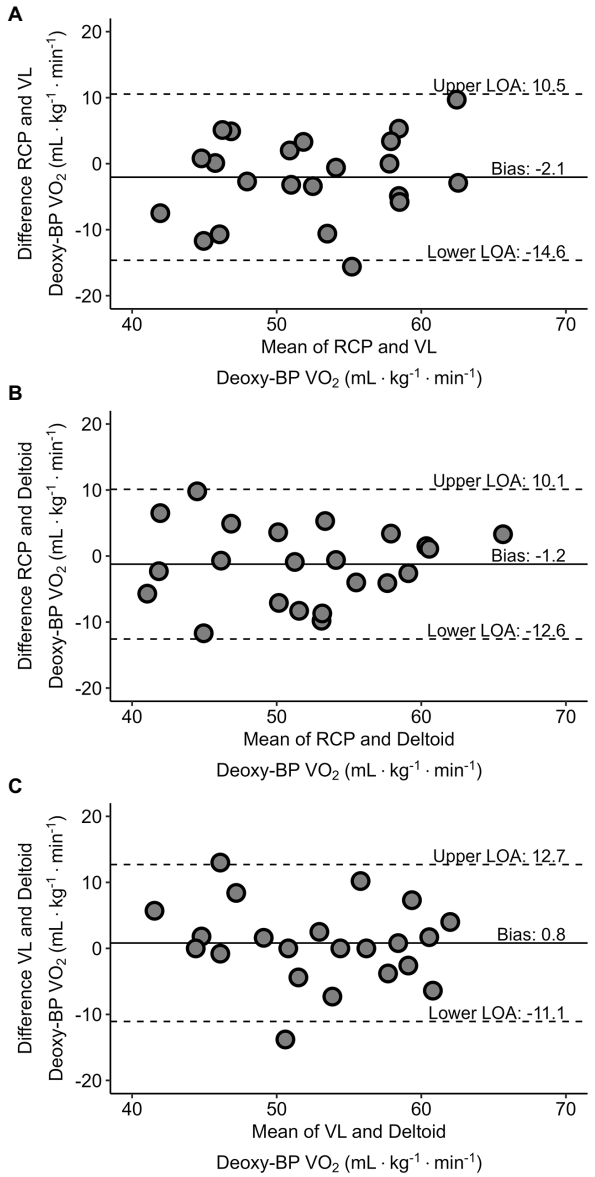

FIGURE 5 | Bland–Altman plots displaying agreement between $\dot{V}O_2$ (ml·kg^{-1}·min^{-1}) corresponding with RCP and VL Deoxy-BP (panel **A**), RCP and deltoid Deoxy-BP (panel **B**), and VL and deltoid Deoxy-BP (panel **C**). The horizontal solid line represents the mean difference between each of the two measurements. The paired horizontal dotted lines represent the 95% limits of agreement for each of the comparisons.

addition to calculating the MRT-adjusted $\dot{V}O_2$ and PO that were associated with those breakpoints.

The analysis methods chosen for the detection of the NIRS-derived Deoxy-BP in this study and in others are based on well-established methods used to determine ventilatory thresholds (Davis, 1985; Beaver et al., 1986; Murias et al., 2013; Iannetta et al., 2019). The commonly used incremental ramp protocol allows for easy comparison to ventilatory thresholds for identification of intensity domains. However, like all methods of assessing physiological breakpoint, the analysis method is specific to the protocol used. The considerable variability in the expression of individual ventilatory thresholds and deoxygenation breakpoints at locomotor and non-locomotor muscle sites among this well-trained subject group may suggest that different assessment protocols may be useful to further explore the sources of this individual heterogeneity. For example, by design, the relatively fast incremental ramp rate (30 W/min) used in the present study does not allow for the kinetics of either pulmonary ventilation or muscle oxygenation to be fully expressed at any particular workload. It could be that a longer multi-stage "step test" protocol could be used to observe the full expression of oxygenation kinetics across multiple locomotor and non-locomotor muscle sites at progressively increasing workloads, in order to better appreciate the interaction of local metabolic responses and their contribution to systemic measurements like pulmonary gas exchange. Future experiments will be able to optimize exercise assessment protocols to the specific advantages of NIRS, rather than be bound to design constraints imposed by unrelated measurement techniques.

Lastly, the default variable, SmO_2, generated by the Moxy sensor may be more sensitive to changes in blood flow compared to [HHb+Mb] measured with frequency-domain NIRS (Grassi et al., 2003). Because of this setting, it is possible that the high individual variation seen in our study is related to exercise induced vasodilation (Grassi et al., 2003).

CONCLUSION

In conclusion, our findings show that a commercially available wearable NIRS sensor can detect the Deoxy-BP in both VL and deltoid muscles, and that there were no differences between the mean Deoxy-BP and mean RCP; however, the high degree of individual variability suggests caution should be taken when translating between these protocol-dependent metabolic breakpoints. As such, further investigations remain warranted in order for practitioners and athletes to use wearable NIRS to detect physiological breakpoints that may be used to prescribe training, predict race performance pacing, and monitor athlete development, from a single incremental ramp exercise test.

DATA AVAILABILITY STATEMENT

The raw data supporting the conclusions of this article will be made available by the authors, without undue reservation.

ETHICS STATEMENT

The studies involving human participants were reviewed and approved by UBC Clinical Research Ethics Board. The patients/participants provided their written informed consent to participate in this study.

AUTHOR CONTRIBUTIONS

AY and JA have equally contributed to the study design, data acquisition, and write up, under the supervision of MK, and guidance of the remaining listed authors. All authors contributed to the article and approved the submitted version.

FUNDING

This study was funded by a Natural Sciences and Engineering Research Council Discovery Grant and an equipment grant from the British Columbia Sport and Exercise Medicine Research Foundation.

REFERENCES

Barstow, T. J. (2019). Understanding near Infrared spectroscopy and its application to skeletal muscle research. *J. App. Physiol. Am. Physiol. Soc.* 126, 1360–1376. doi: 10.1152/japplphysiol.00166.2018

Beaver, W. L., Wasserman, K., and Whipp, B. J. (1986). A new method for detecting anaerobic threshold by gas exchange. *J. Appl. Physiol.* 60, 2020–2027. doi: 10.1152/jappl.1986.60.6.2020

Boone, J., Barstow, T. J., Celie, B., Prieur, F., and Bourgois, J. (2014). The impact of pedal rate on muscle oxygenation, muscle activation and whole-body VO_2 during ramp exercise in healthy subjects. *Eur. J. Appl. Physiol.* 115, 57–70. doi: 10.1007/s00421-014-2991-x

Boone, J., Barstow, T. J., Celie, B., Prieur, F., and Bourgois, J. (2015). The interrelationship between muscle oxygenation, muscle activation, and pulmonary oxygen uptake to incremental ramp exercise: influence of aerobic fitness. *Appl. Physiol. Nutr. Metab.* 41, 55–62. doi: 10.1139/apnm-2015-0261

Caen, K., Vermeire, K., Bourgois, J. G., and Boone, J. (2018). Exercise thresholds on trial: are they really equivalent? *Med. Sci. Sports Exerc.* 50, 1277–1284. doi: 10.1249/MSS.0000000000001547

Contreras-Briceño, F., Espinosa-Ramirez, M., Hevia, G., Llambias, D., Carrasco, M., Cerda, F., et al. (2019). Reliability of NIRS portable device for measuring intercostal muscles oxygenation during exercise. *J. Sports Sci.* 37, 2653–2659. doi: 10.1080/02640414.2019.1653422

Crum, E. M., O'Connor, W. J., Van Loo, L., Valckx, M., and Stannard, S. R. (2017). Validity and reliability of the Moxy oxygen monitor during incremental cycling exercise. *Eur. J. Sport Sci.* 17, 1037–1043. doi: 10.1080/17461391.2017.1330899

Davis, J. A. (1985). Anaerobic threshold: review of the concept and directions for future research. *Med. Sci. Sports Exerc.* 17, 6–21. doi: 10.1249/00005768-198502000-00003

Feldmann, A., Schmitz, R., and Erlacher, D. (2019). Near-infrared spectroscopy-derived muscle oxygen saturation on a 0 to 100% scale: reliability and validity of the Moxy monitor. *J. Biomed. Opt.* 24, 1–11. doi: 10.1117/1.jbo.24.11.115001

Fontana, F. Y., Keir, D. A., Bellotti, C., De Roia, G. F., Murias, J. M., and Pogliaghi, S. (2015). Determination of respiratory point compensation in healthy adults: can non-invasive near-infrared spectroscopy help? *J. Sci. Med. Sport* 18, 590–595. doi: 10.1016/j.jsams.2014.07.016

Grassi, B., Pogliaghi, S., Rampichini, S., Quaresima, V., Ferrari, M., Marconi, C., et al. (2003). Muscle oxygenation and pulmonary gas exchange kinetics during cycling exercise on-transitions in humans. *J. Appl. Physiol.* 95, 149–158. doi: 10.1152/japplphysiol.00695.2002

Iannetta, D., Inglis, E. C., Fullerton, C., Passfield, L., and Murias, J. M. (2018). Metabolic and performance-related consequences of exercising at and slightly above MLSS. *Scand. J. Med. Sci. Sports* 28, 2481–2493. doi: 10.1111/sms.13280

Iannetta, D., Murias, J. M., and Keir, D. A. (2019). A simple method to quantify the V-O 2 mean response time of ramp-incremental exercise. *Med. Sci. Sports Exerc.* 51, 1080–1086. doi: 10.1249/MSS.0000000000001880

Iannetta, D., Qahtani, A., Maturana, F. M., and Murias, J. M. (2017a). The near-infrared spectroscopy-derived deoxygenated Haemoglobin breaking-point is a repeatable measure That demarcates exercise intensity domains. *J. Sci. Med. Sport* 20, 873–877. doi: 10.1016/j.jsams.2017.01.237

Iannetta, D., Qahtani, A., Millet, G. Y., and Murias, J. M. (2017b). Quadriceps muscles O_2 extraction and Emg breakpoints during a ramp incremental test. *Front. Physiol.* 8:686. doi: 10.3389/fphys.2017.00686

Inglis, C., Erin, D. I., and Murias, J. M. (2017). The plateau in the NIRS-derived [HHb] signal near the end of a ramp incremental test does not indicate the upper limit of O_2 extraction in the Vastus Lateralis. *Am. J. Physiol. Regul. Integr. Comp. Physiol.* 313, R723–R729. doi: 10.1152/ajpregu.00261.2017

Inglis, E. C., Iannetta, D., Keir, D. A., and Murias, J. M. (2019). Training-induced changes in the RCP, [HHb]BP and MLSS: evidence of equivalence. *Int. J. Sports Physiol. Perform.* 15, 119–125. doi: 10.1123/ijspp.2019-0046

Keir, D. A., Fontana, F. Y., Robertson, T. C., Murias, J. M., Paterson, D. H., Kowalchuk, J. M., et al. (2015). Exercise intensity thresholds: identifying the boundaries of sustainable performance. *Med. Sci. Sports Exerc.* 47, 1932–1940. doi: 10.1249/MSS.0000000000000613

Kirby, B. S., Clark, D. A., Bradley, E. M., and Wilkins, B. W. (2021). The balance of muscle oxygen supply and demand reveals critical metabolic rate and predicts time to exhaustion. *J. Appl. Physiol.* 130, 1915–1927. doi: 10.1152/japplphysiol.00058.2021

Legrand, R., Marles, A., Prieur, F., and Lazzari, S. (2007). Related trends in Locomotor and respiratory muscle oxygenation during exercise. *Med. Sci. Sports Exerc.* 39, 91–100. doi: 10.1249/01.mss.0000241638.90348.67

Manchado-Gobatto, F. B., Marostegan, A. B., Rasteiro, F. M., Cirino, C., Cruz, J. P., Moreno, M. A., et al. (2020). New insights into mechanical, metabolic and muscle oxygenation signals During and After high-intensity tethered running. *Sci. Rep.* 10, 6336–6314. doi: 10.1038/s41598-020-63297-w

McManus, C. J., Collison, J., and Cooper, C. E. (2018). Performance comparison of the MOXY and PortaMon near-infrared spectroscopy muscle Oximeters at rest and during exercise. *J. Biomed. Opt.* 23, 1–14. doi: 10.1117/1.jbo.23.1.015007

Mukaka, M. M. (2012). Statistics corner: A guide to appropriate use of correlation coefficient in medical research. *J. Med. Assoc. Malawi* 24, 69–71.

Murias, J. M., Keir, D. A., Spencer, M. D., and Paterson, D. H. (2013). Sex-related differences in muscle Deoxygenation during ramp incremental exercise. *Resp. Physiol. Neurobiol.* 189, 530–536. doi: 10.1016/j.resp.2013.08.011

Ogata, H., Reyihan, A., and Yano, T. (2004). Kinetics of oxygenation in inactive forearm muscle during ramp leg cycling. *J. Physiol. Anthropol. Appl. Hum. Sci.* 23, 7–17. doi: 10.2114/jpa.23.7

Özyener, F., Whipp, B. J., and Ward, S. A. (2012). The contribution of 'resting' body muscles to the slow component of pulmonary oxygen uptake during high-intensity cycling. *J. Sports Sci. Med.* 11, 759–767.

Perrey, S., and Ferrari, M. (2018). Muscle oximetry in sports science: a systematic review. *Sports Med.* 48, 597–616. doi: 10.1007/s40279-017-0820-1

Racinais, S., Buchheit, M., Girard, O., and Perrey, S. (2014). Breakpoints in ventilation, cerebral and muscle oxygenation, and muscle activity during an incremental cycling exercise. *Front. Physiol.* 5:142. doi: 10.3389/fphys.2014.00142

Rodrigo-Carranza, V., González-Mohíno, F., Turner, A. P., Rodriguez-Barbero, S., and González-Ravé, J. M. (2021). Using a portable near-infrared spectroscopy device to estimate the second Ventilatory threshold. *Int. J. Sports Med.* 42, 905–910. doi: 10.1055/a-1343-2127

Shiroishi, K., Kime, R., Osada, T., Murase, N., Shimomura, K., and Katsumura, T. (2010). Decreased muscle oxygenation and increased arterial blood flow in the non-exercising limb during leg exercise. *Adv. Exp. Med. Biol.* 662, 379–384. doi: 10.1007/978-1-4419-1241-1_55

Tanaka, H., Shimizu, S., Ohmori, F., Muraoka, Y., Kumagai, M., Yoshizawa, M., et al. (2006). Increases in blood flow and shear stress to nonworking limbs during incremental exercise. *Med. Sci. Sports Exerc.* 38, 81–85. doi: 10.1249/01.mss.0000191166.81789.de

Zwaard, S., Jaspers, R. T., Blokland, I. J., Achterberg, C., Visser, J. M., Den Uil, A. R., et al. (2016). Oxygenation threshold derived from near-infrared spectroscopy: reliability and its relationship with the first

Ventilatory threshold. *PLoS One* 11, 1–16. doi: 10.1371/journal.pone.0162914

Conflict of Interest: The authors declare that the research was conducted in the absence of any commercial or financial relationships that could be construed as a potential conflict of interest.

Publisher's Note: All claims expressed in this article are solely those of the authors and do not necessarily represent those of their affiliated organizations, or those of the publisher, the editors and the reviewers. Any product that may be evaluated in this article, or claim that may be made by its manufacturer, is not guaranteed or endorsed by the publisher.

frontiers | Frontiers in Physiology

ORIGINAL RESEARCH
published: 08 July 2022
doi: 10.3389/fphys.2022.919754

Skeletal Muscle Tissue Saturation Changes Measured Using Near Infrared Spectroscopy During Exercise Are Associated With Post-Occlusive Reactive Hyperaemia

Siana Jones, Therese Tillin, Suzanne Williams, Alicja Rapala, Nishi Chaturvedi and Alun D. Hughes*

MRC Unit for Lifelong Health & Ageing at UCL, Department of Population Science and Experimental Medicine, Institute for Cardiovascular Science, University College London, London, United Kingdom

Measuring local haemodynamics in skeletal muscle has the potential to provide valuable insight into the oxygen delivery to tissue, especially during high demand situations such as exercise. The aim of this study was to compare the skeletal muscle microvascular response during post-occlusive reactive hyperaemia (PORH) with the response to exercise, each measured using near-infrared spectroscopy (NIRS) and to establish if associations exist between muscle measures and exercise capacity or sex. Participants were from a population-based cohort study, the Southall and Brent Revisited (SABRE) study. Skeletal muscle measures included changes in tissue saturation index at the onset of exercise ($\Delta TSI_{BL\text{-}INC}$) and across the whole of exercise ($\Delta TSI_{BL\text{-}EE}$), time to 50%, 95% and 100% PORH, rate of PORH recovery, area under the curve (AUC) and total oxygenated Haemoglobin (oxy-Hb) change during PORH. Exercise capacity was measured using a 6-min stepper test (6MST). Analysis was by multiple linear regression. In total, 558 participants completed the 6MST with NIRS measures of TSI (mean age±SD: 73 ± 7years, 59% male). A sub-set of 149 participants also undertook the arterial occlusion. Time to 100% PORH, recovery rate, AUC and Δoxy-Hb were all associated with $\Delta TSI_{BL\text{-}EE}$ (β-coefficient (95%CI): 0.05 (0.01, 0.09), $p = 0.012$; –47 (-85, –9.9), $p = 0.014$; 1.7 (0.62, 2.8), $p = 0.002$; 0.04 (0.002.0.108), $p = 0.041$, respectively). Time to 95% & 100% PORH, AUC and Δoxy-Hb were all associated with $\Delta TSI_{BL\text{-}INC}$ (β-coefficient (95%CI): –0.07 (–0.12,–0.02), $p = 0.02$; –0.03 (–0.05, –0.003), $p = 0.028$; 0.85 (0.18, 1.5), $p = 0.013$ & 0.05 (0.02, 0.09), $p = 0.001$, respectively). AUC and ΔOxy-Hb were associated with steps achieved (β-coefficient (95%CI): 18.0 (2.3, 33.7), $p = 0.025$; 0.86 (0.10, 1.6), $p = 0.027$). $\Delta TSI_{BL\text{-}EE}$ was associated with steps and highest VO_2 (1.7 (0.49, 2.9), $p = 0.006$; 7.7 (3.2, 12.3), $p = 0.001$). $\Delta TSI_{BL\text{-}INC}$ was associated with steps and VO_2 but this difference was attenuated towards the null after adjustment for age, sex and ethnicity. $\Delta TSI_{BL\text{-}EE}$ was greater in women (3.4 (0.4, 8.9) versus 2.1 (0.3, 7.4), $p = 0.017$) and $\Delta TSI_{BL\text{-}INC}$ was lower in women versus men (2.4 (0.2, 10.2) versus 3.2 (0.2, 18.2), $p = 0.016$). These Local microvascular NIRS-measures are associated with exercise capacity in older adults and several measures can detect differences in microvascular reactivity between a community-based sample of men and women.

OPEN ACCESS

Edited by:
Giancarlo Condello, University of Parma, Italy

Reviewed by:
Ben Jones, University of Essex, United Kingdom
Yumie Ono, Meiji University, Japan

***Correspondence:**
Siana Jones
siana.jones@ucl.ac.uk

Specialty section:
This article was submitted to Exercise Physiology, a section of the journal Frontiers in Physiology

Received: *13 April 2022*
Accepted: *17 June 2022*
Published: *08 July 2022*

Citation:
Jones S, Tillin T, Williams S, Rapala A, Chaturvedi N and Hughes AD (2022) Skeletal Muscle Tissue Saturation Changes Measured Using Near Infrared Spectroscopy During Exercise Are Associated With Post-Occlusive Reactive Hyperaemia. Front. Physiol. 13:919754. doi: 10.3389/fphys.2022.919754

Keywords: near-infrared spectroscopy, skeletal muscle, reactive hyperaemia, exercise, microvascular

BACKGROUND

Reduced aerobic exercise capacity is a risk factor for future CVD morbidity and mortality. (Laukkanen et al., 2007; Kodama et al., 2009; Hamer et al., 2020). As adequate supply of oxygenated blood to skeletal muscle is one of the primary components of aerobic exercise capacity, measuring local haemodynamics in skeletal muscle during exercise has the potential to provide valuable insight into the oxygen transport pathway. However, assessment of skeletal muscle haemodynamics during exercise, particularly at the microvascular level, is challenging.

Near-infrared Spectroscopy (NIRS) offers a simple non-invasive technique that measures changes in oxygenated and deoxygenated haemoglobin and myoglobin (oxy-Hb & deoxy-Hb) and tissue saturation index (TSI) specifically from small blood vessels and myocytes. (Scholkmann et al., 2014). Development of NIRS technology into small, wireless devices permits measurements to be captured during exercise. A number of reports suggest that greater drops in TSI during exercise represent local impairment in oxygen delivery (Boezeman et al., 2016) and there is good evidence for the use of TSI in clinical setting for assessment of peripheral vascular diseases. (Bauer et al., 2004; Mesquita et al., 2013). However, NIRS has not yet been adopted in routine clinical practice and evidence investigating its sensitivity to detect differences in non-clinical population-based samples, particularly in older adults, is limited. Despite recognised sex differences in the pattern of cardiovascular aging, (Redfield et al., 2005; Chung et al., 2006) including a differential pathophysiology in development of heart failure that involves microvascular dysfunction in women, (Beale et al., 2018) NIRS has been under-employed in investigating these differences. (Jones et al., 2021a).

NIRS can also be applied during and following a cuff-induced arterial occlusion, the subsequent post occlusive reactive hyperaemia (PORH) can be quantified to provide fairly well established indices of microvascular reactivity. (Rosenberry and Nelson, 2020). The PORH reperfusion slope is associated with post-occlusive brachial artery blood flow. (Bopp et al., 2014). Strong evidence suggests the reperfusion slope is slower and time to peak recovery longer in the presence of peripheral arterial disease (PAD). (Cheatle et al., 1991; Kooijman et al., 1997; Chung et al., 2018). Surprisingly, a comparison of the outcomes derived from application of NIRS to assess TSI during exercise and its application during PORH has not previously been carried out. Furthermore, the TSI increase at initiation of exercise (oxy-Hb over-shoot), which has the potential to provide a crude indicator of vasodilatory capacity at initiation of exercise, is not widely described and limited prior work examining an 'overshoot' in oxy- or deoxy-Hb has used measurements derived from single distance NIRS devices which are unable to spatially resolve the signals. (Bowen et al., 19852012; Salzmann et al., 2021).

Therefore, the objectives of this study are: 1) to compare changes in skeletal muscle tissue saturation index (TSI) during exercise with indices of microvascular function captured during PORH 2) to determine if NIRS-derived measures of microvascular function are associated with exercise capacity in older adults, and 3) to compare skeletal muscle microvascular function in men versus women in a population-based sample of older adults.

METHODS

Participants

Participants were drawn from a population-based, tri-ethnic cohort study of older adults resident in West London, United Kingdom: the Southall and Brent Revisited (SABRE) study. (Tillin et al., 2012). Data presented in this study were collected at the 25–30 years follow-up visit (2015–2018). Participants were excluded from undertaking exercise tests according to co-morbidity contraindications given in the American College of Sports Medicine (ACSM) guidelines. (American College of Sports Medicine, 2018).

All procedures were in accordance with the principles of the Helsinki declaration, all participants gave written informed consent and the study was approved by the National Research Ethics Service (NRES) Committee London—North Fulham.

Anthropometrics and Questionnaires

Height was measured barefoot using a stadiometer (Seca 217; Seca, Hamburg, Germany). Weight was measured using digital bio-impedance scales (BC-418; Tanita, IL, United States). Adipose tissue thickness (ATT) overlaying the NIRS measurement site was measured using an ultrasound device (Vivid I; GE, Boston, MA, United States) fitted with a high frequency transducer (12L-RS; 6–13 MHz; GE).

Information on physical activity, smoking, history of cardiovascular disease (CVD), hypertension and medication use were obtained by questionnaire. Diabetes was defined as self-reported physician diagnosis, reported use of glucose-lowering medication or an elevated measurement of HbA_{1c} above the guideline cut-off value for diagnosis of type 2 diabetes (≥48 mmol/mol [>6.5%]) (Chung et al., 2018). HbA_{1c} was measured using an immunoassay (cobas HbA_{1c} test) on the Cobas c311 automated analyser (Roche Diagnostics, Burgess Hill, United Kingdom). Non-fasting blood samples were obtained in the morning of the clinic visit.

Aerobic Exercise Capacity and Blood Pressure and Arterial Saturation During Exercise

A sub-maximal, self-paced, 6-min stepper test (6MST) was performed. Participants were all given the same instructions for the 6MST: to start at a pace they felt they could continue at for 6 min with the objective of completing as many steps as possible within 6 min. Full details are presented elsewhere. (Jones et al., 2017). This has previously been validated in this age-group against walking pace and sub-maximal oxygen consumption

achieved in the 6 min walk test. (Jones et al., 2017). A portable expired gas analysis system including a Polar heart rate monitor (K4B2; COSMED, Rome, Italy) was used to measure breath-by-breath whole-body oxygen consumption ($\dot{V}O_2$) and heart rate during the 6MST. Exercise capacity was defined using 2 variables: 1) the number of steps achieved during the test and 2) the highest $\dot{V}O_2$ of a rolling 60 s average during exercise. The workload achieved during the test was estimated in Watts using methods previously described. (Jones et al., 2017).

Systolic and diastolic blood pressure (SBP and DBP) were measured during exercise using a specialist motion-tolerant blood pressure monitor (Tango M2 Stress Test Monitor, SunTech Medical, United States). Measurements were made one minute into the exercise test (during the second minute of exercise). Mean arterial pressure was calculated as *DBP+⅓(SBP-DBP)*.

Arterial saturation was measured from the finger throughout rest, exercise and recovery using a basic battery-powered clip-on pulse oximeter. This was checked periodically by the operator and the lowest value observed was recorded.

Near-Infrared Spectroscopy Measurements

For both exercise and the arterial occlusion, a NIRS device (Portamon, Artinis Medical Systems, Netherlands) (Grassi and Quaresima, 2016; Jones et al., 2016) was positioned on the lateral head of the gastrocnemius where the calf girth was greatest, orientation was standardized, the device was secured and covered completely using a neoprene sleeve. TSI was estimated using spatially solved spectroscopy. The device was set to sample at 10 Hz. The 6MST was performed as specified above. During recovery a rapid inflation cuff (Hokanson, SC10D/E20; Washington, United States) was placed on the thigh proximal to the location of NIRS measurement. A protocol of short transient arterial occlusions was performed for 3 min immediately following the exercise test (data presented elsewhere). (Jones et al., 2021b). The staff member conducting the measurement then observed the NIRS signals until the participant was fully recovered and a steady-state had been reached before the cuff was inflated to a supra-systolic pressure (>250 mmHg) to induce complete arterial occlusion for at least 2 min.

Analysis of NIRS data was conducted using custom written programs in MATLAB R2014a (MathWorks Inc.). TSI was averaged over 5 s at each measurement time point: at rest, at the peak of the initial increment at onset of exercise, at the minimum observed during exercise and at the end of exercise. (Boezeman et al., 2016). The difference between TSI at rest (baseline) and at the initial increment ($\Delta TSI_{BL\text{-}INC}$) was calculated as the increment minus the baseline value. The TSI change from baseline to the end of exercise ($\Delta TSI_{BL\text{-}EE}$) was calculated as the baseline value minus the value at the end of exercise. The TSI change from the increment to the minimum $\Delta TSI_{INC\text{-}MIN}$ was calculated as the increment value minus the minimum value. All values were presented as positive despite $\Delta TSI_{BL\text{-}EE}$ being a negative change.

Time to 50%, 95% and 100% peak PORH and area under the curve (AUC) for the PORH were calculated by following previously presented methods. (Bopp et al., 2014; Willingham et al., 2016). In short, all traces were inspected by eye, the point at which the cuff was released was identified from the oxy-Hb trace as the moment the first upward inflection point could be visualized and the peak response was identified as the maximum value captured within 2 min from cuff release. The change in oxy-Hb from the start to the end of the PORH (ΔOxyHb) was calculated as the peak value minus the start value (**Figure 1**). Because the response to ischaemia is time-sensitive, we used single values rather than a 5-s average. The recovery rate was calculated as 1 divided by the time to 100% peak PORH. The oxy-Hb and TSI signals were not smoothed prior to post-processing analysis and all analysis was done by a single observer.

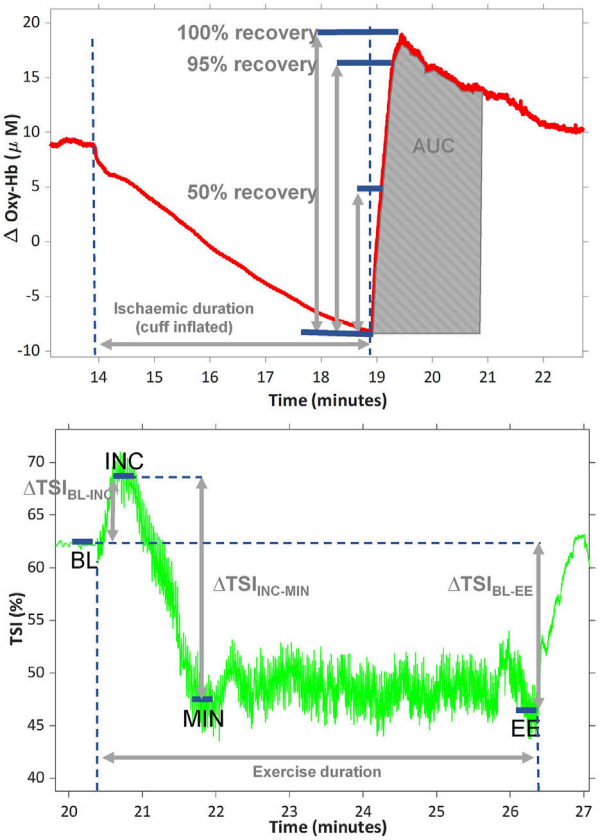

FIGURE 1 | representative traces showing the change in oxygenated haemoglobin (oxy-Hb) during ischaemia and post occlusive reactive hyperaemia (PORH) (top) and change in tissue saturation index (TSI%) during exercise (bottom). Area under the curve (AUC) was calculated after normalising the start of PORH to zero. TSI was averaged over 5 s at baseline (BL), at the peak of the initial increment at onset of exercise (INC), at the minimum observed during exercise (MIN) and at the end of exercise (EE). $\Delta TSI_{BL\text{-}INC}$ is the difference between TSI at BL and INC; $\Delta TSI_{BL\text{-}EE}$ is the TSI change from BL-EE; $\Delta TSI_{INC\text{-}MIN}$ is the TSI change from INC to MIN. All values are presented as positive values, despite $\Delta TSI_{BL\text{-}EE}$ being a negative change.

Statistical Methods

Statistical analysis was carried out in STATA 17 (StataCorp College Station, TX, United States). Categorical data are

presented as frequency (%). Continuous data were examined for normality; normally distributed sample data are summarised as means ± SD and skewed data as medians (interquartile range). Comparison of participant characteristics by sex was done using an unpaired Student's *t* test for normally distributed continuous data, χ^2 test for categorical data and a Wilcoxon Rank Sum test for skewed data (ATT).

Associations between exposures and outcomes are presented as unadjusted (unadj.) and adjusted (adj.) β-coefficients. Model 1a (M1a) is adjusted for confounders: age, sex and ethnicity and for the estimated workload achieved during the stepping test as an auxiliary co-variate. Model 1b (M1b) is adjusted for age, sex, ethnicity and mean arterial pressure (MAP) change at the start of exercise to account for the change in driving pressure at initiation of exercise. Models where indices of PORH are included as exposures are additionally adjusted for height, as an auxiliary co-variate to account for differences in hydrostatic pressure between participants and for the duration of the ischaemic stimulus.

RESULTS

Participant Characteristics

In total, 711 participants who attended the SABRE visit 3 clinic undertook the 6-min stepper test and, of these, 558 participants underwent NIRS measures of TSI during exercise (mean age±SD: 73 ± 7years, 59% male). It was not possible to fit the NIRS-device to the lower leg in 153 participants due to either tight fitting clothing, broken or sensitive skin or because the participant declined to have the device fitted. In a sub-set of 149 participants, a leg cuff was fitted to the upper leg and participants were able to tolerate a ≥2 min arterial occlusion.

Participant characteristics are provided in **Table 1** stratified by men and women for all participants and for the PORH sub-group only. By design the SABRE study recruited more men than women. (Tillin et al., 2012). On average, women were younger, had a higher BMI and a thicker layer of adipose over the measurement site and achieved lower exercise capacity.

ΔTSI During 6MST Versus Post-Occlusive Reactive Hyperaemia Measurements

Greater changes in TSI from rest to the end of exercise ($\Delta TSI_{BL\text{-}EE}$) indicate larger drops in TSI during exercise. A positive association was observed between the time to recovery during PORH and $\Delta TSI_{BL\text{-}EE}$, such that slower times to recovery (time to 95% and 100% PORH) were associated with larger drops in TSI (**table 2**). Coefficients were similar after adjusting for co-variates in model 1a (**table 2**). The overall recovery rate during PORH (1/time to 100% PORH) was negatively associated with $\Delta TSI_{BL\text{-}EE}$. AUC and ΔOxy-Hb during PORH were positively associated with $\Delta TSI_{BL\text{-}EE}$. Adjustment for co-variates did not alter these associations (**table 2**).

PORH recovery times and rate were not associated with the change in TSI from the increment to the minimum value ($\Delta TSI_{INC\text{-}MIN}$). AUC and ΔOxy-Hb during PORH were positively associated with $\Delta TSI_{INC\text{-}MIN}$ and adjustment for co-variates did not alter these associations (**table 2**).

PORH recovery times (time to 50%, 95% and 100% PORH) were negatively associated with the change in TSI from rest to the initial increment ($\Delta TSI_{BL\text{-}INC}$), these associations were similar even after adjustment for co-variates including the change in MAP at the start of exercise (**table 2**). The rate of PORH recovery was positively associated with $\Delta TSI_{BL\text{-}INC}$, but this association was attenuated by over half after adjustment for co-variates. AUC and ΔOxy-Hb during PORH were positively associated with $\Delta TSI_{BL\text{-}INC}$ (**table 2**).

Exercise Capacity and Post-Occlusive Reactive Hyperaemia

PORH recovery times were negatively associated with steps and VO_2 achieved during the 6MST. These associations were largely explained by co-variates age, sex and ethnicity (**table 3**). Recovery rate, AUC and ΔOxy-Hb were all positively associated with steps and VO_2 achieved during the 6MST. The associations between AUC and ΔOxy-Hb with steps achieved were only partially explained by co-variates (**Table 3**).

TABLE 1 | Participant characteristics stratified by sex. Values are mean ± SD or median (inter-quartile range) for the whole study group and those who undertook an ischaemic occlusion. ATT, adipose tissue thickness at the NIRS measurement site, BMI, body mass index, CVD, cardiovascular disease, ethnicity is E, European; SA, South Asian ; AFC, African Caribbean or OT, Other; T2DM, type-2 diabetes mellitus.

Characteristic	Mean ± SD or median (IQR) or *n(%)*					
	All (*n* = 558)			Sub-group (*n* = 149)		
	Women (*n* = 231)	Men (*n* = 327)	*p*	Women (*n* = 42)	Men (*n* = 107)	*p*
Age (years)	71 ± 6	75 ± 6	*<0.001*	71 ± 5	75 ± 6	*<0.001*
Ethnicity, *n* (E, SA, AFC, OT)	92,54,80,5	156,117,54,0	*<0.001*	18,9,14,1	43,50,14,0	*0.003*
BMI (kg/m^2)	28.3 ± 4.9	27.2 ± 3.6	*0.004*	26.1 ± 4.1	26.6 ± 3.1	*0.481*
ATT (cm) (*n = 492*)	0.90 (0.71, 1.2)	0.53 (0.41, 0.67)	*<0.001*	0.78 (0.62, 1.09)	0.51 (0.40, 0.62)	*<0.001*
T2DM *n* (%)	51 (22)	75 (23)	*0.057*	5 (12)	26 (24)	*0.094*
CVD *n* (%) (*n = 539*)	13 (6)	57 (18)	*<0.001*	4 (10)	22 (21)	*0.135*
Steps achieved	190 ± 73	227 ± 78	*<0.001*	216 ± 65	238 ± 76	*0.073*
VO_2 achieved (ml/kg/min) (*n = 495*)	14.7 ± 3.8	17.1 ± 4.4	*<0.001*	16.8 ± 3.6	17.9 ± 4.2	*0.125*
Occlusion duration (s)	-	-	-	208 ± 77	211 ± 66	*0.830*
Arterial saturation <95% during exercise *n* (%) (*n = 446*)	16 (8.3)	15 (6.0)	*0.345*	3 (8.6)	4 (4.6)	*0.393*

TABLE 2 | Associations between TSI, tissue saturation index; changes during exercise and indices of post-occlusive reactive hyperaemia (PORH); measured in the lower-limb skeletal muscle. ΔTSI_{BL-EE} is the change in tissue saturation index (TSI); between rest (baseline, BL) and the EE, end of exercise ; $\Delta TSI_{INC-MIN}$ is the change in TSI from it is highest point at the INC, increment; to it is MIN, minimum; ΔTSI_{BL-INC} is the change in TSI from the BL to the highest point (INC). unadj, Unadjusted; and adjusted β-coefficients, 95% confidence intervals and *p*-values are presented for each association. M1a, Model 1a; is adjusted for age, sex, ethnicity, the duration of the ischaemic stimulus and the estimated workload achieved during the stepping test. M1b, Model 1b; is adjusted for age, sex, ethnicity and the duration of the ischaemic stimulus. M2, Model 2; is adjusted for age, sex, ethnicity, mean arterial pressure (MAP); change at the start of exercise.

	B-coefficient (95%CI) ***p-value***						
	ΔTSI_{BL-EE}		**$\Delta TSI_{INC-MIN}$**		**ΔTSI_{BL-INC}**		
NIRS measure of PORH	**Unadj. (*n* = 149)**	**M1a (*n* = 149)**	**Unadj. (*n* = 149)**	**M1a (*n* = 149)**	**Unadj. (*n* = 129)**	**M1b (*n* = 129)**	**M2 (*n* = 129)**
Time to 50% PORH (s)	0.20 (–0.09, 0.49) *0.169*	0.14 (–0.17, 0.44) *0.366*	0.06 (–0.25, 0.36) *0.720*	–0.01 (–0.33, 0.31) *0.935*	–0.25 (–0.42, 0.07) *0.006*	–0.19 (–0.37, 0.006) 0.043	–0.18 (–0.36, 0.005) *0.056*
Time to 95% PORH (s)	0.09 (0.008, 0.17) *0.031*	0.08 (–0.01, 0.17) *0.085*	0.02 (–0.07, 0.10) *0.683*	–0.003 (–0.09, 0.10) *0.945*	–0.09 (–0.13, 0.04) *0.001*	–0.07 (–0.12, 0.02) 0.009	–0.07 (–0.12, 0.02) *0.012*
Time to 100% PORH (s)	0.05 (0.01, 0.08) *0.009*	0.05 (0.01, 0.09) *0.012*	–0.002 (–0.04, 0.04) *0.937*	0.003 (–0.04, 0.04) *0.903*	–0.04 (–0.06, 0.02) *0.001*	–0.03 (–0.05, 0.004) 0.024	–0.03 (–0.05, 0.003) *0.028*
Recovery rate PORH (1/s)	–47 (–81, 13) *0.006*	–47 (–85, 9.9) *0.014*	–11 (–48, 25) *0.538*	–9.8 (–49.6, 29.9) *0.626*	20 (–0.88, 40.7) *0.060*	8.3 (–14, 31) 0.468	7.2 (–15.4, 29.9) *0.530*
(log)AUC PORH (μM x s)	1.6 (0.62, 2.6) *0.002*	1.7 (0.62, 2.8) *0.002*	1.5 (0.45, 2.5) *0.005*	1.6 (0.45, 2.7) *0.007*	0.68 (0.06, 1.3) *0.032*	0.80 (0.14, 1.5) 0.018	0.85 (0.18, 1.5) *0.013*
ΔOxyHb PORH (μM)	0.05 (0.02, 0.10) *0.042*	0.04 (0.002, 0.108) *0.041*	0.08 (0.03, 0.13) *0.003*	0.08 (0.03, 0.13) *0.004*	0.06 (0.03, 0.09) *<0.001*	0.06 (0.02, 0.07) 0.001	0.05 (0.02, 0.09) *0.001*

TABLE 3 | Associations between exercise capacity measures (steps achieved and measured VO_2) and indices of post-occlusive reactive hyperaemia (PORH); or tissue saturation index (TSI); changes during exercise measured in the lower-limb. ΔTSI_{BL-EE} is the change in TSI, between rest (baseline, BL) and the end of exercise (EE); $\Delta TSI_{INC-MIN}$ is the change in TSI from its highest point at the INC, increment; to its MIN, minimum; ΔTSI_{BL-INC} is the change in TSI from the BL to the highest point (INC).unadj, Unadjusted; and adjusted β-coefficients, 95% confidence intervals and *p*-values are presented for each association. M1, Model 1; is adjusted for age, sex and ethnicity. Associations between PORH measures and exercise capacity were also adjusted for height and ischaemic duration in M1. *indicates models also adjusted for estimated workload (W).

NIRS measures	**Exercise capacity measured β-coefficient (95%CI)**			
	Steps achieved		**VO_2 achieved (ml/min)**	
	Unadj	**M1**	**Unadj**	**M1**
	n = 153	***n = 153***	***n = 148***	***n = 148***
Time to 50% PORH (s)	–5.3 (–10.0,-0.66) *0.026*	–2.7 (–7.1.1.7) *0.221*	–21.9 (–44.8.1.0) *0.061*	–6.2 (–25.7.13.2) *0.528*
Time to 95% PORH (s)	–1.3 (–2.6.0.04) *0.056*	–0.42 (–1.7.0.87) *0.525*	–6.1 (–12.5.0.36) *0.064*	–0.54 (–6.3.5.2) *0.852*
Time to 100% PORH (s)	–0.29 (–0.86.0.28) *0.315*	0.11 (-0.48.0.70) *0.709*	–1.3 (–4.1.1.4) *0.339*	1.1 (–1.5.3.7) *0.406*
Recovery rate PORH (1/s)	699 (140,1259) *0.015*	306 (–235,848) *0.266*	3835 (1127,6542) *0.006*	1383 (–1016,3782) *0.256*
AUC PORH (μM x s)	20.8 (4.8.36.7) *0.011*	18.0 (2.3.33.7) *0.025*	90.8 (12.0,169.6) *0.024*	22.5 (–48.2.93.1) *0.531*
ΔOxyHb PORH (μM)	1.3 (0.46.2.1) *0.002* *n = 558*	0.86 (0.10.1.6) *0.027* *n = 558*	4.4 (0.21.8.7) *0.040* *n = 495*	–0.13 (–3.8.3.5) *0.944* *n = 495*
ΔTSI_{BL-EE}	4.1 (2.6.5.6) *<0.001*	1.7 (0.49.2.9) *0.006**	24.7 (17.8.31.7) *<0.001*	7.7 (3.2.12.3) *0.001**
$\Delta TSI_{INC-MIN}$	3.6 (1.9.5.2) *<0.001* *n = 478*	2.5 (1.3.3.8) *<0.001** *n = 478*	16.4 (8.7.24.1) *<0.001* *n = 427*	6.6 (1.9.11.3) *0.006** *n = 427*
ΔTSI_{BL-INC}	2.8 (0.14.5.4) *0.039*	–1.2 (-3.6.1.3) *0.352*	24.0 (11.8.36.1) *<0.001*	1.7 (-9.3.12.7) *0.764*
ΔTSI_{BL-INC} Adj. ΔMAP	2.9 (0.22.5.5) *0.034*	–1.1 (–3.5.1.3) *0.381*	24.9 (13.0.36.9) *<0.001*	2.2 (–8.5.12.8) *0.687*

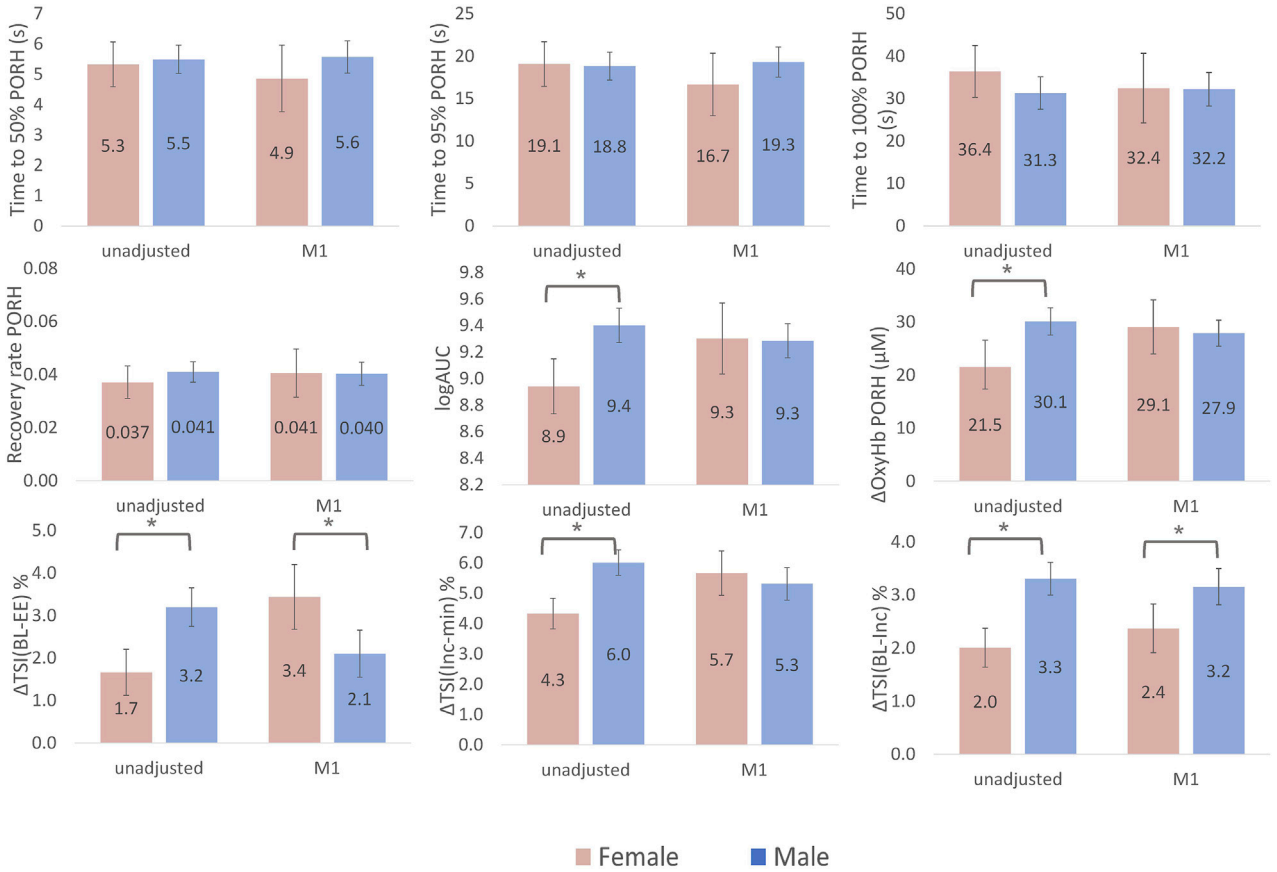

FIGURE 2 | Sex differences in NIRS-measured skeletal muscle microvascular response to cuff-induced ischaemia and exercise. Bars represent marginal means for female (pink) and male (blue). Error bars are 95% confidence intervals. $\Delta TSI_{BL\text{-}EE}$ is the change in tissue saturation index (TSI) between rest (baseline, BL) and the end of exercise (EE); $\Delta TSI_{INC\text{-}MIN}$ is the change in TSI from it is highest point at the increment (INC) to it is minimum (MIN); $\Delta TSI_{BL\text{-}INC}$ is the change in TSI from the BL to the highest point (INC). Area under the curve (AUC) had a skewed distribution and so log transformed values are presented. Model 1 (M1) is adjusted for age, ethnicity, adipose tissue thickness (ATT), height, ischaemic duration and presence of type 2 Diabetes and cardiovascular disease. The change in tissue saturation index (ΔTSI) from baseline to end of exercise (BL-EE) and ΔTSI from increment to minimum (Inc-min) were additionally adjusted for workload achieved during exercise and the ΔTSI from baseline to the initial increment (BL-Inc) was additionally adjusted for change in mean arterial pressure at the beginning of exercise in model 1.

$\Delta TSI_{BL\text{-}EE}$ and $\Delta TSI_{INC\text{-}MIN}$ were positively associated with exercise capacity outcomes, these associations were only partially explained by co-variates age, sex and ethnicity (**table 3**). $\Delta TSI_{BL\text{-}INC}$ was positively associated with both exercise capacity outcomes, these associations were largely explained by co-variates age, sex and ethnicity, however, adjustment for ΔMAP at the start of exercise did not affect β-coefficients (**table 3**).

Time to 50%, 95% and 100% recovery during PORH and the overall recovery rate were not different in men versus women (**Figure 2**). The AUC and Δoxy-Hb were smaller in women versus men, however, both differences were explained by adjustment for co-variates (age, ethnicity, ATT, T2DM and CVD). $\Delta TSI_{BL\text{-}EE}$ was 1.5% greater in men versus women, however, after adjustment for co-variates (including estimated workload achieved during stepping), this difference was reversed to a 1.3% greater change in women (**Figure 2**). A similar pattern was observed for $\Delta TSI_{INC\text{-}MIN}$ but values were similar between men and women after adjustment. $\Delta TSI_{BL\text{-}INC}$ was 1.3% greater in men versus women, this difference persisted after adjusting for co-variates (**Figure 2**).

DISCUSSION

This study presents evidence that improved microvascular reactivity in response to ischaemia is associated with greater increments in TSI pattern at initiation of exercise and smaller overall drops in TSI during exercise. In addition, we show that these local microvascular measures are associated with exercise capacity in older adults and that differences between men and women enrolled in a population-based cohort can be detected using NIRS.

Exercise Deoxygenation and Post-Occlusive Reactive Hyperaemia

For the first time, we describe a relationship between greater skeletal muscle deoxygenation from the start to the end of exercise (greater

$\Delta TSI_{BL\text{-}EE}$ values) and blunted (slower) PORH recovery rates. Previously, greater deoxygenation during exercise has been described in various conditions of vascular dysfunction, (Bauer et al., 2004; Boezeman et al., 2016) including PAD (Bauer et al., 2004; Vardi and Nini, 2008; Mesquita et al., 2013) and chronic lower limb compartment syndrome. (van den Brand et al., 2005). A blunted reactive hyperaemia, irrespective of measurement method, is widely accepted as a measure of impaired vascular function (Rosenberry and Nelson, 2020) and predictor of future cardiovascular events. (Anderson et al., 2011). NIRS has previously been applied to assessed PORH and measures found to be impaired in patients with PAD, (Kragelj et al., 2001) various other clinical populations (Doerschug et al., 2007; Mayeur et al., 2011) and in old, compared to young, adults. (Rosenberry et al., 2018). As both response to exercise and PORH response measures are thought to represent a haemodynamic insufficiency, our finding that these measures are associated was expected. We did not observe statistically significant associations between $\Delta TSI_{BL\text{-}EE}$ and time to 50% PORH and the association between $\Delta TSI_{BL\text{-}EE}$ and time to 95% PORH was attenuated after adjustment for co-variates. This could be due to different physiological components underpinning the initial versus the final stages of the PORH response curve. However, these associations were positive and the β-coefficient for time to 95% PORH was only marginally altered after adjustment which is in line with the robust associations we observed between $\Delta TSI_{BL\text{-}EE}$ and time to 100% PORH, recovery rate, AUC and Δoxy-Hb. Further work is necessary to establish if the initial fast PORH response versus the slow response differ in their relationship with skeletal muscle deoxygenation during exercise.

Conversely, the TSI change from its highest point (the initial increment) to its lowest ($\Delta TSI_{INC\text{-}MIN}$) was only associated with AUC and ΔOxyHb derived from PORH. The lack of association between $\Delta TSI_{INC\text{-}MIN}$ and the PORH recovery rate and times, could be due to this parameter also encompassing the change in TSI at initiation of exercise ($\Delta TSI_{BL\text{-}INC}$) which may have amplified $\Delta TSI_{INC\text{-}MIN}$ if there were favourable vasodilatory response at initiation of exercise.

We speculate that larger $\Delta TSI_{BL\text{-}INC}$ values indicate better peripheral vasodilatory capacity at exercise onset. We observed strong associations between the change in TSI at initiation of exercise and PORH measures. Larger values of $\Delta TSI_{BL\text{-}INC}$ were associated with faster PORH recovery times suggesting this novel parameter is closely related to an appropriate haemodynamic response to demand for oxygenated blood. Adjustment for the change in MAP at the start of exercise, to account for the increased driving pressure, did not alter associations, it is therefore likely that greater values of $\Delta TSI_{BL\text{-}INC}$ indicate adequate perfusion, or perhaps over-perfusion, in response to the increase in metabolic demand within skeletal muscle at the onset of exercise. As this was a sub-maximal, self-paced exercise test, it is unlikely that participants would have initiated exercise at a workload near to their maximum, therefore maximum circulatory capacity would not have been achieved and over-perfusion would be possible. Future research is necessary to verify these findings and $\Delta TSI_{BL\text{-}INC}$ merits investigation in clinical studies in order to determine threshold values that could inform on peripheral haemodynamic insufficiency.

Exercise Capacity

Blunted skeletal muscle oxygen kinetics during PORH were associated with poorer exercise capacity, both in terms of steps completed and VO_2 achieved. Adjustment for co-variates, age, sex and ethnicity attenuated these estimates towards the null which is expected given the known decline in microvascular function with age. However, the associations between AUC, ΔOxyHb and steps remained statistically significant after adjustment for co-variates. This is in line with previous findings linking microvascular reactivity and physical activity levels. (Montero et al., 2015; Lanting et al., 2017). However, this association has not previously been described using NIRS-measured PORH. Previous studies typically investigate downstream PORH using venous occlusion plethysmography or laser-Doppler. While these techniques inform us on 1) the overall blood influx to the whole of the lower limb (plethysmography) and 2) the response within the cutaneous circulation (laser Doppler), NIRS provides assessment of changes specifically in microvasculature and, typically, a large portion of the signal is from skeletal muscle. Therefore, our findings highlight the importance of developing complementary methods of assessing skeletal muscle.

Deoxygenation across exercise ($\Delta TSI_{BL\text{-}EE}$) was positively associated with exercise capacity measures. However, the use of $\Delta TSI_{BL\text{-}EE}$ to assess microvascular function in the context of the self-paced exercise test carried out here is limited because this association is heavily confounded by the effect of the achieved workload during exercise. After adjustment for estimated workload, effect sizes were attenuated by half for steps completed and nearly 3 times for VO_2 achieved. The change in TSI at exercise onset, $\Delta TSI_{BL\text{-}INC}$, is likely to be less dependent of workload achieved and has not previously been explored in the context of microvascular function and exercise capacity. These results show positive associations between $\Delta TSI_{BL\text{-}INC}$ and both exercise capacity outcomes suggesting that improved vasodilatory capacity in the microvasculature of skeletal muscle is associated with improved exercise capacity. Adjustment for ΔMAP at the start of exercise did not affect β-coefficients.

Sex Differences in Microvascular Reactive Hyperaemia in Older Adults

During PORH, only AUC and Δoxy-Hb differed by sex, with smaller values in women suggesting reduced microvascular reactivity. Although the time to 100% recovery and the recovery rate were slightly faster in men, these differences did not reach statistical significance. Our findings are in line with two previous studies that detected more rapid and greater magnitude of downstream reactive hyperaemia in men versus women using NIRS. (Fellahi et al., 2014; Rasica et al., 2022). These studies enrolled young healthy individuals and were unable to adjust for confounding factors, such as ATT, due to small sample sizes. The differences presented here were largely explained by adjustment for co-variates (age, ethnicity, ATT, T2DM and CVD). Studies investigating sex-differences in the upstream response to ischaemia, examined using flow-mediated dilatation (FMD), have yielded conflicting results. (Levenson et al., 2001).

Inconsistencies are thought to be related to confounding from the differences in vessel diameter at rest by sex. This further highlights the importance of developing additional complementary techniques that directly assess downstream reactive hyperaemia.

Deoxygenation during exercise was lower in women when differences were unadjusted, however, after adjustment (Model 1) deoxygenation was greater in women. Adjusting for the workload achieved during exercise and ATT contributed to this reversal of effect as men achieved a higher estimated workload during exercise (a contributor towards greater deoxygenation) and women had greater ATT. Greater ATT can attenuate the signal from skeletal muscle resulting the appearance of less deoxygenation. The $\Delta TSI_{BL\text{-}INC}$ was greater in men than women despite adjustment for all co-variates. Together this pattern of tissue oxygenation change during exercise suggests that, in older adults, women have a reduced vasodilatory capacity at the start of exercise and haemodynamic insufficiency at the microvascular level throughout exercise. This finding is in line with previously described sex differences in the pattern of cardiovascular aging at the population level. (Redfield et al., 2005; Chung et al., 2006). The higher prevalence of heart failure with preserved ejection fraction in ageing women versus men is thought to be underpinned by, among other things, greater microvascular dysfunction. (Beale et al., 2018). Early detection of dysfunction within skeletal muscle could lead to a more targeted intervention to mitigate risk in women.

Study Limitations

We used a self-paced exercise test to measure exercise capacity in our older adult population. As workload was not controlled, we cannot be certain that changes in TSI measured during exercise were not due to self-selected higher workloads and we cannot be sure participants did not change the rate they were stepping at throughout the test. However, we endeavoured to address this via adjustment of statistical models for an estimate of the workload achieved. Furthermore, activities of daily living rarely occur at peak exercise capacity, therefore, a self-paced exercise stimulus may provide more appropriate insight into daily exercise limitations in older adults compared to traditional graded exercise tests. The occlusion duration used to apply ischaemic changes was variable between participants. We targeted a 5-min duration in all participants but found that this duration was poorly tolerated in our study population. We report ischemic duration in table one and show no difference between men and women, we also adjusted statistical models for the duration of the ischaemic stimulus. Furthermore, previous work suggests that above a threshold stimulus of 1.5 min of cuff occlusion there is an association between flow and vessel dilatation as measured by FMD. (Leeson et al., 1997). we therefore selected an arterial occlusion >2 min as our threshold for inclusion in results and present an average tolerated duration of ~3.5 min which is well above this threshold.

CONCLUSION

This study suggests that NIRS-derived PORH parameters and the pattern of TSI change measured during exercise offer a simple approach to evaluation of microvascular function. Furthermore, these methods are both sensitive enough to detect sex differences in the skeletal muscle microvasculature of ageing populations. Developing methods that capture local changes from skeletal muscle is an important step towards understanding the reduction in exercise capacity with age and detection of early, pre-clinical changes which may lead to onset of cardiovascular disease.

DATA AVAILABILITY STATEMENT

The raw data supporting the conclusions of this article will be made available by the authors, without undue reservation.

ETHICS STATEMENT

The studies involving human participants were reviewed and approved by The study was approved by the National Research Ethics Service (NRES) Committee London-North Fulham. The ethics committee waived the requirement of written informed consent for participation.

AUTHOR CONTRIBUTIONS

All authors contributed to study design, data interpretation, and revision of the manuscript. All authors approved the final version and agree to be accountable for the work, taking responsibility for the integrity of the data and the accuracy of the data analysis. SJ collected and processed data, performed the statistical analysis and drafted the initial manuscript. SW collected and processed data and reviewed the manuscript. TT and AR were involved in study design, data collection and reviewing all methods and manuscripts. NC and AH are the principal investigators of the SABRE study and contributed to all aspects of study design and revision of analysis and results.

FUNDING

This work was supported by the Wellcome Trust (grant numbers 067100, 60337055891 and 086676/7/08/Z), the British Heart Foundation (grant numbers PG/06/145, PG/08/103/26133, PG/12/29/29497 and CS/13/1/30327) and Diabetes United Kingdom (grant number 13/0004774). The study team also acknowledges the support of the National Institute of Health Research Clinical Research Network. NC and ADH work in a unit that receives support from the United Kingdom Medical Research Council (grant number MC_UU_12019/1). The authors have no conflicts of interest to declare.

ACKNOWLEDGMENTS

We are extremely grateful to all the people who took part in the SABRE study and past and present members of the SABRE team who helped to collect the data.

REFERENCES

American College of Sports Medicine (2018). *ACSM's Guidelines for Exercise Testing and Prescription*. Tenth edition. Philadelphia: Wolters Kluwer. xxx, 472.

Anderson, T. J., Charbonneau, F., Title, L. M., Buithieu, J., Rose, M. S., Conradson, H., et al. (2011). Microvascular Function Predicts Cardiovascular Events in Primary Prevention: Long-Term Results from the Firefighters and Their Endothelium (FATE) Study. *Circulation* 123 (2), 163–169. doi:10.1161/CIRCULATIONAHA.110.953653

Bauer, T. A., Brass, E. P., and Hiatt, W. R. (2004). Impaired Muscle Oxygen Use at Onset of Exercise in Peripheral Arterial Disease. *J. Vasc. Surg.* 40 (3), 488–493. doi:10.1016/j.jvs.2004.06.025

Beale, A. L., Meyer, P., Marwick, T. H., Lam, C. S. P., and Kaye, D. M. (2018). Sex Differences in Cardiovascular Pathophysiology. *Circulation* 138 (2), 198–205. doi:10.1161/circulationaha.118.034271

Boezeman, R. P. E., Moll, F. L., Ünlü, Ç., and de Vries, J.-P. P. M. (2016). Systematic Review of Clinical Applications of Monitoring Muscle Tissue Oxygenation with Near-Infrared Spectroscopy in Vascular Disease. *Microvasc. Res.* 104, 11–22. doi:10.1016/j.mvr.2015.11.004

Bopp, C. M., Townsend, D. K., Warren, S., and Barstow, T. J. (2014). Relationship between Brachial Artery Blood Flow and Total [hemoglobin+myoglobin] during Post-occlusive Reactive Hyperemia. *Microvasc. Res.* 91, 37–43. doi:10.1016/j.mvr.2013.10.004

Bowen, T. S., Cannon, D. T., Murgatroyd, S. R., Birch, K. M., Witte, K. K., and Rossiter, H. B. (19852012). The Intramuscular Contribution to the Slow Oxygen Uptake Kinetics during Exercise in Chronic Heart Failure Is Related to the Severity of the Condition. *J. Appl. Physiol. (1985)* 112 (3), 378–387. doi:10.1152/japplphysiol.00779.2011

Cheatle, T. R., Potter, L. A., Cope, M., Delpy, D. T., Coleridge Smith, P. D., and Scurr, J. H. (1991). Near-infrared Spectroscopy in Peripheral Vascular Disease. *Br. J. Surg.* 78 (4), 405–408. doi:10.1002/bjs.1800780408

Chung, A. K., Das, S. R., Leonard, D., Peshock, R. M., Kazi, F., Abdullah, S. M., et al. (2006). Women Have Higher Left Ventricular Ejection Fractions Than Men Independent of Differences in Left Ventricular Volume. *Circulation* 113 (12), 1597–1604. doi:10.1161/circulationaha.105.574400

Chung, S., Rosenberry, R., Ryan, T. E., Munson, M., Dombrowsky, T., Park, S., et al. (2018). Near-infrared Spectroscopy Detects Age-Related Differences in Skeletal Muscle Oxidative Function: Promising Implications for Geroscience. *Physiol. Rep.* 6 (3). doi:10.14814/phy2.13588

Doerschug, K. C., Delsing, A. S., Schmidt, G. A., and Haynes, W. G. (2007). Impairments in Microvascular Reactivity Are Related to Organ Failure in Human Sepsis. *Am. J. Physiol. Heart Circ. Physiol.* 293 (2), H1065–H1071. doi:10.1152/ajpheart.01237.2006

Fellahi, J. L., Butin, G., Zamparini, G., Fischer, M-O., Gérard, J-L., Hanouz, J-L., et al. (2014). Lower Limb Peripheral NIRS Parameters during a Vascular Occlusion Test: an Experimental Study in Healthy Volunteers. *Ann. Fr. Anesth. Reanim.* 33, e9–14. doi:10.1016/j.annfar.2013.11.014

Grassi, B., and Quaresima, V. (2016). Near-infrared Spectroscopy and Skeletal Muscle Oxidative Functionin Vivoin Health and Disease: a Review from an Exercise Physiology Perspective. *J. Biomed. Opt.* 21 (9), 091313. doi:10.1117/1.jbo.21.9.091313

Hamer, M., O'Donovan, G., Batty, G. D., and Stamatakis, E. (2020). Estimated Cardiorespiratory Fitness in Childhood and Cardiometabolic Health in Adulthood: 1970 British Cohort Study. *Scand. J. Med. Sci. Sports* 30 (5), 932–938. doi:10.1111/sms.13637

Jones, S. A.-O., Schultz, M. G., Tillin, T., Park, C., Williams, S., Chaturvedi, N., et al. (2021). Sex Differences in the Contribution of Different Physiological Systems to Physical Function in Older Adults. *Geroscienc* 43 (1), 443–455. doi:10.1007/s11357-021-00328-y

Jones, S., Chiesa, S. T., Chaturvedi, N., and Hughes, A. D. (2016). Recent Developments in Near-Infrared Spectroscopy (NIRS) for the Assessment of Local Skeletal Muscle Microvascular Function and Capacity to Utilise Oxygen. *Artres* 16, 25–33. doi:10.1016/j.artres.2016.09.001

Jones, S., Schultz, M. G., Tillin, T., Park, C., Williams, S., Chaturvedi, N., et al. (2021). Sex Differences in the Contribution of Different Physiological Systems to Physical Function in Older Adults. *Geroscience* 43 (1), 443–455. doi:10.1007/s11357-021-00328-y

Jones, S., Tillin, T., Williams, S., Coady, E., Chaturvedi, N., Hughes, A. D., et al. (2017). Assessment of Exercise Capacity and Oxygen Consumption Using a 6 Min Stepper Test in Older Adults. *Front. Pharmacol.* 8, 408. doi:10.3389/fphys.2017.00408

Kodama, S., Saito, K., Tanaka, S., Maki, M., Yachi, Y., Asumi, M., et al. (2009). Cardiorespiratory Fitness as a Quantitative Predictor of All-Cause Mortality and Cardiovascular Events in Healthy Men and Women. *JAMA* 301 (19), 2024–2035. doi:10.1001/jama.2009.681

Kooijman, H. M., Hopman, M. T. E., Colier, W. N. J. M., van der Vliet, J. A., and Oeseburg, B. (1997). Near Infrared Spectroscopy for Noninvasive Assessment of Claudication. *J. Surg. Res.* 72 (1), 1–7. doi:10.1006/jsre.1997.5164

Kragelj, R., Jarm, T., Erjavec, T., Prešern-Štrukelj, M., and Miklavčič, D. (2001). Parameters of Postocclusive Reactive Hyperemia Measured by Near Infrared Spectroscopy in Patients with Peripheral Vascular Disease and in Healthy Volunteers. *Ann. Biomed. Eng.* 29 (4), 311–320. doi:10.1114/1.1359451

Lanting, S. M., Johnson, N. A., Baker, M. K., Caterson, I. D., and Chuter, V. H. (2017). The Effect of Exercise Training on Cutaneous Microvascular Reactivity: A Systematic Review and Meta-Analysis. *J. Sci. Med. Sport* 20 (2), 170–177. doi:10.1016/j.jsams.2016.04.002

Laukkanen, J. A., Rauramaa, R., Salonen, J. T., and Kurl, S. (2007). The Predictive Value of Cardiorespiratory Fitness Combined with Coronary Risk Evaluation and the Risk of Cardiovascular and All-Cause Death. *J. Intern Med.* 262 (2), 263–272. doi:10.1111/j.1365-2796.2007.01807.x

Leeson, P., Thorne, S., Donald, A., Mullen, M., Clarkson, P., and Deanfield, J. (1997). Non-invasive Measurement of Endothelial Function: Effect on Brachial Artery Dilatation of Graded Endothelial Dependent and Independent Stimuli. *Heart* 78 (1), 22–27. doi:10.1136/hrt.78.1.22

Levenson, J., Pessana, F., Gariepy, J., Armentano, R., and Simon, A. (2001). Gender Differences in Wall Shear-Mediated Brachial Artery Vasoconstriction and Vasodilation. *J. Am. Coll. Cardiol.* 38 (6), 1668–1674. doi:10.1016/s0735-1097(01)01604-7

Mayeur, C., Campard, S., Richard, C., and Teboul, J.-L. (2011). Comparison of Four Different Vascular Occlusion Tests for Assessing Reactive Hyperemia Using Near-Infrared Spectroscopy. *Crit. care Med.* 39 (4), 695–701. doi:10.1097/ccm.0b013e318206d256

Mesquita, R. C., Putt, M. E., Chandra, M., Yu, G., Xing, X., Han, S. W., et al. (2013). Diffuse Optical Characterization of an Exercising Patient Group with Peripheral Artery Disease. *J. Biomed. Opt.* 18 (5), 057007. doi:10.1117/1.JBO.18.5.057007

Montero, D., Walther, G., Diaz-Cañestro, C., Pyke, K. E., and Padilla, J. (2015). Microvascular Dilator Function in Athletes: A Systematic Review and Meta-Analysis. *Med. Sci. Sports Exerc* 47 (7), 1485–1494. doi:10.1249/MSS.0000000000000567

Rasica, L., Inglis, E. C., Iannetta, D., Soares, R. N., and Murias, J. M. (2022). Fitness Level- and Sex-Related Differences in Macrovascular and Microvascular Responses during Reactive Hyperemia. *Med. Sci. Sports Exerc.* 54 (3). doi:10.1249/mss.0000000000002806

Redfield, M. M., Jacobsen, S. J., Borlaug, B. A., Rodeheffer, R. J., and Kass, D. A. (2005). Age- and Gender-Related Ventricular-Vascular Stiffening. *Circulation* 112 (15), 2254–2262. doi:10.1161/circulationaha.105.541078

Rosenberry, R., Munson, M., Chung, S., Samuel, T. J., Patik, J., Tucker, W. J., et al. (2018). Age-related Microvascular Dysfunction: Novel Insight from Near-Infrared Spectroscopy. *Exp. Physiol.* 103 (2), 190–200. doi:10.1113/ep086639

Rosenberry, R., and Nelson, M. D. (2020). Reactive Hyperemia: a Review of Methods, Mechanisms, and Considerations. *Am. J. Physiology-Regulatory, Integr. Comp. Physiology* 318 (3), R605–r618. doi:10.1152/ajpregu.00339.2019

Salzmann, K., Sanchez, A. M. J., and Borrani, F. (2021). Effects of Blood Flow Restriction on O2 Muscle Extraction and O2 Pulmonary Uptake Kinetics during Heavy Exercise. *Front. Physiol.* 12, 722848. doi:10.3389/fphys.2021.722848

Scholkmann, F., Kleiser, S., Metz, A. J., Zimmermann, R., Mata Pavia, J., Wolf, U., et al. (2014). A Review on Continuous Wave Functional Near-Infrared

Spectroscopy and Imaging Instrumentation and Methodology. *Neuroimage* 85, 6–27. doi:10.1016/j.neuroimage.2013.05.004

Tillin, T., Forouhi, N. G., McKeigue, P. M., and Chaturvedi, N. (2012). Southall and Brent REvisited: Cohort Profile of SABRE, a UK Population-Based Comparison of Cardiovascular Disease and Diabetes in People of European, Indian Asian and African Caribbean Origins. *Int. J. Epidemiol.* 41 (1), 33–42. doi:10.1093/ije/dyq175

van den Brand, J. G. H., Nelson, T., Verleisdonk, E. J. M. M., and Van Der Werken, C. (2005). The Diagnostic Value of Intracompartmental Pressure Measurement, Magnetic Resonance Imaging, and Near-Infrared Spectroscopy in Chronic Exertional Compartment Syndrome. *Am. J. Sports Med.* 33 (5), 699–704. doi:10.1177/0363546504270565

Vardi, M., and Nini, A. (2008). Near-infrared spectroscopy for evaluation of peripheral vascular disease. A systematic review of literature. *Eur. J. Vasc. Endovascular Surg.* 35 (1), 68–74. doi:10.1016/j.ejvs.2007.07.015

Willingham, T. B., Southern, W. M., and McCully, K. K. (2016). Measuring reactive hyperemia in the lower limb using near-infrared spectroscopy. *J. Biomed. Opt.* 21 (9), 091302. doi:10.1117/1.jbo.21.9.091302

Conflict of Interest: The authors declare that the research was conducted in the absence of any commercial or financial relationships that could be construed as a potential conflict of interest.

Publisher's Note: All claims expressed in this article are solely those of the authors and do not necessarily represent those of their affiliated organizations, or those of the publisher, the editors and the reviewers. Any product that may be evaluated in this article, or claim that may be made by its manufacturer, is not guaranteed or endorsed by the publisher.

frontiers | Frontiers in Physiology

TYPE Original Research
PUBLISHED 09 August 2022
DOI 10.3389/fphys.2022.794473

OPEN ACCESS

EDITED BY
Wei-Peng Teo,
Nanyang Technological University, Singapore

REVIEWED BY
Nattai Borges,
The University of Newcastle, Australia
Congcong Huo,
Shandong University, China

*CORRESPONDENCE
Atsuhiro Tsubaki,
tsubaki@nuhw.ac.jp

SPECIALTY SECTION
This article was submitted to Exercise Physiology, a section of the journal Frontiers in Physiology

RECEIVED 13 October 2021
ACCEPTED 07 July 2022
PUBLISHED 09 August 2022

CITATION
Kojima S, Morishita S, Hotta K, Qin W, Usui N and Tsubaki A (2022), Temporal changes in cortical oxygenation in the motor-related areas and bilateral prefrontal cortex based on exercise intensity and respiratory metabolism during incremental exercise in male subjects: A near-Infrared spectroscopy study.
Front. Physiol. 13:794473.
doi: 10.3389/fphys.2022.794473

Temporal changes in cortical oxygenation in the motor-related areas and bilateral prefrontal cortex based on exercise intensity and respiratory metabolism during incremental exercise in male subjects: A near-Infrared spectroscopy study

Sho Kojima[1,2], Shinichiro Morishita[3], Kazuki Hotta[1], Weixiang Qin[1], Naoto Usui[2] and Atsuhiro Tsubaki[1]*

[1]Institute for Human Movement and Medical Sciences, Niigata University of Health and Welfare, Niigata, Japan, [2]Department of Physical Therapy, Kisen Hospital, Tokyo, Japan, [3]Department of Physical Therapy, Fukushima Medical University, Fukushima, Japan

A recent study has reported that prefrontal cortex (PFC) activity during incremental exercise may be related to exercise termination on exhaustion. However, few studies have focused on motor-related areas during incremental exercise. This study investigated changes in the oxygenation of the PFC and motor-related areas using near-infrared spectroscopy during incremental exercise. Moreover, we analyzed the effect of exercise termination on changes in cortical oxygenation based on exercise intensity and respiratory metabolism. Sixteen healthy young male patients participated in this study. After a 4-min rest and 4-min warm-up period, incremental exercise was started at an incremental load corresponding to 20 W/min. Oxyhemoglobin (O_2Hb), deoxyhemoglobin (HHb), and total hemoglobin (THb) in the bilateral PFC, supplementary motor area, and primary motor cortex were measured. We evaluated changes in oxygenation in each cortex before and after the anaerobic threshold (AT) and respiratory compensation point to identify changes due to respiratory metabolism. O_2Hb and THb increased from moderate intensity or after AT to maximal exercise, and HHb increased slowly compared to O_2Hb and THb; these changes in hemoglobin levels were consistent in all cortical areas we measured. However, the increase in each hemoglobin level in the bilateral PFC during incremental exercise was faster than that in motor-related areas. Moreover, changes in cortical oxygenation in the right PFC were faster than those in the left PFC. These results suggest changes based on differences in neural activity due to the cortical area.

KEYWORDS

cortical oxygenation, near-infrared spectroscopy, incremental exercise, prefrontal cortex, supplementary motor area, primary motor cortex, anaerobic threshold, respiratory compensation point

1 Introduction

Near-infrared spectroscopy (NIRS) can evaluate changes in cortical oxygenation during dynamic exercise such as running and cycling. Recently, changes in cortical oxygenation during submaximal exercise have received attention because brain activity is related to exercise termination on exhaustion (Robertson and Marino, 2016), but the underlying mechanisms are not clear. A previous study reported that oxyhemoglobin (O_2Hb) in the prefrontal cortex (PFC) during incremental exercise reaches a peak at the respiratory compensation point (RCP) and decreases after RCP to maximal exercise, and deoxyhemoglobin (HHb) increases until maximal exercise (Rupp et al., 2008). In addition, the increase in O_2Hb during incremental exercise for subjects with high exercise capacity is higher than that in subjects with low exercise capacity (Rupp et al., 2008; Oussaidene et al., 2015). The PFC has controlled cognitive and affective function (Ridderinkhof et al., 2004; Etkin et al., 2011), and motor-related areas such as the supplementary motor area (SMA), premotor area, and primary motor cortex (M1) have controlled motor output, coordination, and execution of movement (Nachev et al., 2008; Green et al., 2018; Côté et al., 2020). The PFC, SMA and M1 have indirect connectivity by premotor area (Robertson and Marino, 2016). The PFC is the region upstream of the motor-related area for motor control and determines exercise termination due to the integration of afferent feedback such as fatigue levels, physiological sensations and internal motivation levels (Robertson and Marino, 2016). The PFC may be activated earlier or higher than motor-related areas because aggregates multiple afferent feedback and forward to motor-related areas. Therefore, we have considered that activation in the PFC and motor-related areas during incremental exercise varied due to the different functions of these areas.

Several studies have reported different changes in cortical oxygenation between the PFC and motor-related areas during incremental exercise (Subudhi et al., 2009; Jung et al., 2015). Subudhi et al. (Subudhi et al., 2009) reported strong correlations between the left PFC, premotor, and motor regions with respect to HHb and total hemoglobin (THb), but not O_2Hb or right PFC. Moreover, the increasing O_2Hb in the PFC was greater in the right PFC than in the left. Therefore, right-PFC oxygenation during incremental exercise may change specifically, unlike in other areas. In addition, Jung et al. (Jung et al., 2015) reported that O_2Hb in the PFC during incremental exercise significantly increased with rising exercise intensity, except in the motor cortex. Thus, cortical oxygenation in the PFC and motor-related areas may be different. However, previous studies have only compared exercise intensity with workload, and have not compared PFC and motor-related areas based on respiratory metabolism. Respiratory metabolism has two change points. The first point is the anaerobic threshold (AT), when as aerobic metabolism switches to anaerobic. The second point is the RCP, where the discharge of carbon dioxide is increased to buffer acidosis. Following AT point, arterial pH decreases until maximal exercise and more decreases from RCP (Wasserman et al., 1973). In addition, arterial partial pressure of carbon dioxide ($PaCO_2$) decreases until maximal exercise after RCP (Wasserman et al., 1973; Smith and Ainslie, 2017). Decrease of arterial pH associate with vasodilatation, and increase cerebral blood flow due to vasodilatation (Kontos et al., 1977; Yoon et al., 2012). On the other hand, Decrease of $PaCO_2$ related to decrease cerebral blood flow by the intermediary of vasoconstriction (Yoon et al., 2012; Smith and Ainslie, 2017). Cortical oxygenation may change based on the AT and RCP because they affect the circulation dynamics of the whole body. Therefore, measurement of changes in metabolism based on AT and RCP are important to understand changes in cortical oxygenation during incremental exercise. Breakpoints of cerebral oxygenation reported that both O_2Hb and HHb increased concomitantly from the AT, and the HHb further increased while the O_2Hb reached a plateau or decreased after the RCP (Racinais et al., 2014). We previously reported that O_2Hb during incremental exercise only increases in the PFC, but not the premotor area, SMA or M1. However, the measurements our previous study were not differentiated by right or left PFC, and we included mostly female subjects (Kojima et al., 2020). The O_2Hb, HHb and THb levels during exercise are reported higher male subjects compared with female subjects (Auger et al., 2016; Inagaki et al., 2021). Moreover, cerebral circulation in female is reportedly influenced by reproductive hormones (Barnes and Charkoudian, 2021). Therefore, sex difference is a factor to consider. The results of our previous study (Kojima et al., 2020) may include effects of sex difference; we need to exclude this effect. In addition, cerebral oxygenation reported to affect by changes of skin blood flow (SBF) (Miyazawa et al., 2013). Thus, measuring cortical oxygenation during incremental exercise need with consideration for effect of respiratory metabolism, sex, cortical areas and SBF. This study aimed to investigate changes in cortical oxygenation in the PFC and motor-related areas based on exercise intensity and respiratory metabolism during incremental exercise, and only include male subjects to consider sex difference. We hypothesized that cortical oxygenation of the right PFC at the AT changes independently from the left PFC and motor-related areas. This study may

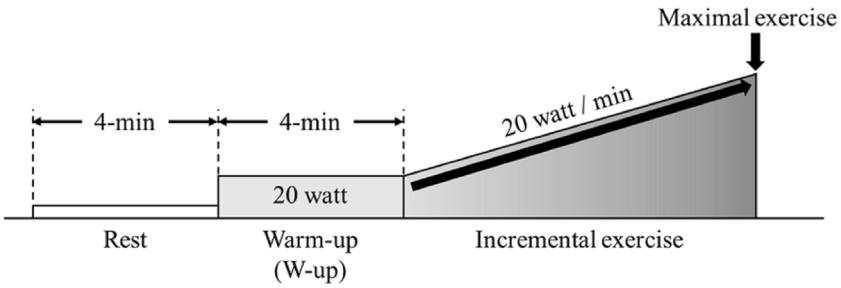

FIGURE 1
Experimental protocol. Participants performed incremental load exercise corresponding to 20 W/min after a 4-min resting state and warm up (W-up).

provide cortical oxygenation changes in multi-cortical areas during incremental exercise from a respiratory metabolism perspective. Our results may be an important for understanding the relationship between exercise and cortical oxygenation.

2 Materials and methods

2.1 Subjects

Sixteen healthy young male patients participated in this study. Participants had no fitness habits or history of neurological or orthopedic disorders and were unmedicated within the last 3 months. The study was approved by the Ethics Committee of Niigata University of Health and Welfare (approval number: 18082–181010) and conducted in accordance with the Declaration of Helsinki.

2.2 Experimental protocol

Participants were instructed not to consume alcohol or caffeine 24 h before the experiment. They were allowed to consume food and drink until 3 h before the experiments. Participants arrived 1 h prior to the start of experiment into the laboratory, wore experimental equipment, and had enough rest. Patients performed incremental exercise using the ramp load method on a cycle ergometer (Aerobike 75XLII; Combi, Tokyo, Japan) until exhaustion. Following a 4min rest, participants completed a 4 min warm up (W-up) pedaling at 20 W. Following the warm up the incremental protocol began increasing at a rate of 20W/min (Figure 1). The participants were instructed to maintain a cadence of 50–60 rpm. NIRS parameters, respiratory gas parameters, and skin blood flow (SBF) were measured from rest to the end of the incremental exercise.

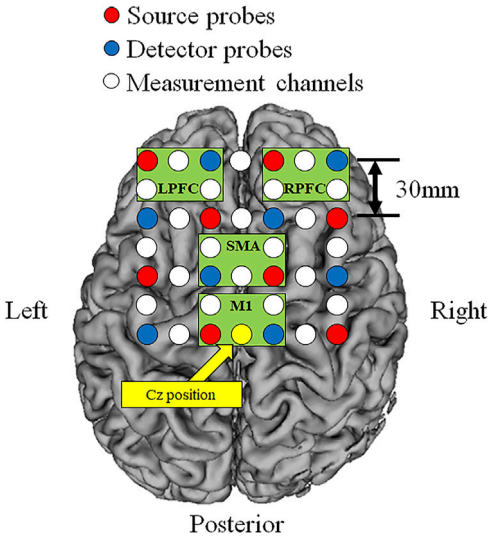

FIGURE 2
Locations of the source and detector probes and measurement channels. Red circles show source probes, blue circles show detector probes, white circles show measurement channels, and yellow circle show the vertex position (Cz). Green frames show measurement region of each cortex (L-PFC: left prefrontal cortex, R-PFC: right prefrontal cortex, SMA: supplementary motor area, M1: primary motor cortex).

2.3 Cortical oxygenation

Cortical O_2Hb, HHb, and THb during incremental exercise were measured using a multi-channel NIRS imaging system (LABNIRS, Shimadzu Co., Kyoto, Japan) with multiple continuous wavelengths (780 nm, 805 nm, and 830 nm) based on the modified Beer-Lambert law. The regions of interest were the bilateral prefrontal cortex (left: L-PFC and right: R-PFC) and motor-related areas [including the SMA and primary motor cortex (M1)]. The measurement regions were standardized based on the vertex (Cz) position according to the

international 10–20 system (Suzuki et al., 2008). The measurement channels included a total of 24 channels that used eight source probes and eight detector probes, and the probe distance was 30 mm (Figure 2). Measurement was performed at a sampling interval of 130 ms. Artifacts of head motion and heartbeat oscillations were filtered by a 0.1-Hz low pass filter (Qin et al., 2021). A repeat measurement was performed if obvious artifacts due to misalignment between head and NIRS system were confirmed.

2.4 Skin blood flow

We measured the SBF because a previous study reported the relationship between the SBF and cortical oxygenation (Miyazawa et al., 2013). The SBF during incremental exercise was measured with the midline of the forehead on 10 mm upward from the nasion of the international 10–20 system using a laser-tissue blood flow oxygen monitor (Omegaflow, FLO-Cl, Omega Wave Inc., Osaka, Japan). Analog data were converted to digital data using an A/D converter (PowerLab, AD Instruments, Australia) at a 130-Hz sampling rate.

2.5 Respiratory metabolism

Changes in oxygen uptake (VO_2), carbon dioxide output (VCO_2), minute ventilation (VE), partial pressure end-tidal oxygen ($P_{ET}O_2$), and partial pressure end-tidal carbon dioxide ($P_{ET}CO_2$) during incremental exercise were measured using a gas analyzer (AE-310, Minato Medical Science, Osaka, Japan). Respiratory metabolism data were obtained from breath-by-breath gas exchange data. We determined the AT and RCP based on previous studies (Wasserman and McIlroy, 1964; Wasserman et al., 1973). AT was determined by each point as follows: accelerating increase of VCO_2 compared with VO_2, increase of VE/VCO_2 but not VE/VCO_2, increase of respiratory exchange ratio, increase of $P_{ET}O_2$ but not $P_{ET}CO_2$. RCP determined by each point as follows: more increase of VE/VO_2, $P_{ET}O_2$ and VE, increase of VE/VCO_2, decrease of $P_{ET}CO_2$. Moreover, we calculated the peak value of VO_2 (VO_{2peak}) and VO_2 at the AT and RCP and calculated the work rate (WR) and exercise time at the AT, RCP, and maximal exercise. Exhaustion was defined as follows: 1) a plateau in VO_2; 2) respiratory exchange ratio >1.1; 3) heart rate values near the age-predicted maximal heart rate, calculated as 220—(0.65 × age); and 4) a decrease in the cycling cadence to <50 rpm, despite strong verbal encouragement (Morishita et al., 2018).

2.6 Statical analysis

Changes in O_2Hb, HHb, THb, and SBF were calculated as the amount of change from the average of 4-min of rest. These parameters during rest and W-up were calculated from the average over 4-min. These parameters during incremental exercise were calculated from the average values of each 10th percentile (10%–100%) of the individual's exercise time period from initiation to end exercise. In addition, these parameters were calculated as averages of 5-s intervals at timepoints where AT, RCP maximal exercise point (MAX), before 1-min of AT (before AT), and before 1-min of RCP (before RCP) occurred. Changes in O_2Hb, HHb, THb, and SBF from rest to at W-up and during incremental exercise were compared using the one-way analysis of variance and the Bonferroni multiple comparisons test. Statistical analyses were performed using SPSS 21.0 (SPSS Japan Inc., Tokyo, Japan), with statistical significance set at $p < 0.05$.

3 Results

The patient age was 20.8 ± 0.4 years, BMI was 22.5 ± 2.7 kg/m^2, VO_2peak was 35.4 ± 5.4 ml/min/kg, WR at maximal exercise was 172.7 ± 34.3 W, exercise time at maximal exercise was 518.1 ± 102.9 s. The percentiles of maximal exercise time at the AT and RCP were 42.5 ± 5.7% and 86.3 ± 4.9%, respectively. VO_2, exercise load, and exercise time at the AT and RCP are summarized in Table 1.

3.1 Changes in cortical oxygenation and SBF based on metabolism

The O_2Hb significantly increased from AT in the L-PFC (AT: $p = 0.04$; before RCP, RCP and MAX: $p < 0.001$) and R-PFC (AT: $p = 0.01$; before RCP, RCP and MAX: $p < 0.001$) compared with rest. The O_2Hb in the SMA and M1 showed significant increase from before RCP compared with rest ($p < 0.001$, respectively). The HHb significantly increased from before RCP in the R-PFC ($p < 0.001$, respectively) compared with rest. The HHb in the L-PFC and M1 showed significant increase from RCP compared with rest (L-PFC, RCP: $p = 0.002$, MAX: $p < 0.001$; M1, RCP: $p = 0.01$, MAX: $p < 0.001$), and the SMA showed significant increase of the HHb at MAX compared with rest ($p = 0.006$). The THb significantly increased from AT in the L-PFC (AT: $p = 0.01$; before RCP, RCP and MAX: $p < 0.001$) and R-PFC (AT: $p = 0.003$; before RCP, RCP and MAX: $p < 0.001$) compared with rest. The SMA and M1 showed significant increase of THb from before RCP compared with rest ($p < 0.001$, respectively). Moreover, the HHb significantly increased at MAX in the L-PFC ($p = 0.03$) and R-PFC ($p < 0.001$) compared with RCP. The SBF significantly increased before RCP compared with rest (Before RCP: $p = 0.01$; RCP and MAX: $p < 0.001$). These results are shown in Table 2 and Supplementary Table 1 and 2.

TABLE 1 Power output, oxygen uptake and exercise time during incremental exercise.

Variable	Mean ± SD
VO_2 at AT (ml/min/kg)	17.4 ± 2.3
VO_2 at RCP (ml/min/kg)	29.5 ± 4.0
VO_2peak (ml/min/kg)	35.4 ± 5.4
%VO_2peak at AT	49.6 ± 5.2
%VO_2peak at RCP	83.8 ± 6.7
Exercise load at AT (watt)	74.0 ± 20.9
Exercise load at RCP (watt)	148.3 ± 27.2
Exercise load at maximal exercise (watt)	172.7 ± 34.3
time at AT (sec)	222.0 ± 62.8
time at RCP (sec)	444.9 ± 81.7
time at maxiaml exercise (sec)	518.1 ± 102.9
%maxmal exercise time at AT	42.5 ± 5.7
%maxmal exercise time at RCP	86.3 ± 4.9

VO_2: oxygen uptake, VO_{2peak}: peak oxygen uptake, AT: anerobic threshold, RCP: respiratory compensation point

3.2 Changes in cortical oxygenation and SBF at percentile

As shown in Figure 3 and Supplementary Tables 3 and 4, the O_2Hb significantly increased from 50% to 100% in the R-PFC compared with rest (50%: $p = 0.02$; 60%–100%: $p < 0.001$). The O_2Hb in the L-PFC and M1 showed significant increase from 60% to 100% compared with rest (L-PFC, 60%: $p = 0.005$, 70%–100%: $p < 0.001$; M1, 60%: $p = 0.001$, 70%–100%: $p < 0.001$). The SMA showed significant increase of the O_2Hb from 70 to 100% compared with rest (70%: $p = 0.003$, 80%–100%: $p < 0.001$). The HHb in the R-PFC significantly increased from 70% to 100% compared with rest ($p < 0.001$). The L-PFC and M1 showed significant increase of the HHb from 80% to 100% compared with rest (L-PFC, 80%: $p = 0.005$, 90% and 100%: $p < 0.001$; M1, 80%: $p = 0.03$, 90% and 100%: $p < 0.001$). The HHb in the SMA significantly increased from 100% compared with rest ($p = 0.001$). The THb significantly increased from 50% to 100% in the L-PFC (50%: $p = 0.01$, 60%–100%: $p < 0.001$) and R-PFC (50%: $p = 0.002$, 60%–100%: $p < 0.001$) compared with rest. The THb in the SMA and M1 significantly increased from 60% to 100% compared with rest (SMA, 60%: $p = 0.04$, 70%: $p = 0.001$, 80%–100%: $p < 0.001$; M1, 60%: $p = 0.001$, 70%–100%: $p < 0.001$). The SBF significantly increased from 70% to 100% compared to rest (70%: $p = 0.006$, 80%–100%: $p < 0.001$).

4 Discussion

We investigated changes in cerebral oxygenation in the bilateral PFC and motor-related areas based on changes in respiratory metabolism during incremental exercise. The main finding of our study was that the HHb in the R-PFC increased faster than in other cortical areas, and the HHb in the bilateral PFC further increased from RCP to MAX. In addition, the O_2Hb and THb in the bilateral PFC during incremental exercise increased faster than those in the SMA and M1. This study is the first to reveal differences in cortical oxygenation changes between the PFC and motor-related areas based on respiratory metabolism.

4.1 Cerebral oxygenation during incremental exercise

In this study, we showed an increase in O_2Hb, HHb, and THb with increasing intensity. These findings support previous findings regarding cerebral oxygenation during incremental exercise (Rupp et al., 2008; Giles et al., 2014; Kojima et al., 2020). Changes in cerebral oxygenation are reportedly affected by changes in SBF, cerebral blood flow (CBF), and cortical activity (Lindauer et al., 2010; Miyazawa et al., 2013). In general, NIRS signal at neural activity is related to an increase of O_2Hb, decrease of HHb and an increase of THb, because the CBF increases with the cerebral metabolic rate of oxygen ($CMRO_2$) (Lindauer et al., 2010). Increase in the HHb is caused by cortical activation, hypoxia, ischemia, or vein congestion (Murata et al., 2006; Subudhi et al., 2007; Lindauer et al., 2010). Subjective symptoms of hypoxia and ischemia were not observed in the subjects. Our study showed different timings of increase between SBF and cerebral oxygenation. The timepoint of significant increase in the O_2Hb and THb were 50–60% during incremental exercise, while the SBF was 70% during incremental exercise (Figure 3). Moreover, previous studies reported none or negative correlation between the SBF and O_2Hb at high intensity exercise and cool-down (Tsubaki et al., 2016; Kojima et al., 2021). Although SBF and O_2Hb appear to increase simultaneously, we considered that changes in cerebral oxygenation were related to increased cerebral blood flow or cortical activation. CBF during incremental exercise increases with an increase in exercise intensity and reaches a plateau/decrease after high-intensity exercise (Smith and Ainslie, 2017). Changes in CBF and O_2Hb during incremental exercise are similar and can be explained by arterial constriction/dilatation with $P_{ET}CO_2$ changes. However, a previous study reported that CBF increased with clamped $P_{ET}CO_2$ after RCP but did not increase O_2Hb (Hansen et al., 2020). In addition, our previous study demonstrated no correlation between changes in cerebral oxygenation and $P_{ET}CO_2$ after RCP, and THb increased until maximal exercise (Kojima et al., 2021). Thus, changes in cerebral oxygenation during incremental exercise can be partially explained by CBF

TABLE 2 Changes in cerebral oxygenation and skin blood flow based on respiratory metabolism.

Variable	Time						
	Rest	W-up	Before AT	AT	Before RCP	RCP	MAX
$O_2Hb \times 10^{-2}$ (mM·cm)							
L-PFC	0.0 ± 0.0	0.7 ± 2.1	2.4 ± 3.3	4.2 ± 3.2*	7.7 ± 3.8*	8.7 ± 4.1*	7.3 ± 6.2*
R-PFC	0.0 ± 0.0	0.6 ± 1.6	2.2 ± 2.4	3.8 ± 2.5*	6.9 ± 2.7*	7.7 ± 3.4*	6.7 ± 5.2*
SMA	0.0 ± 0.0	0.2 ± 2.1	1.4 ± 2.3	3.0 ± 2.2	5.5 ± 2.6*	6.2 ± 3.7*	5.0 ± 5.6*
M1	0.0 ± 0.0	-0.1 ± 1.9	1.5 ± 2.4	2.6 ± 2.5	5.2 ± 2.7*	5.6 ± 3.1*	4.1 ± 3.5*
HHb $\times 10^{-2}$ (mM·cm)							
L-PFC	0.0 ± 0.0	0.0 ± 1.0	0.1 ± 1.6	0.6 ± 1.5	1.9 ± 2.3	3.2 ± 2.9*	5.7 ± 3.7*†
R-PFC	0.0 ± 0.0	0.3 ± 0.6	0.6 ± 1.0	0.9 ± 0.9	2.5 ± 1.4*	3.8 ± 1.8*	6.5 ± 2.5*†
SMA	0.0 ± 0.0	-0.1 ± 0.6	0.2 ± 1.1	0.4 ± 1.3	1.4 ± 1.6	2.2 ± 2.1	2.9 ± 4.7*
M1	0.0 ± 0.0	-0.8 ± 0.9	-0.6 ± 1.7	-0.2 ± 1.6	1.3 ± 1.8	2.4 ± 2.2*	4.5 ± 3.1*
THb $\times 10^{-2}$ (mM·cm)							
L-PFC	0.0 ± 0.0	0.7 ± 1.6	2.5 ± 2.9	4.8 ± 2.9*	9.7 ± 3.8*	11.9 ± 5.1*	13.1 ± 6.6*
R-PFC	0.0 ± 0.0	0.9 ± 1.5	2.8 ± 2.1	4.7 ± 2.4*	9.4 ± 3.1*	11.5 ± 4.0*	13.2 ± 5.9*
SMA	0.0 ± 0.0	0.2 ± 2.0	1.6 ± 1.9	3.4 ± 2.1	6.9 ± 2.9*	8.4 ± 4.3*	7.9 ± 9.2*
M1	0.0 ± 0.0	-0.9 ± 1.9	0.9 ± 2.6	2.4 ± 2.9	6.6 ± 3.4*	8.0 ± 3.6*	8.7 ± 4.8*
SBF (a.u.)	0.0 ± 0.1	-0.2 ± 0.6	0.8 ± 1.4	1.7 ± 2.1	4.6 ± 3.3*	7.5 ± 4.1*	8.8 ± 7.9*

O_2Hb, oxyhemoglobin, HHb, deoxyhemoglobin, THb, total hemoglobin, SBF, skin blood flow, L-PFC, left prefrontal cortex, R-PFC, right prefrontal cortex, SMA, supplementary motor area, M1, primary motor cortex, W-up, warm-up, AT, anaerobic threshold, RCP, respiratory compensation point, MAX, maximal exercise point.
[a]$p<0.05$: significant different from the rest.
[b]$p<0.05$: significant different from the RCP.
Mean ± standard deviation.

changes, while not explaining the changes from RCP to maximal exercise.

On the other hand, changes in cerebral oxygenation from the RCP to maximal exercise may be affected by neural activity in each cortex. Oxygen metabolism by neural activity accelerates conversion from the O_2Hb to the HHb, whereas an increase in regional CBF exceeds the cerebral metabolic rate of oxygen ($CMRO_2$) by a factor of 2–10, resulting in washout of HHb from the activation area, an increase in O_2Hb, and a decrease in HHb (Lindauer et al., 2010). The PFC can aggregate afferent signals of affect, physical sensations, fatigue levels, and control to modify the exercise pace due to out via the pre-motor area and the basal ganglia (Robertson and Marino, 2016). Motor-related areas activation increases with the PFC because motor-related areas increase the power output of muscles with incremental exercise intensity (Brümmer et al., 2011). Cortical activation during incremental exercise is possibly increased from RCP to MAX owing to the maintenance of the exercise pace. However, neural activity in the PFC and motor cortex during incremental exercise, measured using electroencephalogram (EEG), was reported to decrease from RCP to maximal exercise (Robertson and Marino, 2015). In contrast, $CMRO_2$ has been reported to increase until maximal exercise (Smith and Ainslie, 2017). Additionally, the systemic vascular conductance (VC) index and cerebral VC index increased with increasing load (Fisher et al., 2013), and systemic VC may increase the pulsatility index in the straight sinus, which shows resistance to venous outflow (Stolz et al., 2009). Imbalanced cerebral oxygenation from RCP to maximal exercise might be caused by a decrease in CBF, an increase in cerebral metabolic rate of oxygen, and a larger resistance to venous outflow, and these results may lead to a decline in neural activation.

4.2 Different of cerebral oxygenation in the prefrontal and motor-related areas

The O_2Hb and THb in the bilateral PFC increased faster than in the SMA and M1, and the HHb in the R-PFC increased faster than in other cortical areas. A previous study that measured oxygenation in the PFC during incremental exercise reported that the non-linear changes in cerebral oxygenation were concomitant with both AT and RCP (Racinais et al., 2014). The O_2Hb and THb levels in the PFC significantly increased from AT, and these results correspond with those of a previous study. On the other hand, the O_2Hb and THb in the motor-related areas increased later compared to the bilateral PFC. This result shows that regional oxygenation changes during incremental exercise differ between PFC and motor-related areas.

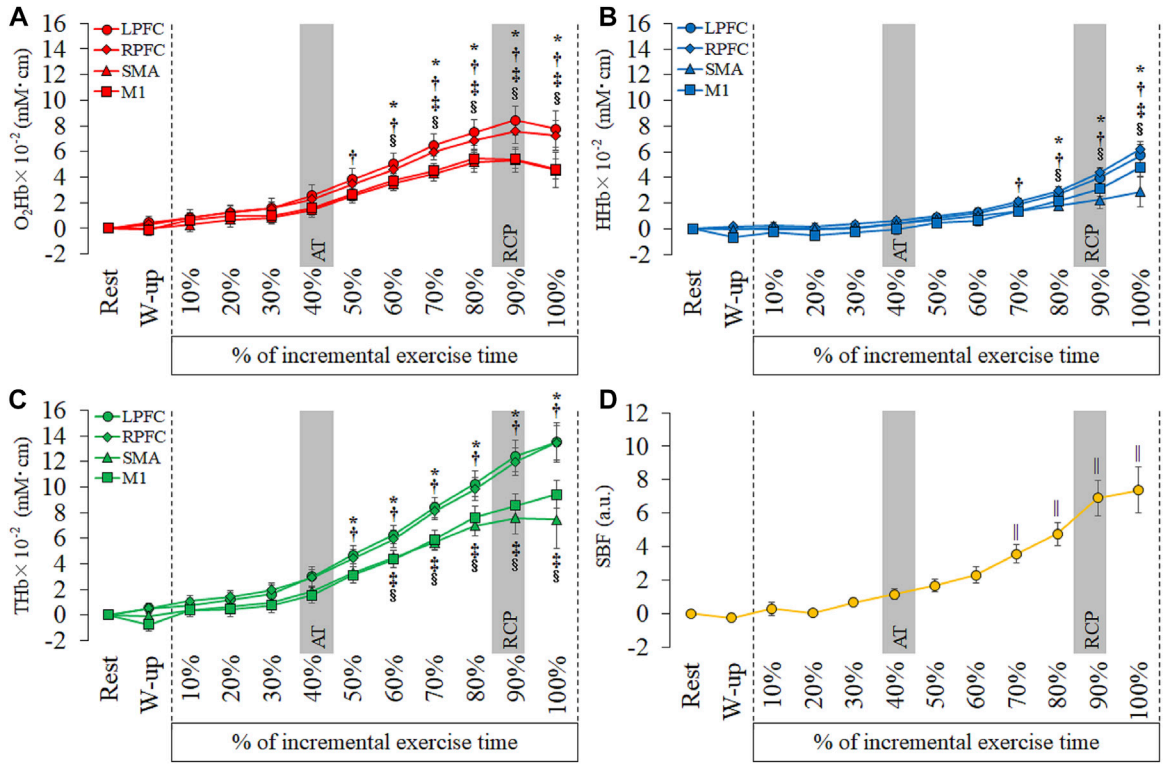

FIGURE 3
Temporal changes in each hemoglobin and skin blood flow (SBF) at each period of every 10th of incremental exercise. **(A)**: oxyhemoglobin (O2Hb), **(B)**: deoxyhemoglobin (HHb), **(C)**: total hemoglobin (THb) and **(D)**: SBF. Region of interests are left prefrontal cortex (L-PFC), right prefrontal cortex (R-PFC), supplementary motor area (SMA) and primary motor cortex (M1). Gray bars show approximate position in the AT and RCP calculated from all participants. Significant different compared with rest: *$p < 0.05$.

Moreover, the HHb in the bilateral PFC increased MAX compared with the RCP. Increased HHb was not identified in motor-related areas. A previous study investigated the relationship between affective responses and cerebral oxygenation and reported a relationship between an increase in unpleasant emotion and an increase in the O_2Hb at RCP and at the end of the exercise (Tempest et al., 2014). However, a previous study did not report a relationship between affective responses and HHb. Therefore, early increases in O_2Hb and THb in the bilateral PFC and rapid increase in HHb from RCP to MAX may be affected by affective responses. Some studies have reported the extension of exercise time during incremental exercise by transcranial direct current stimulation (tDCS), which modulates cortical activity (Okano et al., 2015; Baldari et al., 2018). Anodal tDCS for the motor cortex extended the exercise time but did not change affective responses (Baldari et al., 2018). On the other hand, anodal tDCS for the insular cortex delayed the increase in the rating of perceived exertion and heart rate in addition to prolonged exercise time (Okano et al., 2015). The insular cortex has functional connectivity with the PFC and sends afferent feedback during exercise (Robertson and Marino, 2016; McMorris et al., 2018). The PFC is an important region that integrates afferent signals, such as fatigue, emotion, and perception of movement during exercise. Therefore, the oxygenation of the PFC may have increased earlier than in motor-related areas.

4.3 Limitations and strength

In this study, cortical activity, affective response, $CMRO_2$, and CBF were not measured during the incremental exercise. Thus, differences in cortical oxygenation by function explicitly were not explained. Moreover, the amygdala and insular cortex related to affect are located deep in the brain. To understand cortical oxygenation and neural activity during incremental exercise, an overall assessment based on magnetic resonance imaging, positron-emission tomography, EEG, and NIRS is required.

We measured SBF using laser tissue blood flow oxygen monitoring. Measurement of the SBF is a strength of our research and removes the effect of extra-cerebral tissue. However, SBF was measured on the forehead. In particular, M1 is distant from the forehead, which is a limitation of this

study. In addition, systemic physiological factors of cardiac output, mean arterial pressure and peripheral vascular resistance influence cerebral blood flow (Smith and Ainslie, 2017). We could not measure physiological factors other than skin blood flow, and this missing information is a limitation of our study. Future studies should assess SBF using short-channel regression methods and should measure physiological factors associated with cerebral blood flow and oxygenation.

However, few studies have measured NIRS during incremental exercise in multiple regions, and our study is the first to evaluate regional changes in cerebral oxygenation based on AT and RCP during incremental exercise. The present study may be an important study that increases the understanding of cortical oxygenation and neural activity during incremental exercise.

5 Conclusion

We found different changes in cerebral oxygenation in the PFC and motor-related areas during incremental exercise. The PFC during incremental exercise may be more active than the motor-related areas to continue exercise. Future studies are need to investigate the relationship between cerebral oxygenation in the multi-cortical area during incremental exercise, neural activity, fatigue, and emotion.

Data availability statement

The raw data supporting the conclusions of this article will be made available by the authors, without undue reservation.

Ethics statement

The studies involving human participants were reviewed and approved by Niigata University Health and Welfare. The patients/participants provided their written informed consent to participate in this study.

Author contributions

SK and AT were responsible for the design of the study, execution of the study, data collection, data analysis, interpretation of data, drafting the manuscript, revising the manuscript, and approving the final submitted version. SM, KH, and AT were responsible for data analysis, interpretation of data, drafting the manuscript, revising the manuscript, and approving the final submitted version. WQ and NU were interpretation of data, drafting the manuscript, revising the manuscript, and approving the final submitted version.

Funding

A part of this research was funded by a Grant-in-Aid for Scientific Research (B) from the JSPS (20H04042, AT) and Grant-in-Aid for Scientific Research (A) from Niigata University of Health and Welfare, 2020 (R02B18, AT).

Acknowledgments

This study was supported by a Grant-in-Aid for Scientific Research (B) from the Japan Society for the Promotion of Science (AT) and a Grant-in-Aid for Exploratory Research (A) from Niigata University of Health and Welfare (AT).

Conflict of interest

The authors declare that the research was conducted in the absence of any commercial or financial relationships that could be construed as a potential conflict of interest.

Publisher's note

Supplementary material

The Supplementary Material for this article can be found online at: https://www.frontiersin.org/articles/10.3389/fphys.2022.794473/full#supplementary-material

References

Auger, H., Bherer, L., Boucher, É., Hoge, R., Lesage, F., and Dehaes, M. (2016). Quantification of extra-cerebral and cerebral hemoglobin concentrations during physical exercise using time-domain near infrared spectroscopy. *Biomed. Opt. Express* 7 (10), 3826–3842. doi:10.1364/BOE.7.003826

Baldari, C., Buzzachera, C. F., Vitor-Costa, M., Gabardo, J. M., Bernardes, A. G., Altimari, L. R., et al. (2018). Effects of transcranial direct current stimulation on psychophysiological responses to maximal incremental exercise test in recreational endurance runners. *Front. Psychol.* 9, 1867. doi:10.3389/fpsyg.2018.01867

Barnes, J. N., and Charkoudian, N. (2021). Integrative cardiovascular control in women: Regulation of blood pressure, body temperature, and cerebrovascular responsiveness. *Faseb J.* 35 (2), e21143. doi:10.1096/fj.202001387R

Brümmer, V., Schneider, S., Strüder, H. K., and Askew, C. D. (2011). Primary motor cortex activity is elevated with incremental exercise intensity. *Neuroscience* 181, 150–162. doi:10.1016/j.neuroscience.2011.02.006

Côté, S. L., Elgbeili, G., Quessy, S., and Dancause, N. (2020). Modulatory effects of the supplementary motor area on primary motor cortex outputs. *J. Neurophysiol.* 123 (1), 407–419. doi:10.1152/jn.00391.2019

Etkin, A., Egner, T., and Kalisch, R. (2011). Emotional processing in anterior cingulate and medial prefrontal cortex. *Trends Cogn. Sci.* 15 (2), 85–93. doi:10.1016/j.tics.2010.11.004

Fisher, J. P., Hartwich, D., Seifert, T., Olesen, N. D., McNulty, C. L., Nielsen, H. B., et al. (2013). Cerebral perfusion, oxygenation and metabolism during exercise in young and elderly individuals. *J. Physiol.* 591 (7), 1859–1870. doi:10.1113/jphysiol.2012.244905

Giles, G. E., Brunye, T. T., Eddy, M. D., Mahoney, C. R., Gagnon, S. A., Taylor, H. A., et al. (2014). Acute exercise increases oxygenated and deoxygenated hemoglobin in the prefrontal cortex. *Neuroreport* 25 (16), 1320–1325. doi:10.1097/WNR.0000000000000266

Green, P. E., Ridding, M. C., Hill, K. D., Semmler, J. G., Drummond, P. D., and Vallence, A. M. (2018). Supplementary motor area-primary motor cortex facilitation in younger but not older adults. *Neurobiol. Aging* 64, 85–91. doi:10.1016/j.neurobiolaging.2017.12.016

Hansen, R. K., Nielsen, P. S., Schelske, M. W., Secher, N. H., and Volianitis, S. (2020). CO(2) supplementation dissociates cerebral oxygenation and middle cerebral artery blood velocity during maximal cycling. *Scand. J. Med. Sci. Sports* 30 (3), 399–407. doi:10.1111/sms.13582

Inagaki, Y., Sato, R., Uchiyama, T., Kojima, S., Morishita, S., Qin, W., et al. (2021). Sex differences in the oxygenation of the left and right prefrontal cortex during moderate-intensity exercise. *Int. J. Environ. Res. Public Health* 18 (10), 5212. doi:10.3390/ijerph18105212

Jung, R., Moser, M., Baucsek, S., Dern, S., and Schneider, S. (2015). Activation patterns of different brain areas during incremental exercise measured by near-infrared spectroscopy. *Exp. Brain Res.* 233 (4), 1175–1180. doi:10.1007/s00221-015-4201-4

Kojima, S., Morishita, S., Hotta, K., Qin, W., Kato, T., Oyama, K., et al. (2021). Relationship between decrease of oxygenation during incremental exercise and partial pressure end-tidal carbon dioxide: near-infrared spectroscopy vector analysis. *Adv. Exp. Med. Biol.* 1269, 119–124. doi:10.1007/978-3-030-48238-1_19

Kojima, S., Morishita, S., Qin, W., and Tsubaki, A. (2020). Cerebral oxygenation dynamics of the prefrontal cortex and motor-related area during cardiopulmonary exercise test: a near-infrared spectroscopy study. *Adv. Exp. Med. Biol.* 1232, 231–237. doi:10.1007/978-3-030-34461-0_29

Kontos, H. A., Raper, A. J., and Patterson, J. L. (1977). Analysis of vasoactivity of local pH, PCO2 and bicarbonate on pial vessels. *Stroke* 8 (3), 358–360. doi:10.1161/01.str.8.3.358

Lindauer, U., Dirnagl, U., Fuchtemeier, M., Bottiger, C., Offenhauser, N., Leithner, C., et al. (2010). Pathophysiological interference with neurovascular coupling - when imaging based on hemoglobin might go blind. *Front. Neuroenergetics* 2, 25. doi:10.3389/fnene.2010.00025

McMorris, T., Barwood, M., and Corbett, J. (2018). Central fatigue theory and endurance exercise: toward an interoceptive model. *Neurosci. Biobehav. Rev.* 93, 93–107. doi:10.1016/j.neubiorev.2018.03.024

Miyazawa, T., Horiuchi, M., Komine, H., Sugawara, J., Fadel, P. J., and Ogoh, S. (2013). Skin blood flow influences cerebral oxygenation measured by near-infrared spectroscopy during dynamic exercise. *Eur. J. Appl. Physiol.* 113 (11), 2841–2848. doi:10.1007/s00421-013-2723-7

Morishita, S., Tsubaki, A., Nashimoto, S., Fu, J. B., and Onishi, H. (2018). Face scale rating of perceived exertion during cardiopulmonary exercise test. *BMJ Open Sport Exerc. Med.* 4 (1), e000474. doi:10.1136/bmjsem-2018-000474

Murata, Y., Sakatani, K., Hoshino, T., Fujiwara, N., Kano, T., Nakamura, S., et al. (2006). Effects of cerebral ischemia on evoked cerebral blood oxygenation responses and BOLD contrast functional MRI in stroke patients. *Stroke* 37 (10), 2514–2520. doi:10.1161/01.STR.0000239698.50656.3b

Nachev, P., Kennard, C., and Husain, M. (2008). Functional role of the supplementary and pre-supplementary motor areas. *Nat. Rev. Neurosci.* 9 (11), 856–869. doi:10.1038/nrn2478

Okano, A. H., Fontes, E. B., Montenegro, R. A., Farinatti Pde, T., Cyrino, E. S., Li, L. M., et al. (2015). Brain stimulation modulates the autonomic nervous system, rating of perceived exertion and performance during maximal exercise. *Br. J. Sports Med.* 49 (18), 1213–1218. doi:10.1136/bjsports-2012-091658

Oussaidene, K., Prieur, F., Tagougui, S., Abaidia, A., Matran, R., and Mucci, P. (2015). Aerobic fitness influences cerebral oxygenation response to maximal exercise in healthy subjects. *Respir. Physiol. Neurobiol.* 205, 53–60. doi:10.1016/j.resp.2014.10.009

Qin, W., Kojima, S., Yamazaki, Y., Morishita, S., Hotta, K., Inoue, T., et al. (2021). Relationship between the difference in oxygenated hemoglobin concentration changes in the left and right prefrontal cortex and cognitive function during moderate-intensity aerobic exercise. *Appl. Sci.* 11 (4), 1643. doi:10.3390/app11041643

Racinais, S., Buchheit, M., and Girard, O. (2014). Breakpoints in ventilation, cerebral and muscle oxygenation, and muscle activity during an incremental cycling exercise. *Front. Physiol.* 5, 142. doi:10.3389/fphys.2014.00142

Ridderinkhof, K. R., van den Wildenberg, W. P., Segalowitz, S. J., and Carter, C. S. (2004). Neurocognitive mechanisms of cognitive control: the role of prefrontal cortex in action selection, response inhibition, performance monitoring, and reward-based learning. *Brain Cogn.* 56 (2), 129–140. doi:10.1016/j.bandc.2004.09.016

Robertson, C. V., and Marino, F. E. (2016). A role for the prefrontal cortex in exercise tolerance and termination. *J. Appl. Physiol.* 120 (4), 464–466. doi:10.1152/japplphysiol.00363.2015

Robertson, C. V., and Marino, F. E. (2015). Prefrontal and motor cortex EEG responses and their relationship to ventilatory thresholds during exhaustive incremental exercise. *Eur. J. Appl. Physiol.* 115 (9), 1939–1948. doi:10.1007/s00421-015-3177-x

Rupp, T., Perrey, S., and Stephane, P. (2008). Prefrontal cortex oxygenation and neuromuscular responses to exhaustive exercise. *Eur. J. Appl. Physiol.* 102 (2), 153–163. doi:10.1007/s00421-007-0568-7

Smith, K. J., and Ainslie, P. N. (2017). Regulation of cerebral blood flow and metabolism during exercise. *Exp. Physiol.* 102 (11), 1356–1371. doi:10.1113/EP086249

Stolz, E., Fox, B. C., Hoffmann, O., Gerriets, T., Blaes, F., Kraus, J., et al. (2009). Cranial venous outflow under lower body positive and negative pressure conditions and head-up and -down tilts. *J. Neuroimaging* 19 (1), 31–36. doi:10.1111/j.1552-6569.2008.00250.x

Subudhi, A. W., Dimmen, A. C., and Roach, R. C. (2007). Effects of acute hypoxia on cerebral and muscle oxygenation during incremental exercise. *J. Appl. Physiol.* 103 (1), 177–183. doi:10.1152/japplphysiol.01460.2006

Subudhi, A. W., Miramon, B. R., Granger, M. E., and Roach, R. C. (2009). Frontal and motor cortex oxygenation during maximal exercise in normoxia and hypoxia. *J. Appl. Physiol.* 106 (4), 1153–1158. doi:10.1152/japplphysiol.91475.2008

Suzuki, M., Miyai, I., Ono, T., and Kubota, K. (2008). Activities in the frontal cortex and gait performance are modulated by preparation. An fNIRS study. *Neuroimage* 39 (2), 600–607. doi:10.1016/j.neuroimage.2007.08.044

Tempest, G. D., Eston, R. G., and Parfitt, G. (2014). Prefrontal cortex haemodynamics and affective responses during exercise: a multi-channel near infrared spectroscopy study. *PLoS One* 9 (5), e95924. doi:10.1371/journal.pone.0095924

Tsubaki, A., Takai, H., Oyanagi, K., Kojima, S., Tokunaga, Y., Miyaguchi, S., et al. (2016). Correlation between the cerebral oxyhaemoglobin signal and physiological signals during cycling exercise: a near-infrared spectroscopy study. *Adv. Exp. Med. Biol.* 923, 159–166. doi:10.1007/978-3-319-38810-6_21

Wasserman, K., and McIlroy, M. B. (1964). Detecting the threshold of anaerobic metabolism in cardiac patients during exercise. *Am. J. Cardiol.* 14, 844–852. doi:10.1016/0002-9149(64)90012-8

Wasserman, K., Whipp, B. J., Koyl, S. N., and Beaver, W. L. (1973). Anaerobic threshold and respiratory gas exchange during exercise. *J. Appl. Physiol.* 35 (2), 236–243. doi:10.1152/jappl.1973.35.2.236

Yoon, S., Zuccarello, M., and Rapoport, R. M. (2012). pCO(2) and pH regulation of cerebral blood flow. *Front. Physiol.* 3, 365. doi:10.3389/fphys.2012.00365

frontiers | Frontiers in Sports and Active Living

TYPE Original Research
PUBLISHED 12 September 2022
DOI 10.3389/fspor.2022.838189

OPEN ACCESS

EDITED BY
Wei-Peng Teo,
Nanyang Technological University, Singapore

REVIEWED BY
Christopher Latella,
Edith Cowan University, Australia
Nathan Nuzum,
Deakin Univeristy, Australia

*CORRESPONDENCE
Toshinori Kato
kato@katobrain.com

SPECIALTY SECTION
This article was submitted to Exercise Physiology, a section of the journal Frontiers in Sports and Active Living

RECEIVED 17 December 2021
ACCEPTED 17 August 2022
PUBLISHED 12 September 2022

CITATION
Kato T (2022) Vector-based analysis of cortical activity associated with dumbbell exercise using functional near-infrared spectroscopy. *Front. Sports Act. Living* 4:838189. doi: 10.3389/fspor.2022.838189

Vector-based analysis of cortical activity associated with dumbbell exercise using functional near-infrared spectroscopy

Toshinori Kato*

Department of Brain Environmental Research, KatoBrain Co., Ltd., Tokyo, Japan

The mechanisms *via* which the brain and muscles work together remain poorly understood. The use of vector-based fNIRS, to propose a new metric and imaging method to understand neural activation during dumbbell-lifting exercises. This method can simultaneously measure oxyhemoglobin (oxyHb) and deoxyHb levels so that the angle *k*: Arctan (deoxyHb/oxyHb) represents the degree of oxygen exchange in the brain and can be used to quantify the distribution of oxygen consumption. The amplitude L of the vector reflects the intensity of the response caused by the amount of change in Hb. This study used vector-based fNIRS to simultaneously measure the left primary motor cortex (left M1), multiple peripheral regions, and the right biceps brachii muscle. The subjects were seven healthy adults. The task was a dumbbell-lifting exercise involving flexion and extension of the elbow joints of both arms. Dumbbell weights of 0 (no dumbbell), 4.5, and 9.5 kg were used. During dumbbell exercise, oxygen exchange increased in the left M1, indicating increased local oxygen consumption. Around the left M1, the cerebral oxygen exchange decreased, and oxygen supply increased without cerebral oxygen consumption. The spatial agreement between the maximum value of oxygen exchange *k* and L during the task was <20%. Therefore, the dumbbell-lifting exercise task study reported here supported the hypothesis that cerebral oxygen consumption associated with neural activation does not coincide with the distribution of cerebral oxygen supply. The relationship between the brain oxygen supply from the site of increased oxygen exchange in the brain and its surrounding areas can be quantified using the vector method fNIRS.

KEYWORDS

phase, motor, brain, function, vector analysis, near-infrared spectroscopy, fNIRS, dumbbell exercise

Introduction

Studies of brain oxygenation during high-intensity exercise (Rupp and Perrey, 2008) and walking (Khan et al., 2021) have been performed using functional near-infrared spectroscopy (fNIRS). Physical activity induces local cerebral oxygen consumption and demand for oxygen supply. However, conventional brain functional imaging currently does not include a method for distinguishing oxygen consumption from oxygen supply simultaneously. Thus, the spatial distribution between oxygen consumption and supply in the brain that accompanies exercise remains largely unknown.

In fNIRS, variations in the ratio between changes in oxyhemoglobin (oxyHb) and deoxyHb are observed according to the site, thus reflecting the spatial distribution of oxygen consumption and supply. It is known that fNIRS is capable of measuring the fast oxygen response in capillary events (FORCE) associated with neuronal responses, defined as the FORCE effect (Kato, 2004).

The FORCE effect indicates tissue hypoxia with an increase in deoxyHb and a decrease in oxyHb, reflecting increased oxygen consumption. It has been reported that a temporary FORCE occurred in the primary motor cortex (M1) at the onset of a hand grasping task, and deoxyHb decreased and oxyHb increased around M1, reflecting oxygen supply (Akiyama et al., 2006). In a task that activated the supplementary motor area (SMA), deoxyHb and oxyHb were increased in the SMA. OxyHb increased and deoxyHb fell slightly in the sensory-motor cortex and the pre-SMA (Hatakenaka et al., 2007). Several reports have shown that oxyHb analysis alone cannot accurately detect the localization of neuroactivation (Cyranoski, 2011; Takahashi et al., 2011) and that functional images of increasing oxyHb may differ from the actual distribution of oxygen consumption (Kato, 2018, 2021).

Detecting changes in early deoxygenation has been considered a more useful spatial indicator of neuronal activity than increases in oxyHb or cerebral blood volume (CBV) because they occur in a more limited area (Ances, 2003; Kato, 2004; Khan et al., 2021). However, the oxygen consumption and supply triggered by neuroactivation cannot be evaluated simultaneously based on deoxyHb alone. In terms of technological advances, earlier NIRS was used as a cerebral oxygen monitor that could be measured over the scalp, and it was not until July 1991 that it was first successfully demonstrated that fNIRS could detect regional brain function (Kato, 2018). In addition, there was a lack of theory to quantitatively integrate neural activation from multiple sites (channels) and indices (Kato et al., 1993; Ferrari and Quaresima, 2012).

A vector-based model of cerebral oxygen regulation (CORE model; Kato, 2006, 2013) can explain variations in the ratios of concentration changes in oxyHb and deoxyHb without exception. Vector-based fNIRS allows the integration of the dynamics of oxyHb and deoxyHb changes in multiple channels on the same vector coordinates, thus enabling the detection of oxygen dynamics as differences between CORE vectors. Oxygen consumption associated with neuroactivation can be classified into one of eight phases according to the combination of the CORE vector components, i.e., oxyHb, deoxyHb, CBV, and cerebral oxygen exchange (COE). Using vector-based fNIRS, the patterns of FORCE in the language area were analyzed and classified into five levels based on variations in oxygen consumption (Yoshino and Kato, 2012).

A technique has been proposed for detecting and imaging the spatial distribution of neuroactivation by differentiating the phase distributions of oxygen consumption and oxygen supply (Kato et al., 2003; Kato, 2018). Temporal FORCE effects were reported to be detected 2–3 s after the onset of the stimulus task. Therefore, it was hypothesized that when neural activity is strongly induced, the FORCE effect occurs over a larger spatial area and for a longer period of time. Furthermore, it is assumed that the oxygen consumption and oxygen supply distributions do not coincide with the oxygen consumption distribution due to neural activation during exercise when the FORCE effect strongly appears. As a result, when oxygen consumption increases in the M1 and a strong FORCE effect is induced, a mechanism to supply fresh blood to the area around M1 could be detected. Therefore, the task of lifting heavier dumbbells has been chosen, which could be predicted to elicit strong neural activity in M1.

To identify differences in the strength of neuroactivation, measurements were taken from the M1 and surrounding sites using vector-based fNIRS during exercise tasks using three different dumbbell weights and report a new imaging method for differentiating between oxygen consumption and supply.

Materials and methods

Subjects

The subjects of this study were seven healthy adults: six males and one female; the mean age was 33.3 ± 8.0 years. The participants had some experience in sports before age 20, but had not received any intensive strength training for at least 1 year.

All participants were identified as being right-handed based on the Edinburgh Handedness Inventory. The study was explained to the subjects in writing and orally, and they provided prior written consent for participation in and reporting of this study.

The experimental procedure complied with the principles of the Declaration of Helsinki. All subjects received full explanation of the procedures and provided written informed consent for participation in the study. This study was reviewed and approved by the Ethics Committee of KatoBrain Co., Ltd. which included outside members.

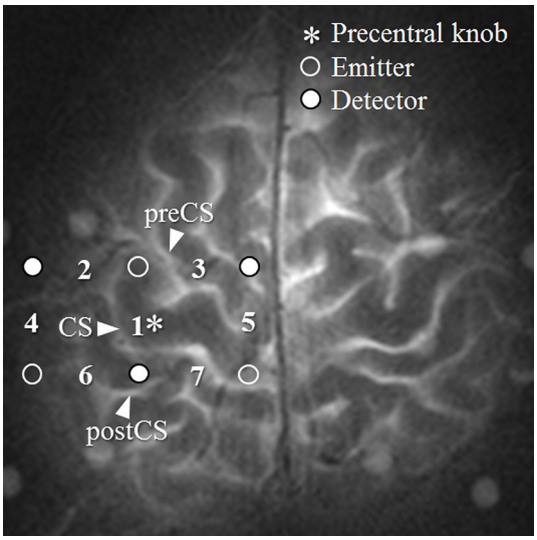

FIGURE 1
Region of measurement. The numbers between the detectors and emitters are channel numbers. CS, central sulcus.

fNIRS measurement

A multi-channel NIRS apparatus (ETG-100) monitored localized changes in oxyHb and deoxyHb. The scalp was irradiated at each site with two wavelengths of near-infrared light (780 and 830 nm) from a semi-conductor laser using three optical fibers. Three avalanche photodiodes detected light passing through the head. Hb concentration measurements were recorded at a sampling rate of 10 Hz.

Measurements were collected from a total of seven channels (Figure 1). Channel 1 was positioned directly over the left M1, and the remaining six channels were arranged around it: channel 2 lateral to the precentral knob, channel 3 in the premotor area, channel 5 in the SMA, and channels 4, 6, and 7 over the postcentral gyrus. The distance between emitter and detector probes was 30 mm. The M1 was identified using a technique for pre-measurement identification of target cortex sites that utilizes the distance between points of reference on the scalp from the subject's MRI (Murakoshi and Kato, 2006). The right M1 was measured by fNIRS simultaneously with the left M1. However, the analysis was limited to the left-hemisphere channel.

Experimental procedure

The task used in this study to investigate the effects of the strength of neural activity was a dumbbell-lifting exercise that involved flexing and extending the elbow joints of both arms. It has been reported that movement-related cortical potentials increase more for isometric contractions of the elbow flexors under a heavy load than they do under a light load (Oda et al., 1996). Therefore, there were three different weights: 0 kg (no dumbbell), and dumbbells weighing 4.5 and 9.5 kg. One trial consisted of flexing and extending a given weight 12 times. Repetitions were paced at 3 s (Tamaki et al., 1994), for a total of 36 s per trial, with a 60 s resting period between trials. Each repetition lasted for 1.5 s, for a total of 3 s. Five trials with each weight made up a trial set. After completing a trial set for one weight, the subject went on to the next, heavier weight. The training order was always from lightest to heaviest, with participants always set to be most fatigued on the heaviest trial set.

For the 0 and 4.5 kg tasks, a total of 35 trials performed by the seven subjects were used for analysis. For the 9.5 kg task, one subject completed only one trial and another subject only four because the weight was too heavy, and a total of 30 trials were used for analysis.

The weight of the dumbbells that can be lifted could be different for each individual.

However, the neural activity to M1 and its surrounding sites is expected to be higher with the dumbbell weighing more. Therefore, instead of selecting the dumbbell weight that produces maximal voluntary muscle contraction, a uniform dumbbell weight was set.

Theory of vector-based analysis

A vector-based model of CORE

The CORE model (Kato, 2004, 2006, 2013) can simultaneously detect seven indices reflecting the oxygen consumption and supply caused by neuroactivation. OxyHb and deoxyHb have different chemical properties (paramagnetic or diamagnetic) arising from differences in the bonding of oxygen molecules (Pauling and Coryell, 1936). The axes oxyHb (ΔO) and deoxyHb (ΔD) define an orthogonal vector coordinate plane. Rotating this $\Delta O/\Delta D$ vector plane by 45° counterclockwise results in an orthogonal vector coordinate plane comprising a ($\Delta O + \Delta D$) axis and a ($\Delta D - \Delta O$) axis. The ($\Delta O + \Delta D$) vector can be defined as the CBV vector (ΔCBV), and the ($\Delta D - \Delta O$) vector can be considered as the COE vector (ΔCOE).

The relationship among the four axes, ΔO, ΔD, ΔCBV, and ΔCOE, is described by the following square matrix:

$$\begin{pmatrix} \Delta O + \Delta D \\ -\Delta O + \Delta D \end{pmatrix} = \begin{pmatrix} 1 & 1 \\ -1 & 1 \end{pmatrix} \begin{pmatrix} \Delta O \\ \Delta D \end{pmatrix} = \begin{pmatrix} \Delta CBV \\ \Delta COE \end{pmatrix} \quad (1)$$

$$\begin{pmatrix} \Delta O \\ \Delta D \end{pmatrix} = \frac{1}{2} \begin{pmatrix} 1 & -1 \\ 1 & 1 \end{pmatrix} \begin{pmatrix} \Delta CBV \\ \Delta COE \end{pmatrix} \quad (2)$$

The polar coordinate plane comprising these four axes is termed as the CORE vector plane and the vector tracks on the polar

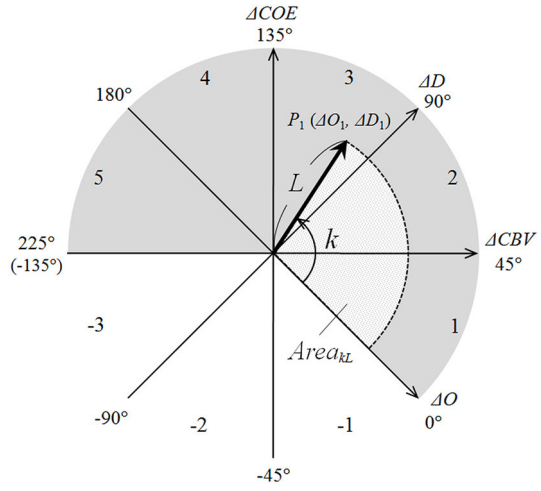

FIGURE 2
CORE vector coordinates. Values for k (in degrees) are shown at the tips of the axes. Phase numbers are shown in each octant arc.

coordinate as CORE vectors (Figure 2). The vectors have four components, i.e., ΔO, ΔD, ΔCBV, and ΔCOE, and the analysis of the CORE vectors allows handling these four Hb indices as the components of a wave.

On the CORE vector plane, a positive value for ΔCBV indicates increasing ΔCBV and a negative value for ΔCBV indicates decreasing ΔCBV; moreover, a positive value for ΔCOE indicates increasing ΔCOE and shows hypoxic change, and a negative value for ΔCOE indicates decreasing ΔCOE and shows hyperoxic change. In other words, ΔCOE reflects increasing or decreasing cerebral oxygen extraction from the capillaries to the cells.

Phase components of CORE vectors

The phases on the CORE vector plane are quantitatively defined indices of the degree of oxygen exchange that reflect the strength of oxygen consumption. Phase is defined by the angle k, the ratio of ΔD to ΔO. k is the angle between a CORE vector and the positive ΔO axis and is determined as follows:

$$k = Arc\ \tan\left(\frac{\Delta D}{\Delta O}\right) = Arc\ \tan\left(\frac{\Delta COE}{\Delta CBV}\right) + 45^\circ \quad \left(-135^\circ \leqq k \leqq 225^\circ\right) \tag{3}$$

It is a quantitative index indicating the degree of oxygen consumption over a certain period. $k = 0^\circ$ is on the positive ΔO axis and coincides with the oxygen density of arterial blood. Thus, an increase or decrease in k indicates a change in oxygen density. The eight octants of 45° on the vector plane in Figure 1 can be classified into activation phases (Phases 1 through 5) and non-activation phases (Phases −1 through −3). Phase 1 ($0 < \Delta D < \Delta O$; $\Delta COE < 0 < \Delta CBV$) and Phase 2 ($0 < \Delta O < \Delta D$; $0 < \Delta COE < \Delta CBV$) are canonical activation, showing increases in both ΔD and ΔO. Phase 3 ($\Delta O < 0 < \Delta D$; $0 < \Delta CBV < \Delta COE$) is hypoxic–hyperemic activation, showing a decrease in ΔO together with an increase in ΔCBV. Phase 4 ($\Delta O < 0 < \Delta D$; $\Delta CBV < 0 < \Delta COE$) and Phase 5 ($\Delta O < \Delta D < 0$; $\Delta CBV < 0 < \Delta COE$) are hypoxic–ischemic activation, showing an increase in ΔCOE together with a decrease in ΔCBV. Conversely, Phases −1 through −3 indicate non-activation and show decreases in both ΔD and ΔCOE. Oxygen consumption during neuroactivation can be considered higher during the activation phases vs. the non-activation phases.

The scalar L

The scalar L between point P_1 (ΔO_1, ΔD_1) and the origin can be described by the following equation:

$$L = \sqrt{(\Delta O_1)^2 + (\Delta D_1)^2} = \frac{1}{\sqrt{2}}\sqrt{(\Delta COE_1)^2 + (\Delta CBV_1)^2}, \tag{4}$$

where L represents the intensity of Hb changes (oxyHb and deoxyHb); i.e., the scalar component L of the CORE vector also includes ΔCBV and ΔCOE.

The contribution percentage of ΔO and ΔD to L is calculated by squaring both sides of Equation (4).

$$1 = \left(\frac{\Delta O}{L}\right)^2 + \left(\frac{\Delta D}{L}\right)^2 \tag{5}$$

$$\text{Percentage contributed by } \Delta O: \left(\frac{\Delta O}{L}\right)^2 \times 100\ (\%) \tag{6}$$

$$\text{Percentage contributed by } \Delta D: \left(\frac{\Delta D}{L}\right)^2 \times 100\ (\%) \tag{7}$$

The following relationship exists between L and the angle k:

$$\begin{pmatrix}\Delta COE \\ \Delta CBV\end{pmatrix} = L\begin{pmatrix}\cos k \\ \sin k\end{pmatrix} \tag{8}$$

In this way, CORE vectors have properties of waves: phase (k) and intensity (L). The imaging of k indicates the phase distribution of oxygen consumption, whereas the imaging of ΔO shows the distribution of oxygen supply. The distribution of the percentages of contribution by ΔO indicates the relative contribution of ΔO that is affected by changes in k with respect to L.

Oxygen regulation index

A new index was created to reflect phase and amplitude (L). The area created by the rotational motion of the CORE vector is defined on the vector plane using L_t and the radian of k (k_t^{rad}), as follows:

$$Area_{kL} = \sum_{n=1}^{n} \frac{1}{2}\ k^{rad}{}_t \bullet {L_t}^2, \tag{9}$$

where n is the number of trials analyzed for all subjects An $Area_{kL}$ is a cumulative area encompassed by the CORE vector track; that is, the area swept out by L_t over the range of k_t degrees from the positive ΔO axis ($k = 0^\circ$) during t seconds from task initiation. A positive value for $Area_{kL}$ indicates an area increasing in the direction of increased oxygen exchange degree ($0^\circ < k$), and a negative value indicates an area increasing in the direction of increased oxygen not used for oxygen exchange ($k < 0^\circ$).

Vector-based analysis

Measurements performed over 36 s during a trial and 36 s after a trial were used for analysis. Functional imaging was performed using seven indices: the four-vector components (ΔO, ΔD, ΔCBV, and ΔCOE) of the addition vectors during the tasks, phase (k), the scalar (L), and the oxygen regulation index ($Area_{kL}$).

The time-course changes were averaged, with each trial onset set as zero. The time-course changes in ΔCBV and ΔCOE were calculated from the time-course changes in ΔO and ΔD using Equations (1) and (2). Vector tracks were plotted using task onset as the origin and the grand averages calculated for all trials for each component. No baseline normalization or motion correction was performed as a preprocessing step for the analysis, as these may distort the phase of oxygen exchange (Kato, 2021).

CORE addition vectors during and after the tasks were calculated to observe total changes across the task time. The cumulative sums of ΔCBV and ΔCOE grand averages were determined, and the CORE addition vectors were plotted using those values. Imaging of each vector component (ΔO, ΔD, ΔCBV, and ΔCOE) was carried out using the cumulative sums recorded during the task. Imaging of k and L was performed using Equations (3) and (4), with values determined from the CORE addition vectors. Imaging of $Area_{kL}$ was carried out based on Equation (9) based on the cumulative sums of the area determined from k and L of the single-trial CORE addition vectors.

The phase distribution of a CORE vector was determined by first classifying k for each trial into the appropriate octant and then calculating the ratio of the number of trials in each phase to the total number of trials for analysis for each task. Phase distribution for the sites surrounding the left M1 was calculated by averaging the phase distributions of all surrounding channels.

Spatial concordance between k and L was calculated as the ratio of the number of trials in which the maximum values for k and L coincided with the number of trials in the analysis of each task.

The percent contribution of ΔO and ΔD to L was calculated using Equations (6) and (7). Values for L of the CORE addition vectors and the cumulative sums of ΔD and ΔO were used for the calculation. The contribution rates for the sites surrounding the left M1 were averaged from the contribution rates of all channels. Differences in contribution rates were calculated by subtracting the percentages for ΔO from those for ΔD.

Statistics

Multiple analysis of variance and *post-hoc* multiple comparison tests (Scheffe's) were performed using ΔCBV and ΔCOE for all trials to determine the significance of differences between the left M1 and the averages of the surrounding sites. Statistical tests were performed for k, L, and the $Area_{kL}$, to determine the significance of differences between the left M1 and the averages of surrounding sites. Independent t-tests were used for L and the $Area_{kL}$, and Watson's U2 test was used for k. Differences in phase distribution between the left M1 and the surrounding sites were compared using Fisher's exact test for each phase.

Results

Time courses and functional images of CORE vector components

Figure 3A shows the average time courses for each vector component during and after the tasks. Figure 3B is a functional image of the four-vector components during a task. At the left M1 (channel 1), ΔO decreased for the 4.5 and 9.5 kg tasks, whereas ΔD and ΔCBV increased. However, in the surrounding sites, ΔO increased, and ΔD and ΔCOE decreased. The left M1, where the maximum decrease in ΔO occurred, was surrounded by a high oxygen supply (increased ΔO), in a donut-like shape. The sites of maximum increase in ΔD and ΔCOE were the left M1 for the 4.5 and 9.5 kg tasks and the SMA (channel 5) for the 0 kg task. ΔCBV increased in both the left M1 and the surrounding sites, not indicating localization. At 9.5 kg, the rate of the maximum increase of each vector component at the left M1 was 0% for ΔO, 0% for ΔCBV, 56.7% for ΔD, and 63.3% for ΔCOE.

Functional images using k, L, and the new index $Area_{kL}$

Figure 4 provides functional images of k, L, and the $Area_{kL}$. The SMA was the site with the maximum increase in k at 0 kg. At 4.5 and 9.5 kg, the left M1 showed the maximum increase in k, whereas oxygen consumption decreased in the surrounding area. The maximum increase in L appeared not at the left M1, but in the surrounding area. The spatial concordance of the

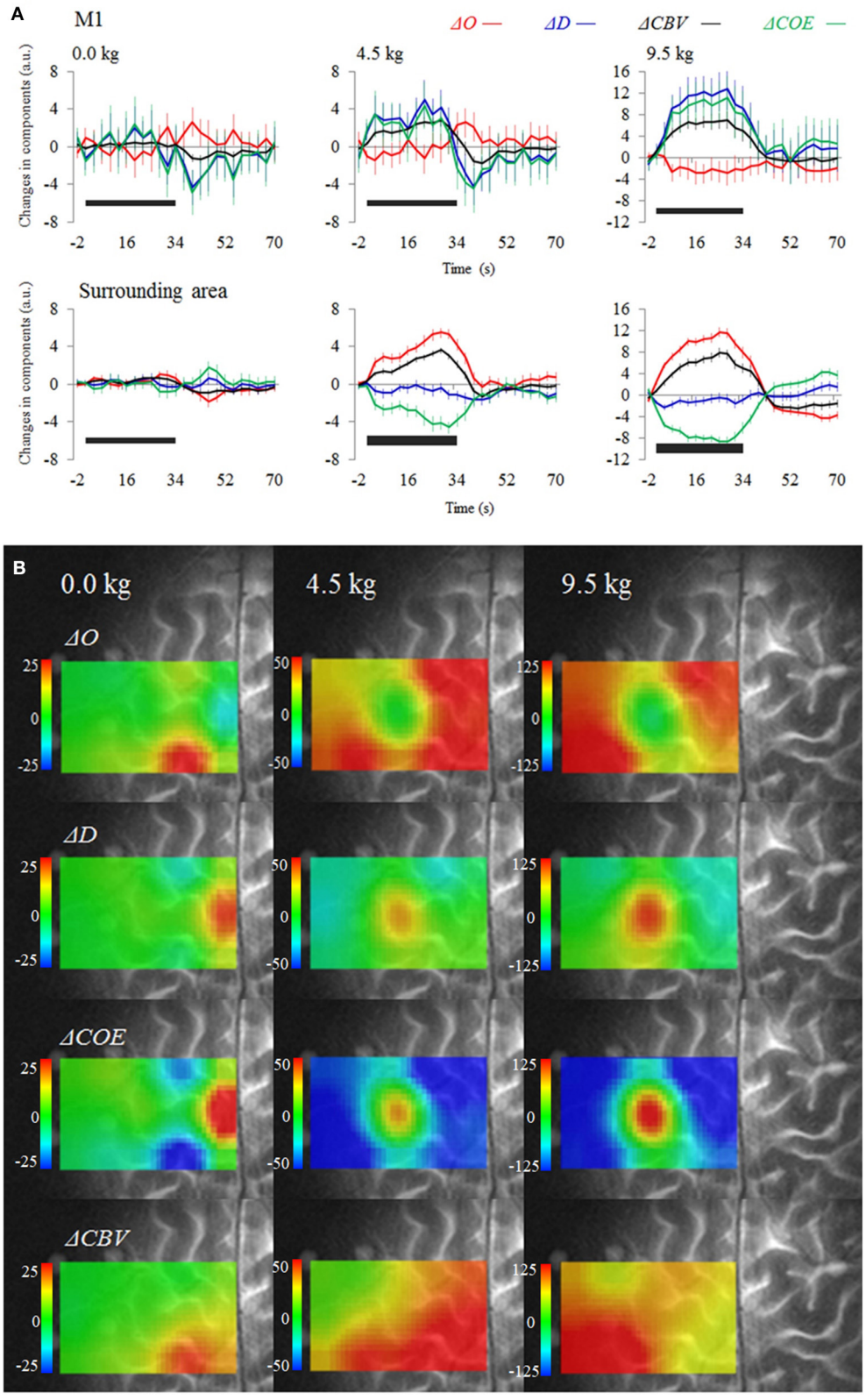

FIGURE 3
(A) Average time courses and standard error for the four-vector components at the left M1 and surrounding sites (averaged). **(B)** Functional images show changes in the vector components during a task. The black bars on the figure represent the period of the dumbbell exercise.

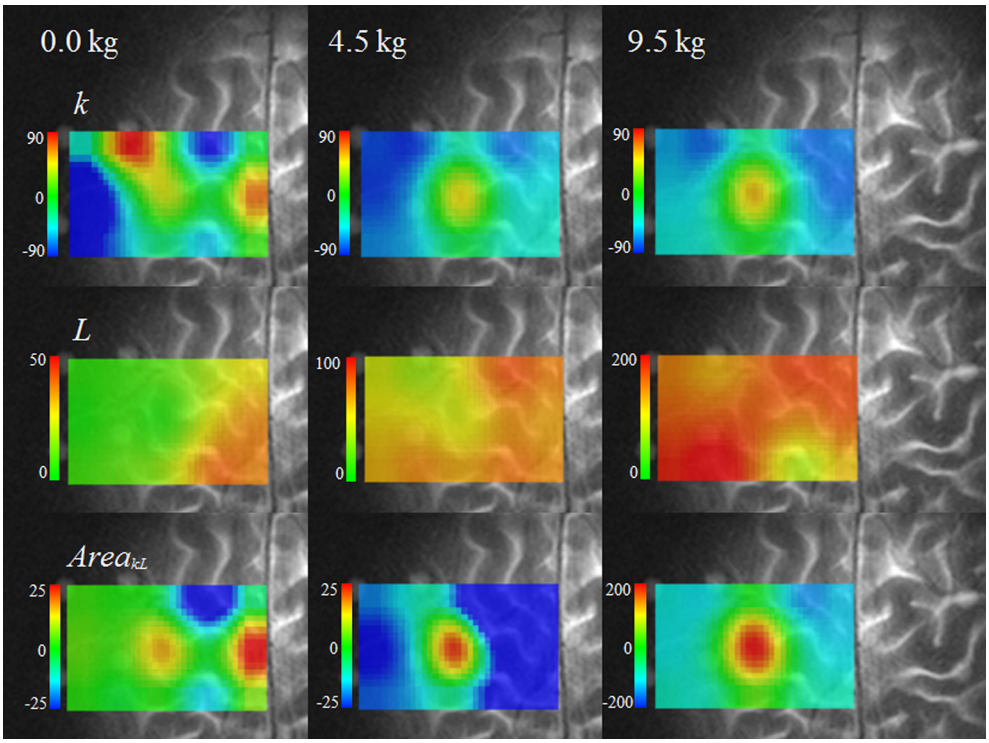

FIGURE 4
Functional images of three indices (*k*, *L*, and $Area_{kL}$) during tasks.

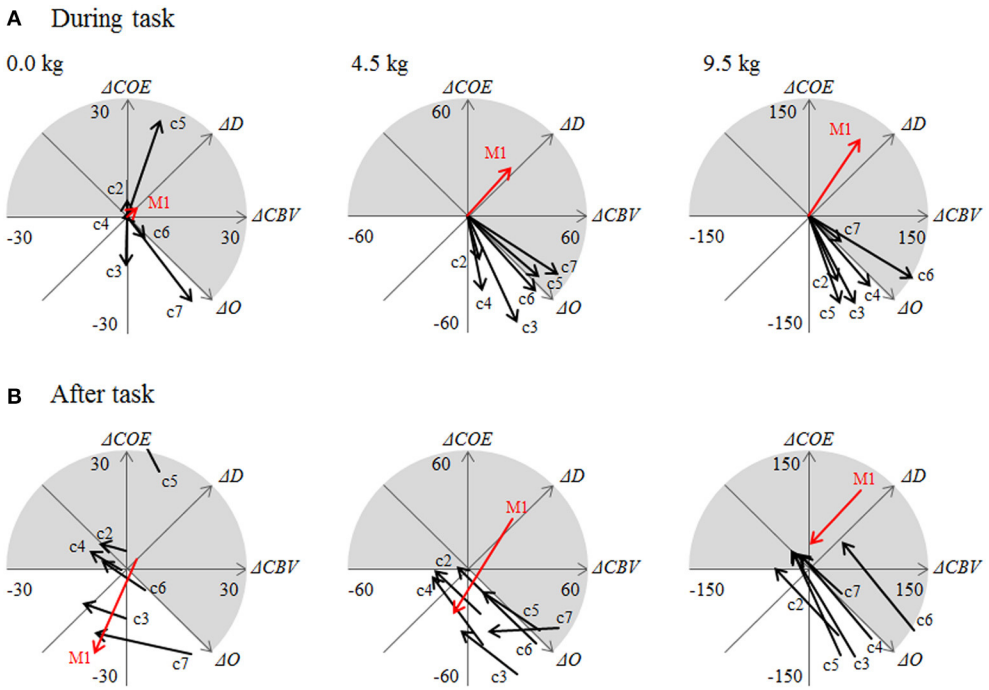

FIGURE 5
(A) Addition vectors during a task (0–36 s) and **(B)** after the task (36–72 s). c2 through c7 are the numbers of channels in the area surrounding the left M1, as shown in Figure 2.

maximum increases in k and L was low; 11.4% at 0 kg, 17.1% at 4.5 kg, and 20.0% at 9.5 kg.

The spatial concordance of the maximum increases in k and $Area_{kL}$ increased as the dumbbell weight increased; 37.1% at 0 kg, 54.3% at 4.5 kg, and 76.7% at 9.5 kg. $Area_{kL}$ showed a significantly greater increase at the left M1 compared with the surrounding area (4.5 and 9.5 kg) ($P < 0.01$), indicating increased oxygen consumption. The site of maximum increase in $Area_{kL}$ was the SMA at 0 kg. The imaging of $Area_{kL}$ emphasized the changes at the left M1 and SMA and allowed the detection of a small increase in oxygen consumption at the left M1 that could not be detected in images of the single-vector components or L.

Differentiation of phase during and after motor exercise

Figure 5 displays the CORE addition vectors during the task (36 s) and after the task (36 s) at each channel.

Table 1 shows the phase distribution of the CORE addition vectors at the left M1 and surrounding sites.

Vectors for the 4.5 and 9.5 kg tasks showed significant differences between the left M1 and the surrounding sites ($P < 0.01$). The most common phase at the left M1 was Phase 3, indicating hypoxic–hyperemic activation. The percent occurrence of Phase 3 at the left M1 was 31.4% at 0 kg, 54.3% at 4.5 kg, and 46.7% at 9.5 kg, which were all significantly higher than those detected in the surrounding sites (Table 1). At this time, k was 83.9° at 0 kg, 93.8° at 4.5 kg, and 101.6° at 9.5 kg, which were also significantly higher than those detected in the surrounding sites ($P < 0.05$). Vectors in the surrounding sites were significantly concentrated in Phases −1 and −2, which are non-activation phases. In the surrounding area, k ranged from −118.3° to 135.2° at 0 kg, from −34.0° to 11.6° at 4.5 kg, and from −25.5° to 14.0° at 9.5 kg.

After the tasks, the phase differences between the left M1 and the surrounding sites disappeared. The direction of the vectors changed and moved toward the origin.

During the task, L increased significantly with increased dumbbell weight at both the left M1 and the surrounding area ($P < 0.01$). In the 4.5 and 9.5 kg tasks, there was no significant difference between L at the left M1 and the surrounding sites. In this way, the CORE vectors showed specific phase distributions according to site and task.

Contribution rate of ΔO and ΔD related to L change

Table 2 reports the relative contributions of ΔO and ΔD to L during the tasks. The contribution percentages from ΔO and ΔD were different for each measurement channel. At the left M1, the contribution of ΔO was small, at <4.0%, whereas the contribution of ΔD was more than 96%, which represented a difference of ∼92%.

At the sites surrounding the left M1, the contribution rate was higher for ΔO than for ΔD. Differences in the contribution rates of ΔO and ΔD increased as the dumbbell weights became heavier: 12.8% at 0 kg, 65.8% at 4.5 kg, and 83.8% at 9.5 kg. Namely, the donut-shaped image surrounding the site of maximum increase in oxygen consumption became clearer as the dumbbell weight increased from 0 to 4.5 kg and then to 9.5 kg, reflecting the increase in oxygen supply (ΔO increase) in the area surrounding the M1 unaccompanied by oxygen consumption as the dumbbell weight increased.

Although at 0 kg L was smaller at the left M1 than it was at the surrounding sites (Figure 5), the contribution of ΔO at the left M1 was lower (1.1%) than it was at the surrounding sites (56.4%).

Discussion

Spatial distribution of COE

Differences in the distribution of oxygen consumption are quantifiable using the images of k, which represents the degree of oxygen exchange. During dumbbell exercises, oxygen exchange increased at the left M1, indicating a localized increase in oxygen consumption. In the area surrounding the left M1, oxygen exchange decreased, and oxygen supply increased unaccompanied by oxygen consumption. The spatial concordance between the maximum values for the degree of oxygen exchange during a task and L, which reflects the intensity of Hb changes, was <20%. The contribution rates of ΔO and ΔD differed according to the measurement site. Therefore, the hypothesis that the distribution of oxygen consumption associated with neural activation does not coincide with the distribution of oxygen supply was supported in the motor task study.

Interestingly, an increasing difference in the relative contribution of ΔO and ΔD in the area surrounding the M1 was found as the dumbbell weights increased, which suggests that oxygen supply in the surrounding area is regulated concerning the site of increasing oxygen consumption. Even at sites of increased oxygen consumption, the contribution of ΔO was found to be low. It is believed that neural activity and local cerebral blood flow (CBF) increase or decrease relatively correlatedly. Similarly, local CBF and local CBV are also thought to increase or decrease in correlation. However, it is thought that, in brain regions where COE has increased markedly because of a rapid and sustained increase in oxygen consumption relative to oxygen supply, there is a mechanism

TABLE 1 Phase distribution (%) of the CORE vectors during the tasks.

Phase	0.0 kg		4.5 kg		9.5 kg	
	MI	Surrounding area	MI	Surrounding area	MI	Surrounding area
1	2.9	9.0	5.7	19.0	10.0	22.2
2	2.9	10.5	2.9	6.7	10.0	7.2
3	31.4*	16.2	54.3**	11.0	46.7**	3.9
4	5.7	12.4	5.7	4.3	0.0	0.6
5	2.9	9.5	0.0	7.1	0.0	0.0
−1	11.4	18.6	20.0	38.1*	16.7	43.3**
−2	42.9**	16.7	8.6	9.0	16.7	15.6
−3	0.0	7.1	2.9	4.8	0.0	7.2
Total (%)	100.0	100.0	100.0	100.0	100.0	100.0

The asterisks indicate significant differences between the left M1 and the surrounding sites for the same phase (*$P < 0.1$, **$P < 0.01$).

TABLE 2 Average contribution to *L* and differences in the relative contributions of ΔD and ΔO during a task.

Site	Task (kg)	ΔO (%)	ΔD (%)	Differences (%)
M1	0	1.1	98.9	97.7
	4.5	0.4	99.6	99.1
	9.5	4.0	96.0	91.9
Surrounding area	0	56.4	43.6	−12.8
	4.5	87.9	12.1	−75.7
	9.5	91.9	8.1	83.8

Differences were determined by subtracting the contribution of ΔO from that of ΔD.

of cerebral blood circulation that promotes replenishment from surrounding sites with sufficient oxygen supply.

Neural activity may not always correlate with local CBV or CBF when it has a strong impact on the COE homeostasis for the whole brain, as in the results of this study. The detection of an excessive increase in ΔCBV rather than an increase in ΔCOE around the near regions of rapidly increasing oxygen consumption was not previously known and therefore has not been incorporated into conventional models of cerebral circulation regulation (Roy and Sherrington, 1890; Lassen, 1959). A new model of whole brain circulation regulation is needed that can explain the mechanisms that maintain COE homeostasis for the whole brain.

Using the vector method fNIRS, it is necessary to study further how the oxygen supply in the brain is regulated from the site of increased oxygen exchange in the brain and its surrounding areas. The nature of the mechanisms that regulate the simultaneous oxygen supply at sites of increased oxygen exchange is also an important research topic at the level of whole brain regulation and at the level of more microscopic cell populations. As the weight of dumbbells lifted increases or the subject's muscle fatigue increases, the mechanisms that attempts to maintain COE homeostasis for the whole brain may be more likely to be strongly detected by vector method fNIRS. Thus, the closer to maximal voluntary muscle contraction, the more brain-muscle coordination may be required.

Compared with previous studies using verbal tasks (Kato et al., 2003; Yoshino and Kato, 2012), the present results suggest that, during muscle training, oxygen consumption and oxygen supply are controlled in areas of the cortex within a few centimeters square.

The FORCE, which is an oxygen-consuming response that occurs in a high neuroactivation site, has been observed in invasive human studies using optical imaging (Suh et al., 2006). However, it does not report that the phenomenon of oxygen supply surrounding the FORCE effect in the form of a doughnut has occurred, as obtained in this experiment. The strong and persistent FORCE effect on the homeostasis of oxygen exchange for the whole brain, as obtained in this experiment, may be a different brain mechanism from the temporary FORCE that has been previously reported (Kato, 2004, 2018).

It has been shown that γ-aminobutyric acid (GABA) concentrations during a motor learning task decrease in the left M1 and increase around it (Gudberg et al., 2012).

Studies using proton magnetic resonance spectroscopy have shown interactions between M1 and its surrounding sites in neurotransmitters (Umesawa et al., 2020; Maruyama et al., 2021). Although this method cannot measure intracellular

and extracellular GABA separately, it could be used in conjunction with the vector method fNIRS to clarify the relationship between oxygen metabolism and GABA. However, because the dumbbell task is not a motor learning task, it does not necessarily elicit the same response as the strength training task. Further evidence and discussion of the physiological link between GABA and oxygen kinetics are needed.

Advantages of vector-based analysis

The CORE model of 2-dimensional analysis of ΔO and ΔD was used to simultaneously generate functional distribution images using seven indices, including oxygen exchange.

The advantage of vector-based fNIRS is that multiple indices with different physiological significance can be compared to understand better neurovascular-coupling mechanisms and neuro-oxygen coupling that accompany neuroactivation. Conversely, these indices cannot be separately detected using the fMRI BOLD signal, which includes the effects of both oxyHb and deoxyHb changes (Yamamoto and Kato, 2002).

Unlike the other component images, the oxygen exchange images were able to indicate both high oxygen exchange sites, such as Phase 3 sites (common in the M1), and reduced oxygen exchange sites, such as Phase −1 (more common in the surrounding area), even though ΔCBV increased in the same way in both types of sites. The fact that the M1 site was most frequently a Phase 3 site (ΔCOE increased more than ΔCBV) reflects the fact that the increase in ΔD attributable to oxygen consumption exceeds the increase in ΔO from oxygen supply. Together with k, the ΔD and ΔCOE indices (reflecting oxygen consumption) increased most at the SMA for 0 kg, and at the M1 for 4.5 and 9.5 kg. However, the sites showing maximum increases in the ΔO, ΔCBV, and L indices (strongly affected by blood supply) did not coincide with the M1. Phase −1 is a non-activation phase, and I also observed that it did not reflect neuroactivation in a language task (Yoshino and Kato, 2012). In Phase −1, ΔO increases and ΔD decreases, which has been considered a typical fNIRS activation pattern; however, oxygen consumption is low in this phase, and it has become clear that it does not indicate a site where activation is strong. Based on our results, an increase in ΔCBV at a site does not necessarily imply an increase in oxygen demand. Variations were found in the oxygen exchange response concerning the amount of increase in ΔO or ΔCBV. For example, it was reported that, during a motor task, $CMRO_2$ did not increase significantly at the M1, whereas CBF did (Vafaee et al., 2012); conversely, CBF did not increase significantly in the visual cortex, although $CMRO_2$ did (Mintun et al., 2001).

Possibilities and limitations of vector-based fNIRS

$Area_{kL}$, which combines the indices k and L, proved to be useful for clearly imaging slight neuroactivation at the left M1 and SMA during a 0 kg task. Increased oxygen exchange, rather than the intensity of oxygen supply, coincided with the neuroactivation site. This result shows that the location and intensity of neuroactivation cannot be accurately estimated from the intensity of Hb concentration changes. Mintun et al. (2001) strongly suggested that increased CBF is caused by factors other than oxygen demand. The response at the M1 was in danger of being overlooked, masked by the intensity of ΔO. However, even small Hb changes, such as those from cognitive tasks, can provide dynamic oxygen consumption and oxygen supply images if $Area_{kL}$ is used.

Because the dumbbell load in our study was sufficient to cause a systemic cardiovascular response, it is possible that systemic circulatory changes or scalp perfusion were included in the ΔO increases in the sites surrounding M1 (Kato et al., 1999). However, the donut-shaped excessive oxygen supply response generated in the area surrounding the neuroactivation site cannot be explained simply by changes in the systemic circulation. The most recent study (Kato, 2021) showed that vector-based fNIRS was less susceptible to artifacts from whole-body cardiovascular responses and motion. In other words, detecting localized increases in k may allow us to discount the broader influence of circulation and the autonomous nervous system.

I also observed an increase in k in a prior study of passive word listening (1.5-s tasks) that was unlikely to cause systemic circulation changes (Yoshino and Kato, 2012). It is important to note that the use of baseline normalization or motion correction to preprocess the data for analysis may distort the phase of oxygen exchange. For a rigorous study, it is interesting to use data from short channels where the distance between probes detects only the scalp. Even in such a comparative study, it may not be possible to conclude that systemic changes are not involved in brain responses.

When describing the exercise during validation, the loads used were 0, 4.5, and 9.5 kg, citing previous research showing that cortical potentials increase more with heavier loads (Tamaki et al., 1994). Due to the lack of information on the maximum voluntary muscle contraction of the participants' biceps curls, it is impossible to determine whether these loads were truly heavy for the participants. Bearability for loads varies from person to person; what may be light for one person may be heavy for another. It is necessary to study the COE distribution when using dumbbells of a weight that cannot be lifted and the relationship between maximal voluntary muscle contraction and oxygen exchange. By focusing on the strong FORCE effect and the surrounding oxygen supply response using the vector-based

fNIRS, it may be possible to distinguish whether the subject's inability to lift the dumbbell is due to muscle fatigue or brain fatigue, or whether the patient is capable of lifting the dumbbell but does not intentionally try to do so.

Conclusion

Vector-based fNIRS allows to image the spatial dissociation between oxygen consumption and supply in the brain during the dumbbell exercises. Based on seven indexes, vector-based fNIRS can image aspects of motor activation that other brain functional imaging modalities cannot detect. Moreover, vector-based fNIRS is a useful brain measurement method for understanding how increased oxygen exchange in M1 causes hypoxia and how the area surrounding the M1 provides fresh blood volume. The comparison of *k*, *L*, an index reflecting the local oxygen exchange distribution and its intensity obtained from vector-based fNIRS, with indices such as CBV, COE, OxyHb, DeoxyHb, CBF, and CMRO2 will be an important topic for future fNIRS studies to interpret oxygen dynamics better.

Data availability statement

The raw data supporting the conclusions of this article will be made available by the author, without undue reservation.

Ethics statement

The studies involving human participants were reviewed and approved by the Ethics Committee of KatoBrain Co. Ltd. The patients/participants provided their written informed consent to participate in this study.

Author contributions

TK contributed to conception and design of the study, organized the data, and wrote the draft of the manuscript.

Acknowledgments

This study was partly supported by Akira Endo, M.D., Ph.D. for supervision of task design and the physical care of subjects during the experiment, and Patricia Yonemura, Hiroshi Kato and Enago (www.enago.jp) for the English language review.

Conflict of interest

Author TK was employed by KatoBrain Co., Ltd.

Publisher's note

All claims expressed in this article are solely those of the authors and do not necessarily represent those of their affiliated organizations, or those of the publisher, the editors and the reviewers. Any product that may be evaluated in this article, or claim that may be made by its manufacturer, is not guaranteed or endorsed by the publisher.

References

Akiyama, T., Ohira, T., Kawase, T., and Kato, T. (2006). TMS orientation for NIRS-functional motor mapping. *Brain Topogr.* 19, 1–9. doi: 10.1007/s10548-006-0007-9

Ances, B. M. (2003). Coupling of changes in cerebral blood flow with neural activity: what must initially dip must come back up. *J. Cereb. Blood Flow Metab.* 24, 1–6. doi: 10.1097/01.WCB.0000103920.96801.12

Cyranoski, D. (2011). Thought experiment. *Nature* 469, 148–149. doi: 10.1038/469148a

Ferrari, M., and Quaresima, V. (2012). A brief review on the history of human functional near-infrared spectroscopy (fNIRS) development and fields of application. *Neuroimage* 63, 921–935. doi: 10.1016/j.neuroimage.2012.03.049

Gudberg, C. A., Stagg, C. J., Near, J., and Johansen-Berg, H. (2012). "Motor learning and offline processes of consolidation associated with rapid GABA modulation," in *18th Annual Meeting of the Organization for Human Brain Mapping* (Beijing).

Hatakenaka, M., Miyai, I., Mihara, M., Sakoda, S., and Kubota, K. (2007). Frontal regions involved in learning of motor skill-A functional NIRS study. *Neuroimage* 34, 109–116. doi: 10.1016/j.neuroimage.2006.08.014

Kato, T. (2004). Principle and technique of NIRS imaging for human brain FORCE: fast-oxygen response in capillary event. *Proc. ISBET* 1270, 85–90. doi: 10.1016/j.ics.2004.05.052

Kato, T. (2006). *Apparatus for Evaluating Biological Function*. U.S. Patent No 7,065,392. Washington, DC: U.S. Patent and Trademark Office.

Kato, T. (2013). *Apparatus for Evaluating Biological Function, a Method for Evaluating Biological Function, a Living Body Probe, a Living Body Probe Mounting Device, a Living Body Probe Support Device and a Living Body Probe Mounting Accessory*. U.S. Patent No 8,406,838. Washington, DC: U.S. Patent and Trademark Office.

Kato, T. (2018). *Vector-Based Approach for the Detection of Initial Dips Using Functional Near-Infrared Spectroscopy, Neuroimaging - Structure, Function and Mind, Sanja Josef Golubic*. IntechOpen. Available online at: https://www.intechopen.com/chapters/63385 (accessed August 30, 2022).

Kato, T. (2021). *Biological Function Measurement Device, and Biological Function Measurement Method, and Program*. U.K. Patent GB2595162, Application Number 202,111,659. Newport: Intellectual Property Office.

Kato, T., Kamei, A., Takashima, S., and Ozaki, T. (1993). Human visual cortical function during photic stimulation monitoring by means of near-infrared spectroscopy. *J. Cereb. Blood Flow Metab.* 13, 516–520 doi: 10.1038/jcbfm.1993.66

Kato, T., Kumoi, M., and Koike, T. (2003). "Temporal spatial imaging of k-ratio and k-angle as oxygen exchange ratio between oxyhemoglobin and deoxyhemoglobin," in *9th Annual Meeting of the Organization for Human Brain Mapping, Vol. 19 (Suppl)* (New York, NY), 673.

Kato, T., Yamashita, Y., Sugihara, K., Furusho, J., Tazaki, I., Tanaka, D., et al. (1999). "Cerebral autonomic functional test using human functional near-infraredgraphy (fNIR)," in *5th Annual Meeting of the Organization for Human Brain Mapping, Vol. 9* (Dusseldorf).

Khan, H., Naseer, N., Yazidi, A., Eide, P. K., Hassan, H. W., and Mirtaheri, P. (2021). Analysis of human gait using hybrid EEG-fNIRS-based BCI system: a review. *Front. Hum. Neurosci.* 14, 613254. doi: 10.3389/fnhum.2020.613254

Lassen, N. A. (1959). Cerebral blood flow and oxygen consumption in man. *Physiol. Rev.* 39,183–238. doi: 10.1152/physrev.1959.39.2.183

Maruyama, S., Fukunaga, M., Sugawara, S. K., Hamano, Y. H., Yamamoto, T., and Sadato, N. (2021). Cognitive control affects motor learning through local variations in GABA within the primary motor cortex. *Sci. Rep.* 11, 18566. doi: 10.1038/s41598-021-97974-1

Mintun, M. A., Lundstrom, B. N., Snyder, A. Z., Vlassenko, A. Z., Shulman, G. L., and Raichle, M. E. (2001). Blood flow and oxygen delivery to human brain during functional activity: theoretical modeling and experimental data. *Proc. Natl. Acad. Sci. U. S. A.* 98, 6859–6864. doi: 10.1073/pnas.111164398

Murakoshi, A., and Kato, T. (2006). "Navigating system of cranio-cerebral anatomical correlation for COE: Cerebral functional mapping of oxygen exchange," in *12th Annual Meeting of the Organization for Human Brain Mapping, Vol. 31(suppl)* (Florence). Available online at: https://www.sciencedirect.com/journal/neuroimage/vol/31/suppl/S1

Oda, S., Shibata, M., and Moritani, T. (1996). Force-dependent changes in movement-related cortical potentials. *J. Electromyogr. Kinesiol.* 6, 247–252. doi: 10.1016/S1050-6411(96)00010-7

Pauling, L., and Coryell, C. D. (1936). The magnetic properties and structure of hemoglobin, oxyhemoglobin and carbonmonoxyhemoglobin. *Proc. Natl. Acad. Sci. U. S. A.* 22, 210–216. doi: 10.1073/pnas.22.4.210

Roy, C., and Sherrington, C. (1890). On the regulation of the blood-supply of the brain. *J. Physiol.* 11, 85–158. doi: 10.1113/jphysiol.1890.sp000321

Rupp, T., and Perrey, S. (2008). Prefrontal cortex oxygenation and neuromuscular responses to exhaustive exercise. *Eur. J. Appl. Physiol.* 102, 153–163. doi: 10.1007/s00421-007-0568-7

Suh, M., Bahar, S., Mehta, A., and Schwartz, T. (2006). Blood volume and hemoglobin oxygenation response following electrical stimulation of human cortex. *Neuroimage* 31, 66–75. doi: 10.1016/j.neuroimage.2005.11.030

Takahashi, T., Takikawa, Y., Kawagoe, R., Shibuya, S., Iwano, T., and Kitazawa, S. (2011). Influence of skin blood flow on near-infrared spectroscopy signals measured on the forehead during a verbal fluency task. *Neuroimage* 57, 991–1002 doi: 10.1016/j.neuroimage.2011.05.012

Tamaki, T., Uchiyama, S., Tamura, T., and Nakano, S. (1994). Changes in muscle oxygenation during weight-lifting exercise. *Eur. J. Appl. Physiol.* 68, 465–469. doi: 10.1007/BF00599514

Umesawa, Y., Matsushima, K., Atsumi, T., Kato, T., Fukatsu, R., Wada, M., et al. (2020). Altered GABA concentration in brain motor area is associated with the severity of motor disabilities in individuals with autism spectrum disorder. *J. Autism Dev. Disord.* 50, 2710–2722. doi: 10.1007/s10803-020-04382-x

Vafaee, M. S., Vang, K., Bergersen, L. H., and Gjedde, A. (2012). Oxygen consumption and blood flow coupling in human motor cortex during intense finger tapping: implication for a role of lactate. *J. Cereb. Blood Flow Metab.* 32, 1859–1868. doi: 10.1038/jcbfm.2012.89

Yamamoto, T., and Kato, T. (2002). Paradoxical correlation between signal in functional magnetic resonance imaging and deoxygenated haemoglobin content in capillaries: a new theoretical explanation. *Phys. Med. Biol.* 47, 1121–1141. doi: 10.1088/0031-9155/47/7/309

Yoshino, K., and Kato, T. (2012). Vector-based phase classification of initial dips during word listening using near-infrared spectroscopy. *Neuroreport* 23, 947–951. doi: 10.1097/WNR.0b013e328359833b

frontiers | Frontiers in Physiology

TYPE Original Research
PUBLISHED 23 September 2022
DOI 10.3389/fphys.2022.833871

OPEN ACCESS

EDITED BY
Wei-Peng Teo,
Nanyang Technological University, Singapore

REVIEWED BY
Daniel Milej,
Lawson Health Research Institute, Canada
Yoshihiro Inoue,
Shimadzu Corporation, Japan

*CORRESPONDENCE
Toshinori Kato,
kato@katobrain.com

SPECIALTY SECTION
This article was submitted to Exercise Physiology, a section of the journal Frontiers in Physiology

RECEIVED 12 December 2021
ACCEPTED 05 September 2022
PUBLISHED 23 September 2022

CITATION
Arai M, Kato H and Kato T (2022), Functional quantification of oral motor cortex at rest and during tasks using activity phase ratio: A zero-setting vector functional near-infrared spectroscopy study.
Front. Physiol. 13:833871.
doi: 10.3389/fphys.2022.833871

Functional quantification of oral motor cortex at rest and during tasks using activity phase ratio: A zero-setting vector functional near-infrared spectroscopy study

Masaaki Arai[1], Hikaru Kato[2] and Toshinori Kato[2]*

[1]Department of Oral Biomedical Research, Total Health Advisers Co., Chiba, Japan, [2]Department of Brain Environmental Research, KatoBrain Co., Ltd., Tokyo, Japan

Oral frailty associated with oral hypokinesia may cause dementia. Functional near-infrared spectroscopy (fNIRS) can be used while the participants are in seating position with few restrictions. Thus, it is useful for assessing brain function, particularly oral motor activity. However, methods for identifying oral motor cortex (OMC) activation *via* the scalp have not been established. The current study aimed to detect OMC activation, an indicator of activity phase ratio (APR), which reflects increased oxygen consumption (0 < [deoxyhemoglobin (*ΔDeoxyHb*) or 0 < {[*ΔDeoxyHb*- oxyhemoglobin (*ΔOxyHb*)/$\sqrt{2}$]}, *via* fNIRS to accurately identify local brain activity. The APR, calculated *via* zero-set vector analysis, is a novel index for quantifying brain function both temporally and spatially at rest and during tasks. In total, 14 healthy participants performed bite tasks for 3 s per side for 10 times while in the sitting position. Then, time-series data on concentration changes in *ΔOxyHb* and *ΔDeoxyHb* were obtained *via* fNIRS. The anatomical location of the OMC was determined using a pooled data set of three-dimensional magnetic resonance images collected in advance from 40 healthy adults. In the zero-set vector analysis, the average change in *ΔOxyHb* and *ΔDeoxyHb* concentrations was utilized to calculate the APR percentage in 140 trials. The significant regions (z-score of ≥2.0) of the APR and ΔOxyHb in the task were compared. During the bite task, the APR significantly increased within the estimated OMC region (56–84 mm lateral to Cz and 4–20 mm anterior to Cz) in both the right and left hemispheres. By contrast, the *ΔOxyHb* concentrations increased on the bite side alone beyond the OMC region. The mean APR at rest for 2 s before the task showed 59.5%–62.2% in the left and right OMCs. The average APR for 3 s during the task showed 75.3% for the left OMC and 75.7% for the right OMC during the left bite task, and 65.9% for the left OMC and 80.9% for the right OMC during the right bite task. Interestingly, the average increase in APR for the left and right OMCs for the left bite task and the right bite task was 13.9% and 13.7%, respectively, showing almost a close match. The time course of the APR was more limited to the bite task segment than that of *ΔOxyHb* or *ΔDexyHb* concentration, and it

increased in the OMC. Hence, the APR can quantitatively monitor both the resting and active states of the OMC in the left and right hemispheres. Using the zero-set vector-based fNIRS, the APR can be a valid indicator of oral motor function and bite force.

KEYWORDS

oral frailty, initial dip, activity phase ratio, cerebral oxygen metabolism, dental medicine, fNIRS, functional near-infrared spectroscopy, oral motor cortex

Introduction

Oral frailty should be prevented to maintain brain health (Horibe et al., 2018). Recent studies have shown that cognitive function decline and oral motor function decline are correlated with each other (Kugimiya et al., 2019; Takeuchi et al., 2017). The oral motor cortex (OMC), which is associated with oral movement, was first investigated *via* positron emission tomography (PET) (Fox et al., 2001). Subsequently, brain activation during gum chewing (Onozuka et al., 2002), clenching (Tamura et al., 2002), and mastication (Matsushima et al., 2005) was assessed *via* functional magnetic resonance imaging (fMRI). Thus, it is extremely important to understand the association between oral exercise and brain function from the perspective of dementia prevention.

Brain activity during rest differs between the supine and sitting positions (Thibault et al., 2014). In addition, gravity-induced mandibular retracted position may occur in the supine position. Prefrontal activation varies between the mandibular retracted and normal mandibular positions (Otsuka et al., 2015). However, patients who undergo PET or fMRI for the assessment of brain activity, including the OMC, should be in the supine position.

Functional near-infrared spectroscopy (fNIRS) has few limitations in terms of posture and movement during measurement (Kato et al., 1993; Kato, 2018). Therefore, fNIRS can be an optimal technique for assessing brain function during daily activities performed in the sitting or standing position (Kasahara et al., 2007; Kasahara et al., 2008). Brain activity during swallowing (Kober et al., 2015), oral care (Fujii et al., 2015), and clenching (Shibusawa et al., 2009) was evaluated *via* fNIRS. However, brain responses localized in the primary motor cortex (M1) were not detected. Clenching is an involuntary, forceful biting of the upper and lower teeth. Several aspects of this mechanism, such as bite duration, are unknown. By contrast, first bite is an oral movement that lasts only for a few seconds, and it plays an important role in the process of mastication (Dan et al., 2007). fNIRS methods for measuring OMC activity for a few seconds during bite have not been established yet.

Thus, fMRI and fNIRS have been used to evaluate brain function, particularly oral motor activity. Both modalities have a common method of detecting brain response to a task by comparing the resting state with a certain task. However, challenges in the quantitative assessment of the resting state of either modality remains unresolved.

Reports of many fNIRS studies have used increases in oxyhemoglobin concentration (OxyHb) and decreases in deoxyhemoglobin concentration (DeoxyHb) as brain activity. However, these are indicators of cerebral oxygen supply, and there is a possibility that cerebral blood supply also occurs around the area where the brain activity occurred (Kato, 2004). In addition, it has been pointed out that distinguishing between cutaneous blood flow and motion artifact contamination from the cortical activity is difficult when using OxyHb as the sole indicator of measurement (Kirilina et al., 2012; Kirilina et al., 2012; Miyazawa et al., 2013). Therefore, in order to identify brain activity more accurately, it is necessary to detect the initial dip caused by a decrease in OxyHb and an increase in DeoxyHb as an indicator of cerebral oxygen consumption and to use the indicator from the vector-based fNIRS, which simultaneously uses DeoxyHb and OxyHb (Kato, 2022).

The vector-based fNIRS has been applied for early dip detection and brain–computer interface studies (Hong and Naseer, 2016; Kato, 2013; Kato, 2018; Yoshino and Kato, 2012). Recently, it has played a role in the identification of oxygen metabolism during exercise training (Kato, 2022). Zero-set vector-based fNIRS has been utilized to quantitatively monitor the resting state of individual brain measurement channels (Kato, 2021).

We hypothesized that OMC function in biting movements such as eating can be validated using the activity phase ratio (APR), a novel index calculated *via* vector-based fNIRS. The current study aimed to quantitatively monitor OMC activity in the resting state and during a 3-s bite period *via* zero-set vector-based fNIRS using APR.

Methods

Participants

In total, 14 healthy adults who were right-handed based on the Edinburgh Handedness Inventory [mean age: 20.1 years, standard deviation (SD): 0.3 years; 11 men, 3 women] were included in the analysis. The experimental procedure was performed in accordance with the principles of the Declaration of Helsinki. Furthermore, this research was approved by the ethics committee of KatoBrain Co., Ltd. All

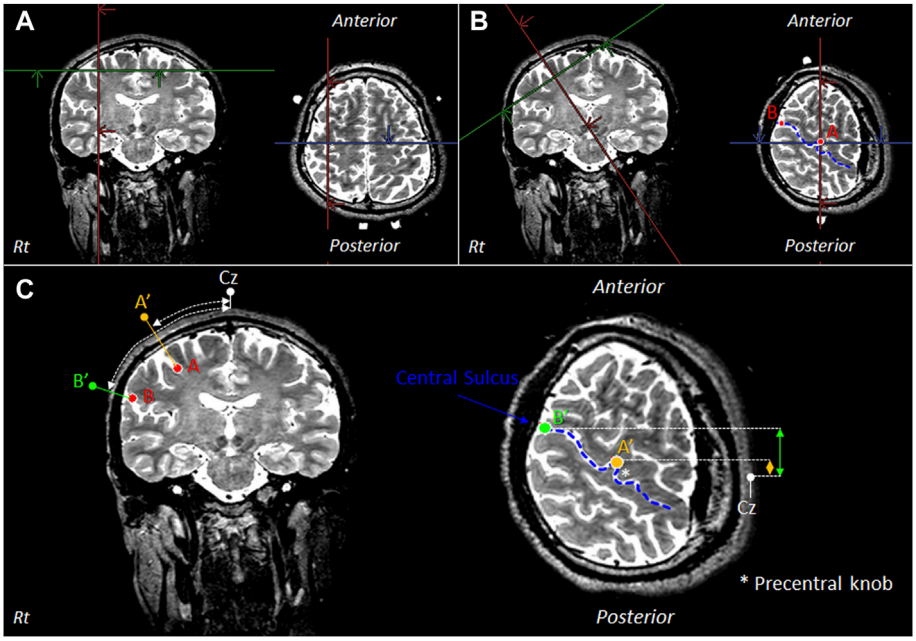

FIGURE 1
MRI for selecting the OMC measurement region. **(A)** Extract the outer edge of the precentral knob in the primary motor cortex (M1) and define it as point A. **(B)** Display an image in which point A is tilted as an axis perpendicular to the skull. In the displayed image, the outer edge of the central sulcus is defined as point B. The blue line indicates the central sulcus of the right hemisphere. **(C)** Points A′ and B′ are defined as points passing through points A and B and perpendicular to the skull. There is OMC in the area between points A′ and B′. Thus, the distances between Cz, point A′, and point B′ in the longitudinal direction and lateral direction were measured. OMC: oral motor cortex. Cz: location of vertex on the scalp. Rt: right.

participants received full explanation of the procedures and provided a written informed consent for study participation.

Determination of chewing side preferences

Chewing side preferences (CSPs) were defined as the initial chewing side of the participants (Ozaki, 2002). A cotton roll (1.0 cm × 0.8 cm) was placed in the center of the tongue. Then, the initial chewing side was observed and recorded by a dentist. The side used for ≥2 times in three trials was considered as the CSP. In total, 10 participants (71.4%; seven men, three women) had right CSP, and four participants (28.6%; all men) had left CSP. The percentage of participants with right CSP was consistent with that in previous reports (Ozaki, 2002; Zamanlu et al., 2012).

Measurement areas

OMC identification was performed *via* pre-measured identification of the target cortical sites (Murakoshi and Kato, 2006), using distances between reference points on the scalp from the MRI images of 40 healthy adults [average age: 32.2 (SD: 5.8) years; 20 men and 20 women]. The OMC region was defined as the region of interest (ROI). The OMC measurement sites were established using three-dimensional (3D) T2-weighted data. The Achieva 3.0-T Quasar Dual MRI Scanner (Philips Co.) was used. The pulse sequence was as follows: spin-echo sequence–TE: 255 ms, TR: 2,700 ms, flip angle: 90°, matrix: 25 cm × 25 cm, and resolution: 1.0 × 1.0 × 1.0 mm^3. For MRI data analysis, the AZEWIN DICOM viewer (AZE Co.) was utilized. Figure 1A,B,C show the MRI method used to select the OMC measurement region. The OMC is estimated to be located outside the precentral knob (Yousry et al., 1997), which is the region of hand movement. The blue line in the Figure 1B,C indicates the central sulcus of the right hemisphere.

Figure 2A shows the position of the OMC measured to determine the location where the probe should be attached before starting the fNIRS experiment. The measurement ranges were 24 mm forward, 56 mm rearward, and 84 mm outside bilaterally from the Cz reference point. Cz is a landmark of the international 10–20 system for electroencephalogram electrode placement. The left and right OMCs were considered as the ROI surrounded by the dotted rectangle. The positions of the OMC on the scalp were 56–84 mm outside and 4–20 mm anterior based on Cz. The estimated right

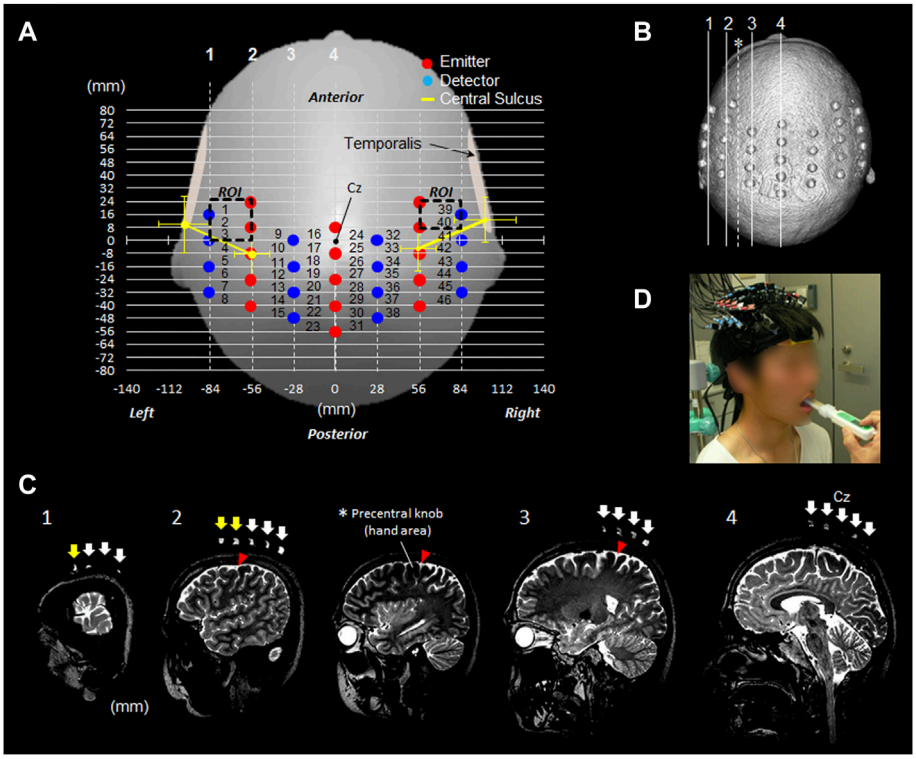

FIGURE 2
fNIRS measurement settings. **(A)** fNIRS 46-channel arrangement and the estimated bilateral OMC. **(B)** Head image reconstructed from 3D T2-weighted MRI taken with a registration marker, which indicates the probe position. The four lines from 1 to 4 correspond to the positions in the image in Figure **(C)**. **(C)** Sagittal images 1–4 along the registration marker are shown. The sagittal image presented with an asterisk indicates a slice passing through the precentral knob between rows 2 and 3. Among the arrows indicating the probe position, the yellow arrow of slices 1 and 2 indicates the position of the pair probe sandwiching the part corresponding to the OMC. **(D)** Participant wearing a probe during experimental tasks. OMC: oral motor cortex. ROI: region of interest. Cz: location of vertex on the scalp.

OMC was located at channels 39 and 40 and the estimated left OMC at channels 1, 2, and 3.

The attachment was mounted corresponding with Cz between the first and second emitter probes in the center. The red and blue circles indicated the emitter and detector, respectively. The distance between the emitter and detector was 3.0 cm. The distances between the channels were set to 2.8 cm in the horizontal direction and 0.8 cm in the sagittal direction, which ensured a sufficiently high resolution to secure cortical data (Kawaguchi et al., 2004). The yellow line in the Figure 2A indicated the estimated direction of the central sulcus outside the precentral knob corresponding to the region of voluntary hand movement (Figure 1A,B). With reference to Cz on the scalp, in the left hemisphere, the central sulcus runs outside the precentral knob in the direction connecting the points 8.6 ± 6.9 mm (mean ± SD) posterior to Cz and 56.0 ± 5.9 mm outside from the points 9.7 ± 8.7 mm anterior and 101.3 ± 8.5 mm outside Cz.

In the right hemisphere, the central sulcus runs outside the precentral knob in the direction connecting the points 5.0 ± 6.9 mm posterior to Cz and 55.9 ± 5.9 mm outside from the points 12.5 ± 6.8 mm anterior and 101.1 ± 9.0 mm outside Cz.

fNIRS measurement

A multichannel fNIRS (FOIRE-3000; Shimadzu Corporation, Japan) with 15 irradiation probes and 16 detection probes was used. Furthermore, a self-made measurement probe with 46 channels was utilized (Figure 2A,D). Changes in oxyhemoglobin (ΔOxyHb) and deoxyhemoglobin (ΔDeoxyHb) concentrations were monitored by detecting scattered light with three wavelengths of near-infrared light (780, 805, and 830 nm) irradiated to the scalp. Conversion from absorbance to ΔOxyHb was performed inside the device using a method by Matcher et al., 1995. Measurement was performed in a continuous mode. The sampling time of ΔOxyHb was 85 ms. Event marks were recorded at the task start and end. To prevent temporal muscle artifacts, the measurement channel was mounted more inside the origin of the temporalis muscle.

To prevent artifacts in the temporalis muscle, the measurement channel was mounted medial to the origin of the temporalis muscle. In addition, to evaluate the presence of motion artifacts in the scalp and temporalis muscles, the participants were instructed to open and close their mouths and perform a trial bite on a bite force meter prior to the experiment. Results confirmed the absence of artifacts in the OxyHb and DeoxyHb measurement waveforms, with rapid fluctuations caused by movement during the bite task. However, the presence of slow artifacts persisted until after the task was not confirmed.

After the experiment, a registration marker was placed at the probe placement site in one participant, and T2-weighted images were taken with 3-T MRI to confirm the probe location (Figure 2B,C). The other 13 participants did not undergo MRI after the experiment because the probes were placed using a pre-measured identification technique at the target cortical sites with distances between reference points on the scalp *via* MRI in healthy adults (Murakoshi and Kato, 2006).

As shown in Figures 1, 2, the position of the OMC in 40 participants was less sensitive to temporal muscle movements.

Experimental procedures

The experimental task was set as the maximum bite task for 3 s with consideration of the characteristics of M1 related to force output (Cheney and Fetz, 1980; Hoffman and Luschei, 1980). The participants bit the bite force meter (GM10; Nagano Keiki Co., Ltd., Japan) with maximum force for 3 s in accordance with the vocal cue (Figure 2D). In the experimental task, the dentist placed the bite force meter sensor at the contact point between the first molar and second premolar on the lower jaw. The maximum bite force for 3 s was recorded using a bite force meter.

The right bite force was 49.0 ± 15.0 kg, and the left bite force was 50.0 ± 15.7 kg. Hence, there was no significant difference between the two bite forces (p = 0.405; paired t-test).

The participants performed right and left bite each for 10 trials. After each trial, the bite force meter was pulled from the oral cavity and maintained at rest. The interval between each trial varied from 10 to 15 s. Approximately 5 s before the next trial, the bite force meter was again set in the oral cavity. Therefore, it did not include jaw movement during the task. The data of the left and right bite tasks were obtained for each of the 140 trials. The left and right bite tasks were performed randomly to eliminate the order effect.

Preparation of zero-set vector for fNIRS data

Five preparatory processing steps were required to calculate *ΔOxyHb* and *ΔDeoxyHb* concentrations and APR. The first step

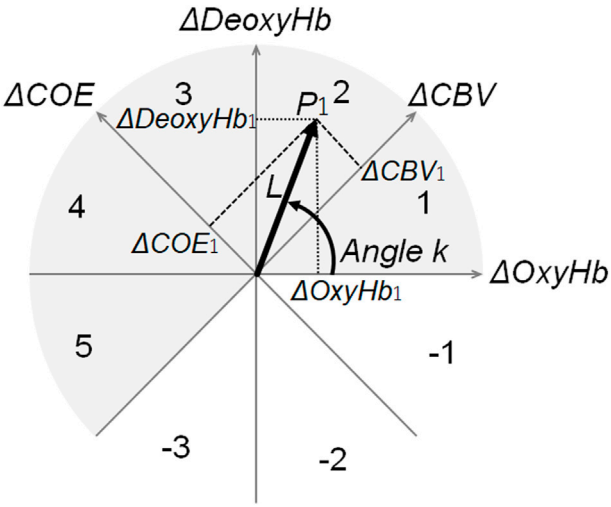

FIGURE 3
Polar coordinates for vector analysis. Vector polar coordinate plane used for vector analysis. By converting the vector connecting the origin and an arbitrary point P_1 ($\Delta OxyHb_1$, $\Delta DeoxyHb_1$) to the *ΔCOE* axis and the *ΔCBV* axis, the coordinates of ΔCOE_1 and ΔCBV_1 are obtained. The number on the arc indicates the phase number. Among the eight quadrants divided by the four axes, the phase of the gray portion (*ΔDeoxyHb* > 0 or *ΔCOE* > 0) implies low oxygenation or deoxygenation. Thus, these phases indicate increased brain activity (activation phase). By contrast, the phase of white (*ΔDeoxyHb* < 0 or *ΔCOE* < 0) showed minimal enhancement of brain activity (non-activation phase). *k* quantitatively indicates the phase of these oxygen metabolisms. *ΔOxyHb*: oxyhemoglobin. *ΔDeoxyHb*: deoxyhemoglobin. *ΔCOE*: cerebral oxygen exchange. *ΔCBV*: cerebral blood volume.

was the smoothing of OxyHb and DeoxyHb time-series data *via* fNIRS. The raw OxyHb and DeoxyHb data were low-pass filtered at 0.1 Hz (first-order Butterworth filter).

Baseline normalization and motion correction were not performed as the preprocessing step in the analysis due to the risk of distorting the phase of oxygen exchange (Kato., 2022).

The second step was the calculation of *ΔCOE* and *ΔCBV* in each trial using *ΔOxyHb* and *ΔDeoxyHb* data with Eqs 1, 2:

$$\Delta COE = \frac{1}{\sqrt{2}}\left(\Delta Deoxy Hb - \Delta Oxy Hb\right) \quad (1)$$

$$\Delta CBV = \frac{1}{\sqrt{2}}\left(\Delta Deoxy Hb + \Delta Oxy Hb\right). \quad (2)$$

An orthogonal vector plane spanned by *ΔOxyHb* and *ΔDeoxyHb* (Kato, 2006; Kato, 2018) was used in the analysis of hemodynamic responses (Figure 3).

The third step was the offset of the start of each bite task in *ΔOxyHb* and *ΔDeoxyHb* to the vector origin to observe event-related responses.

The fourth step is the creation of a group of zero-set vectors of time-series changes in *ΔOxyHb* and *ΔDeoxyHb* concentrations

at each given sampling time based on the two-dimensional diagram, as shown in Figure 3. This was defined as the zero-set vector.

The phase *k* and norm *L* values could be calculated using the zero-set vectors.

The fifth step was the calculation of all the phases (angles *k*) of the zero-set vector using Eq. 3.

The angle *k* between the zero-set vector and the positive *ΔOxyHb* axis could be calculated using Eq. 3.

The angle *k* between a vector and the positive *ΔOxyHb* axes could be calculated using Eq. 3:

$$k = \mathrm{Arctan}\left(\frac{\Delta Deoxy Hb}{\Delta Oxy Hb}\right) = \mathrm{Arctan}\left(\frac{\Delta CBV}{\Delta COE}\right) + 45^{\circ}\,(-135^{\circ} \leqq k \leqq 225^{\circ}). \quad (3)$$

The oxygen exchange degree (*k* angle) was defined as a quantitative index of oxygen metabolism intensity based on the *ΔCOE*-to-*ΔCBV* ratio (or *ΔDeoxyHb*-to-*ΔOxyHb* ratio) obtained using Eqs 1, 2 (Kato, 2006; Kato, 2018).

The norm *L* between point P_1 ($\Delta Oxy Hb_1$, $\Delta Deoxy Hb_1$) in Figure 3 and the origin can be described using the following equation:

$$L = \sqrt{(\Delta Oxy Hb_1)^2 + (\Delta Deoxy Hb_1)^2} = \frac{1}{\sqrt{2}}\sqrt{(\Delta COE_1)^2 + (\Delta CBV_1)^2}, \quad (4)$$

where *L* represents the intensity of Hb changes (OxyHb and DeoxyHb).

Each norm *L* value reflected the intensity of each zero-set vector, which is not analyzed in this study.

The phase *k* and norm *L* values could be calculated using the zero-set vectors. Each norm *L* value reflects the intensity of each zero-set vector, which was not analyzed in this study.

Quantitative analysis of APR

After calculating the phases of the zero-set vector, the APR was calculated using Eq. 5.

As shown in Figure 3, phases 1–5 were defined as the activity phase. Therefore, the APR (%) was defined as the percentage of trials, with an activity phase out of the total number of trials. It was calculated for each measurement channel in each task.

The APR could be calculated using Eqs 5, 6, 7 (Kato, 2021):

$$\mathrm{APR}\ (\%) = \frac{\text{Number of trials shown in the activity phase at the sampling time (n)}}{\text{Total number of trials at the sampling time (n = 140)}} \times 100, \quad (5)$$

$$APR\ denominator = (\text{number of participants}) \text{ x } (\text{number of sites measured}), \quad (6)$$

$$APR\ numerator = \text{number of activity phase trials among the total number of trials used as the denominator.} \quad (7)$$

This zero-set vector-based fNIRS study identified the areas where the task caused cortical activity in the ROI, since the resting state was quantified by the APR. The OMC was defined as the area of increased APR and oxygen metabolism in the combined force output task.

A measurement channel in which the z-score of the APR was ≥2.0 was considered a high ratio activity site. The OMC site was defined as the high ratio activity site in the bite force task.

In addition, we detected the measurement channels with z-scores of ≥2.0 for concentration changes in *ΔOxyHb*, which is a conventional activity index. Then, differences in the identifying sites of the OMC based on APR and *ΔOxyHb* concentrations were compared.

The cumulative sum of the four vector components (*ΔOxyHb*, *ΔDeoxyHb*, *ΔCOE*, and *ΔCBV*) for 3 s during the task was used for APR and *ΔOxyHb* mapping.

Time trends in APR and *ΔOxyHb* and *ΔDeoxyHb* concentrations in the OMC

The APR was calculated every 0.51 s of sampling time to plot the time course of synchronicity between the increase in APR, and the task time was evaluated from the time course series for APR changes in the OMC. The *k* angle was calculated using the cumulative sum of *ΔCOE* and *ΔCBV* every 0.51 s, and the time-series change in the APR every 0.51 s was plotted. Using the APRs of the left and right bite tasks of each participant as paired data, differences in the APR between tasks were examined (paired *t*-test). Similarly, the waveforms of *ΔOxyHb* and *ΔDeoxyHb* plotted every 0.51 s were detected. A *p*-value of 0.05 was considered statistically significant.

Result

Quantitative mapping using the APR for identifying OMC location

Figure 4 shows mapping using the average value of the APR (%) and *ΔOxyHb* during the right and left biting tasks. In the analysis using the APR, channels 1, 2, and 40 had statistically significant results (z-score of >2.0) in the left bite task, and channels 1 and 40 had statistically significant results (z-score of >2.0) in the right bite task. Channels 1 and 40 were within the OMC area assessed *via* MRI. The area between these probes was located above the precentral gyrus and outside the area of the precentral knob, as shown in Figures 2C1,C2. These measurement channels were located in front of the outermost

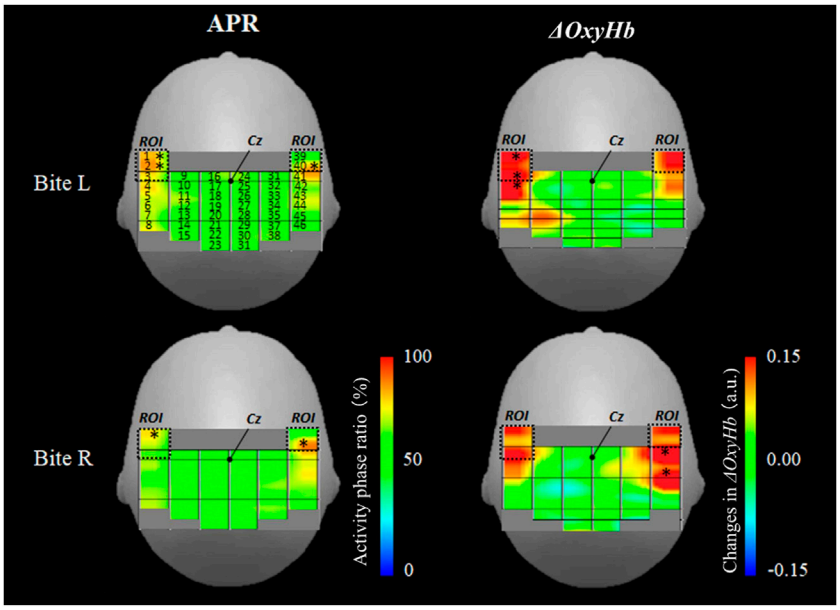

FIGURE 4
Activation map during unilateral bite task. The left column shows APR mapping in the right and left biting tasks. The right column shows *ΔOxyHb* mapping in the right and left biting tasks. An asterisk indicates a high ratio active site (z-score of >2.0). APR: activity phase ratio. L: left. R: right. *ΔOxyHb*: oxyhemoglobin.

row of measurement probes, and these two channels had bilaterally symmetrical positions merely displaced by 8 mm in the anterior–posterior direction. Based on these results, the APR significantly increased only in the ROI channel corresponding to the OMC on both sides with respect to one-side bite.

In the analysis using *ΔOxyHb*, channels 1, 3, and 4 had statistically significant results in the left bite task, and channels 41 and 43 had statistically significant results in the right bite task (z-score of >2.0). The *ΔOxyHb* concentration significantly increased during the one-sided bite task only on the bite side and not on the opposite side. Hence, the *ΔOxyHb* concentration outside the OMC region increased on MRI. In the left biting task, the area in front of the central sulcus also increased. However, the most evident increase was detected behind the central sulcus (left bite: ch1 z-score = 2.8, ch3 z-score = 2.5, and ch4 z-score = 2.1; right bite: ch41 z-score = 3.0, ch43 z-score = 2.5).

Quantitative detection of changes in the OMC at rest and during tasks using APR

Figure 5 shows the time-series changes in APR and *ΔOxyHb* and *ΔDeoxyHb* concentrations in the left and right OMCs (left OMC: channels 1 and 2 and right OMC: channel 40). The APR on the bilateral OMC increased only during the 3-s task period for both right and left bite tasks. Meanwhile, the *ΔOxyHb* and *ΔDeoxyHb* concentrations increased after the task. The average APR for 2 s before the task, which can quantitatively indicate the level of oxygen metabolism in the OMC during the resting state, was 62.2% in the left OMC and 61.2% in the right OMC during the left bite task, and 60.0% in the left OMC and 59.5% in the right OMC during the right bite task.

The average APR for 3 s during the task showed 75.3% for the left OMC and 75.7% for the right OMC during the left bite task, 65.9% for the left OMC and 80.9% for the right OMC during the right bite task. Therefore, the average APR during the task increased by 13.2% in the left OMC and 14.5% in the right OMC of the left bite task and by 5.9% in the left OMC and 21.2% in the right OMC of the right bite task, compared with that before the tasks. This means that the percentage increase in oxygen consumption was about 1.1 times greater in the right OMC than in the left OMC for the left bite task and about 3.6 times greater for the right bite task. Thus, the difference in left and right OMC activities, which was scarcely observed during the left bite task, became more significant during the right bite task. Interestingly, the average increase in APR for the left and right OMCs for the left bite task and the right bite task was 13.9% and 13.7%, respectively, showing almost a close match.

In the left bite task, there was no significant difference between the APRs in the left and right OMCs in any time zone ($p > 0.05$). In the right bite task, the APR was significantly higher on average 16.7% in the right OMC than in the left OMC within 1.02–3.06 s ($2.500 < t\ (13) < 3.553$, $p < 0.05$).

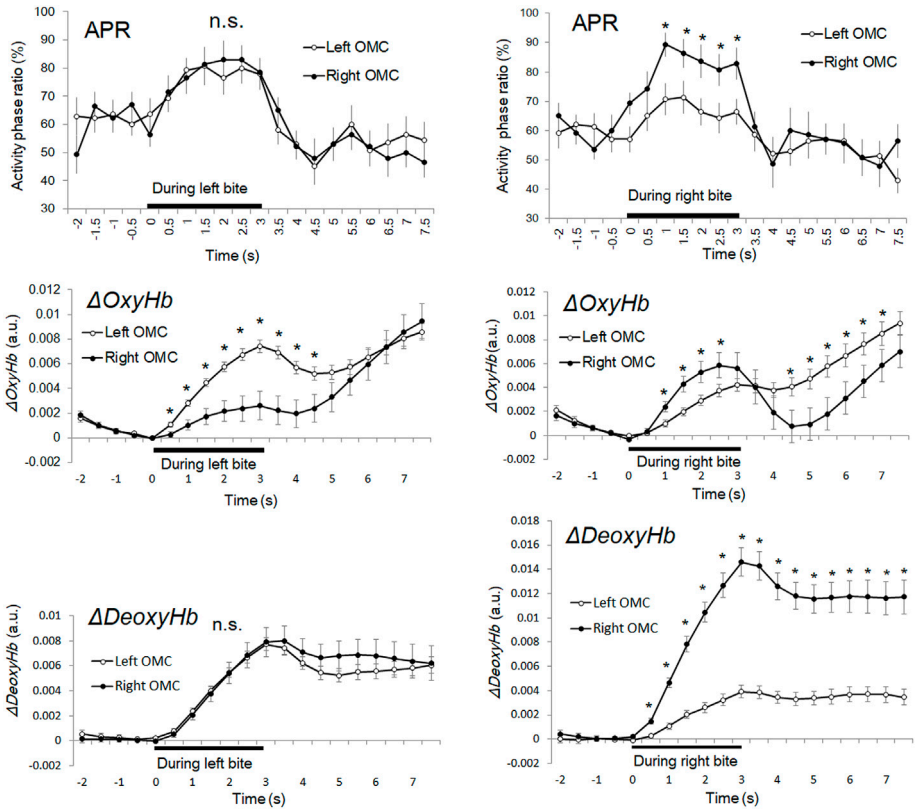

FIGURE 5
Time course series of APR, *ΔOxyHb*, and *ΔDeoxyHb* during unilateral bite task. The left column shows the time courses of the average APR of the right and left OMCs, respectively. The bar shows the standard error of the mean. An asterisk indicates a high signal site (z-score of >2.0) in which there was a significant difference between the right and left OMC. APR: activity phase ratio. APR: activity phase ratio. *ΔOxyHb*: oxyhemoglobin. *ΔDeoxyHb*: deoxyhemoglobin. OMC: oral motor cortex.

The maximum peak APR values in the left bite task were 82.9% (z-score = 2.2, n = 140) at 2 s after task onset in the right OMC and 80.7% (z-score = 2.0, n = 140) in the left OMC, 1.5 s after task onset.

The maximum peak APR values in the right bite task were 89.3% (z-score = 3.2, n = 140) at 1 s after task onset in the right OMC and 71.4% (z-score = 2.0, n = 140) in the left OMC, 1.5 s after task onset.

Average APR for 4.5 s after the task showed 53.7% for the left OMC and 52.3% for the right OMC in the left bite task, 53.2% for the left OMC and 55.4% for the right OMC in the right bite task. Thus, compared to the pre-task, the average APR after the task showed a decrease of 8.4% in the left OMC and 8.9% in the right OMC for the left bite task, and a decrease of 6.8% in the left OMC and 4.3% in the right OMC for the right bite task, respectively. This means that the inactive phase, reflecting the oxygen supply, increased in the left and right OMCs after the task and remained in a state that did not return to the state before the task. Therefore, the peak APR value can be an indicator for detecting activities during short tasks within 3 s.

Elevated *ΔOxyHb* and *ΔDeoxyHb* concentrations sustained after bite task

In both left and right bite tasks, *ΔOxyHb* showed a bimodal waveform and was increased at the beginning of the task and 1–2 s after the task (Figure 5). In the left bite task, the *ΔOxyHb* concentration of the left OMC was significantly higher than that of the right OMC (0.51–4.06 s; $p < 0.001$). The average ΔOxyHb concentration change in the left OMC during the task was approximately 2.7 times greater than the value in the right OMC. In the right biting task, the *ΔOxyHb* concentration of the right OMC was significantly higher than that of the left OMC (4.49–7.14 s and 1.02–2.55 s; p = 0.000–0.034). Thus, *ΔOxyHb* occurred strongly on the same side as the bite side, both in the left and right bite tasks.

The *ΔDeoxyHb* concentration of the bilateral OMC increased steadily from the beginning to the end of the right and left bite tasks. Subsequently, it decreased slightly, not returning to the starting point, but showing flattening with an increase. In the left bite task, there was no significant difference in *ΔDeoxyHb*

TABLE 1 Functional brain studies of human mandibular movement *via* PET, fMRI, and fNIRS.

Author	Device	Index	Task	Task side	Performance data	M1[a] activation
Fox et al. 2001	PET	rCBF ($H_2{}^{15}O$)	Speaking and reading aloud[b]	Bilateral	None	Bilateral
Onozuka et al. 2002	fMRI	BOLD	Gum chewing	Bilateral	None	Bilateral
Matsushima et al. 2005	fMRI	BOLD	Mastication (1 Hz)	Left or right	None	Left or bilateral
Shibusawa et al. 2009	fNIRS	OxyHb	Clenching	Right	% MVC[c]	Left (right is not measured)
Iida et al. 2012	fNIRS fMRI	OxyHb BOLD	Teeth tapping (1 Hz)	Bilateral	EMG[d] activity	Bilateral
Kanayama et al. 2015	fMRI	BOLD	Clenching	Bilateral	None	Bilateral
Arai et al. (present study)	Vector-based fNIRS	APR[e] *ΔOxyHb* *ΔDeoxyHb*	Object biting	Left or right	Bite force strength	Bilateral

[a]Primary moto area (M1).
[b]This was not a mandibular movement task study. However, it was the first study that identified OMC spatially using functional activation.
[c]Percent maximum voluntary contraction (MVC).
[d]Electromyography (EMG).
[e]Activity phase ratio (APR) (%).

concentrations between the left and right OMCs at any time point ($p > 0.05$), as in the APR time-series data. In the right bite task, the *ΔDeoxyHb* concentration of the right OMC was significantly higher than that of the left OMC (0.51–7.65 s; $p < 0.001$). The average *ΔDeoxyHb* concentration change in the right OMC during the task was approximately 4.4 times greater than the value in the left OMC.

Time-series data of both ΔOxyHb and ΔDeoxyHb concentrations increased during the task but showed divergence in post-task trends. In addition, the time-series data for ΔOxyHb and ΔDeoxyHb concentrations showed a rather different trend from the APR data for both right and left bite tasks.

Discussion

Identification of OMC using APR and MRI

This study showed that left and right OMC activation occurs even during unilateral bite. Based on previous studies on human mandibular movements, bilateral M1 activity is enhanced in oral motor tasks that do not distinguish between left and right bites. However, although unilateral dominance of movement increases bilateral OMC activity was unclear. The active sites of OMCs obtained from the scalp ranged from 56 to 84 mm laterally and from 4 to 20 mm anteriorly with respect to Cz. It showed an increase in APR during unilateral bite, which is consistent with the location of OMC assessed *via* MRI in 40 participants.

Since the APR activity in the OMC, indicating oxygen metabolism, occurs in the left and right hemispheres, bite movements are not significantly inhibited unless the bilateral OMCs are damaged. In a study comparing force production on the paralyzed and healthy sides (Kemppainen et al., 1999), it was difficult to recover the loss of finger palmar grip strength on the paralyzed side. However, there was no difference in maximum bite force between the left and right sides. The results of this study were consistent with those of previous ones. Closure muscles (e.g., the masseter, medial pterygoid muscle, and temporal muscle) are involved in biting and controlled by the trigeminal nerve motor branch from the OMC *via* the corticopontine tract. In the upper part of the trigeminal nucleus, the closure muscles are dually controlled by the bilateral cerebral hemispheres (Berkovitz, 2005). The results of this study are consistent with those of previous anatomical ones.

By contrast, ΔOxyHb, which is widely used in fNIRS analysis, had significant responses to not only the activity of the OMC itself but also the activity around the OMC. Meanwhile, the responses of APR and *ΔOxyHb* occurred 8 mm (1 channel width) apart. As shown in Table 1, previous functional brain studies were not able to individually detect the identified OMCs and surrounding brain activity.

With the use of phase *k*, not only the areas of increased oxygen consumption in brain activity but also the surrounding oxygen supplying regions can be detected. However, they are considered indistinguishable if BOLD or ΔOxyHb is used as an indicator (Kato, 2022).

Temporal advantage of APR using zero-set vector-based fNIRS

The APR had different time-series changes compared with *ΔOxyHb* and *ΔDeoxyHb* concentrations and could quantify brain activity during oral movements. The APR trend could not be predicted *via* gross observation based on the trend of *ΔOxyHb*

and *ΔDeoxyHb* time-series data. The APR was about 1.1 times higher in the right OMC than in the left OMC for the left bite task and about 3.6 times higher in the right bite task. Interestingly, the average increase in APR for the left and right OMCs for the left bite task and the right bite task was 13.9% and 13.7%, respectively, showing almost a close match. Since the participants did not show significant differences in the left and right bite strength, this suggests that in the absence of differences in bite strength, it is possible that bite muscles are controlled by the sum of activation of the left and right OMCs. Moreover, since all participants were right-handed, the APR results could be different for left-handed participants or children with deciduous teeth.

The APR recovered to about 60% of its pre-task value 1 s after the task. On the other hand, once the task is completed, neural activity is also expected to decrease, and as a result, ΔOxyHb and ΔDeoxyHb would be expected to return to their pre-task values. However, ΔOxyHb and ΔDeoxyHb increased after the task and did not return to their pre-task values. Thus, the use of ΔOxyHb and ΔDeoxyHb alone as indicators of neural activity may be misleading, as if neural activity is ongoing. The re-elevation of *ΔOxyHb* after the task may indicate cerebral blood supply to the OMC. However, the reason why the post-task *ΔDeoxyHb* did not return to pre-task values remains unclear.

An increase in APR indicates an elevated frequency of the initial dip, which represents increased oxygen consumption. The initial dip is more spatially limited than that associated with increased *ΔOxyHb* or blood volume changes (Ances et al., 2001; Kato, 2004; Kato, 2018; Suh et al., 2006). In fact, the initial dip is a spatially selective response in hand motor tasks (Akiyama et al., 2006). A brief 4-s increase in oxygen metabolism can be detected *via* phase evaluations using vector analysis (Kato, 2018). Values of 60%–70% at rest reflect the total percentage of phases -1, -2, and -3 in Figure 3, which is 30%–40%. Kato (2021) showed that the total APR of activity phases 1–5 was 65.7%, and the total percentage of inactivity phases -1, -2, and -3 was 34.3%, based on the APR measured from the right frontal region during 5 min of closed-eye rest.

In this study, the mean APR values (%) from the zero-set vector at rest exhibited different phase variations, with approximately 60% in the active phase and 40% in the inactive phase. In a previous study, the time course of the mean APR value (%) was examined in the Broca's area of the left frontal lobe for approximately 4 s before subjects heard and spoke the word "lion" and thereafter. The results showed that the APR was about 60% in the 2 s before the task started, reached a maximum of 90% at 2 s after the task started, decreased to 30% at 5 s, and returned to 50% at 6 s (Kato, 2021). Thus, the reproducibility of the results, even if the measurement site and task differ, confirms that APR values are a novel quantitative measure of brain activity, not just in the resting state.

Oral motor function in the sitting position

In the present study, the mean resting APR decreased by about 7% from about 60% before and after the bite task. It would be very interesting to see how the resting APR changes in daily life. Furthermore, the APR, which quantitatively indicates the state of brain activity at rest, may be a useful indicator of left and right OMC function and bite force change with aging. It is important to evaluate how the activation of OMC and the function of other brain regions should be enhanced to prevent cognitive decline. We hypothesized that improving oral motor function can improve brain function. This study was conducted in the sitting position. The association between the left and right OMC function and bite force in the supine position in the same participants can be an interesting topic of future research. Using APR, it is possible to compare the resting brain activity status of OMC in the sitting and supine positions without using an oral motor task.

Oral movements should be assessed in the sitting position as it is advantageous to evaluate differences in one-sided biting habits in an environment similar to real-life behavior. In the current study, the participants had a higher *ΔOxyHb* in the ipsilateral OMC than in the contralateral side. There was no difference in APR and *ΔDeoxyHb* between the left and right sides during left-side bite, and the ipsilateral side increased more than the contralateral side in the right-side bite. The results could have been affected by the fact that 78.1% of participants had a right bite CSP. An fMRI study on tongue movement was reported by determining the participant's CSP and extracting the left CSP group (Shinagawa, et al., 2004). Results showed that when participants moved their tongues after chewing gum, activation increased in the motor and sensory cortices ipsilateral to the CSP side. Data on the right side of the CSP group were not described.

In this study, the association between the CSP and the left and right OMCs was not analyzed. Although a sufficient number of participants are required, the association between CSP and the left and right OMCs is an interesting research topic.

Potential for the zero-set vector-based fNIRS study

The use of APR values obtained *via* zero-set vector fNIRS is a novel method for evaluating differences in the resting state of the brain. Using APR, the resting state of oxygen metabolism can be simultaneously quantified from multiple sites with time resolution in the order of milliseconds.

fNIRS has been reported to be an effective method for neurorehabilitation compared to fMRI (Klein et al., 2022). However, when multiple sites are measured with a continuous wave multi-channel fNIRS system, the optical path lengths of each site are treated as identical even if they are different.

Moreover, the concentration change of each hemoglobin has been qualitatively mapped.

The measurement of optical path length using time-resolved spectroscopy (TRS) or phase-resolved spectroscopy requires several minutes at rest. Hence, changes in the order of milliseconds or meters were not quantified in real time. In fact, the TRS takes approximately 5 min to measure the resting cerebral oxygen saturation at one location on the scalp. Using the OxyHb and DeoxyHb signals to calculate changes in tissue saturation (Robu et al., 2020) and to compare them to the time course of the APR may characterize the physiology of the APR and confirm that they are excellent markers. The physiological significance of APR values in the resting state *via* zero-set vector analysis should be further evaluated.

The time course of the APR can more accurately indicate bite task-related responses in OMC than *ΔOxyHb* or *ΔDexyHb*. Baseline normalization and motion correction as preprocesses for analysis may distort the phase of oxygen exchange (Kato, 2021). Hence, only data smoothing of *ΔOxyHb* and *ΔDexyHb* concentrations at 0.1-Hz low-pass filter was performed.

The phase k and norm L are obtained from the zero-set vector. Since the norm L reflects the signal intensity, the motion artifact may be more susceptible than the phase k. By contrast, phase k is less sensitive to trends in signal strength (Kato, 2021).

The technical challenges in fNIRS measurements are motion artifact and skin blood flow correction. Therefore, researchers have developed several artifact correction processes, such as wavelet-based motion correction (Perpetuini et al., 2021). The association between zero-set vectors and measurement noise should be further assessed.

Study limitations

Scalp blood flow was not simultaneously measured. The extent to which APR and L obtained from the zero-set vectors that are affected by the use of preprocessing techniques must be determined.

If the population in Eq. 5 is greater, the APR can be calculated more accurately. Hence, the accuracy of the APR is dependent on the population of the zero-set vector group.

The APR was calculated as the population in all 140 trials. However, this study did not determine the minimum number of trials sufficient for analysis.

Determining the minimum number of trials required to unambiguously detect a task-dependent response by the APR could allow for an appropriate number of tasks in the experimental design. The APR may provide accurate quantitative values even with a small number of trials.

In this study, the duration of the resting period was only a few seconds, which was insufficient to assess each site at rest. A controlled study at rest for more than 1 min could be useful in the future.

This study was conducted using a pre-measured identification method (Murakoshi and Kato, 2006) of target cortical sites using the distance between reference points on the scalp from the participant's MRI to place the measurement probes. Therefore, only one participant underwent MRI after the measurement to validate the OMC location. fNIRS is a measurement method, using a probe pair attached to the scalp. The brain region where the probe pair can detect the signal is limited to the nearest region of the probe pair. Therefore, it is necessary to detect location information with a higher accuracy in preparation for probe placement.

A recent study has assessed the optimization of fNIRS optodevice placement based on a transcranial brain atlas (Zhao et al., 2021). Pre-identifying transcranial brain regions that must be measured on MRI images from a population may be possible even with a portable type of fNIRS with a reduced number of channels, with good accuracy. In addition, it can help reduce the participants' burden and research costs.

Conclusion

Unlike conventional analysis methods, which are dependent on *ΔOxyHb* and *ΔDeoxyHb* signal intensities, APR can reflect the state of oxygen metabolism and can quantify and monitor changes in the resting state of the brain at each measurement site. In comparison to APR, ΔOxyHb and ΔDeoxyHb alone may overestimate the spatial extent of brain activity more broadly or the duration of brain activity longer. Using the zero-set vector-based fNIRS, APR can be a valid indicator to evaluate the relationship between OMC activity and oral motor function and bite force.

Data availability statement

The raw data supporting the conclusions of this article will be made available by the authors, without undue reservation.

Ethics statement

The studies involving human participants were reviewed and approved by the ethics committee of KatoBrain Co., Ltd. The patients/participants provided their written informed consent to participate in this study.

Author contributions

MA, HK, and TK contributed to conception and design of the study. TK organized the data. TK wrote the draft of the manuscript with their discussion with HK and MA. MA and HK wrote the dental medicine sections of the manuscript. All authors contributed to manuscript revision, read, and approved the submitted version.

Acknowledgments

The authors wish to thank Hiroshi Kato and Enago (www.enago.jp) for the English language review.

Conflict of interest

MA was employed by the company Total Health Advisers Co. HK and TK were employed by the company KatoBrain Co., Ltd.

Publisher's note

All claims expressed in this article are solely those of the authors and do not necessarily represent those of their affiliated organizations, or those of the publisher, the editors, and the reviewers. Any product that may be evaluated in this article, or claim that may be made by its manufacturer, is not guaranteed or endorsed by the publisher.

References

Akiyama, T., Ohira, T., Kawase, T., and Kato, T. (2006). TMS orientation for NIRS-functional motor mapping. *Brain Topogr.* 19, 1–9. doi:10.1007/s10548-006-0007-9

Ances, B. M., Buerk, D. G., Greenberg, J. H., and Detre, J. A. (2001). Temporal dynamics of the partial pressure of brain tissue oxygen during functional forepaw stimulation in rats. *Neurosci. Lett.* 306, 106–110. doi:10.1016/s0304-3940(01)01868-7

Berkovitz, B. K. (2005). "Infratemporal region and temporomandibular joint," in *Gray's anatomy: The anatomical basis of clinical practice*. Editor S. Standring. 39th ed. (Edinburgh: Elsevier Churchill Livingstone), 526.

Cheney, P. D., and Fetz, E. E. (1980). Functional classes of primate corticomotoneuronal cells and their relation to active force. *J. Neurophysiol.* 44, 773–791. doi:10.1152/jn.1980.44.4.773

Dan, H., Okamoto, M., Wada, Y., Dan, I., and Kohyama, K. (2007). First bite for hardness judgment as haptic exploratory procedure. *Physiol. Behav.* 92, 601–610. doi:10.1016/j.physbeh.2007.05.006

Fox, P. T., Huang, A., Parsons, L. M., Xiong, J., Zamarippa, F., Rainey, L., et al. (2001). Location-probability profiles for the mouth region of human primary motor-sensory cortex: Model and validation. *NeuroImage* 13, 196–209. doi:10.1006/nimg.2000.0659

Fujii, W., Kanamori, D., Nagata, C., Sakaguchi, K., and Watanabe, R. (2015). Does oral care contributed to brain activation?: One case of functional near-infrared spectroscopy study in patients with a persistent disturbance of consciousness. *Clin. Case Rep.* 2, 143–146. doi:10.1002/ccr3.81

Hoffman, D. S., and Luschei, E. S. (1980). Responses of monkey precentral cortical cells during a controlled jaw bite task. *J. Neurophysiol.* 44, 333–348. doi:10.1152/jn.1980.44.2.333

Hong, K. S., and Naseer, N. (2016). Reduction of delay in detecting initial dips from functional near-infrared spectroscopy signals using vector-based phase analysis. *Int. J. Neural Syst.* 26, 1650012. doi:10.1142/S012906571650012X

Horibe, Y., Ueda, T., Watanabe, Y., Motokawa, K., Edahiro, A., Hirano, H., et al. (2018). A 2-year longitudinal study of the relationship between mastica- tory function and progression to frailty or pre-frailty among community-dwelling Japanese aged 65 and older. *J. Oral Rehabil.* 45, 864–870. doi:10.1111/joor.12700

Iida, T., Sakayanagi, M., Sevensson, P., Komiyama, O., Hirayama, T., Kaneda, T., et al. (2012). Influence of periodontal afferent inputs for human cerebral blood oxygenation during jaw movements. *Exp. Brain Res.* 216, 375–384. doi:10.1007/s00221-011-2941-3

Kanayama, T., Miyamoto, H., Yokoyama, A., and Shibuya, Y. (2015). The influence of bite force strength on brain activity: A functional magnetic resonance imaging study. *J. Biomed. Graph. Comput.* 5, 28–32. doi:10.5430/jbgc.v5n1p28

Kasahara, S., Kato, T., and Kimura, K. (2008). Changes in cerebral function associated with oral pain caused by dentures. *Prosthodont. Res. Pract.* 7, 180–182. doi:10.2186/prp.7.180

Kasahara, S., Kato, T., and Kimura, K. (2007). "Measurement of human cerebral function caused by oral pain," in *Interface oral health science*. Editors K. Sasaki, M. Watanabe, N. Takahashi, O. Okuno, and O. Suzuki (Tokyo: Springer), 203

Kato, T. (2006). *Apparatus for evaluating biological function*. U.S. Patent No 7,065,392 (Washington, DC: U.S. Patent and Trademark Office)

Kato, T. (2013). *Apparatus for evaluating biological function, a method for evaluating biological function, a living body probe, a living body probe mounting device, a living body probe support device and a living body probe mounting accessory*. U.S. Patent No 8,406,838 (Washington, DC: U.S. Patent and Trademark Office)

Kato, T. (2021). *Biological function measurement device, and biological function measurement method, and program*. U.K. Patent GB2595162, Application Number 202,111,659 (Newport, South Wales: Intellectual Property Office)

Kato, T., Kamei, A., Takashima, S., and Ozaki, T. (1993). Human visual cortical function during photic stimulation monitoring by means of near-infrared spectroscopy. *J. Cereb. Blood Flow. Metab.* 13, 516–520. doi:10.1038/jcbfm.1993.66

Kato, T. (2004). Principle and technique of NIRS imaging for human brain FORCE: Fast-oxygen response in capillary event. *Int. Congr. Ser.* 1270, 85–90. doi:10.1016/j.ics.2004.05.052

Kato, T. (2022). Vector-based analysis of cortical activity associated with dumbbell exercise using functional near-infrared spectroscopy. *Front. Sports Act. Living Front.* 4, 838189. doi:10.3389/fspor.2022.838189

Kato, T. (2018). Vector-based approach for the detection of initial dips using functional near-infrared spectroscopy, Neuroimaging - structure, Function and Mind, Sanja Josef Golubic. IntechOpen. Available at: https://www.intechopen.com/chapters/63385.

Kawaguchi, H., Hayashi, T., Kato, T., and Okada, E. (2004). Theoretical evaluation of accuracy in position and size of brain activity obtained by near-infrared topography. *Phys. Med. Biol.* 49, 2753–2765. doi:10.1088/0031-9155/49/12/019

Kemppainen, P., Waltimo, A., Palomäki, H., Salonen, O., Könönen, M., and Kaste, M. (1999). Masticatory force and function in patients with hemispheric brain infarction and hemiplegia. *J. Dent. Res.* 78, 1810–1814. doi:10.1177/00220345990780120701

Kirilina, E., Jelzow, A., Heine, A., Niessing, M., Wabnitz, H., Bruhl, R., et al. (2012). The physiological origin of task-evoked systemic artefacts in functional near infrared spectroscopy. *NeuroImage* 61, 70–81. doi:10.1016/j.neuroimage.2012.02.074

Klein, F., Debener, S., Witt, K., and Kranczioch, C. (2022). fMRI-based validation of continuous-wave fNIRS of supplementary motor area activation during motor execution and motor imagery. *Sci. Rep.* 12, 3570. doi:10.1038/s41598-022-06519-7

Kober, S. E., Gressenberger, B., Kurzmann, J., Neuper, C., and Wood, G. (2015). Voluntary modulation of hemodynamic responses in swallowing related motor areas: A near-infrared spectroscopy-based neurofeedback study. *PLoS One* 10, e0143314. doi:10.1371/journal.pone.0143314

Kugimiya, Y., Ueda, T., Watanabe, Y., Takano, T., Edahiro, A., Awata, S., et al. (2019). Relationship between mild cognitive decline and oral motor functions in metropolitan community-dwelling older Japanese: The takashimadaira study. *Arch. Gerontol. Geriatr.* 81, 53–58. doi:10.1016/j.archger.2018.11.008

Matcher, S. J., Elwell, C. E., Cooper, C. E., Cope, M., and Delpy, D. T. (1995). Performance comparison of several published tissue near-infrared spectroscopy algorithms. *Anal. Biochem.* 227, 54–68. doi:10.1006/abio.1995.1252

Matsushima, Y., Kusumoto, T., and Kawazoe, T. (2005). Influence of the language dominant hemisphere on the activation region of the cerebral cortex during mastication. *Shika Igaku. J. Osaka Odontol. Soc.* 68, 111–119. (In Japanese). doi:10.18905/shikaigaku.68.1_111

Miyazawa, T., Horiuchi, M., Komine, H., Sugawara, J., Fadel, P. J., and Ogoh, S. (2013). Skin blood flow influences cerebral oxygenation measured by near-infrared spectroscopy during dynamic exercise. *Eur. J. Appl. Physiol.* 113, 2841–2848. doi:10.1007/s00421-013-2723-7

Murakoshi, A., and Kato, T. (2006). "Navigating system of cranio-cerebral anatomical correlation for COE: Cerebral functional mapping of oxygen exchange," in 12th Annual Meeting of the Organization for Human Brain Mapping. NeuroImage.

Onozuka, M., Fujita, M., Watanabe, K., Hirano, Y., Niwa, M., Nishiyama, K., et al. (2002). Mapping brain region activity during chewing: A functional magnetic resonance imaging study. *J. Dent. Res.* 81, 743–746. doi:10.1177/0810743

Otsuka, T., Yamasaki, R., Shimazaki, T., Yoshino, F., Sasaguri, K., and Kawata, T. (2015). Effects of mandibular retrusive deviation on prefrontal cortex activation: A functional near-infrared spectroscopy study. *Biomed. Res. Int.* 2015, 373769. doi:10.1155/2015/373769

Ozaki, H. (2002). Laterality of stomatognathic function and reliability of determination of preferred chewing side. *Hiroshima Daigaku Shigaku Zasshi* 34, 48–59. in Japanese.

Perpetuini, D., Cardone, D., Filippini, C., Chiarelli, A. M., and Merla, A. (2021). A motion artifact correction procedure for fNIRS signals based on wavelet transform and infrared thermography Video Tracking. *Sensors (Basel).* 21, 5117. doi:10.3390/s21155117

Robu, C. B., Koninckx, A., Docquier, M. A., Grosu, I., De Kerchove, L., Mastrobuoni, S., et al. (2020). Advanced age and sex influence baseline regional cerebral oxygen saturation as measured by near-infrared spectroscopy: Subanalysis of a prospective study. *J. Cardiothorac. Vasc. Anesth.* 34, 3282–3289. doi:10.1053/j.jvca.2020.06.025

Shibusawa, M., Takeda, T., Nakajima, K., Ishigami, K., and Sakatani, K. (2009). Functional near-infrared spectroscopy study on primary motor and sensory cortex response to clenching. *Neurosci. Lett.* 449, 98–102. doi:10.1016/j.neulet.2008.10.073

Shinagawa, H., Ono, T., Handa, E., Sasaki, T., Taira, M., Iriki, A., et al. (2004). Chewing-side preference is involved in differential cortical activation patterns during tongue movements after bilateral gum-chewing: A functional magnetic resonance imaging study. *J. Dent. Res.* 83, 762–766. doi:10.1177/154405910408301005

Suh, M., Bahar, S., Mehta, A., and Schwartz, T. (2006). Blood volume and hemoglobin oxygenation response following electrical stimulation of human cortex. *Neuroimage* 31, 66–75. doi:10.1016/j.neuroimage.2005.11.030

Takeuchi, K., Ohara, T., Furuta, M., Takeshita, T., Shibata, Y., Hatam, J., et al. (2017). Tooth loss and risk of dementia in the community: The hisayama study. *J. Am. Geriatr. Soc.* 65, e95–e100. doi:10.1111/jgs.14791

Tamura, T., Kanayama, T., Yoshida, S., and Kawasaki, T. (2002). Analysis of brain activity during clenching by fMRI. *J. Oral Rehabil.* 29, 467–472. doi:10.1046/j.1365-2842.2002.00880.x

Thibault, R. T., Lifshitz, M., Jones, J. M., and Raz, A. (2014). Posture alters human resting-state. *Cortex.* 58, 199–205. doi:10.1016/j.cortex.2014.06.014

Yoshino, K., and Kato, T. (2012). Vector-based phase classification of initial dips during word listening using near-infrared spectroscopy. *NeuroReport* 23, 947–951. doi:10.1097/WNR.0b013e328359833b

Yousry, T. A., Schmid, U. D., Alkadhi, H., Schmidt, D., Peraud, A., Buettner, A., et al. (1997). Localization of the motor hand area to a knob on the precentral gyrus. A new landmark. *Brain* 120, 141–157. doi:10.1093/brain/120.1.141

Zamanlu, M., Khamnei, S., Salarilak, S., Oskoee, S. S., Shakouri, S. K., Houshyar, Y., et al. (2012). Chewing side preference in first and all mastication cycles for hard and soft morsels. *Int. J. Clin. Exp. Med.* 5, 326–331.

Zhao, Y., Xiao, X., Jiang, Y. H., Sun, P. P., Zhang, Z., Gong, Y. L., et al. (2021). Transcranial brain atlas-based optimization for functional near-infrared spectroscopy optode arrangement: Theory, algorithm, and application. *Hum. Brain Mapp.* 42, 1657–1669. doi:10.1002/hbm.25318

Frontiers in Physiology

Understanding how an organism's components work together to maintain a healthy state

The second most-cited physiology journal, promoting a multidisciplinary approach to the physiology of living systems - from the subcellular and molecular domains to the intact organism and its interaction with the environment.

Discover the latest Research Topics

See more →

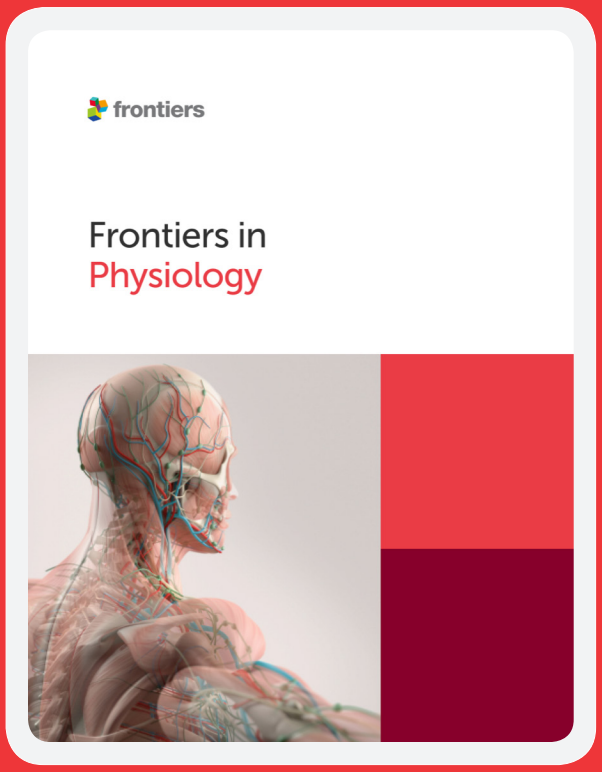

Frontiers

Avenue du Tribunal-Fédéral 34
1005 Lausanne, Switzerland
frontiersin.org

Contact us

+41 (0)21 510 17 00
frontiersin.org/about/contact